ISSN 0021-9673

VOL. 709 NO. 2 18 AUGUST 1995

THIS ISSUE COMPLETES VOL. 709

JOURNAL OF CHROMATOGRAPHY A

INCLUDING ELECTROPHORESIS AND OTHER SEPARATION METHODS

ELSEVIER

JOURNAL OF CHROMATOGRAPHY A

INCLUDING ELECTROPHORESIS AND OTHER SEPARATION METHODS

Scope. The *Journal of Chromatography A* publishes papers on all aspects of **chromatography, electrophoresis** and related methods. Contributions consist mainly of research papers dealing with chromatographic theory, instrumental developments and their applications. In the *Symposium volumes*, which are under separate editorship, proceedings of symposia on chromatography, electrophoresis and related methods are published. *Journal of Chromatography B: Biomedical Applications* —This journal, which is under separate editorship, deals with the following aspects: developments in and applications of chromatographic and electrophoretic techniques related to clinical diagnosis or alterations during medical treatment; screening and profiling of body fluids or tissues related to the analysis of active substances and to metabolic disorders; drug level monitoring and pharmacokinetic studies; clinical toxicology; forensic medicine; veterinary medicine; occupational medicine; results from basic medical research with direct consequences in clinical practice.

Submission of Papers. The preferred medium of submission is on disk with accompanying manuscript (see *Electronic manuscripts* in the Instructions to Authors, which can be obtained from the publisher, Elsevier Science B.V., P.O. Box 330, 1000 AH Amsterdam, Netherlands). Manuscripts (in English; *four* copies are required) should be submitted to: Editorial Office of *Journal of Chromatography A*, P.O. Box 681, 1000 AR Amsterdam, Netherlands, Telefax (+31-20) 485 2304, or to: The Editor of *Journal of Chromatography B: Biomedical Applications*, P.O. Box 681, 1000 AR Amsterdam, Netherlands. Review articles are invited or proposed in writing to the Editors who welcome suggestions for subjects. An outline of the proposed review should first be forwarded to the Editors for preliminary discussion prior to preparation. Submission of an article is understood to imply that the article is original and unpublished and is not being considered for publication elsewhere. For copyright regulations, see below.

Publication information. *Journal of Chromatography A* (ISSN 0021-9673): for 1995 Vols. 683–714 are scheduled for publication. *Journal of Chromatography B: Biomedical Applications* (ISSN 0378-4347): for 1995 Vols. 663–674 are scheduled for publication. Subscription prices for *Journal of Chromatography A*, *Journal of Chromatography B: Biomedical Applications* or a combined subscription are available upon request from the publisher. Subscriptions are accepted on a prepaid basis only and are entered on a calendar year basis. Issues are sent by surface mail except to the following countries where air delivery via SAL is ensured: Argentina, Australia, Brazil, Canada, China, Hong Kong, India, Israel, Japan, Malaysia, Mexico, New Zealand, Pakistan, Singapore, South Africa, South Korea, Taiwan, Thailand, USA. For all other countries airmail rates are available upon request. Claims for missing issues must be made within six months of our publication (mailing) date. Please address all your requests regarding orders and subscription queries to: Elsevier Science B.V., Journal Department, P.O. Box 211, 1000 AE Amsterdam, Netherlands. Tel.: (+31-20) 485 3642; Fax: (+31-20) 485 3598. Customers in the USA and Canada wishing information on this and other Elsevier journals, please contact Journal Information Center, Elsevier Science Inc., 655 Avenue of the Americas, New York, NY 10010, USA, Tel. (+1-212) 633 3750, Telefax (+1-212) 633 3764.

Abstracts/Contents Lists published in Analytical Abstracts, Biochemical Abstracts, Biological Abstracts, Chemical Abstracts, Chemical Titles, Chromatography Abstracts, Current Awareness in Biological Sciences (CABS), Current Contents/Life Sciences, Current Contents/Physical, Chemical & Earth Sciences, Deep-Sea Research/Part B: Oceanographic Literature Review, Excerpta Medica, Index Medicus, Mass Spectrometry Bulletin, PASCAL-CNRS, Referativnyi Zhurnal, Research Alert and Science Citation Index.

US Mailing Notice. *Journal of Chromatography A* (ISSN 0021-9673) is published weekly (total 52 issues) by Elsevier Science B.V., (Sara Burgerhartstraat 25, P.O. Box 211, 1000 AE Amsterdam, Netherlands). Annual subscription price in the USA US$ 5389.00 (US$ price valid in North, Central and South America only) including air speed delivery. Second class postage paid at Jamaica, NY 11431. **USA POSTMASTERS**: Send address changes to *Journal of Chromatography A*, Publications Expediting, Inc., 200 Meacham Avenue, Elmont, NY 11003. Airfreight and mailing in the USA by Publications Expediting.

See inside back cover for Publication Schedule, Information for Authors and information on Advertisements.

0021-9673/95/$09.50

Printed in the Netherlands

VOL. 709, NO. 2 JOURNAL OF CHROMATOGRAPHY A 18 AUGUST 1995

CONTENTS

(Abstracts/Contents Lists published in Analytical Abstracts, Biochemical Abstracts, Biological Abstracts, Chemical Abstracts, Chemical Titles, Chromatography Abstracts, Current Awareness in Biological Sciences (CABS), Current Contents/Life Sciences, Current Contents/Physical, Chemical & Earth Sciences, Deep-Sea Research/Part B: Oceanographic Literature Review, Excerpta Medica, Index Medicus, Mass Spectrometry Bulletin, PASCAL-CNRS, Referativnyi Zhurnal, Research Alert and Science Citation Index)

REGULAR PAPERS

Column Liquid Chromatography

Gas Chromatography

Supercritical Fluid Chromatography

(Continued overleaf)

Contents (continued)

ELSEVIER

Journal of Chromatography A, 709 (1995) 227–239

JOURNAL OF CHROMATOGRAPHY A

Study of the operating conditions of axial compression columns for preparative chromatography

Matilal Sarker[a], Georges Guiochon[a,b,*]

[a]*Department of Chemistry, University of Tennessee, Knoxville, TN 37996-1600, USA*

[b]*Analytical Chemistry Division, Oak Ridge National Laboratory, Oak Ridge, TN 37831, USA*

First received 24 February 1995; revised manuscript received 12 April 1995; accepted 12 April 1995

Abstract

The packing behavior and the stability of a spherical-particle, silica-based packing material and the operation of an axial compression column are discussed. The coupling between the axial compression pressure and the inlet pressure at constant flow-rate was investigated. The results demonstrated also an excellent column efficiency, a rapid packing consolidation, and a long-term stability of the column performance. Reduced height equivalents of theoretical plate (HETPs) around 2 were routinely obtained and the column did not show any sign of degradation of its efficiency or stability after 700 h of continuous use. These results are attributed primarily to the spherical nature of the material used. Finally, a procedure for opening the top flange of a column packed under axial compression without loosing any stationary phase nor degrading the column efficiency is described.

1. Introduction

For over twenty years, a slow debate regarding the relative superiority of spherical- and irregular-shaped particles has been held without yet reaching a conclusion. This problem seems to have been of more serious concern to vendors and manufacturers than to the scientific community, and very few systematic comparative studies have been published. Admittedly, the differences between the hydrodynamic and the kinetic performance observed in analytical applications did not seem very significant compared to the differences of retention properties reported between any two brands of silica material. As reliable, accurate information is nearly priceless, there was little incentive in taking the particle shape into account when separation factors are of so paramount importance.

Things have changed somewhat with the development of preparative chromatography. The cost of the packing material, although not the most critical component of production costs [1–3], has become important. The cost of bulk packing materials is higher when they are made of spherical particles than when made of irregular-shaped particles. For production purposes, several elements other than the separation factors must be taken into account. Therefore, the issues of the relative technical advantages

* Corresponding author. Address for correspondence: Department of Chemistry, University of Tennessee, Knoxville, TN 37996-1600, USA.

0021-9673/95/$09.50
SSDI 0021-9673(95)00474-2

and disadvantages of the two types of packing materials is resurfacing. Although not always convincingly, it is often claimed that the performance of spherical particles is superior to that of irregular-shaped materials.

The most important advantages claimed for spherical particles are as follows. First, because of the conditions under which they are prepared, there is a better control over their particle-size distribution. Whether a narrower size distribution is a real advantage, however, is still open for discussion. It is said that the small particles determine the column permeability whereas the large ones control the column efficiency, but systematic experiments are lacking. Second, spherical particles can tolerate higher compression pressures than irregular particles and they would be less susceptible to fragmentation into smaller particles during handling, packing, and consolidation. This mechanical superiority is suggested by the preeminent strength of the eggshells and cupolas. Packings do suffer during consolidation [4] and materials made of spherical particles seem to consolidate faster, under lower pressures, and into a more compact, more resilient bed than those made of irregular-shaped particles [5]. The practical extent of these advantages remains unclear and several systematic studies are needed to understand the different aspects of this complex issue. It should be underlined that, even in preparative chromatography, the issues of primary importance remain (i) the separation factor and (ii) the saturation capacity. The final choice of a packing should be made between those materials which have the best characteristics for these two properties and give columns with a long useful life.

In previous publications [6–8] we have studied the performance of dynamic radial and axial compression columns packed with irregular-shaped particles. The goal of this paper is the description of experimental results obtained with a material made of spherical particles when using the methods we have previously developed for the packing of dynamic axial compression columns and for testing of these columns for long-time durability.

2. Experimental

2.1. Dynamic axial compression column

The axial compression unit was an LC.50.VE.500.100 Column Skid obtained from Prochrom (Champigneulles, France). The column is made of a stainless steel cylinder (5.0 cm × 59.0 cm) with a maximum working pressure of 100 bar. The axial compression is applied by a hydraulic piston operated by a Haskel pump (Burbank, CA, USA). The Haskel pump in turn is assisted by compressed nitrogen from a cylinder.

2.2. Solvent delivery system

A Kiloprep 100 HPLC pump was obtained from Biotage (Charlottesville, VA, USA). The pump can deliver solvents at flow-rates up to 500 ml/min, at a maximum pressure of 138 bar. The flow-rate is set manually. The system includes also two solvent ports and an injection valve with a 1.5-ml injection loop.

2.3. Stationary phase

All the columns used in this work were packed with Kromasil C_8 (Eka Nobel, Bohus, Sweden). This chemically bonded spherical silica has an average particle size of 13.0 μm and an average pore size of 100 Å. The axial compression column was packed using the procedure previously described [8], at a pressure of 61.5 bar. All experiments were carried out at this axial compression pressure, except for those during which the influence of the compression pressure was studied.

Several analytical columns of different lengths, all with an internal diameter of 0.46 cm, were packed in our laboratory using the same stationary phase, and a conventional slurry packing method at 483 bar, in agreement with the recommendations of the manufacturer. The characteristics of these columns are summarized in Table 1.

Table 1
Characteristics of the columns

Column properties	Axial compression column	Analytical column #1	Analytical column #2	Analytical column #3
Dimension (cm)	20.0 × 5.0	20.0 × 0.46	20.0 × 0.46	10.0 × 0.46
Total porosity (solvent A)	0.72	0.76	0.73	0.71
Total porosity (solvent B)	0.67	0.75	not done	0.70
Total porosity (from mass)	0.74	0.74	0.75	not done
Phase ratio (solvent A)	0.39	0.32	0.37	0.40
Phase ratio (solvent B)	0.48	0.34	not done	0.43
Phase ratio (from mass)	0.35	0.35	0.33	not done
k' (acetone)	0.37 ± 0.01	na[a]	na	0.30 ± 0.01
k' (phenol)	2.82 ± 0.20	na	na	2.84 ± 0.05
k' (cresol)	6.04 ± 0.46	na	na	6.18 ± 0.12

[a] na = not available.

2.4. Chemicals

Acetone, *m*-cresol, phenol, methyl benzoate, toluene, acetonitrile, nitric acid, ammonium bifluoride, isopropanol, and methanol were all purchased from Baxter (Atlanta, GA, USA) and were 99.9% pure. Phenethyl alcohol was purchased from Fluka (Buchs, Switzerland). Distilled water from the chemistry department plant was filtered on a 1.2-μm membrane before use.

2.5. Detector

A UV–Vis detector (Model 203-7083, Linear Scientific, Reno, NV, USA) equipped with a variable path length preparative cell was used to collect chromatograms. With a short cell path length the detector response remains linear up to much higher concentrations than with conventional HPLC detectors. The cell can be operated under high pressures and can easily accommodate a 500 ml/min flow-rate. For HETP measurements, the cell path length was kept to its maximum (3 mm), so that a reasonable response could be obtained with analytical-size injections.

2.6. Pressure sensor

The column inlet pressure was measured with an Omega pressure transducer Model PX603-2KG5V (Omega, Stamford, CT, USA). This transducer gives a 1–5 V d.c. linear output. Its response time is 1 ms. The output was adjusted to read 0.402 V d.c. for 0 bar and 2.022 V d.c. for 138 bar, for compatibility with the data acquisition system. Calibration shows that the inlet pressure [P (bar)] and the voltage output [V (V)] are related by $P = (V - 0.402)/1.1745 \cdot 10^{-2}$). The reading of the sensor at a zero inlet pressure (no flow-rate) was checked periodically.

2.7. Displacement sensor

Dynamic changes of the column length were measured with an Electro-Mike displacement sensor Model PAA1555 (Reagan Controls, Charlotte, NC, USA). This sensor includes a displacement transducer and a transmitter with analog output of 2 to 9 V d.c. for a displacement between 2.0 and 9.0 mm. The output voltage was

attenuated to 2.2 V d.c. for our data system. Calibration of the sensor output with known targets shows the response to be linear in the +2 to +9 mm range, d (distance between target and sensor in mm) and V (output in V) being related by $d = (0.20 \pm 0.01)V + (0.18 \pm 0.06)$.

Unlike in our previous work [8], the sensor was hanged from a stand and the steel target was clamped to the compression piston, in such a way that an increase in target distance means an increase in the column length. Depending on the movement of the piston, the distance between the sensor and the target increases or decreases. Because of the nature of the device, a change of 0.01 mm in the column length can be detected easily, while the actual column length is known within only 0.1 cm. The actual length of a packed column was measured by attaching a long, thin electric wire to the piston rod, just below the piston head, stretching it with a small weight, and measuring the position of a small mark on this wire. The zero reference is obtained by raising the piston in an empty column until it touches the top flange. This device permits a measurement of the column length with an accuracy of 0.1 cm.

2.8. Data acquisition system

The data system consists of a Waters System Interface Module (SIM) with two A/D convertors (Milford, MA, USA). This SIM is capable of the simultaneous monitoring of four sensors and/or detectors and can control three HPLC pumps. The digitized data from the SIM was collected by Waters Maxima 820 version 3.31 software loaded on a NEC computer. All the data files were translated to ASCII format for further use and uploaded to the computer network of the University of Tennessee. For treatment of these data, various DOS- and VMS-based software was developed in our laboratory.

2.9. Methods

In the experiments reported here, two solvents were used as the eluent. These were methanol (solvent A) and a mixture of 40% methanol and 60% water (v/v, solvent B). The test samples were low-concentration solutions of acetone (1.6 ml/l), phenol (0.4 g/l), and *m*-cresol (0.5 g/l) in the eluent. Sample volumes for HETP measurements were 1.5 ml, injected by filling an appropriate loop. For economic and waste management reasons, the solvents were pumped in closed circuit, with a 15–20 l reservoir on the solvent line. The solvent was replaced when the baseline absorbance became significantly higher than that of fresh solvent.

Three outputs were recorded in most of the experiments, the UV-detector signal and the outputs of the displacement and the pressure sensors. The data from the pressure transducer were converted to pressure units (bar), and the output from the sensors to changes in the column length (cm) and the pressure (bar). The chromatographic data were used to calculate the column efficiencies, from the width at peak half-height, and the retention factors. The reduced velocities ($\nu = u\, d_p/D_m$, with u the linear velocity, d_p the average particle size, and D_m the molecular diffusivity) and reduced plate heights ($h = H/d_p$, with H the actual column HETP) were fitted to the van Deemter equation [9], using a nonlinear least-squares fit. The classical Wilke–Chang [10] equation was used to estimate the diffusion coefficients of the compounds used. It gives as the molecular diffusivities of acetone, phenol, and cresol, in solvent B, at 25°C, $7.39 \cdot 10^{-6}$, $6.59 \cdot 10^{-6}$, and $5.98 \cdot 10^{-6}$ cm^2/s, respectively.

3. Results and discussion

The characteristics of the columns studied are summarized in Table 1. The results of a long-term stability test of the axial compression column are reported in Table 2. During this study, several similar determinations of the dependence of the column efficiency on the mobile phase flow-rate were completed. Flow-rates and column efficiencies were converted into reduced parameters, viz., reduced velocity and reduced plate height, and fitted to the classical van

Table 2
Compiled Van Deemter parameters for the axial compression columns

Column no.	Solvent	Sample	a	c	h_{min}	v_{opt}	Hours used
11	A	acetone	1.62	0.089	2.42	4.50	10
11	A	acetone	1.55	0.098	2.39	4.29	20
11	A	acetone	1.68	0.080	2.44	4.74	46
11	B	acetone	2.18	0.042	2.73	6.55	
		phenol	3.03	0.012	3.32	12.25	72
		cresol	2.81	0.015	3.14	10.95	
11	B	acetone	2.09	0.052	2.70	5.88	
		phenol	2.80	0.025	3.22	8.49	123
		cresol	2.86	0.016	3.20	10.61	
11	B	acetone	1.96	0.047	2.54	6.19	
		phenol	2.42	0.028	2.87	8.02	238
		cresol	2.90	0.010	3.17	13.42	
11	B	acetone	1.96	0.051	2.57	5.94	
		phenol	2.67	0.026	3.10	8.32	263
		cresol	2.47	0.024	2.89	8.66	
11	A	acetone	1.63	0.088	2.43	4.52	371
11	A	acetone	1.62	0.084	2.40	4.63	391
11	A	acetone	2.07	0.050	2.67	6.00	
		phenol	1.83	0.047	2.41	6.19	497
		cresol	2.49	0.030	2.96	7.75	

Deemter equation [9]. Since few data points were collected at low flow velocities, the coefficient b of this equation was taken arbitrarily as equal to 1.8, as in our previous study [8]. The values of the coefficients a and c are shown in Table 2. Table 2 also contains the values of the minimum reduced plate height (h_{min}) and the optimum reduced velocity (v_{opt}).

As seen in Table 2, the column performance did not change significantly over a period of 500 h. In fact, several other experiments, different from the conventional testing done during the first 500 h, were performed with this same column for an additional 200 h (experiments reported later, in Sections 3.4–3.8). After 700 h, the column was briefly tested again and dismantled. Although a more limited data set was acquired, the final test showed that the column efficiency had not changed.

3.1. Column performance with pure methanol

As in previous papers [7,8], a preliminary study of the column performance was done using pure methanol as the mobile phase and a 1.5% acetone solution as the sample. The results are given in Table 2. Acetone was used as an unretained compound for the determination of the void volume [8], hence of the total porosity, which is reported in Table 1. The total porosity of analytical columns was also determined by washing the column with pure methanol, unpacking it and weighing the packing material recovered, after drying it in an oven at 110°C for 12 h. The stationary phase volume was determined by assuming the density of silica to be 2.2 g/cm^3.

Fig. 1 shows a typical plot of the reduced plate height versus the reduced mobile phase velocity for both the axial compression column and an analytical column. The lines are derived from the best fit of the respective data to the van Deemter equation. The axial compression column showed better efficiency than the analytical column (Fig. 1). This is not uncommon for spherical particles [11] and might be explained either by a smaller relative contribution of extra-column band broadening or by a genuinely better packed

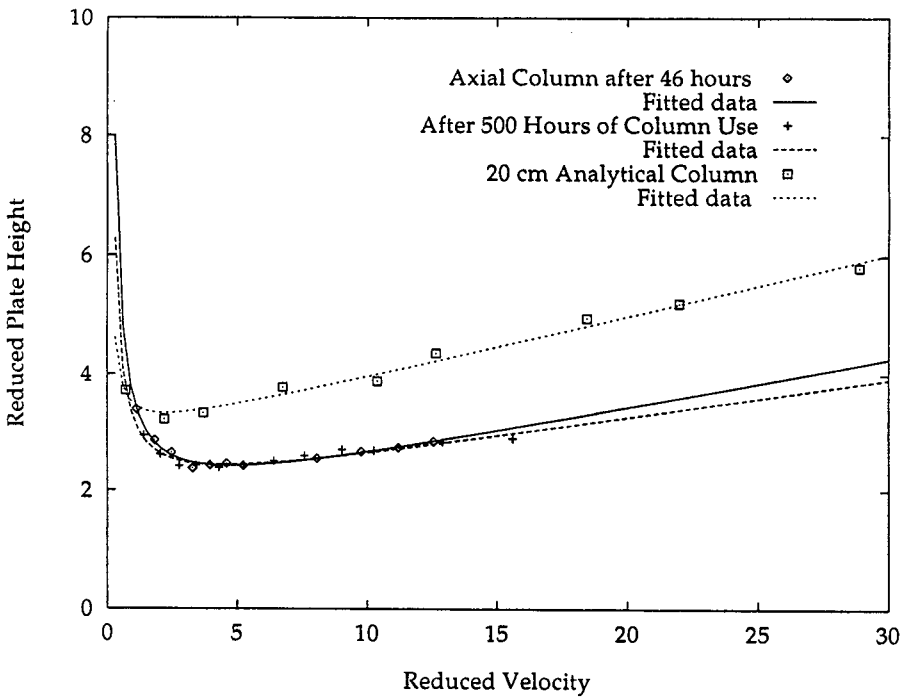

Fig. 1. Typical Van Deemter plot obtained. Plot of the reduced plate height versus the reduced velocity for an axial compression column (20.0 × 5.0 cm) and an analytical column (20.0 × 0.46 cm). The eluent was methanol and the sample a solution of acetone in methanol.

column. Fig. 1 also contains data comparing performance of the axial column after 46 and 500 h of use, respectively. As seen in Fig. 1, the column performance was essentially the same after 500 h of use as immediately after packing. For this column the van Deemter parameters were $a = 1.61$, $b = 1.93$, $c = 0.086$, $h_{min} = 2.42$, $v_{opt} = 4.74$ after 46 h and $a = 1.84$, $b = 1.34$, $c = 0.068$, $h_{min} = 2.44$, $v_{opt} = 4.44$ after 500 h of column use. For the analytical column the van Deemter parameters were $a = 2.86$, $b = 0.53$, $c = 0.105$, $h_{min} = 3.33$, and $v_{opt} = 2.22$.

The data in Table 1 show that the values of the total porosity and the phase ratio of the different columns are consistent. Although there is some scatter of the data for the analytical columns, the axial compression column gives on the average a systematically lower total porosity and a larger phase ratio than the analytical columns.

3.2. Column performance with methanol–water (40:60, v/v)

Solvent B was used for the long-term stability study of the axial compression column. A sample containing acetone ($k' = 0.37$), phenol ($k' = 2.82$), and *m*-cresol ($k' = 6.04$) was used to monitor the efficiency of the column at long time intervals (see Table 2). These values of the retention factors of our standard test compounds are slightly higher than those found with the C_{18} stationary phases previously used [7]. A high surface density of the bonded alkyl chains on the stationary phase could explain this change. It is not due to an error in the mobile phase composition. The values obtained for the retention factors on the axial compression column and the analytical columns are in excellent agreement. It is clear from the data in Table 1 that the

performance of the axial compression column did not degrade significantly after 500 h of use.

3.3. Column permeability and average particle size determination

During the course of this study, the inlet pressure of the axial compression column was determined at different flow-rates, while determining the column efficiency. The values obtained for the inlet pressure were corrected for the contributions from the inlet and outlet frits and the connecting tubes, as done in our previous study [8]. As shown by the plot of a typical set of corrected inlet pressures versus the flow-rate in Fig. 2, these data fit well to a straight line. Introducing the slope of this straight line into the Darcy equation gives a particle size of 12.2 μm. The average particle size determined independently by Coulter counter was 11.5 μm for the material used in the axial compression column and recovered afterward and 11.2 μm for the virgin material. The nominal particle size was 13.0 μm.

3.4. Inlet pressure and axial compression pressure

Several sets of experiments were carried out to investigate the effect of the axial compression on the packing density and the permeability, hence the inlet pressure of the axial compression column. If the axial compression increases the packing density, the permeability should decrease and, in turn, the inlet pressure required to sustain a given flow-rate should increase. In these studies we have set the axial compression pressure to a particular value and measured the inlet pressure at different flow-rates. The results obtained are illustrated in Fig. 3, which shows a

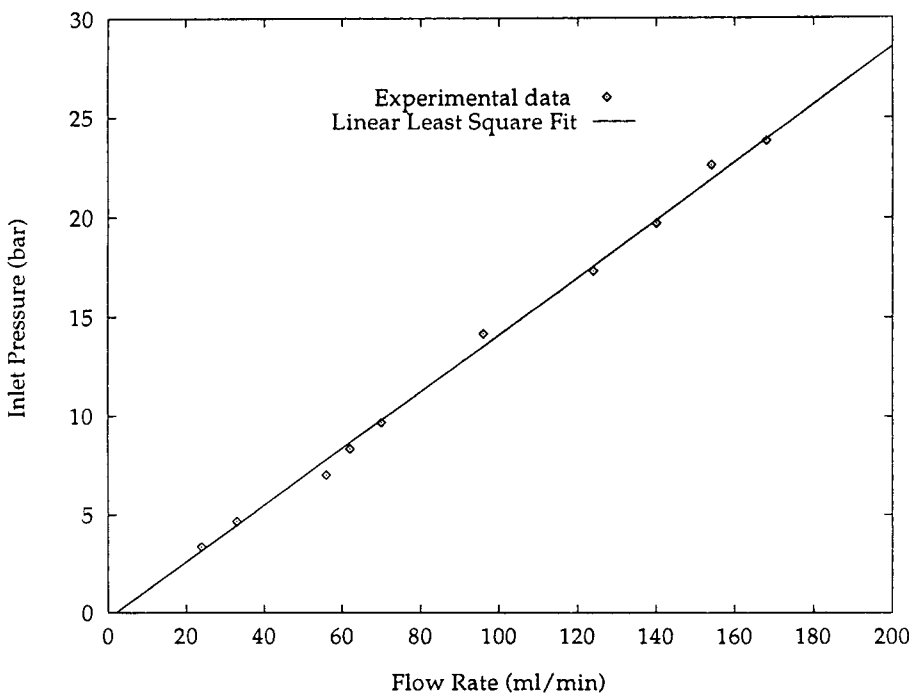

Fig. 2. Plot of the column inlet pressure versus the flow-rate for the axial compression column. The solvent was methanol–water (40:60, v/v). The average particle size obtained from this set of data was 12.2 μm.

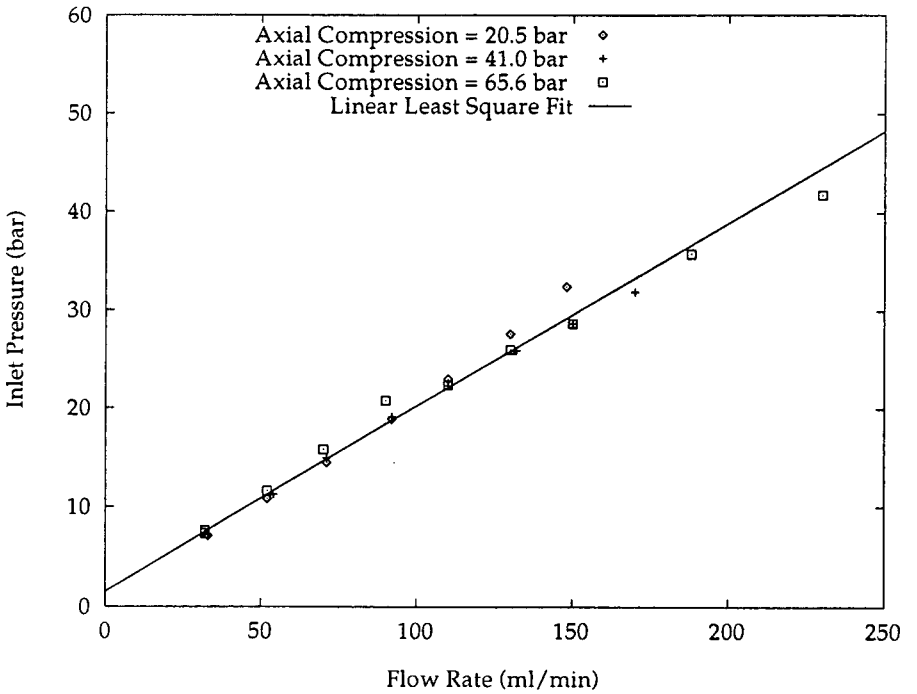

Fig. 3. Plot of the column inlet pressure versus the flow-rate at different axial compression pressures. Solvent methanol–water (40:60, v/v).

plot of the inlet pressure versus the flow-rate at three different axial compression pressures between 20 and 66 bar. The permeability does not change significantly within the range of compression pressures applied. This suggests that the consolidation of the bed has already been achieved when the first experiment was started and that the compressibility of the consolidated bed is small. Indeed, the packed bed had been consolidated under 66 bar during the initial consolidation of the column, prior to these experiments. Both results are in agreement with other experimental findings which will be reported soon [5]. Introducing the slope of the straight line in Fig. 3 into the Darcy equation gives an average particle size of 9.98 μm.

3.5. Effective axial compression pressure (EACP) versus flow-rate

The effective axial compression pressure is the stress applied by the piston against the top of the packing divided by the piston cross-section area. Because a solid, the packing material, is stressed in these compression experiments, the local strain can vary widely across the column. It is useful, however, to follow the variation of this effective compression pressure during the operation of the column. Since the column inlet pressure acts against the axial compression, the effective compression pressure is the difference between the applied axial compression pressure and the inlet pressure. It depends on the flow-rate if, as recommended by Prochrom, the axial compression is kept constant. Results are shown in Fig. 4. The linear decay of the effective compression pressure with increasing flow-rate is expected from what was reported above (Fig. 3). However, it is interesting to note that at high flow-rates the EACP can become negative. This is technically possible because the equipment used in this work for the dynamic axial compression of the column bed is designed in such a way that the piston cannot be pushed back if the

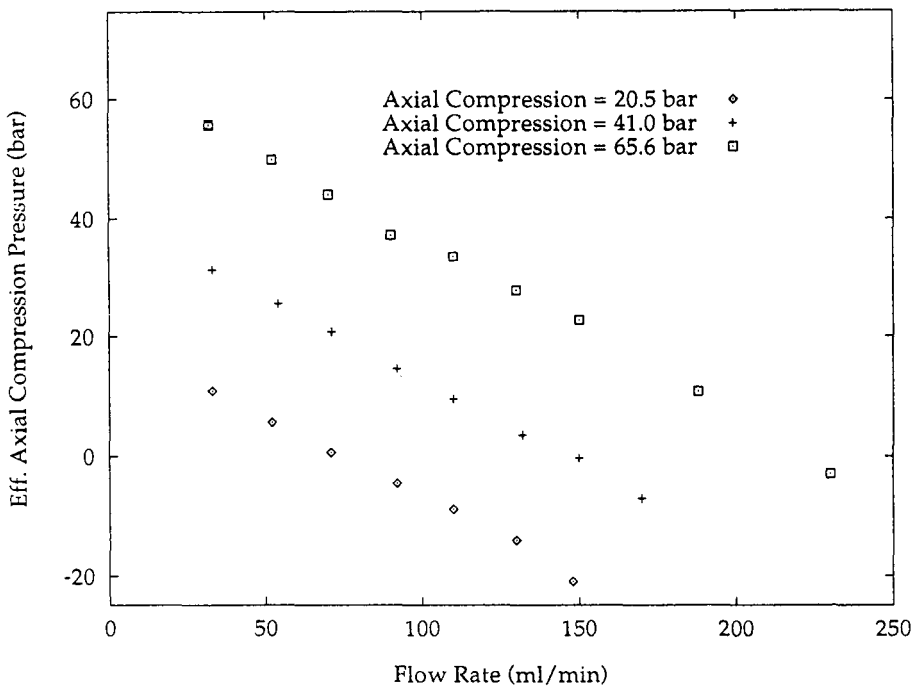

Fig. 4. Plot of the effective axial compression pressure versus the flow-rate for the axial compression column. The initial compression pressures set were 20.5, 41.0, and 65.5 bar. Solvent: methanol–water (40:60, v/v).

compression pressure falls below the inlet pressure. The bed remains compressed like the gas in a tire as long as the pressure in the driving jack is not released. Small leaks are possible, however, and there is a slight compression release of the bed, as we see now.

3.6. Column length and effective axial compression pressure

The column length measured during the experiments just described is plotted against the effective axial compression pressure (EACP) in Fig. 5. In this case, the EACP is varied by varying the flow-rate at constant applied compression pressure. As expected, the column length decreases with increasing EACP and tends toward a constant limit. The higher the axial compression pressure applied, the lower this limit. Fig. 6 shows the result of a complementary experiment. It gives a plot of the column length versus the EACP, at constant flow-rate (110 ml/min) and with different values of the axial compression. A similar behavior is observed. Finally, the plot of the inlet pressure versus the EACP shown in Fig. 7 illustrates the relationship between the effective compression pressure, that is the stress actually applied to the bed, and the inlet pressure for a constant flow-rate. The increase of the column inlet pressure at constant flow-rate corresponding to an increase of the EACP of 30 atm is 6% (31.5 bar to 33.5 bar).

3.7. Replacement of the top flange

It is frequently necessary to open the column and change the top flange. Done without special care, this operation results in a loss of stationary phase, which can cause a problem, for example when the exact amount of packing material used needs to be known. This operation can be done without loss or any disturbance of the packing by the following procedure. A solvent which wets

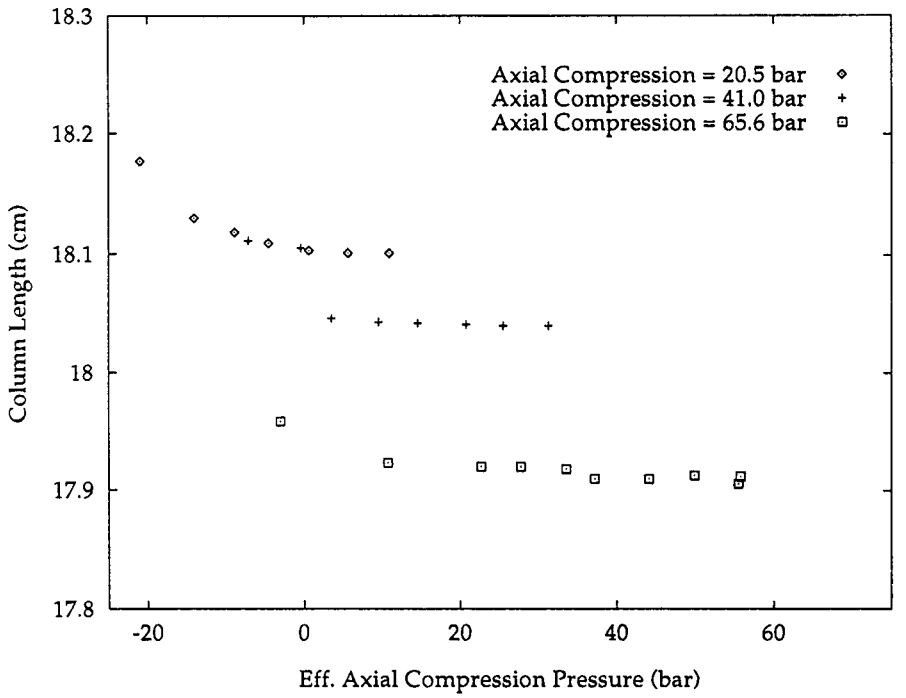

Fig. 5. Plot of the column length versus the effective axial compression pressure during the compression experiments in Fig. 4.

well the packing, methanol in the case of RPLC packings, must be used. First the flow direction of the mobile phase during the experiment is reversed by pumping the solvent into the top flange side. The piston is lowered by 2 cm and held in the neutral position. Solvent is run through the column for five minutes. After flowing several column volumes of solvent while using the top flange as the column inlet, it is safe to open the column top. The top flange is unfastened and opened. A large void, ca. 2 cm deep, is found but the top of the packing is flat. The piston is then moved up slowly by applying a low axial pressure and is stopped when the top flange would barely touch the bed if in position. At this point the top flange is secured in place and the solvent pump is restarted. This procedure is simple. Reversal of the flow direction does not seem to be a problem for a dynamic axial compression column. This procedure allows rapid changes of the top flange or clean/change of the frit.

3.8. Repairing a bad column by axial compression

A void tends to form more or less slowly at the inlet of conventional chromatographic columns, causing a marked degradation of their efficiency. In this last set of experiments, we tried to simulate the formation of a void at the column inlet and to measure its effect on the column efficiency and inlet pressure. The solvent used was methanol and the sample a 3% solution of acetone in methanol. The flow-rate was 151 ml/min. The procedure described in the section above was used to open and close the top of the column and move its top flange. After six hours under a constant stream of mobile phase, the column was tested. The results obtained are shown in row 1 of Table 3. The subsequent operations are also summarized in Table 3. The next day the piston was lowered again by 1 cm as shown in row 3. At this stage, the column efficiency appeared to have been degraded quite

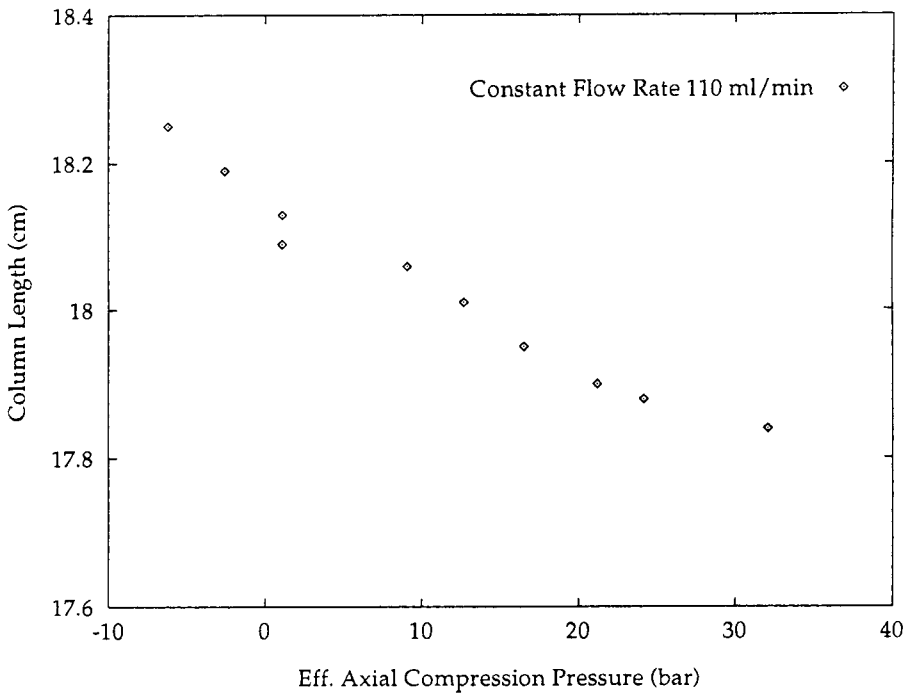

Fig. 6. Plot of the column length versus the effective axial compression pressure at constant flow-rate. The solvent was methanol–water (40:60, v/v).

significantly after eight hours of operation (Table 3, row 5). The previous level of column performance was recovered by a succession of upward movements of the piston (i.e. by decreasing the void space above the piston). The maximum efficiency ever achieved with this column was then obtained (row 9). Finally, the piston was lowered again by 2 cm from the position it occupied when the data in row 9 were being recorded. Comparing the data in rows 5 and 9, we see that an efficiency gain of 69% (from 1488 plates to 2521 plates) in number of theoretical plates was achieved by restoring a sufficiently large, positive effective axial compression and by eliminating the void at the column entrance.

The single most serious disadvantage of the procedure is the increase of inlet pressure by 19%. It was surprising to observe that at no time the column did exhibit any signs of channel formation, even when a 2-cm long void had been created at the column entrance by following a procedure which, in many respects could be qualified as operational failure if it had not been carried out on purpose. The formation of large cavities at the column inlet and their sealing demonstrate the effectiveness of the dynamic compression principle. It permits a change of the flow direction in a dynamic compression column when needed, without any apparent consequences on the column performance.

Acknowledgements

This work has been supported in part by Grant CHE-9201662 of the National Science Foundation and by the cooperative agreement between the University of Tennessee and the Oak Ridge National Laboratory. We acknowledge the long-term free loan from Prochrom (Champigneulles, France) of the 5-cm I.D. stainless-steel column

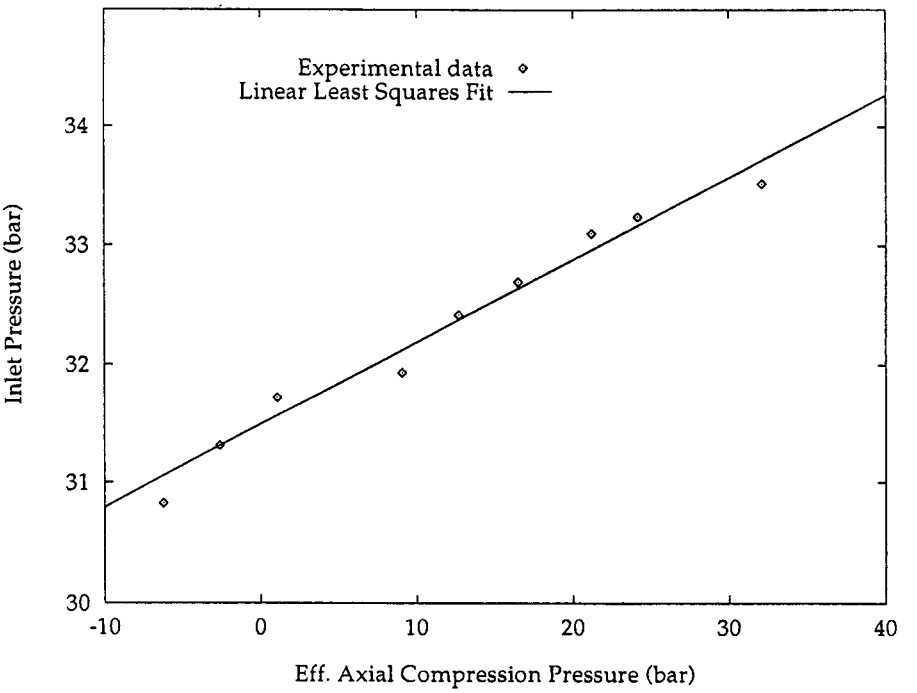

Fig. 7. Plot of the column inlet pressure versus the effective axial compression pressure at constant flow-rate.

and the axial compression unit. We thank Biotage (Charlottesville, VA, USA) for the long-term free loan of their Kiloprep 100 solvent-delivery system and the Linear Scientific Model 204 UV detector equipped with a preparative scale cell. We thank BTR Separation, Wilmington, DE (formerly The PQ Corporation) for their gift of a semi-preparative Linear Scientific Detector and Eka Nobel for their gift of 2 kg of C_8 bonded spherical silica for this study.

Table 3
Repairing a bad axial column by applying axial compression

No.	Condition of experiment	Inlet pressure (bar)	Efficiency of column
1	No ACP[a] applied, piston just touching the bed and the piston held at neutral	13.05	2279
2	Same as #1 after over night (pump not in operation)	13.22	2181
3	Piston position lowered 1 cm from the position at #1	13.05	1534
4	Same as #3, after 2 h of pumping operation	12.88	1517
5	Same as #3, after 8 h of pumping operation	12.80	1488
6	Piston brought up 1 cm with low ACP and held at neutral	12.88	1919
7	Piston brought up 1 cm with low ACP and held at neutral	12.88	2362
8	Piston with ACP = 63 bar. After 2 h of operation, the column length was 17.2 cm	15.35	2482
9	Same as #8, after 6 h of pumping operation	15.18	2521
10	Piston brought down 2 cm from #9	13.22	2017

[a] ACP = axial compression pressure.

References

[1] H. Colin, in G. Ganetsos and P.E. Barker (Editors), Preparative and Production Scale Chromatography, Marcel Dekker, New York, NY, 1993, p. 11.
[2] G. Guiochon, S. Golshan Shirazi and A.M. Katti, Fundamentals of Preparative and Nonlinear Chromatography, Academic Press, Boston, MA, 1994, Ch. XVI.
[3] A. Felinger and G. Guiochon, AIChE J., 40 (1994) 594.
[4] G. Guiochon and M. Sarker, J. Chromatogr. A, 704 (1995) 247.
[5] G. Guiochon, A.M. Katti and M. Sarker, in press.
[6] M. Sarker and G. Guiochon, LC·GC, 12 (1994) 300–306.
[7] M. Sarker and G. Guiochon, J. Chromatogr. A, 683 (1994) 293–309.
[8] M. Sarker and G. Guiochon, J. Chromatogr., 702 (1995) 27.
[9] J.J. van Deemter, F.J. Zuiderweg and A. Klinkenberg, Chem. Eng. Sci., 5 (1956) 271.
[10] C.R. Wilke and P. Chang, AIChE J., 1 (1955) 264.
[11] M. Martin, F. Verillon, C. Eon and G. Guiochon, J. Chromatogr., 125 (1976) 17.

ELSEVIER

Journal of Chromatography A, 709 (1995) 241–247

JOURNAL OF CHROMATOGRAPHY A

Purification of plant polyamines with anion-exchange column clean-up prior to high-performance liquid chromatographic analysis

J. Bernhard Wehr[1]

Department of Horticultural Sciences, University of Stellenbosch, Stellenbosch 7600, South Africa

First received 10 November 1994; revised manuscript received 11 April 1995; accepted 11 April 1995

Abstract

Plant material contains carbohydrates and phenolic compounds that interfere with derivatization and HPLC analysis of polyamines. The use of strong anion-exchange resins was investigated for purification of polyamines in plant samples. Results obtained indicate that anion-exchange resins produce equally good results as cation-exchange resins. Polyamines are eluted from the anion-exchange resin with NaOH, and derivatization can be performed directly on the eluate, resulting in enormous time savings. Optimum results were achieved with low cross-linkage strong anion-exchange resins and the conditions for maximum recoveries of polyamines are reported.

1. Introduction

Since polyamines are involved in numerous metabolic processes in plants [1], they have to be quantified accurately. For HPLC analysis, pre-column derivatization is commonly used [2–7], being easy and relatively quick to perform. Post- and on-column derivatization was also described [8,9]. Since derivatization reagents do not only react with amines but also with plant constituents such as phenolic compounds, organic acids, and carbohydrates, interferences can arise. To avoid these problems, a sample clean-up is necessary. Sample clean-up for polyamines is normally performed with cation-exchange resins [3,10,11] and polyamines are eluted with hydrochloric acid. Before derivatization, HCl has to be removed because most derivatization reagents are acid-chlorides, being inhibited by chloride ions. In addition, these reagents only react with polyamines in alkaline medium. The evaporation of HCl in vacuum is a time-consuming and hazardous step since HCl vapor is highly corrosive. Therefore, the use of anion-exchange resins was investigated as an alternative to cation-exchange resins for sample clean-up. Although anion-exchange clean-up has been explored previously [11], the authors did not elaborate on the resins and procedures employed. In this paper, several anion-exchange resins were tested for their efficacy in removing substances interfering with HPLC analysis. In addition, the parameters affecting the recovery of polyamines from anion-exchange resins are described. The developed

[1] Present address: Department of Agriculture, The University of Queensland, Brisbane, Qld. 4072, Australia.

0021-9673/95/$09.50
SSDI 0021-9673(95)00461-0

procedure was applied to several plant samples to test the applicability of the clean-up procedure and to compare it to cation-exchange clean-up.

2. Experimental

Polyamine standards (putrescine, spermidine, spermine, and diaminooctane) were purchased from Sigma. Various anion-exchange resins were tested for their efficacy in removing interfering substances and for recoveries of polyamines. Type I resins (trialkyl functionality): Bio-Rad AG1-X4 (200–400 mesh), Duolite A101, Duolite A101D, Duolite A113, Amberlite IRA-402, Amberlite IRN-78, and Dowex 1-X8. Type II resins (alkylol-dialkyl functionality): Duolite A102 and Duolite A116. All resins, apart from Bio-Rad AG1-X4, were of technical grade with a 14–50 mesh and were milled to correspond to a 100–200 mesh. Before use, the resins were converted to the OH^- form with 1 *M* NaOH and washed with deionized water to remove excess NaOH.

Plant material was homogenized in 5% (v/v) cold perchloric acid (100 mg fresh mass per ml PCA), extracted for 1 h on ice, and centrifuged at 4200 *g* for 25 min at 10°C. An amount of 1 ml of the supernatant was neutralized with 0.2 ml of 5 *M* NaOH and 0.5 ml loaded onto Poly-Prep columns (Bio-Rad) containing ca. 1.2 ml anion-exchange resin in the OH^- form. Polyamines were eluted with 3.5 ml of a 0.01 *M* NaOH solution. The eluate was collected in vials and mixed with 0.2 ml of 5 *M* NaOH to ensure sufficient alkalinity for derivatization. Polyamines were benzoylated for HPLC analysis according to Refs. [12,13]. NaCl solution was omitted after incubation. Polyamines were separated by HPLC on a Spherisorb ODS2 reverse-phase C_{18} column (250 × 4.6 mm, 10 μm) at 35°C, equipped with a Waters Resolve C_{18} Guard-Pak precolumn, and detected at 245 nm [3]. Separation was achieved isocratically at 1.7 ml min^{-1} with 44% solvent A (water) and 56% solvent B (4% tetrahydrofuran, 96% methanol, v/v).

3. Results and discussion

3.1. Elution profile of polyamines from the anion-exchange column

The elution profile of putrescine, spermidine, and spermine from the Bio-Rad AG1-X4 resin is shown in Fig. 1. A similar elution profile is also obtained with higher and lower molarities of the eluent and with the Duolite A101D resin (data not shown). The results indicate that the first 0.5 ml of the effluent does not contain polyamines (the void volume of the column is ca. 0.3 ml). Thereafter, polyamines elute from the column and elution nears completion after 4.5 ml total volume (1 ml sample volume plus 3.5 ml eluent) have been applied to the column. Benzoylation can be carried out directly on the eluate since a reaction volume of up to 5 ml does not affect the derivatization of individual polyamines (ANOVA, $p > 0.05$, $n = 3$). Hence it is not necessary to concentrate the eluate, resulting in considerable time savings.

3.2. Effect of sample pH and flow-rate on polyamine recovery

Experimental results indicate that if 0.12 ml of 5 *M* NaOH are added to 1 ml of plant extract before loading, the sample pH is neutral and the

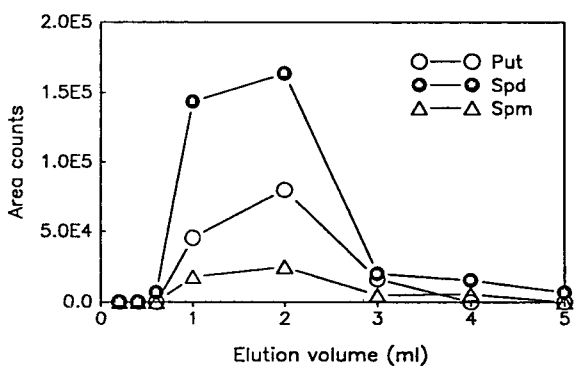

Fig. 1. Elution pattern of putrescine (○), spermidine (●), and spermine (△) from the Bio-Rad AG1-X4 resin in relation to the volume of eluent (1 *M* NaOH) applied. Elution was performed with gravity flow (1 ml min^{-1}).

recoveries of polyamines are unsatisfactory. Using 0.15–0.2 ml of a 5 *M* NaOH solution, the sample pH is alkaline and the recoveries of polyamines are higher (Table 1). Therefore, to achieve maximum recovery of polyamines, 0.15–0.2 ml 5 *M* NaOH should be used to alkalinize the sample extract before loading onto the resin column. An eluent flow-rate of 0.5–2 ml min^{-1} yields constant recoveries of polyamines. Lower recoveries were only observed at a flow-rate of 0.25 ml min^{-1} for spermine (70%), diaminooctane (64%), and spermine (50%), whereas the recovery of putrescine is independent of the flow-rate. Using gravity flow, the flow-rates are normally between 0.75–1.5 ml min^{-1}, which yields constant recoveries for all polyamines. The decreased recovery at low flow-rates is probably due to diffusion and trapping of spermidine, diaminooctane, and spermine in the three-dimensional network of the resin. Also, non-specific retention of polyamines by the anion-exchange column can occur. Thus, to ensure adequate flow, the column should not be packed too tightly.

Table 1
Effect of sample pH on recovery of polyamines from the resin

pH of sample	Area counts ($\times 10^{-6}$)		
	Putrescine	Spermidine	Spermine
pH 6–7	0.39 ± 0.07	1.34 ± 0.30	0.16[a]
pH 13–14	0.57 ± 0.04	1.93 ± 0.01	0.30 ± 0.01

Plum buds were homogenized and 1-ml aliquots of the supernatant were mixed with either 0.12 ml 5 *M* NaOH (corresponding to pH 6–7) or 0.15 ml 5 *M* NaOH (pH 13–14). An amount of 1 ml of the resulting solutions was loaded onto A101D columns. Results are means of three replicates ± standard deviation.

[a] Based on a single determination only due to co-elution of spermine with impurities in the extract.

3.3. Recovery of polyamine standards from various resins

Different anion-exchange resins were tested for the recovery of polyamine standards. Elution was performed with various molarities of NaOH solutions: 2 *M* (pH 14.3), 1 *M* (pH 14), 0.1 *M* (pH 13), 0.01 *M* (pH 12), and with water adjusted to pH 8 with NaOH. Type II resins (Duolite A116, Fig. 2g; Duolite A102, Fig. 2h) had lower recoveries, ranging from 20% for spermine to 70% for putrescine. Thus, type II resins cannot be recommended for clean-up as recoveries of polyamines are unacceptably low, probably due to hydrogen-bridge bonds between the amino groups of polyamines and the alkylol group of the resin. Type I resins had higher recoveries, of up to 100% for putrescine (Figs. 2a–d), especially at lower pH (pH 8, pH 12). The Bio-Rad AG1-X4 (Fig. 2e) resin has a poor performance in comparison to many cheaper resins. Polyamine recovery from the macroporous resin (Duolite A101D, Fig. 2b) is superior to that from the standard type of resin (Duolite A101, Fig. 2f). The high recovery of polyamines from type I resins, especially with weakly alkaline eluents, is possibly due to the fact that the amino groups of the polyamines (pK_a ca. 11) are protonated and therefore repelled by the positively charged functional groups of the resin. Hence, it is suggested that the eluent be adjusted to pH 8–12 for maximum recovery and low cross-linkage or macroporous resins be used. If the eluent is weakly alkaline (e.g. pH 8 or 12), the eluate should be mixed with an additional 0.2 ml of 5 *M* NaOH. This ensures sufficient alkalinity for the derivatization reaction to proceed optimally. If the molarity of the reaction mixture is below 1 *M* NaOH, irreproducible results are obtained (data not shown).

3.4. Polyamine concentrations in plant material

Plant material was subjected to purification with Duolite A101D resin as described or benzoylated directly. Values have been corrected for recoveries of polyamines from the resin (putrescine 89%, spermine 89%, diaminooctane 80%, and spermine 95%) and calculated according to Ref. [14]. Alternatively, polyamines were quantified against external standards, corrected for

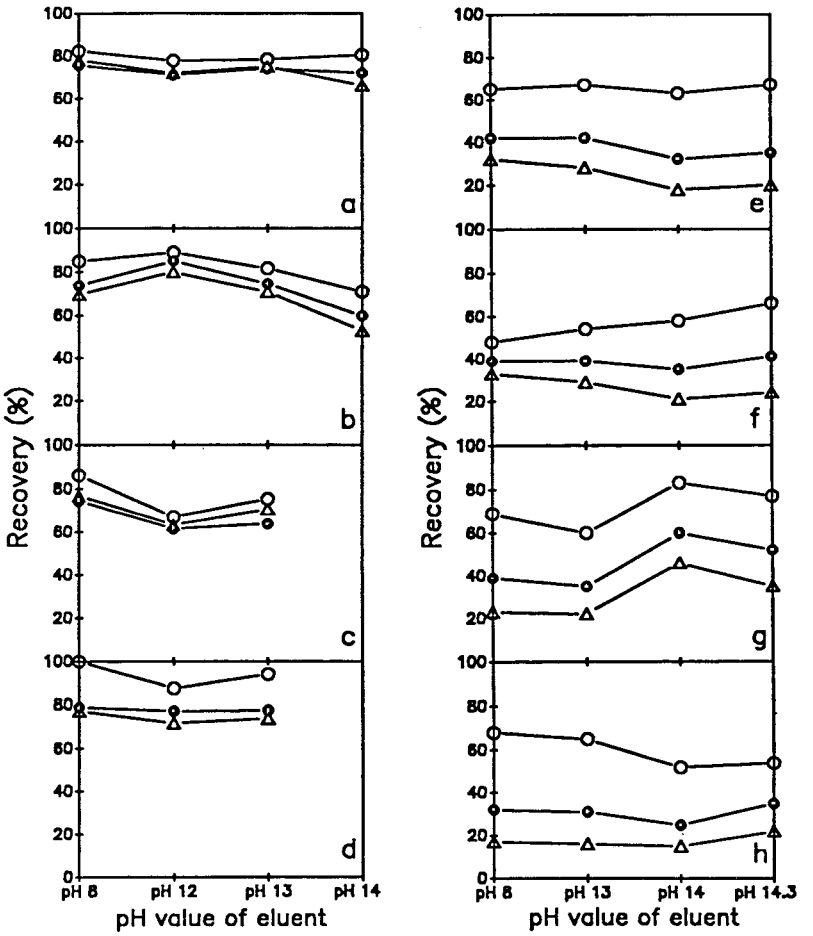

Fig. 2. Recovery of putrescine (○), spermidine (●), and spermine (△) standards from various anion-exchange resins in relation to the pH of the eluent. (a) Duolite A113, (b) Duolite A101D, (c) Amberlite IRN 78, (d) Amberlite IRA 402, (e) Bio-Rad AG1-X4, (f) Duolite A101, (g) Duolite A116, and (h) Duolite A102. Each data point is the average of 2–5 determinations.

recoveries and normalized with the internal standard. Results given in Table 2 indicate that polyamine concentrations can be lower if samples are not purified, and in the case of citrus shoot tips, no peak corresponding to spermine is detected. The recovery of the internal standard (diaminooctane) added to various plant materials ranged between 75–100% (data not shown). It was stated [3] that the benzoylation of polyamines is inhibited by some compounds present in crude plant extracts leading to underestimations of polyamine levels. The authors determined that only 3% of the free polyamines are recovered as benzoylated polyamines if no clean-up is done. However, other researchers, using different plant materials, determined recoveries of 70–95% even without a clean-up [15–17]. To resolve this discrepancy, plum shoot tip homogenates were also spiked with known amounts of authentic polyamines and the recoveries evaluated. The recoveries were 88% for putrescine, 82% for spermidine, and 67% for spermine for column-purified samples and 108% for putrescine, 90% for spermidine, and 69% for spermine in control samples. Since the recoveries are similar, it can be assumed that substances inhib-

Table 2
Polyamine contents in plant material

		Putrescine[a]	Spermidine[a]	Spermine[a]
Pear shoot tips				
A	Control	31 ± 4	78 ± 7	22 ± 9
	Column	38 ± 2	95 ± 8	19 ± 7
B	Control	21 ± 4	73 ± 7	21 ± 8
	Column	26 ± 2	88 ± 9	18 ± 8
Citrus shoot tips				
A	Control	33 ± 3	38 ± 2	0
	Column	44 ± 2	43 ± 7	4 ± 0
B	Control	37 ± 4	42 ± 4	0
	Column	47 ± 5	47 ± 10	5 ± 0
Apple shoot tips				
A	Control	Not calculated because of co-elution of impurities with DOC		
	Column	116 ± 0	484 ± 21	39 ± 5
B	Control	115 ± 3	476 ± 42	45 ± 7
	Column	119 ± 4	498 ± 38	39 ± 6
Plum shoot tips				
A	Control	103 ± 6	379 ± 17	90 ± 11
	Column	107 ± 4	434 ± 16	102 ± 20
B	Control	100 ± 1	373 ± 36	87 ± 15
	Column	101 ± 3	425 ± 42	99 ± 25

Plant extract was either purified with A101D resin (column) or benzoylated directly (control). Results are means ± standard deviation ($n = 3$). Quantification was performed with either DOC (diaminooctane) as internal standard (A) or against external standards (B).
[a] In nmol g^{-1} fresh mass.

iting the derivatization are apparently not present in plum shoot tips. However, mature Citrus leaves may contain inhibiting factors since measured concentrations are lower for unpurified material. More importantly, no spermine could be detected without a sample clean-up, highlighting the necessity of the sample clean-up to obtain meaningful results.

3.5. Qualitative results

In Fig. 3a, a chromatogram of polyamines in plum shoot tips is shown. No clean-up was done and a number of interfering peaks are present that impair quantification of polyamines due to co-elution. By comparison, Fig. 3b shows a HPLC chromatogram of the identical sample purified on Duolite A101D resin and eluted with water adjusted to pH 8.

In Fig. 4a, plum leaf extract was purified with a cation-exchange resin (Dowex 50W-X8) and the polyamines eluted according to Ref. [3]. By contrast, Fig. 4b shows a HPLC chromatogram of the identical sample which was purified on a Duolite A101D resin. The chromatograms in Figs. 3 and 4 show that the clean-up is effective in removing substances that give rise to interfering peaks on HPLC and also that the degree of purification with the anion-exchange column clean-up is similar to cation-exchange clean-up. The purity of the sample is better if the eluent is more alkaline (pH 13 or 14, data not shown). However, since recoveries are lower, it should be determined to what extent the sample needs to be purified to obtain an optimum balance between purity and recovery. Samples being low in interfering substances can be eluted with water adjusted to pH 8 to 12, whereas samples

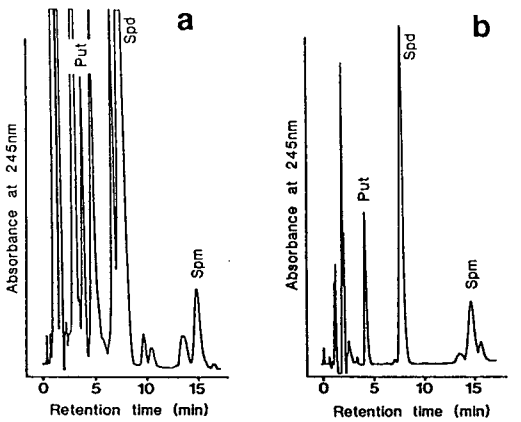

Fig. 3. (a) HPLC-chromatogram of benzoylated polyamines in plum shoot tips. No clean-up was done and a number of interfering peaks are present. The concentrations of the polyamine peaks are: putrescine = 1.4 nmol, spermidine = 3.4 nmol, and spermine = 0.5 nmol. (b) HPLC-chromatogram of plum shoot extract purified with Duolite A101D resin. Polyamines were eluted with water adjusted to pH 8. Concentration of polyamines: putrescine = 0.7 nmol, spermine = 1.7 nmol, and spermidine = 0.3 nmol.

having numerous interfering peaks require a higher molarity NaOH (0.1 or 1 *M*) to obtain samples of suitable purity.

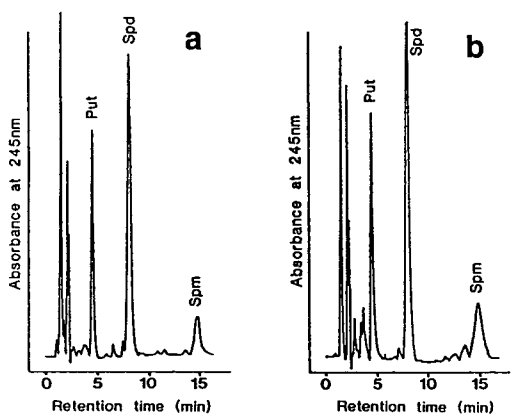

Fig. 4. (a) HPLC-chromatogram of plum leaf extract purified with Dowex 50W-X8 cation-exchange resin. The polyamines were eluted according to Ref. [3]. Concentration of polyamines: putrescine = 0.9 nmol, spermidine = 1.6 nmol, and spermine = 0.2 nmol. (b) HPLC-chromatogram of the identical sample which was purified on a Duolite A101D resin. Concentration of polyamines: putrescine = 1.2 nmol, spermidine = 1.8 nmol, and spermine = 0.4 nmol.

4. Conclusion

Using anion-exchange column clean-up, plant extracts can be successfully purified prior to HPLC analysis. Polyamines can be eluted from the anion-exchange resin without the need to concentrate the eluate, resulting in tremendous time savings. Therefore, the use of anion-exchange resins is a better option and many more samples can be processed per day. In comparison to cation-exchange clean-up, the recoveries of polyamines are similar and the quality of purification is comparable if not superior. The original procedure of Ref. [13] was developed mainly on herbaceous plants that have few interfering substances, unlike woody perennials. However, with the method outlined, it is possible to effectively remove these substances. Furthermore, if the anion-exchange resin is used in the OH^- form, no complicating anions are present in the eluate, allowing for simple and rapid derivatization by benzoylation. Phenolic substances, organic acids and carbohydrates [18–21] are optimally retained on anion-exchange resins in alkaline medium. Since polyamines do not carry a net charge in alkaline medium, they are unretained and elute in the void fraction. It should also be determined beforehand whether a sample clean-up is necessary, as an increase in experimental error is normally observed [16] due to the additional experimental variables included.

Acknowledgements

Anatech (Cape Town) and NCP (Germiston) are greatly acknowledged for kindly supplying samples of various anion-exchange resins. Thanks are due to E. Rabe, M. Huysamer, and P. Swart for editorial advice.

References

[1] P.T. Evans and R.L. Malmberg, Annu. Rev. Plant Physiol. Plant Mol. Biol., 40 (1989) 235.
[2] T. Bartok, G. Borcsok and F. Sagi, J. Liq. Chromatogr., 15 (1992) 777.

[3] J.L. Corbin, B.H. Marsh and G.A. Peters, Plant Physiol., 90 (1989) 434.
[4] M.A. Cichy, D.L. Stegmeier, H. Veening and H.-D. Becker, J. Chromatogr., 613 (1993) 15.
[5] J.-K. Lin and C.-C. Lai, J. Chromatogr., 227 (1982) 369.
[6] N.P.J. Price, J.L. Firmin and D.O. Gray, J. Chromatogr., 598 (1992) 51.
[7] B.P. Spragg and A.D. Hutchings, J. Chromatogr., 258 (1983) 289.
[8] H. Ohta, Y. Takeda, K.-I. Yoza and Y. Nogata, J. Chromatogr., 628 (1993) 369.
[9] K. Saito, M. Horie., N. Nose, K. Nakagomi and H. Nakazawa, Anal. Sci., 8 (1992) 675.
[10] H. Inoue and A. Mizutani, Anal. Biochem., 56 (1973) 408.
[11] V.R. Villanueva, R.C. Adlakha and A.M. Cantera-Soler, Phytochemistry, 17 (1978) 1245.
[12] M.Z. Hauschild, J. Chromatogr., 630 (1993) 397.
[13] H.E. Flores and A.W. Galston, Plant Physiol., 69 (1982) 701.
[14] J. Asshauer and H. Ullner, in H. Engelhardt (Editor), Practice of High Performance Liquid Chromatography, Springer Verlag, Berlin, 1986, p. 73.
[15] J.M. diTomaso, J.J. Hart and L.V. Kochian, Plant Physiol., 98 (1992) 611.
[16] D.R. Roberts, M.A. Walker and E.B. Dumbroff, Phytochemistry, 24 (1985) 1089.
[17] T.A. Smith and G.R. Best, Phytochemistry, 16 (1977) 841.
[18] B. Marescau, P. De Deyn, L. van Gorp and A. Lowenthal, J. Chromatogr., 377 (1986) 334.
[19] R.D. Rocklin and C.A. Pohl, J. Liq. Chromatogr., 6 (1983) 1577.
[20] O. Samuelson, Ion Exchangers in Analytical Chemistry, John Wiley and Sons, New York, 1953.
[21] Duolite Ion Exchange Manual, Western Division, Diamond Alkali Company, Redwood City, 1960.

ELSEVIER

Journal of Chromatography A, 709 (1995) 249–256

JOURNAL OF CHROMATOGRAPHY A

Development of an analytical reversed-phase high-performance liquid chromatography assay for transforming growth factor β3

William J. Lambert*, Geoffrey F. Stamper

Pharmaceutical Research and Development, Pfizer Central Research, Eastern Point Road, Groton, CT 06340, USA

First received 24 March 1995; revised manuscript received 10 April 1995; accepted 10 April 1995

Abstract

Transforming growth factor β3 (TGF-β3) is a dimeric protein (M_r 25 444) which regulates the proliferation of epithelial cells. A reversed-phase high-performance liquid chromatography (RP-HPLC) method was developed for TGF-β3 in order to investigate the solution stability of TGF-β3. Peak width and retention time were evaluated as a function of (1) the initial percent of acetonitrile, (2) the gradient slope, (3) the percentage of trifluoracetic acid, and (4) column temperature. By varying the above conditions, particularly temperature, it was possible to reduce retention times and peak widths by a factor of 2 and 6, respectively. The observed temperature effects on peak width were consistent with the concept that conformational changes can be induced in the protein during the chromatographic migration. A balance was found between on-column degradation and improved peak width at elevated temperatures. The final assay was found to be linear over a 10–150 μg/ml drug range with a correlation coefficient of 0.998 and acceptable reproducibility (R.S.D. 2.09%, $n = 6$). The assay has been useful for monitoring drug loss in ongoing stability studies; however, it was found to have poor resolving power when certain stressed samples of TGF-β3 were applied, suggesting that complimentary assay methodologies must be developed.

1. Introduction

Transforming growth factors β (TGF-β) are a family of structurally related dimeric proteins which exhibit a wide variety of biological actions, and in particular regulate the proliferation of epithelial cells [1]. They are unique in that each monomer contains nine strictly conserved cysteines, one of which stabilizes the dimer via an interchain disulfide bond [2,3]. The monomers, each with a molecular mass of approximately 12 500, are stabilized by two identical hydrophobic surfaces [3].

The objective of the present study was to develop an analytical reversed-phase high-performance liquid chromatography (RP-HPLC) assay for TGF-β3 which can be used to investigate the solution stability of the protein. The literature suggests that a number of variables can affect chromatographic performance for RP-HPLC of proteins [4,5]. Unlike small molecules, proteins have the added challenge that altered conformation can impart on retention. The change in conformation may occur due to interaction with the hydrophobic stationary phase, the column temperature, or the mobile phase components [5]. If more than one conformation exists during the separation, broader bands are expected relative to conditions where only on conformer exists. Thus, one strategy to improv-

* Corresponding author.

0021-9673/95/$09.50
SSDI 0021-9673(95)00452-1

ing chromatographic performance is to purposefully induce denaturation of the protein [5].

Most RP-HPLC assays for proteins utilize an acetonitrile (ACN) gradient with trifluoracetic acid (TFA) to reduce the pH and silanol ionization [4]. In addition to modifying the pH, the TFA may also act as a hydrophobic ion-pairing agent and as a denaturant [4,5]. The choice of the initial organic concentration can impact on total assay time since at low organic concentrations proteins generally remain adsorbed on the stationary phase until the appropriate concentration of organic is reached [6,7]. This results in an extremely steep negative slope when the logarithm of capacity factor is plotted versus the percent organic [8]. It has been shown that increasing the gradient rate can dramatically decrease peak width, and may lead to improved recovery [4,5]. Increasing flow-rate can improve resolution for some peptides; however, this may also lead to a significant loss in sensitivity [4]. Thus, no attempt was made to vary flow-rate as part of the present study. Effects of column temperature on protein chromatography have been proposed due to increased solubility in the mobile phase, more rapid transfer between the stationary and mobile phases, and on-column conformational changes [5,9–11]. Improvements in band width with increasing temperatures have been noted for some proteins and peptides [5,9,12]; however, this is apparently not generally true [13,14]. Temperature can also be utilized to vary selectivity [13].

Based on the above literature observations, our approach for TGF-β3 was to evaluate the effect of altering (1) the initial percent of ACN, (2) the gradient slope, (3) the percentage of TFA, and (4) column temperature in order to optimize overall chromatographic performance, and peak width in particular.

2. Experimental

Samples (at 5°C) containing 120 μg/ml of TGF-β3 were injected using a BIO-RAD Model AS-100 HRLC automatic sampling system with a 20-μl loop. The gradient for the assay was provided by the ConstaMetric 4100 solvent delivery system by LDC Analytical operated at 1 ml/min. A Vydac C_4 column (250 × 4.6 mm I.D.) and guard column were kept at a constant 45°C (except during temperature studies) using a BIO-RAD column heater. Samples were detected at 210 nm using the BIO-Dimension UV–Vis monitor. Integration was performed using the BIO-RAD HRLC system interface and the BIO-RAD Series 800 HRLC system. The acetonitrile (ACN, Fisher Scientific) and the trifluoracetic acid (TFA, J.T. Baker) were both HPLC grade. Milli-Q water was utilized for all studies. TGF-β3 (lot PO1 1409) was used as provided by Ciba Geigy.

Sodium dodecyl sulfate polyacrylamide gel electrophoresis (SDS-PAGE) was performed under non-reducing conditions using a Pharmacia Phast System (Pharmacia technique number 110). Pharmacia 8–25 gradient gels were utilized, and staining was performed with Coomassie Blue (Pharmacia technique number 200).

3. Results and discussion

An RP-HPLC assay using a C_{18} stationary phase, 0.1% TFA, and an acetonitrile gradient has previously been reported by Ogawa et al. [15] for TGF-β2.3, a heterodimer of the TGF-β2 and TGF-β3 monomers. These authors observed a peak width at half-height of approximately 1 min for this protein, which eluted at approximately 17 min with a linear acetonitrile gradient and 0.1% TFA. Preliminary attempts to assay TGF-β3 under similar conditions in our lab led to peaks with this breadth or even wider. Thus, we attempted to analyze those variables which could lead to improvements in the peak width, and thereby improve resolution from potential degradation products.

The effects of altering the initial percent organic modifier are shown in Table 1. As expected, shorter retention times were found with increased initial ACN concentrations. However, there was little or no change in peak width at half-height. Increasing TFA concentrations

Table 1
Observed changes in retention

Initial ACN conc. (%)	TFA (%)	ACN/min (%)	Temp. (°C)	Retention time (min)	Width at $\frac{1}{2}h$ (min)
35	0.1	1.0	30	10.87	1.41
32	0.1	1.0	30	12.95	1.29
30	0.1	1.0	30	15.72	1.14
27	0.1	1.0	30	18.15	1.19
25	0.1	1.0	30	20.02	1.22
27	**0.2**	1.0	30	17.82	1.19
27	**0.4**	1.0	30	20.20	0.99
27	0.1	**2.0**	30	11.56	0.60
27	0.1	**1.5**	30	12.91	0.88
27	0.1	**1.0**	30	15.37	1.26
27	0.1	**0.5**	30	22.13	3.32
27	0.1	1.0	**30**	15.81	1.17
27	0.1	1.0	**35**	16.08	0.93
27	0.1	1.0	**40**	16.12	0.70
27	0.1	1.0	**45**	15.83	0.47
27	0.1	1.0	**50**	15.93	0.23
27	0.1	1.0	**55**	15.84	0.23
27	0.1	1.0	**60**	15.75	0.23
27	0.1	1.0	**65**	15.94	0.23

Values in bold face indicate the changed values.

altered peak width to a small degree only, and complicated detection due to increased background. By increasing the gradient slope, it was found that peak width could be reduced; however, the peaks appeared to be somewhat asymmetric. Significant improvements were made in the peak shape by increasing temperature (Fig. 1). With a 20 min gradient time and a 27–47% acetonitrile linear gradient, the peak width decreased from 1.17 to 0.23 min on going from 30 to 50°C, respectively. No additional improvement was seen at 55 to 65°C.

The retention of proteins in reversed-phase chromatography is complicated by conformational changes that can occur on the column [16,17]. Hearn and co-workers [9] suggest that at a constant gradient time, significant changes in peak width are typically observed over a discrete temperature range. They attribute the temperature effects to alterations in the conformation of the protein in both the mobile and stationary phases. Our observation of a five-fold decrease in peak width over a 20°C range (30–50°C) is consistent with this hypothesis. No improvement in peak width was observed above 50°C, suggesting that conformational changes were no longer being induced.

One concern with the elevated temperatures is that degradation might occur on the column. In fact, at 50°C small shoulders were observed after the main peak which were not observed at lower temperatures (see Fig. 2). Were these due to improved resolution or to degradation? The areas of the peaks were analyzed to determine if their size increased with increasing temperature. The peak areas of the two late-eluting peaks do increase with temperature, and thus, may represent degradation of TGF-β3 on the column (Fig. 3). These data suggest that on-column degradation should be minimal if a temperature of 45°C or less is utilized. To study this further, a short-term stability study of 0.1 mg/ml drug in mobile phase under approximate elution conditions was conducted. Elution was calculated to

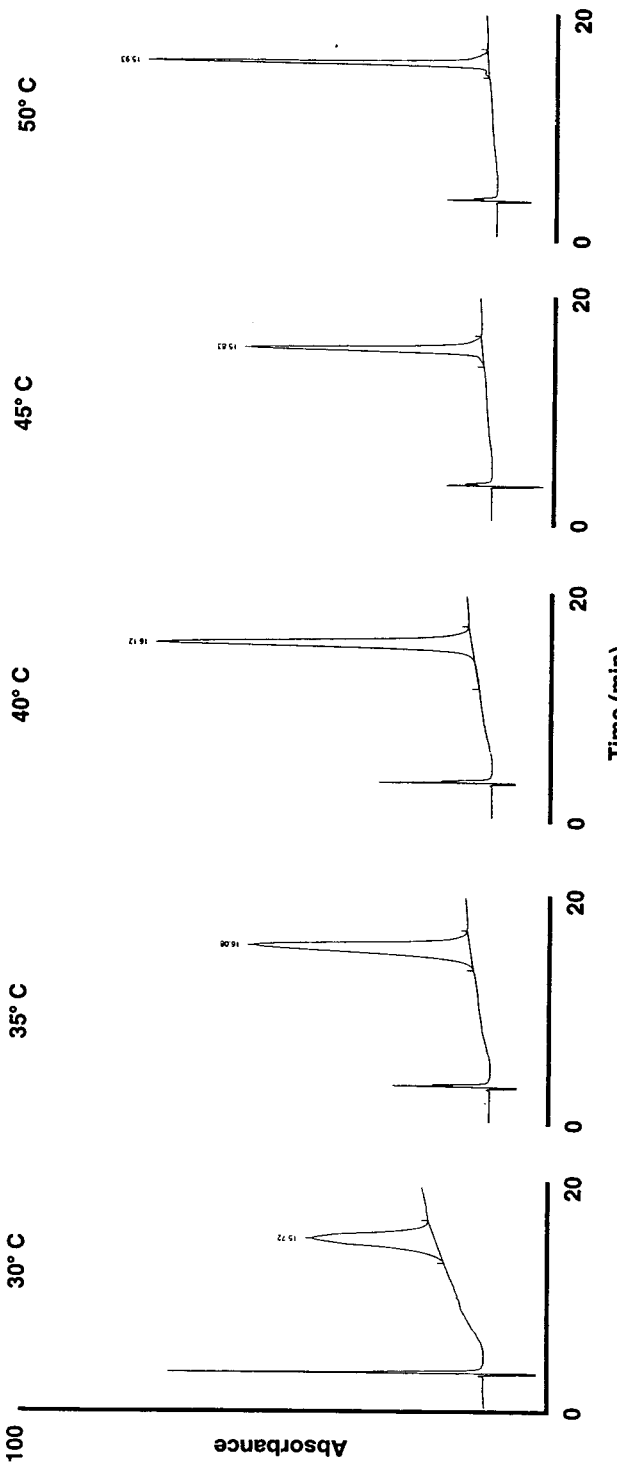

Fig. 1. Chromatograms of TGF-β3 as a function of column temperature. A gradient slope of 1% acetonitrile per min was utilized (27% initial). The detector range was two-fold higher for the 45 and 50°C conditions than for the lower-temperature conditions.

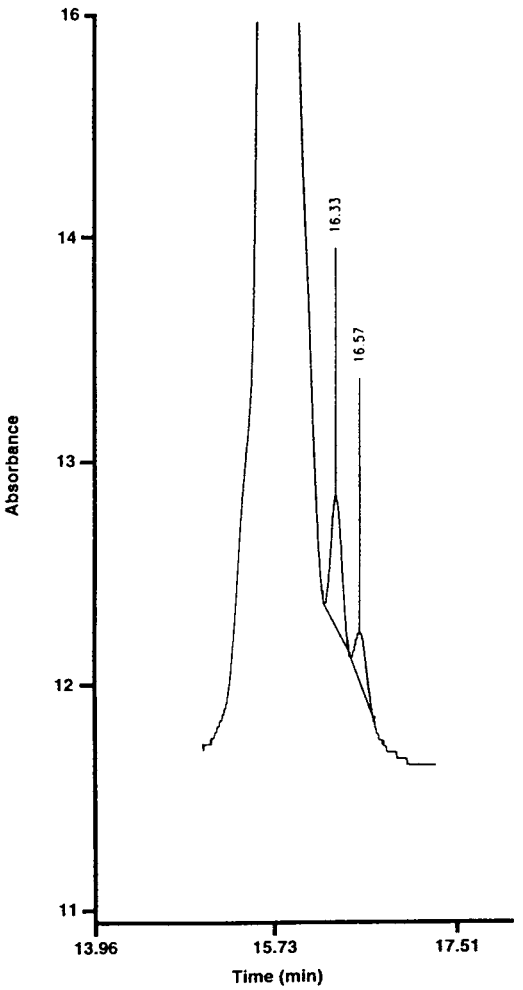

Fig. 2. Chromatogram produced at 65°C column temperature showing late-eluting shoulders which are present on TGF-β3 peak.

occur at approximately 41% acetonitrile. Thus, TGF-β3 was stored in a solution of ACN–H_2O (41:59, v/v) with 0.1% TFA at 45°C for 90 min. No increase in the area of the late-eluting shoulders was observed for up to 90 min at 45°C, which is consistent with the lack of degradation of the drug on the column. Based on the results of both studies, it appears that a 45°C column temperature achieves a balance of on-column stability and chromatographic performance. It is interesting to note that the two shoulder peaks are relatively sharp bands, suggesting that degradation occurred while the TGF-β3 was adsorbed to the stationary phase. Had the degradation occurred in the mobile phase while elution was occurring, the bands would presumably have been broader. Thus, it is possible that degradation could be minimized further by starting the separation at a higher percentage of acetonitrile.

Based on the above analysis, subsequent studies were performed using a RP-HPLC assay which utilized an initial acetonitrile level of 27%, a gradient of 1%/min for 33 min, 0.1% TFA, and a column temperature of 45°C. The other chromatographic conditions are given in the experimental section. A reproducibility study was conducted using 100 μg/ml standards prepared in 20 m*M* acetic acid buffer, 20 m*M* acetic acid in 25% acetonitrile, and 20 m*M* acetic acid in 25% isopropanol. Each sample was injected six times and the peak areas were recorded. The relative standard deviations were 7.57%, 0.75%, and 2.09%, respectively. A trend was observed in the peak areas for the aqueous standards, with peak areas increasing from the first injection to the last by 18.6%. This trend is significant and is characteristic of protein adsorption to the system. The addition of an organic solvent would appear to hinder adsorption. The linearity of the assay was investigated over the 10–150 μg/ml drug range for samples diluted with either 20 m*M* acetic acid in 25% acetonitrile or 20 m*M* acetic acid in 25% isopropanol. The standard curves for these solutions are given in Fig. 4. The correlation coefficients were 0.999 and 0.998, respectively. As a final assessment, the assay was utilized to analyze a 100 μg/ml solution of TGF-β3 in 25% isopropanol and 20 m*M* acetic acid which had been stressed under a number of conditions. These conditions included pH 12.0 (NaOH) and 25°C for 28 h, treatment with a 1000:1 molar ratio of hydrogen peroxide/protein for 6 h at 5°C, heat treatment at 95°C for 2 h, pH 2.0 (HCl) and 25°C for 28 h, and fluorescence light (intensity 6200 lm, 35°C) for 28 h. The RP-HPLC results indicate no significant drug loss for the low-pH and the light-box samples (<4% loss of potency; chromatogram not shown). However, the high-pH, peroxide, and heat-treated samples did show significant degra-

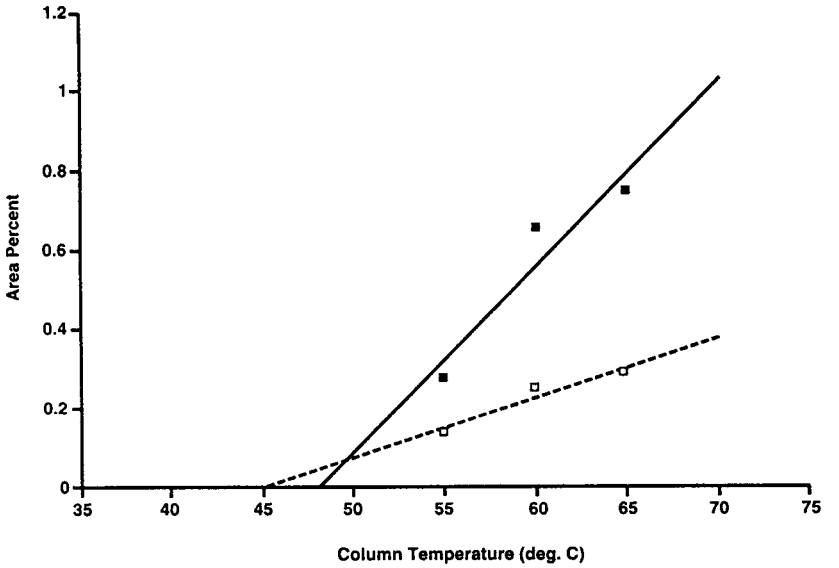

Fig. 3. Area percent of late-eluting shoulders shown in Fig. 2 as a function of column temperature. (■) Peak at 16.33 min; (□) peak at 16.57 min.

dation peaks. The chromatogram of the high-pH sample (Fig. 5) shows two broad peaks, the parent peak (conc. = 0.026 mg/ml) with a retention time of 15.12 min, and a late eluting peak with a relative retention time of 1.19 (the peak at 15.12 min was determined to be TGF-β3 by spiking the sample with additional drug). Sodium dodecyl sulfate polyacrylamide gel electrophoresis (SDS-PAGE) of this sample indicated that the late-eluting peak had a molecular

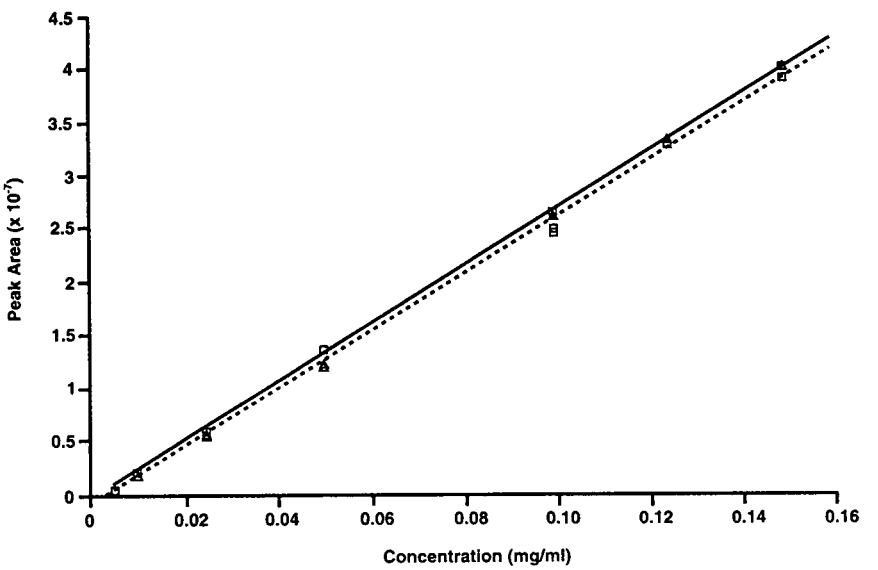

Fig. 4. Standard curves for the assay using two different sample matrices. (△) 25% Acetonitrile; (□) 25% isopropanol.

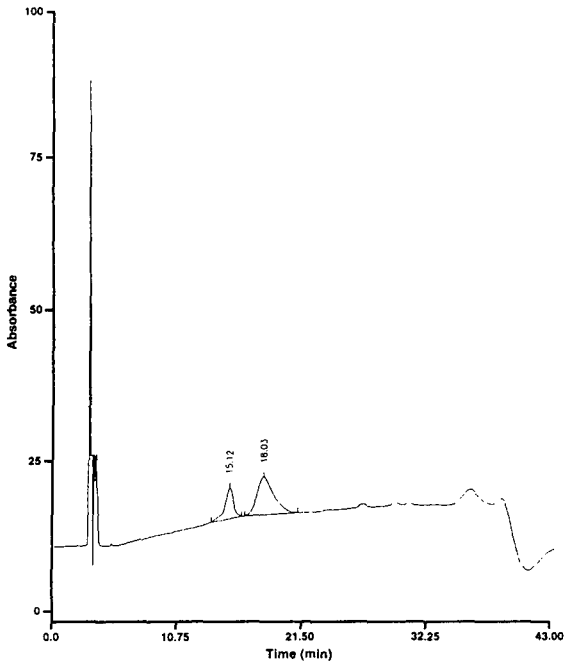

Fig. 5. Chromatogram of a TGF-β3 sample degraded at pH 12 (NaOH) and 25°C for 28 h.

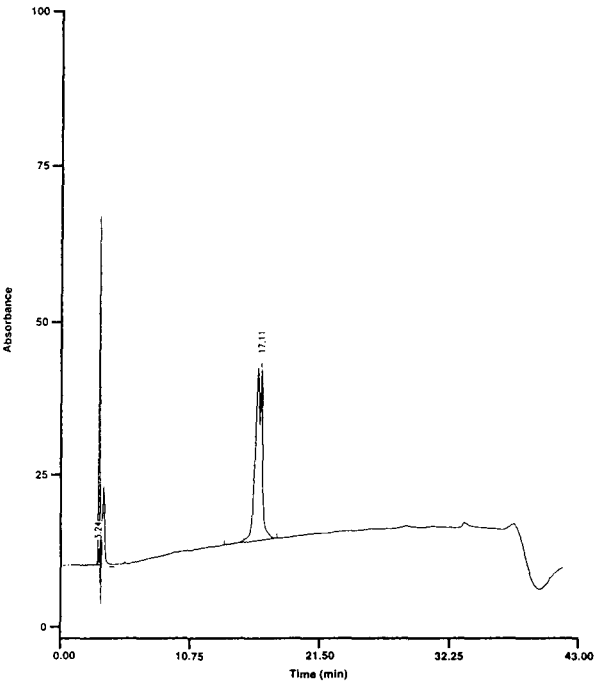

Fig. 6. Chromatogram of a TGF-β3 sample treated with excess hydrogen peroxide for 6 h at 5°C.

mass indicative of the monomer. The degradation product observed in the chromatogram for the peroxide-stressed sample (Fig. 6) has poor resolution from the TGF-β3 peak*. SDS-PAGE of this sample indicates no change in the molecular mass from that of TGF-β3, suggesting that the dimer is still present with some modification (presumably oxidation). Consistent with the temperature study performed during method development, a late-eluting shoulder was observed for the heat-treated sample (Fig. 7)[1]. The area percent of the late-eluting peak was 0.952%. As in the above stressed samples, the assay was unable to resolve this peak from the parent peak. In general, the assay does not provide baseline resolution of TGF-β3 from all potential degradation products. Thus, complimentary analytical techniques will need to be developed in order to assess all of the potential degradation pathways, as is done for most other therapeutic proteins [18].

A significant finding of this study was the fact that of all the variables studied, temperature was the most effective for yielding narrow peaks widths for TGF-β3. Although this large effect on band width might not be expected for all proteins, temperature should certainly be investigated as a method of optimizing chromatographic performance.

[1] At the time this chromatogram was obtained, the retention time for TGF-β3 had changed to just under 17 min. We believe this change occurred due to a partially clogged in-line filter, which led to a slightly reduced flow-rate (replacement of the filter returned retention times to under 16 min).

Acknowledgements

The authors gratefully thank Cheryl Kirkman and Lisa Shaner (both at Pfizer Analytical Research and Development), Lloyd Snyder (LC Resources, Orinda, CA, USA), and Milton Hearn (Monash University, Victoria, Australia) for their helpful discussions.

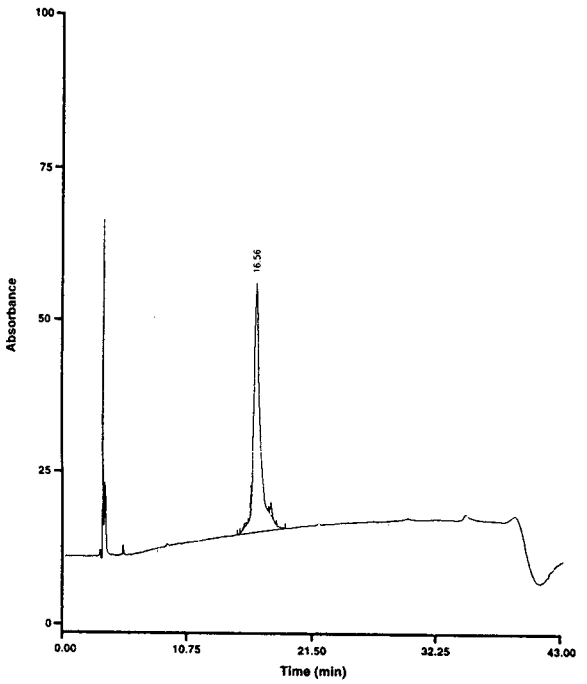

Fig. 7. Chromatogram of a TGF-β3 sample heated at 95°C for 2 h.

References

[1] J.A. Barnard, R.M. Lyons and H.L. Moses, Biochim. Biophys. Acta, 1032 (1990) 79.
[2] S. Daopin, K.A. Piez, Y. Ogawa and D.R. Davies, Science, 257 (1992) 369.
[3] M.P. Schlunegger and M.G. Grutter, Nature, 358 (1992) 430.
[4] R.S. Hodges and C.T. Mant, in C.T. Mant and R.S. Hodges (Editors), High-Performance Liquid Chromatography of Peptides and Proteins: Separation, Analysis, and Conformation, CRC Press, Boca Raton, FL, 1991, pp. 11–22.
[5] K.D. Nugent, W.G. Burton, T.K. Slattery, B.F. Johnson and L.R. Snyder, J. Chromatogr., 443 (1988) 381.
[6] X. Geng and F.E. Regnier, J. Chromatogr., 296 (1984) 15.
[7] C. Simpson, in F. Franks (Editor), Characterization of Proteins, Human Press, Clifton, NJ, 1988, pp. 285–337.
[8] C.T. Mant, T.W.L. Burke and R.S. Hodges, Chromatographia, 24 (1987) 565.
[9] A.W. Purcell, M.I. Aguilar and M.T. Hearn, Anal. Chem., 65 (1993) 3038.
[10] D. Guo, C.T. Mant, A.K. Taneja and R.S. Hodges, J. Chromatrogr., 359 (1986) 519.
[11] H. Lindner and W. Helliger, Chromatographia, 30 (1990) 518–522.
[12] S.A. Cohen, K. Benedek, Y. Tapuhi and B.L. Karger, Anal. Biochem., 144 (1985) 275.
[13] R.C. Chloupek, W.S. Hancock, B.A. Marchylo, J.J. Kirkland, B.E. Boyes and L.R. Snyder, J. Chromatrogr. A, 686 (1994) 45.
[14] L.R. Snyder and M.A. Stadalus, in Cs. Horvath (Editor), High-Performance Liquid Chromatography–Advances and Perspectives, Vol. 4, Academic Press, New York, 1986.
[15] Y. Ogawa, D.K. Schmidt, J.R. Dasch, R.J. Chang and C.B. Glasser, J. Biol. Chem., 267 (1992) 2325.
[16] K. Benedek and R. Rosenfeld, J. Chromatogr., 632 (1993) 29.
[17] P. Oroszian, W. Stanislav, G. Teshima, W. Shiaw-Lin, W. Hancock and B.L. Karger, Anal. Chem., 64 (1992) 1623.
[18] W.S. Hancock, LC·GC, 10 (1992) 96.

ELSEVIER

Journal of Chromatography A, 709 (1995) 257–264

JOURNAL OF CHROMATOGRAPHY A

Improved electrochemical detection of diuretics in high-performance liquid chromatographic analysis by postcolumn on-line photolysis

M. Macher, R. Wintersteiger*

Institute of Pharmaceutical Chemistry, Karl-Franzens-University Graz, Schubertstrasse 1, A-8010 Graz, Austria

Received 2 September 1994; revised manuscript received 5 April 1995; accepted 6 April 1995

Abstract

A sensitive, high-performance liquid chromatographic method including postcolumn on-line UV irradiation and electrochemical detection is described for the determination of pharmaceuticals with diuretic action. The investigations on this liquid chromatography–photolysis–coulometric detection approach indicate that, depending on the substituents of the compounds, oxidation of drugs containing an aromatic chloride and thiazide moiety occurs at potentials as low as +200 mV. Parameters influencing the electrochemical response are given to optimize the reaction conditions. The procedure presented allows the quantification of diuretics, and consequently of chemically related substances, with good reproducibility and high selectivity at the picogram level.

1. Introduction

UV–Vis detection is the technique most commonly used in determinations of pharmaceuticals. As its sensitivity and selectivity are very limited, better systems of detection are necessary in order to quantify low drug dosages. Fluorimetry, which meets these requirements, is usable only for a small group of drugs having native fluorescence. The same problem arises with electrochemical detection. To extend the advantages of this detection mode to a larger group of substances, electrochemical detection was combined with photolysis, because on-line photochemical derivatization or photochemical reaction detection has been found to be an extremely useful technique for converting electrochemically non-responding or poorly responding analytes into easily detectable derivatives [1–4]. In photochemical reaction detection, a photochemical reactor between the column and detector is included in the HPLC system, creating a series of differing derivatization processes [5–8].

Some studies [9–11] have shown that substances with an aromatic chloride are transformed by irradiation with UV light into electrochemically active derivatives. We investigated a group of drugs having this structure, hydrochlorothiazide, bendroflumethiazide, butizide, chlortalidone, furosemide and etacrynic acid. For a few of these diuretic substances, e.g. hydrochlorothiazide and furosemide, there are methods for quantitative analysis with UV [12–14] and electrochemical detection (ED) [15–17]. A disadvantage of these electrochemical methods is the high

* Corresponding author.

0021-9673/95/$09.50
SSDI 0021-9673(95)00440-8

working potential needed to produce electrochemical activity. The main thrust of our work was therefore to use photolysis to reduce the working potential and so to enhance selectivity and sensitivity. In addition, we also tested the influence of photolysis on UV absorption characteristics with a view towards possible improvement of detection limits.

2. Experimental

2.1. Drug standards and standard solutions

Hydrochlorothiazide and chlortalidone were obtained from Ciba-Geigy (Basle, Switzerland), bendroflumethiazide from Kwizda (Vienna, Austria), butizide from Boehringer (Mannheim, Germany), furosemide from Hoechst (Frankfurt, Germany) and etacrynic acid from Merck (Darmstadt, Germany). The substances were weighed with an analytical balance (Sartorius). A stock standard solution of each substance was prepared by dissolving the substance (hydrochlorothiazide 5.5 mg; bendroflumethiazide 5.5 mg; butizide 5.3 mg; chlortalidone 5.3 mg; furosemide 5.1 mg; etacrynic acid 5.1 mg) in doubly distilled methanol (Loba-Chemie, Linz, Austria) and diluted to 10 ml. A 1-ml volume of each solution was diluted to 50 ml with methanol–water (80:20). During our investigations on the influence of irradiation, the final concentration was about 60 ng in 6 μl. Only the working standard solutions of hydrochlorothiazide, bendroflumethiazide and butizide were further diluted 1:1 with methanol–water (80:20). Water for the mobile phase was purified with a Nanopur cartridge purification system (Barnstead, UK).

The HPLC mobile phase was prepared by mixing methanol and water (80:20) and adding 2 g/l of $LiClO_4$. The mobile phase was filtered through a 0.2-μm pore size membrane (Sartorius) and degassed with helium.

2.2. Instrumentation

The HPLC–photolysis–electrochemical system includes a Perkin-Elmer Model 250 binary LC pump and a Rheodyne Model 7125 loop injector with a 6-μl loop. The precolumn (5 × 4 mm I.D.) was packed with LiChrosorb RP-8 (Merck), 10 μm particles. The analytical column was a Brownlee Lab RP-18 (Bartelt, Graz, Austria), Spheri 5 μm, 100 × 4.6 mm I.D. The photochemical reactor was the Beam Roost Reaction Unit (BB) (ICT, Vienna, Austria), which employs a Sylvania GTE 8 W low-pressure UV lamp, emission maximum 254 nm. The irradiation coil was constructed from a PTFE tubing. We used both commercial PTFE coils from ICT, with I.D. 0.3 mm and O.D. 1.3 mm and lengths of 10 and 20 m, and a laboratory-knitted PTFE coil, I.D. 0.33 mm, and O.D. 0.77 mm, 20 m long. Injections were made via a 100-μl syringe (Hamilton, Bonaduz, Switzerland).

Electrochemical detection was effected with a Model 5100A Coulochem electrochemical detector (ESA, Bedford, MS, USA), a model 5020 guard cell and a Model 5010 analytical cell. The working potential of the guard cell was +950 mV vs. palladium as reference electrode. The operating potential of the main cell was between +200 and +500 mV for injections under irradiation and was extended to +900 mV for injections without irradiation. The range was 50 × 10, the response time 0.4 s and the full output scale 10 mV.

The UV detector was a Perkin-Elmer LC 235 diode-array detector with a fixed wavelength of 240 nm, bandwidth 15 and sensitivity 0.05. This detector was connected on-line to the BB and the drug to be tested flowed directly from the BB to the detector. The connections between the column and irradiation coil were Upchurch fingertight fittings.

The integration of the peak areas was carried out with the Omega 235 software package and the results were plotted on an Epson LQ 850.

2.3. Optimization of photochemical reaction conditions

The irradiation time was varied either by mounting two fixed-length PTFE irradiation coils (10 and 20 m) to the photoreactor, or by varying the flow from the normally used 0.5 ml/min to

0.25 ml/min. The influence of the thickness of the coil on the effect of irradiation was tested with the original coil from ICT and with the laboratory-knitted thinner spaghetti coil. The working standard solution of each tested drug was injected into the HPLC–photolysis–electrochemical or HPLC–photolysis–UV detection system and the responses were recorded under the different conditions with and without irradiation. To shorten the equilibration time of the analytical cell, investigations were started at the lowest potential of +200 mV and then raised in steps of +100 mV.

3. Results and discussion

3.1. Electrochemical detection

Influence of chemical structure

The structures of the compounds investigated are given in Table 1. It is known that the chloride substituent in hydrochlorothiazide is replaced by H, OH or OCH_3 in aqueous or methanolic solutions on photolysis [9,10]. Additionally, hydrolysis of the thiazide ring occurs before and after photosubstitution reactions. To investigate the influence of different substituents on the electrochemical response, we chose substances with similar structures, such as bendroflumethizide and butizide.

As the substances flow through a 20-m coil of I.D. 0.3 mm and O.D. 1.3 mm, they are irradiated at 254 nm and then detected electrochemically. The three benzothiazides show an electrochemical response at a working potential of +200 mV vs. palladium. At this potential, these drugs are not electrochemically active without irradiation. Comparing the intensities of the signals for hydrochlorothiazide, bendroflumethiazide and butizide, it could be observed that the signal for bendroflumethiazide is about 20% smaller and that for butizide is about 50% smaller than the signal for hydrochlorothiazide. If these three substances are detected electrochemically at a higher working potential of +500 mV with irradiation, the intensity of the peaks is reversed. This means that the peak for butizide is higher than that for bendroflumethiazide;

Table 1
Structures of the compounds

Substance	Formula
Hydrochlorothiazide	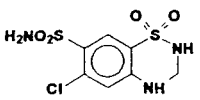
Butizide	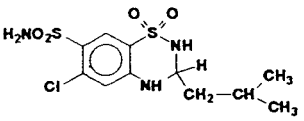
Bendroflumethiazide	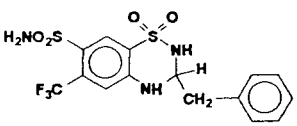
Chlortalidone	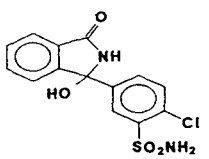
Furosemide	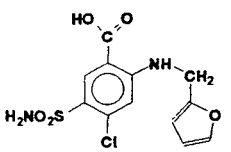
Etacrynic acid	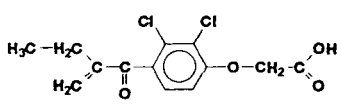

however, neither reaches the intensity of hydrochlorothiazide. Fig. 1 shows the assumed reactions of butizide after UV irradiation.

The different electrochemical signal intensities of bendroflumethiazide and butizide under UV irradiation conditions can be attributed solely to the structures of these drugs. Because there is a similar phenomenon for two neuroleptics, i.e., fluphenazine, which is substituted with CF_3 and not with a chlorine, as in perphenazine, the CF_3 group could be responsible for the reduced signal [18]. The decrease in intensity occurs at higher operating potentials and it appears that chloride

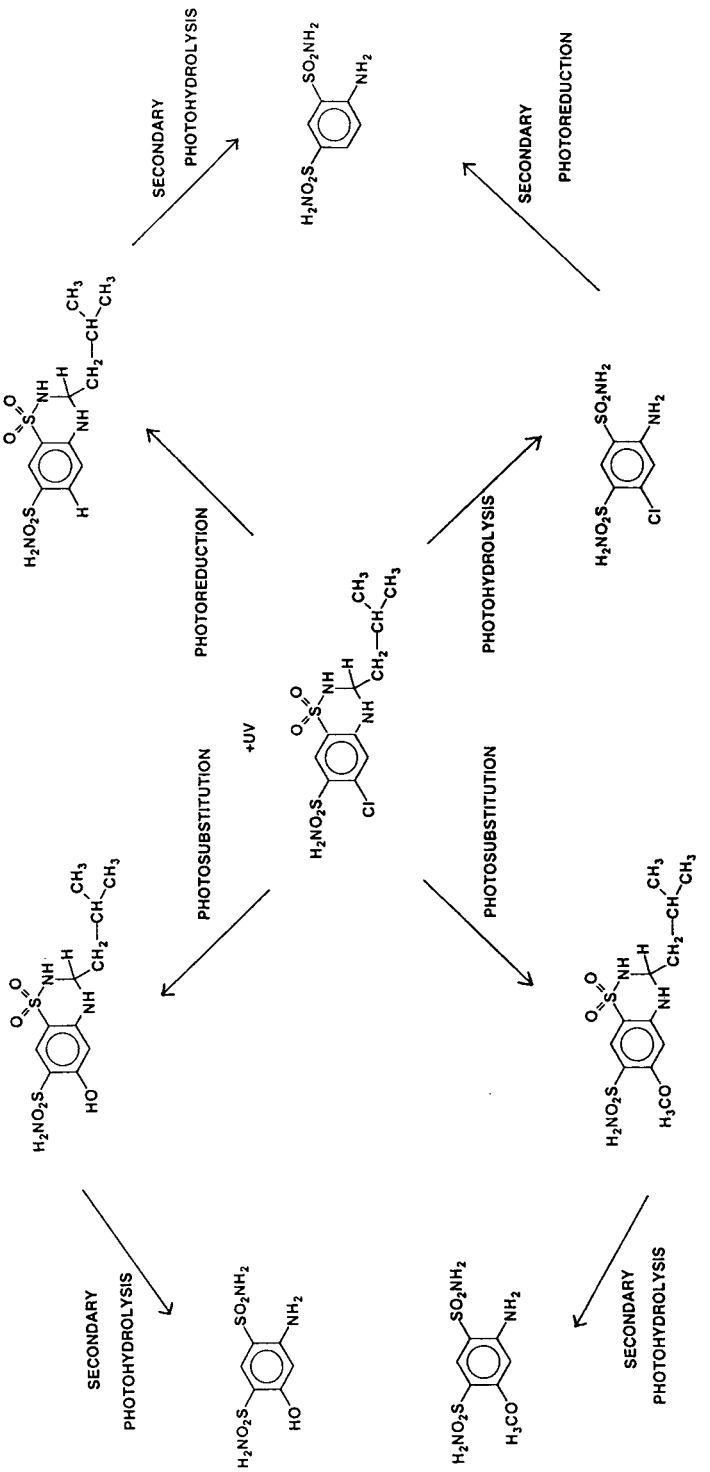

Fig. 1. Proposed butizide reactions induced by photolysis.

could be more easily replaced than CF_3. The substituent at position 3 of the thiazide ring, which is common to both drugs, is a steric hindrance for opening the thiazide ring, thus reducing the signals compared with hydrochlorothiazide.

Fig. 2 shows a comparison of the peak intensities of the three substances at different working potentials. Chlortalidone has the same substituted benzene ring, which a chlorine atom, as butizide and hydrochlorthiazide and it is assumed that photosubstitution occurs here. The acid amide is hydrolysed [19] and a benzophenone and carboxylic group result. Fig. 3 shows the product formed. Without irradiation, chlortalidone has no electrochemical activity at any potential. With photolysis it becomes electrochemically active and is detectable at a working potential of +200 mV. The signal intensity in this case is also only 50% of the intensity of hydrochlorothiazide, which can be explained by the absence of the benzothiazide structure. At higher potential this percentage decreases without reaching the electrochemical response of hydrochlorothiazide.

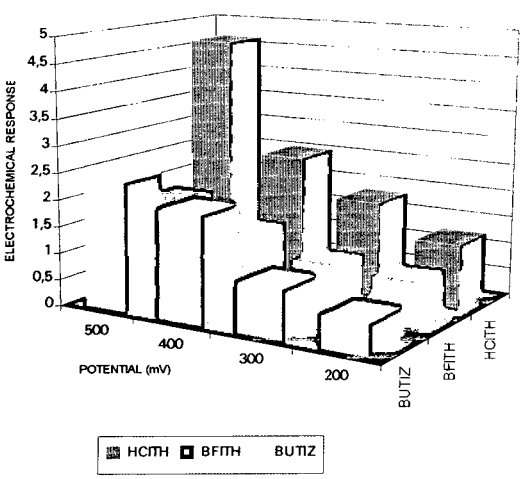

Fig. 2. Comparison of peak intensities of hydrochlorothiazide, bendroflumethiazide and butizide at different working potentials. Hydrochlorothiazide (HCITH) (concentration 30 ng per 6 μl), bendroflumethiazide (BFITH) (30 ng per 6 μl) and butizide (BUTIZ (30 ng per 6 μl). Column, Brownlee RP-18, Spheri 5 μm, 100 × 4.6 mm I.D.; mobile phase, MeOH–H_2O (80:20) + 2 g/l of $LiClO_4$; flow-rate, 0.5 ml/min; coil, 20 m × 1.3 mm O.D.

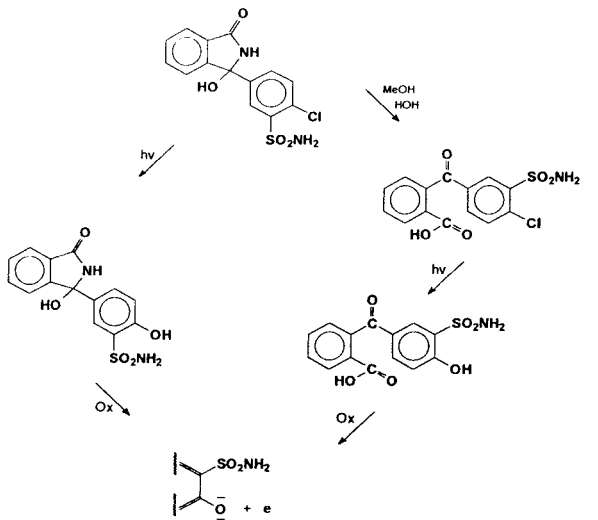

Fig. 3. Proposed formation of chlortalidone derivative by photolysis–ED.

Furosemide was recognized as a photosensitive drug which is photolysed at room temperature under daylight conditions [20]. The chlorine atom is also substituted in this molecule by OH. This characteristic can be utilized for sensitive and selective determination. Furosemide was transformed by photolysis from an electrochemically inactive substance into an electrochemically active derivative at a working potential as low as +200 mV. Etacrynic acid has similar feature. This drug is not electrochemically active without irradiation, but may be detected with irradiation at the same potential of +200 mV.

Stability of different PTFE tubing

The coils for the on-line postcolumn photolyic derivatization are made of PTFE tubing. They display good transparency to UV irradiation in the 230–400 nm range commonly used in organic photochemistry, are resistant to chemical solutions and have oxygen permeability. The reactor coils are made in a specific way by hand [21] or by machine. This, however, produces deformed tubes; this deformation is necessary to reduce the development of parabolic flow profiles and

subsequent peak broadening in the tubing. The commercially available coil is tested for a maximum pressure of 350 p.s.i. The coulometric analytical cell of the detector used produces a back-pressure depending on age and duration of utilization and if this back-pressure is too high, the coil may burst. The ICT coil provides higher stability against fluctuations in pressure because of the greater thickness. The thinner spaghetti coil reacts more quickly to fluctuations in pressure, leading to leakage. Hence the thicker tubing is to be preferred.

Optimization of photolysis conditions

The irradiation intensity influences the production of electrochemically detectable compounds and depends on four parameters: the energy of the lamp used, the distance from the reaction coil to the light source, the thickness of the coil and the duration of irradiation. The energy of the lamp is constant; an 8 W low-pressure lamp was always used. The knitted reaction coil was slipped over the light source to minimize the distance to the coil. Therefore, only the thickness of the coil and the duration of irradiation were considered as parameters that could be varied to optimize the photochemical conditions.

Two coils with different thicknesses were available. They had the same inner diameter to guarantee identical conditions for peak form and flow characteristics. The examinations with all the diuretics resulted in an increased signal intensity when the thicker reaction coil was used for irradiation. These findings are opposite to those produced in additional investigations with benzaldehyde, which produces significantly higher signals when thinner tubing is used. The most advantageous thickness of the coil depends on the structure of the substance. If the highest sensitivity is essential, each compound to be analysed should be tested for optimum thickness of the coil.

The duration of irradiation was tested first by varying the length of the reaction coil; we alternated fixed lengths of 10 and 20 m with an O.D. 1.3 mm, and second by changing the flow to extend or shorten the irradiation time. As photochemical derivatization is an excellent method for improving selectivity in the determination of pharmaceuticals and this advantage is obtained with electrochemical detection at lower potentials, the drugs to be determined were tested for the effect of duration of irradiation at +200, +300 and +400 mV (Table 2).

By comparing the peak areas obtained with the 10- and 20-m coils, the factor increasing signal intensity (F_I) can be calculated. F_I is the ratio of the value for the 20-m coil to that for the 10-m coil. With the exception of butizide at a

Table 2
Influence of the duration of irradiation

Potential (mV)	Coil length (m)	Hydrochlorothiazide	Bendroflumethiazide	Butizide	Chlortalidone	Furosemide	Etacrynic acid
200	10	1.9	1.2	1.8	0.8	0.4	0.06
200	20	2.3	2.0	1.1	1.1	0.9	0.03
F_I		1.2	1.7	0.6	1.4	2.3	0.5
300	10	1.9	0.9	1.8	0.7	0.5	0.6
300	20	3.2	2.2	2.3	2.0	1.6	0.3
F_I		1.7	2.4	1.3	2.9	3.2	0.5
400	10	1.9	1.3	1.9	1.0	0.5	0.8
400	20	4.6	3.0	5.1	4.2	1.4	0.8
F_I		2.4	2.3	2.7	4.2	2.8	1.0

Column, Brownlee RP-18, Spheri 5 μm, 100 × 4.6; I.D. mobile phase, MeOH–H_2O (80:20) + 2g/l of $LiClO_4$; flow-rate, 0.5 ml/min; coil, 20 m × 1.3 mm O.D.

potential of +200 mV and etacrynic acid at +200 and +300 mV, an increase in the detector response was recognized using the longer reaction coil. It appeared that a longer coil corresponding to a longer irradiation time generally produces a higher detector response, but the F_1 is individual and depends on the substance. Fig. 4 shows the different signals of bendroflumethiazide.

The effect of varying the flow-rate was tested with chlortalidone. The irradiation time was doubled by reducing the flow-rate from 0.5 to 0.25 ml/min. Under these, conditions the peak area obtained with longer irradiation is only 23% larger than the peak response obtained with a flow-rate of 0.5 ml/min. The resulting peak broadening is not significant but, together with the longer retention, the sensitivity and selectivity decrease. Therefore, the first method is to be preferred, i.e., influencing the irradiation time by varying the length of the reaction coil.

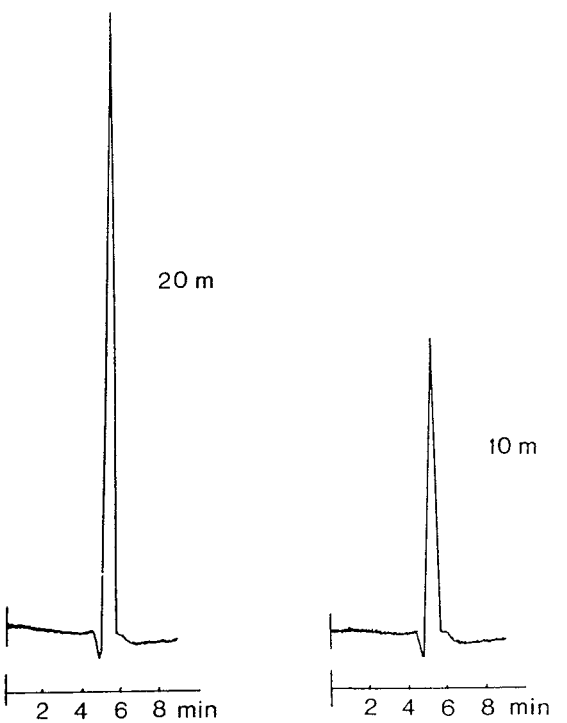

Fig. 4. Influence of coil length on detector response. Bendroflumethiazide concentration, 65 ng per 6 μl; column, Brownlee RP-18, Spheri 5 μm, 100 × 4.6 mm I.D.; mobile phase, MeOH–H_2O (80:20) + 2 g/l of $LiClO_4$; flow-rate, 0.5 ml/min; working potential, +400 mV; with irradiation, coils, 10 and 20 m × 1.3 mm O.D.

Reproducibility and limit of detection (LOD)

The reproducibility of the method under irradiation conditions was determined using 60 ng per 6μl of chlortalidone ($n = 8$). The relative standard deviation was 2.9%. The LOD was measured at a signal-to-noise ratio of 3. The LODs at a potential of +400 mV with UV irradiation were the following: hydrochlorothiazide 0.8, butizide 1, bendroflumethiazide 1.6, chlortalidone 1.6 and etacrynic acid 8 ng per 6 μl. The LOD of hydrochlorothiazide at a potential of +900 mV without UV irradiation is 1 ng per 6 μl and for the other analytes about 2 ng per 6 μl. For etacrynic acid a comparison of the LOD with and without irradiation is impossible because of its lack of electrochemical response without irradiation.

For all substances, a linear response is obtained over the range 2 ng–2 μg, with the exception of etacrynic acid (10 ng–10 μg). The correlation coefficient for the function $y = ax + b$ was between 0.997 and 0.999.

3.2. Influence of irradiation on UV detection

Photolysis may improve the detectability of substances not only by enhancing the electrochemical activity but also by influencing the UV absorption behaviour. Although electrochemical detection is more selective than UV detection, a comparison with respect to sensitivity by irradiation was of interest.

The drugs were detected by UV spectrophotometry at 240 nm without and with irradiation using a 20-cm ICT coil and the peak areas were compared. Only the detector response for bendroflumethiazide increased by about 30% with irradiation. The signals for the other diuretics generally decreased with irradiation. The decrease of the signal of butizide by 40% was the highest and for etacrynic acid by 4% was the lowest.

Comparing the sensitivities of these two detection methods, UV and ED with irradiation, it was found that ED is more sensitive, because the

LOD of hydrochlorothiazide with UV detection was 4 ng per 6 μl. We found the same result for the other substances. This LOD was lower than the LOD for ED with irradiation only for etacrynic acid. Therefore, photolysis in combination with UV detection has no advantages over electrochemical detection and is not recommended for these substances.

4. Conclusion

HPLC–photolysis–ED does not require expensive reagents and is a precise, convenient method for determining diuretics which can be transformed by on-line post-column photolysis into electrochemically active derivatives. The diuretics become electrochemically active by UV irradiation at very low working potentials. Normally they become active at potentials of +800 and +900 mV. This increases the selectivity. HPLC–photolysis–UV detection usually leads to a lower sensitivity.

The expectation that the chloride atom on the benzene ring is replaced and that this substitution is responsible for electrochemical detectability by photolysis could be verified. However, comparison of the signals of hydrochlorothiazide, bendroflumethiazide and butizide indicated that hydrolysis of the benzothiazide ring also has an influence on the transformation into an electrochemically active substance. The effect of the UV irradiation depends on the preparation, thickness and length of the coils and the flow-rate. The method presented will provide the basis for pharmacokinetic studies on real samples and will be published in a subsequent paper.

References

[1] L. Dou and I.S. Krull, Electroanalysis, 4 (1992) 381.
[2] W.R. LaCourse and I.S. Krull, Anal. Chim. Acta, 215 (1988) 45.
[3] L. Dou and I.S. Krull, J. Pharm. Biomed. Anal., 8 (1990) 493.
[4] W.L. Childress, I.S. Krull and C.M. Selavka, J. Chromatogr. Sci., 28 (1990) 76.
[5] R.W. Frei and J.F. Lawrence (Editors), Chemical Derivatization in Analytical Chemistry, Plenum Press, New York, 1981.
[6] J.W. Birks and R.F. Frei, Trends Anal. Chem., 1 (1982) 361.
[7] I.S. Krull and W.R. LaCourse, in I.S. Krull (Editor), Reaction Detection in Liquid Chromatography, Marcel Dekker, New York, 1986, Ch. 7.
[8] W.J. Bachmann and J.T. Stewart, LC·GC, 7 (1989) 38.
[9] S.R. Tamat and D.E. Moore, J. Pharm. Sci., 72 (1983) 180.
[10] W.J. Bachmann and J.T. Stewart, J. Chromatogr. Sci., 28 (1990) 123.
[11] J.R. Poulsen, in J.W. Birks (Editor), Chemiluminiscence and Photochemical Reaction Detection in Chromatography, VCH, New York, 1989, Ch. 6, p. 149.
[12] K.B. Alton, D. Desrivieres and J.E. Patrick, J. Chromatography., 374 (1986) 103.
[13] G.K. Shiu, V.K. Prasad, J. Lin and W. Worsley, J. Chromatogr., 377 (1986) 430.
[14] C.D. Gaitonde and P.P. Jayade, Indian Drugs, 28 (1991) 242.
[15] J.T. Stewart and S.S. Clark, J. Pharm. Sci., 75 (1986) 413.
[16] K. Kunihiro, T. Misako, U. Shinichi, H. Teruhiko, N. Kyoko, A. Kazuyuki and N. Susumu, Iyakuhin Kenkyu, 19 (1988) 103.
[17] M. Koller, Clin. Chem., 34 (1988) 947.
[18] W.A. McKinley, J. Anal. Toxicol., 5 (1981) 209.
[19] M.W. Dong, P.V. Passalacqua and D.R. Choudhury, J. Liq. Chromatogr., 13 (1990) 2135.
[20] N. Yagi, H. Kenmotsu, H. Sekikawa and M. Takada, Chem. Pharm. Bull., 39 (1991) 454.
[21] J.R. Poulson, K.S. Birks, M.S. Gandelman and J.W. Birks, Chromatographia, 22 (1986) 231.

ELSEVIER

Journal of Chromatography A, 709 (1995) 265–273

JOURNAL OF CHROMATOGRAPHY A

Separation of enantiomers of benzodiazepines on the Chiral-AGP column

I. Fitos[a,*], J. Visy[a], M. Simonyi[a], J. Hermansson[b]

[a]*Central Research Institute for Chemistry of the Hungarian Academy of Sciences, P.O. Box 17, H-1525 Budapest, Hungary*
[b]*ChromTech AB, Box 6056, S-12906 Hägersten, Sweden*

First received 16 February 1995; revised manuscript received 7 April 1995; accepted 7 April 1995

Abstract

The resolution of twenty-five 3-chiral and 5-chiral 1,4-benzodiazepines and related compounds was studied on a Chiral-AGP column. Relationship between the structure and enantioselective retention is discussed stressing the role of hydrophobic and hydrogen-bonding interactions as well as the importance of the conformation of the enantiomers. The majority of the benzodiazepines were separated with high separation factors and high resolution. The enantioselectivity was influenced by the nature and the concentration of the organic modifier in the mobile phase, as well as by the pH. Chiral chromatographic separation was compared with stereoselective binding on native AGP.

1. Introduction

Centrally chiral benzodiazepines belong to a special class of chiral compounds. Due to inversion of the boat-shaped diazepine ring the enantiomers have opposite chiral molecular conformation that determines the sign of their optical rotation [1].

Centrally chiral benzodiazepines can be conveniently resolved on various types of synthetic chromatographic chiral stationary phases [2,3]. Among protein phases immobilized human serum albumin (HSA) columns were successfully used for resolution of series of different 3-chiral 1,4-benzodiazepines [4–6], dihydrodiazepam [7], as well as tofisopam and its analogues [8,9]. The importance of these studies lies in the fact that these chromatographic results were useful to get information about the binding stereoselectivity on the native protein [10,11]. Since in plasma protein binding of benzodiazepines the contribution of albumin is dominating [12], binding stereoselectivity on α_1-acid glycoprotein (AGP) has not been studied to our knowledge, and even on the AGP column only very few benzodiazepine separations have been published [13].

In this work we present the HPLC separation on a Chiral-AGP column of a large number of racemic 3-substituted (hydroxy, alkoxy, acyloxy and alkyl) 1,4-benzodiazepines, 5-chiral 1,4-benzodiazepines and analogues as well as a 2,3-benzodiazepine drug, tofisopam. By studying the stereoselective retention of 25 benzodiazepine analogues we tried to get qualitative information of the nature of the chiral discrimination process.

* Corresponding author.

0021-9673/95/$09.50
SSDI 0021-9673(95)00444-0

2. Experimental

2.1. Chromatography

A Chiral-AGP column (ChromTech AB, Hägersten, Sweden) (100 × 4.0 mm I.D.) with a guard column (10 × 3.0 mm I.D.) was used at ambient temperature (22–25°C).

The chromatographic system consisted of a Jasco Model PU-980 HPLC pump, a Rheodyne Model 7125 injector with a 20-μl loop, a Jasco Model UV-975 detector set at 220 nm and B.D.S. software (Barspec, Rehovot, Israel).

The mobile phase was 0.01 *M* phosphate buffer (pH 5.0, 6.0, 7.0) containing 5% or 10% (v/v) of isopropanol (IPA) or acetonitrile (ACN); the flow-rate was 0.9 ml/min.

Sample solutions were prepared by diluting (10 μl/1 ml eluent) the stock solutions (1 mg/2 ml ethanol).

Retention times (t_r) were determined in three parallel runs and corresponding capacity factors ($k' = [t_r - t_o]/t_o$) and separation factors ($\alpha = k'_2/k'_1$) were calculated.

2.2. Chemicals

3-Chiral 1,4-benzodiazepines (compounds 1–18; see Table 1) were synthesized as described previously [4,5,10]. 5-Chiral 1,4-benzodiazepines (compounds 19–22; Table 2) were obtained from Chemical Works of Gedeon Richter (Budapest, Hungary). Compounds 23–25 (Table 2) were kindly donated by Ciba-Geigy (Basle, Switzerland). Tofisopam enantiomers were provided by EGIS Pharmaceuticals (Budapest, Hungary).

2.3. Ultrafiltration

Ultrafiltration (two parallels) was carried out in an Amicon (Oosterhout, Netherlands) MPS-I system with YMT-membranes. Solutions containing racemic compounds 12 or 20 as well as native human AGP (Sigma, St. Louis, MO, USA) were prepared in 0.01 *M* phosphate buffer pH 7.0.

3. Results and discussion

3.1. Separation of 3-chiral 1,4-benzodiazepines

Table 1 summarizes the capacity factors and separation factors for a series of 3-substituted 1,4-benzodiazepines. The mobile phase was 0.01 *M* phosphate buffer pH 7.0 with IPA (isopropanol) or ACN (acetonitrile) modifiers. Comparing the data obtained with 10% IPA and 10% ACN as mobile phase additives it can be observed that in the presence of ACN the enantioselectivity is highly improved. The retention is also somewhat higher. With the exception of compounds 2, 13, 17 and 18 all the racemates could be resolved. In case of the unresolved compounds having either hydroxy, acyloxy or alkyl substituent at the chiral centre, the common structural feature is $R^1 = CH_3$ and $R^{2'} = H$ substitution. When the detached aromatic ring has an ortho chlorine substituent, even the N(1)-methyl derivatives (4,14) could be resolved. Considering the series of oxazepam (1) as well as its methylether (5) and different esters (7–9) it can be seen that increasing hydrophobicity of the R^3 substituent enhances both the capacity and the separation factors. Oxazepam hemisuccinate (10) is a special case. This acidic ligand is bound with low affinity at pH 7 due to the net negative charge of AGP at this pH, nevertheless, its separation was very good (Fig. 1.). Comparing the 3-alkyl derivatives (15 and 16) it can also be observed that the more hydrophobic derivative has the higher retention and somewhat higher enantioselectivity.

Considering the elution orders established by using separated enantiomers, in most cases the (*S*)-enantiomer is the more retained one. It suggests that AGP similarly to other proteins [2,14,15] prefers the "M"-boat conformation (Fig. 2.). Nevertheless, the reversed elution order obtained for the 3-alkyl compounds when 5% IPA mobile phase modifier was used, calls attention to the fact that during chromatography the chiral recognition is a complex process and solvent-induced stereoselectivities may interfere [16].

Summarizing the results obtained for the sepa-

Table 1
Separation of racemic 3-chiral 1,4-benzodiazepines (pH 7.0)

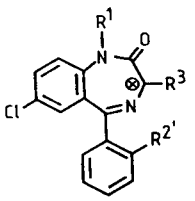

No.	R^1	$R^{2'}$	R^3	5% IPA			10% IPA		10% ACN		
				k'_1	α	Elution order	k'_1	α	k'_1	α	Elution order
1	H	H	OH	4.92	1		2.35	1	2.42	1.17	
2	CH_3	H	OH	4.35	1		2.00	1	2.56	1	
3	H	Cl	OH	6.85	1		2.93	1	3.64	1.41	
4	CH_3	Cl	OH	9.11	1.22				4.48	1.73	
5	H	H	OCH_3	5.67	1		2.08	1	3.15	1.22	
6	H	Cl	OCH_3	6.39	1.10		2.48	1	3.69	1.56	
7	H	H	$OCOCH_3$	7.69	1.18	*R,S*	2.88	1	4.03	2.15	*R,S*
8	H	H	$OCOCH_2CH_3$	11.50	1.58		4.03	1.21	7.18	2.55	
9	H	H	$OCO(CH_2)_2CH_3$	17.33	2.20		5.38	1.65	12.67	2.97	
10	H	H	$OCO(CH_2)_2COOH$	0.40	1.71	*R,S*			0.18	2.93	*R,S*
11	H	H	$OCO(CH_2)_2COOCH_3$	11.23	1.52				5.00	2.44	
12	H	Cl	$OCOCH_3$	9.39	1.33	*R,S*	3.33	1.19	6.69	2.32	*R,S*
13	CH_3	H	$OCOCH_3$	5.68	1		1.92	1	3.08	1	
14	CH_3	Cl	$OCOCH_3$	12.56	1.06		3.77	1	6.67	1.20	
15	H	H	CH_3	6.08	1.19	*S,R*	2.61	1.12	4.10	1.12	*R,S*
16	H	H	CH_2CH_3	11.50	1.29	*S,R*	3.45	1.21	8.20	1.40	*R,S*
17	CH_3	H	CH_3	6.50	1				4.30	1	
18	CH_3	H	CH_2CH_3	11.08	1				8.35	1	

ration of the enantiomers of 3-chiral 1,4-benzodiazepines the following conclusions can be drawn concerning the retention and chiral recognition mechanism: (1) The retention is mainly due to hydrophobic interaction; in this respect isopropanol competes with the solute molecules [16]. (2) The (*S*)-enantiomers having the "M"-conformation are more retained than the (*R*)-"P" enantiomers. The hydrophobic character of R^3 enhances the stereoselectivity. The solvent-induced reversal of the elution order, found for the 3-alkyl derivatives suggests a role of the oxygen atom in R^3 during chiral discrimination. (3) Hydrogen bonding via N(1)-H probably is involved in chiral interaction, since $R^1 = CH_3$ hinders separation. (4) Ortho chlorine substitution on the detached aromatic ring promotes chiral separation, outweighing the effect of $R^1 = CH_3$.

3.2. Separation of 5-chiral 1,4-benzodiazepines

The data in Table 2 present the capacity factors and separation factors obtained at pH 7.0 for 5-chiral 1,4-benzodiazepines as well as for related thiazepine and oxazepine compounds having sulphur or oxygen atom at position 4. It can be seen that compounds with this chiral structure can be easily resolved on Chiral-AGP, the only exception being the highly retained compound 25. Comparing effects of the mobile phase modifiers, the situation is not as simple as

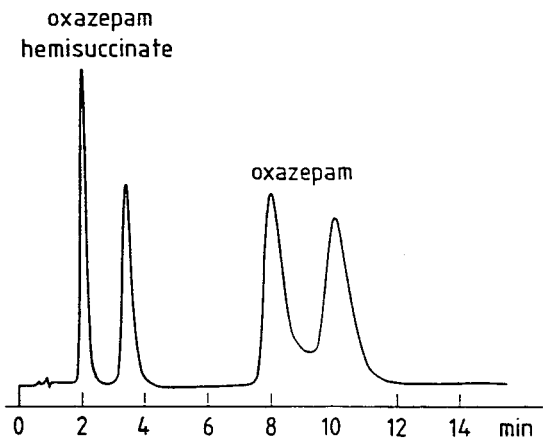

Fig. 1. Separation of *rac*-oxazepam (1) and *rac*-oxazepam hemisuccinate (10) on Chiral-AGP. Mobile phase: 0.01 *M* phosphate buffer pH 7.0 with 5% ACN.

found for the 3-chiral 1,4-benzodiazepines. In the presence of ACN the retention of the first eluted peaks is always higher than with the same concentration of IPA. The enantioselectivity was also affected by the nature of the organic modifier. Higher separation factors were obtained for compounds 21–24 using mobile phases containing ACN, whereas the enantioselectivity was reduced for compounds 19 and 20. Compared to the 3-chiral 1,4-benzodiazepines the effect of $R^1 = CH_3$ substitution on the enantioselectivity is also reversed. Furthermore, whereas for the 3-chiral 1,4-benzodiazepines the N(1)-H group was preferred in chiral discrimination, in this series the presence of an N(1)-methyl group is favoured. The high separation factor of dihydrodiazepam (20) compared to its desmethyl analogue (19) is striking, while the relation of compounds 21 and 22 is less pronounced. Considering the effect of the heteroatom in position

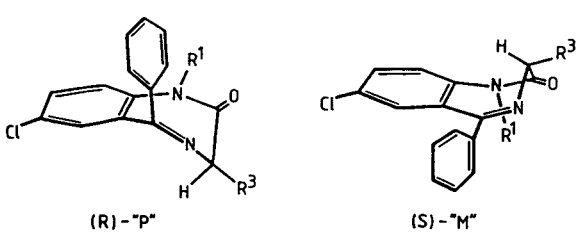

Fig. 2. Dominant conformers of 3-chiral 1,4-benzodiazepines.

4 (cf. 19 vs. 23 and 24) it can be observed that while in the case of the thiazepine (24) the retention of both enantiomers is highly increased, the oxazepine compound (23) has the higher enantioselectivity. Chlorine substitution in the 2′-position provoked very strong retention for both enantiomers of compound 25, and resolution is lost.

The reversed elution order found for dihydrodiazepam (20) and for its N(4)-carbamoyl derivative (22) is not surprising, because carbamoylation exerts inversion of the seven-membered ring (Fig. 3.), even reversing the sign of the optical rotation, as proved by X-ray [17] and chiroptical studies [18]. Thus, the higher affinity of (+)-(*S*)-20 and (+)-(*R*)-22 on Chiral-AGP suggests that discrimination is due to the chiral conformation of the molecule rather than to the absolute configuration at the C(5) centre.

3.3. Separation of tofisopam

Fig. 5 shows the chromatograms of *rac*-tofisopam and its enantiomers obtained at pH 7.0 with 5% IPA and 5% ACN modifiers.

Tofisopam is a 2,3-benzodiazepine having a chiral centre at the C(5) position. It was proved by NMR and chiroptical investigations [19,20] that tofisopam in solution exists in two conformations and conformers of the same enantiomer show opposite optical rotation (Fig. 4.). In crystalline form the molecules are predominantly in the thermodynamically more stable conformation in which the C(5)-ethyl group is pseudo-equatorial with respect to the diazepine ring, while in solution equilibrium is achieved within a few hours [8]. The conformers as diastereomers can be separated even by non-chiral reversed-phase HPLC [21]. On an HSA-Sepharose column it is possible to separate the major conformers of the two enantiomers, as well as the conformers of the (*S*)-enantiomer [8].

The chromatogram obtained on Chiral-AGP with IPA as modifier also indicates the separation of the conformers of (*S*)-absolute configuration (Fig. 5a). The first peak on the chromatogram of the racemate (Fig. 5c) involves the total amount of (*R*)-enantiomer as well as about 20%

Table 2
Separation of racemic 5-chiral 1,4-benzodiazepines and related compounds (pH 7.0)

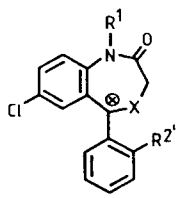

No.	X	R^1	$R^{2'}$	10% IPA			10% ACN		
				k'_1	α	Elution order	k'_1	α	Elution order
19	NH	H	H	2.39	1.46		4.00	1	
20	NH	CH_3	H	2.42	5.03	*R,S*	4.58	2.06	*R,S*
21	N-$CONH_2$	H	H	1.43	1.53		1.65	1.65	
22	N-$CONH_2$	CH_3	H	1.67	2.05	*S,R*	3.88	2.14	*S,R*
23	O	H	H	4.83	2.73		6.80	3.09	
24	S	H	H	7.92	1.36		10.60	1.86	
25	S	H	Cl	18	1		27	1	

of the amount of the other enantiomer corresponding to the (+)-(*S*)-conformer. When ACN modifier was used the conformers of both enantiomers could be separated. It is interesting that in the case of (*S*)-tofisopam the minor conformer is more retained (Fig. 5d), which is opposite to the elution order found with IPA modifier. For the (*R*)-enantiomer, however, the first eluted peak is the minor conformer (Fig. 5e). The chromatogram of the racemate (Fig. 5f) indicates that while the minor conformers are nicely separated, the two major conformers show identical retention. Such variance in elution orders is presumably due to specific solvation effects.

3.4. Effect of pH

Table 3 summarizes the capacity and separation factors measured for several neutral 3-chiral and 5-chiral 1,4-benzodiazepines and analogues at pH 5.0, 6.0 and 7.0, both with ACN and IPA modifiers. The retention of these compounds was only slightly affected by the pH. The fluctuation of the k' values found in some cases is not significant enough to be caused by structural characteristics. By increasing the pH from 5 to 7 using mobile phases containing ACN, the enantioselectivity increases for nine of the ten compounds. For some compounds the effect was more pronounced, i.e. for compounds 6, 7, 10 and 16. A very strong increase of the separation factor was also observed for compound 20, using mobile phases with 5 and 10% IPA. For compound 20, contrary to the other compounds presented in Table 3, it can be noted that a higher enantioselectivity was observed when IPA was used as modifier compared to ACN over the pH range studied. These findings are in accordance with previous observations for neutral compounds made by Hermansson et al. [22,23]. The charge of these compounds can not be affected by pH [24]. This means that the effects on the enantioselectivity could be assigned to changes of the chiral bonding properties of the protein, induced by the charge of the proteolytic amino acid residues.

The acidic compound oxazepam hemisuccinate (10), behaved in a different way with respect to both the retention and the enantioselectivity,

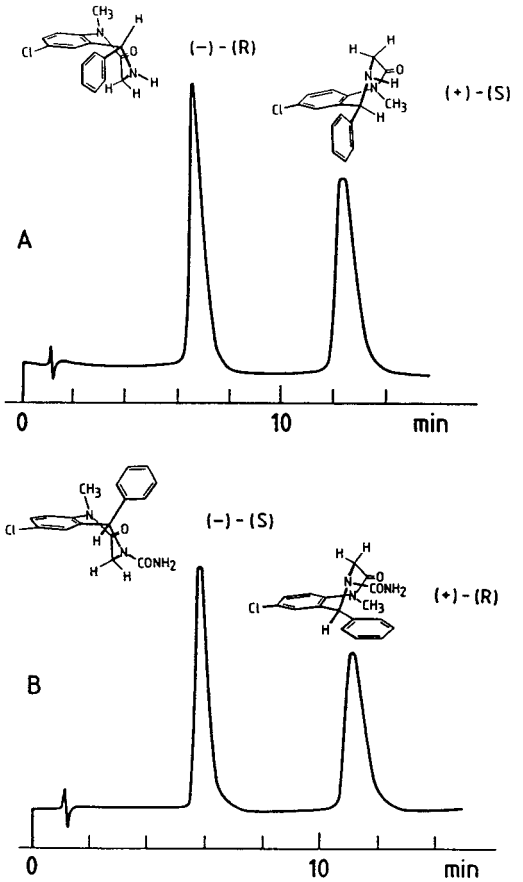

Fig. 3. Separation of (A) *rac*-dihydrodiazepam (20) and (B) *rac*-uxepam (22) on Chiral-AGP. Mobile phase: 0.01 *M* phosphate buffer pH 7.0 with 10% ACN.

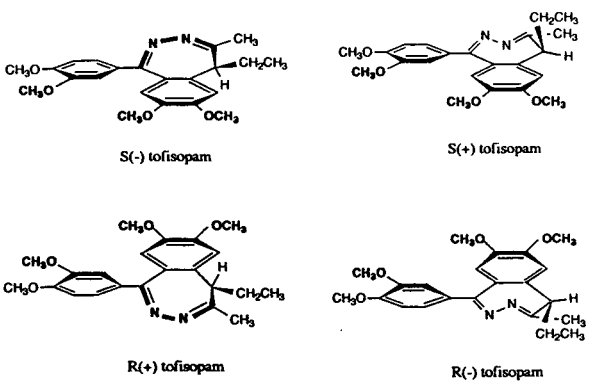

Fig. 4. The four species present in solution of *rac*-tofisopam.

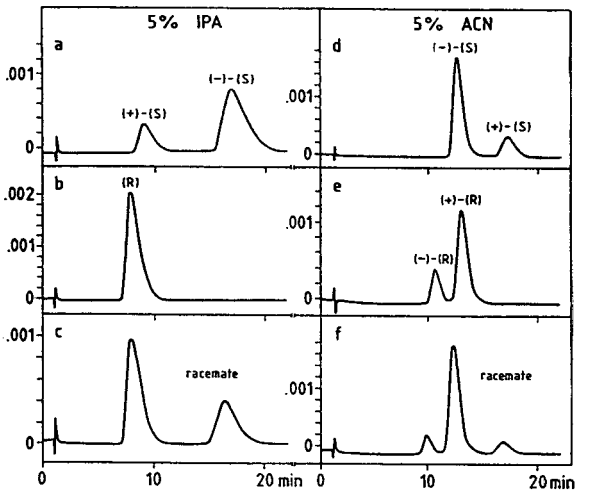

Fig. 5. Chromatograms of (*S*)-, (*R*)- and *rac*-tofisopam obtained on Chiral-AGP. Mobile phase: 0.01 *M* phosphate buffer pH 7.0 with 5% IPA (a,b,c) and 5% ACN (d,e,f).

Table 3
Influence of pH on the capacity factors and separation factors of chiral benzodiazepines

No.		pH 5.0		pH 6.0		pH 7.0	
		k'_1	α	k'_1	α	k'_1	α
1	5% ACN	5.9	1.24	6.8	1.29	6.8	1.29
	5% IPA	3.8	1	4.0	1	4.2	1
3	5% ACN	7.8	1.54	8.1	1.62		
	5% IPA	5.2	1	5.6	1	5.9	1
6	5% ACN	12.3	1.26	10.3	1.60	11.9	1.93
	5% IPA	5.6	1	5.5	1	5.0	1.21
7	10% ACN	4.2	1.62	4.8	1.94	3.8	2.29
	5% IPA	6.0	1.08	6.5	1.16	6.9	1.26
12	10% ACN	5.6	2.34	6.2	2.68	6.4	2.56
	5% IPA	8.0	1.35	8.2	1.46	8.5	1.49
16	10% ACN	9.1	1	7.4	1.22	8.2	1.40
	10% IPA	3.5 (*S*)	1.23	3.4	1.20	3.5	1.21
20	10% ACN	4.8	1.71	4.6	1.72	4.9	1.90
	10% IPA	1.9	2.86	2.2	3.55	2.5	4.23
	5% IPA	4.3	4.53	5.3	5.91	6.2	6.70
23	10% ACN	7.4	2.35	6.8	2.62	6.8	3.09
	10% IPA	4.2	2.01	4.3	1.88	4.7	2.60
24	10% ACN	12.3	1.72	11.1	1.69	10.6	1.68
	10% IPA	6.6	1.54	6.5	1.56	7.2	1.48
25	10% ACN	29	1	27	1	27	1
	10% IPA	16	1	16	1	16	1

compared to the neutral compounds, as demonstrated in Figs. 6A,B. The enantioselectivity was strongly improved by increasing the pH from 5 to 7. It can be noted that the separation factor is 1.0 at pH 5 with ACN as modifier, however, increasing pH to 7 gives a separation factor of 2.4. This behaviour has not been reported previously for acidic compounds. Normally the separation factor increases for acidic compounds by reducing the pH [22,23].

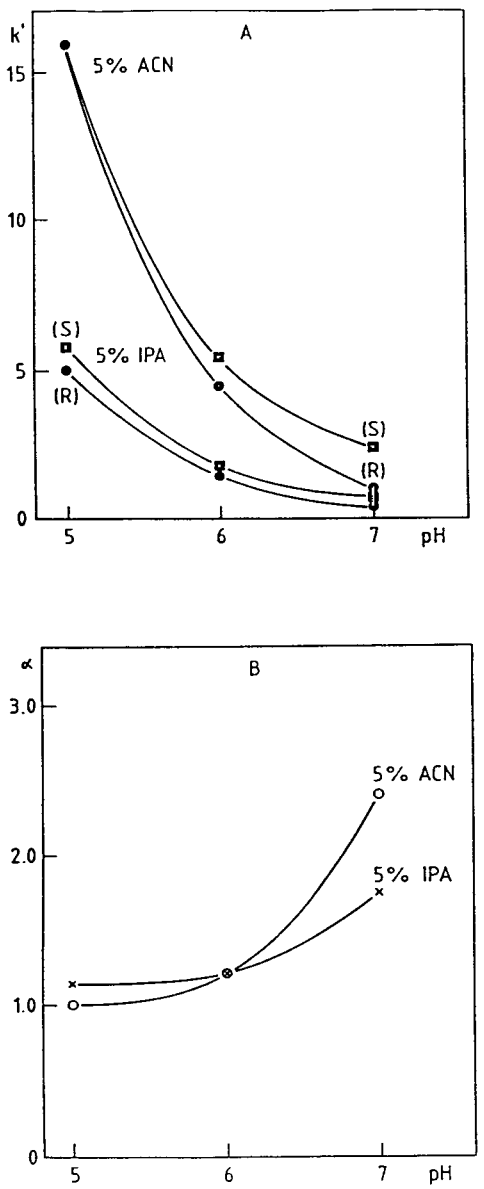

Fig. 6. Effect of pH on the capacity factors (A) and the separation factors (B) of oxazepam hemisuccinate (10) on Chiral-AGP.

3.5. Chromatographic resolution and binding stereoselectivity

Since the majority of the investigated benzodiazepines could be conveniently resolved on Chiral-AGP, it was of interest to check whether these compounds show any stereoselective binding on native AGP. Binding studies were performed with representatives of 5- and 3-chiral compounds, i.e. dihydrodiazepam (20) and lorazepam acetate (12). In case of dihydrodiazepam the chiral separation was very good with both modifiers, exceptionally high with IPA (see Table 2), while the separation of lorazepam acetate enantiomers was better in the presence of ACN (see Table 1). Ultrafiltration of solutions containing the racemic ligand and native AGP were performed, and the free fractions for both enantiomers were determined by comparing the chromatograms obtained on Chiral-AGP for the racemic ligand solution as well as for the ultrafiltrate. The results can be seen in Table 4. In accordance with the chromatographic behaviour, in both cases the more retained (*S*)-enantiomers indicated stronger binding, though to different extents. In the case of dihydrodiazepam the enantiomeric distribution was $R/S = 76/24$, while the chromatogram of lorazepam acetate filtrate indicated only slight excess of the first peak ($R/S = 54/46$). The binding stereoselectivities, i.e. the ratio of enantiomeric binding constants (K^S/K^R) which can be calculated [25] from these data, are 7.7 and 1.4 for compounds 20 and 12, respectively. These enantioselectivities show correlation with the chromatographic results obtained with IPA modifier, but differ from those measured with ACN modifier. Thus, the high chromatographic selectivity of dihydrodiazepam enantiomers on Chiral-AGP is in agreement with its remarkable native binding stereoselectivity. The case of lorazepam acetate, however, indicates that good chromatographic separation on Chiral-AGP does not necessarily

Table 4
Stereoselective binding of dihydrodiazepam (20) and lorazepam acetate (12) studied by chromatographic analysis of ultrafiltrates on Chiral-AGP (eluent: phosphate buffer pH 7.0, 10% ACN)

	Dihydrodiazepam	Lorazepam acetate
C_{rac} (μM)	29	22
C_{AGP} (μM)	50	50
Free fractions (%)	(*R*): 64 ± 2 (*S*): 20 ± 2	(*R*): 47 ± 2 (*S*): 39 ± 2
Binding constants (M^{-1})	$K^R = 1.3 \times 10^4$ $K^S = 1.0 \times 10^5$	$K^R = 2.6 \times 10^4$ $K^S = 3.6 \times 10^4$

require highly stereoselective binding to the native protein.

4. Conclusion

Chiral-AGP can separate the enantiomers of benzodiazepines with a broad range of structures. The effects of substituent on retention and enantioselectivity within homologous series indicate the role of hydrophobic and hydrogen bonding interactions. Exceedingly high chiral separation was found for 4,5-dihydrodiazepam, for which the existence of a remarkably high native binding stereoselectivity favouring the (*S*)-enantiomer was revealed. Discrimination according to chiral molecular conformations, which is the special structural feature of benzodiazepines, plays an important role in the separation mechanism.

Acknowledgements

This work was supported by project OTKA 1764. For providing compounds we gratefully thank the following companies: Chemical Works of Gedeon Richter, Ciba-Geigy and EGIS Pharmaceuticals. The skilful technical assistance by Mrs. Ilona Kawka is acknowledged.

References

[1] V. Šunjić, A. Lisini, A. Sega, T. Kovač, F. Kajfež and B. Ruščić, J. Heterocyclic Chem., 16 (1979) 757.
[2] P. Salvadori, C. Bertucci, E. Domenici and G. Giannaccini, J. Pharm. Biomed. Anal., 7 (1989) 1735.
[3] X.-L. Lu and S.K. Yang, J. Chromatogr., 535 (1990) 229.
[4] I. Fitos, M. Simonyi, Zs. Tegyey, L. Ötvös, J. Kajtár and M. Kajtár, J. Chromatogr., 259 (1983) 494.
[5] I. Fitos, M. Simonyi, Zs. Tegyey, M. Kajtár and L. Ötvös, Arch. Pharm. (Weinheim), 319 (1986) 744.
[6] E. Domenici, C. Bertucci, P. Salvadori, G. Félix, I. Cahagne, S. Motellier and I.W. Wainer, Chromatographia, 29 (1990) 170.
[7] I. Fitos and M. Simonyi, Experientia, 39 (1983) 591.
[8] M. Simonyi and I. Fitos, Biochem. Pharmacol., 32 (1983) 1917.
[9] J. Visy and M. Simonyi, Chirality, 1 (1989) 271.
[10] I. Fitos, Zs. Tegyey, M. Simonyi, I. Sjöholm, T. Larsson and C. Lagercrantz, Biochem. Pharmacol., 35 (1986) 263.
[11] E. Domenici, C. Bertucci, P. Salvadori and I.W. Wainer, J. Pharm. Sci., 80 (1991) 164.
[12] J. Schley and B. Müller-Oerlinghausen, Pharmacopsychiat., 16 (1983) 82.
[13] W. Heitmann, H. Liepmann, U. Mätzel, H. Zeugner, A.M. Fuchs, H. Krähling, M. Ruhland, F. Mol and M.Th.M. Tulp, Eur. J. Med. Chem., 23 (1988) 249.
[14] A. Konoval, G. Snatzke, T. Alebić-Kolbah, F. Kajfež, S. Rendić and V. Šunjić, Biochem. Pharmacol., 28 (1979) 3109.
[15] I. Fitos, J. Visy, J. Kardos and M. Simonyi, Chirality, in press.
[16] M. Enquist and J. Hermansson, J. Chromatogr., 519 (1990) 271.

[17] M. Czugler, A. Kálmán, J. Röhricht, M. Lõw, L. Ürögdi and L. Kisfaludy, Tetrahedron Letters, (1977) 917.
[18] M. Kajtár, J. Kajtár, J. Röhricht and J.G. Ángyán, Croat. Chem. Acta, 62 (1989) 245.
[19] A. Neszmélyi, E. Gács-Baitz, Gy. Horváth, T. Láng and J. Körösi, Chem. Ber., 107 (1974) 3894.
[20] G. Tóth, E. Fogassy, M. Ács, L. Tõke and T. Láng, J. Heterocyclic Chem., 20 (1983) 709.
[21] M. Patthy and J. Salát, J. Chromatogr., 210 (1981) 159.
[22] J. Hermansson and M. Eriksson, J. Liq. Chromatogr., 9 (1986) 621.
[23] J. Hermansson, Trends Anal. Chem., 8 (1989) 251.
[24] T. Sjödin, N. Roosdorp and I. Sjöholm, Biochem. Pharmacol., 25 (1976) 2131.
[25] I. Fitos, J. Visy, M. Simonyi and J. Hermansson, Chirality, 5 (1993) 346.

ELSEVIER

Journal of Chromatography A, 709 (1995) 275–281

JOURNAL OF CHROMATOGRAPHY A

Determination of trace elements in sea water by ion chromatography–inductively coupled plasma mass spectrometry ☆

M. Bettinelli, S. Spezia*

ENEL SpA, DCO, Central Laboratory, via Nino Bixio 39, 29100 Piacenza, Italy

First received 17 December 1994; revised manuscript received 4 April 1995; accepted 11 April 1995

Abstract

The determination of trace elements in sea water was carried out by means of ion chromatography (IC) coupled with inductively coupled plasma mass spectrometry (ICP-MS). The elimination of the matrix by the chromatographic technique allowed the determination of about twenty elements (rare earths, Co, Cu, Mn, Ni, Zn Pb and U) at ultra-trace levels. The calibration of the ICP-MS system was carried out using multi-elemental standard aqueous solutions. The use of a multi-elemental technique such as ICP-MS permitted the throughput of samples to be increased because the separation of the different analytes was not required. The detection limits obtained for most of the elements were in the range 1–50 ng/l and the recovery for all the elements under analysis was quantitative.

1. Introduction

The determination of trace elements, particularly heavy metals, in samples from uncontaminated areas requires powerful techniques to detect extremely low concentrations of analytes. Inductively coupled plasma mass spectrometry (ICP-MS) is applicable to trace multi-elemental and isotopic analysis of a wide range of matrices [1–4], although highly saline samples can cause both spectral interferences and matrix effects [5,6]. Typically, the elements of interest (transition metals and metalloids) are present at trace levels, and the high concentrations of alkaline earth and alkali metals can cause significant interferences in trace element determinations. In this situation, separation of the matrix components and preconcentration of analytes are frequently necessary. In the preconcentration step, metals are generally complexed by chelating agents. The chelating agent could be used in an immobilized form in a resin and packed into a chromatographic column. Metals can be released either by digesting the resin with acid [7] or by changing the ionic form of the resin. One of the most useful and frequently used methods employs an iminodiacetate chelating resin [8,9]. Recently, great importance was assumed by the development of a highly cross-linked macroporous poly(styrene–divinylbenzene) (PS–DVB) resin containing iminodiacetate functional groups with a high degree of physical integrity and

* Corresponding author.

☆ Paper presented at *the International Ion Chromatography Symposium 1994, Turin, 19–22 September 1994.*

0021-9673/95/$09.50
SSDI 0021-9673(95)00454-8

therefore with the possibility of operating at high pressures without physical degradation or alteration of the chemical properties of the resin. In this paper, the use of an automatic chelation system is described for matrix elimination and on-line preconcentration of rare earth elements (REE) and first-row transition metals in sea water prior to determination by ICP-MS.

2. Experimental

2.1. Instrumentation

A metal-free high-pressure chelation system (Chelation System 2; Dionex, Sunnyvale, CA, USA) including a gradient pump (GPM-2, Dionex) and a sample concentration module (SCM-1, Dionex) and equipped with a MetPac CC-1 column was used. The operation of all the components in the system is controlled by the operating program in the chromatography automation system (Autoion-400, Dionex), running on a microcomputer (IBM PS/50) interfaced through a computer interface module (CIM). The gradient pump was employed for delivering reagents during the matrix elimination, metal elution and chelating column reconditioning steps. A single reciprocating piston pump (DPQ, Dionex) was used for sample preconcentration on to the MetPac CC-1 column. The IC system was connected directly to the cross-flow nebulizer of the ICP-MS system with PTFE tubing.

Preconcentration and matrix elimination were carried out on a MetPac CC-1 (Dionex) column (50 mm × 4 mm I.D.) packed with a styrene-based macroporous 12% cross-linked iminodiacetate-functionalized chelating resin. The particle size was about 20 μm and the capacity of the resin was about 0.9 mequiv. Cu(II)/g.

All the elemental measurements were made on a Perkin-Elmer Elan 5000 ICP-mass spectrometer (Perkin-Elmer Sciex, Norwalk, CT, USA), equipped with two mass-flow controllers, a personal computer (IBM PS/2 70/386) and a printer (Epson EPL 7100). The element elution peaks were recorded in real time and stored on a hard disk with Elan V2.2 transient signal analysis software.

2.2. Reagents

Nitric acid (65%, w/v) and ammonia solution (25%, w/v), Suprapur, were obtained from Merck (Darmstadt, Germany) and 2.0 *M* ammonium acetate buffer (pH 5.5), Ultrapure, from Dionex. Deionized water (18 MΩ) was prepared with a Millipore water-purification system.

Synthetic sea water was prepared according to the ASTM D 1141 procedure [10] and subsequently purified by treatment at pH 5.5 with Chelex-100 resin (NH_4^+ form) [11].

Multi-elemental standard solutions were prepared from a 10 mg/l multi-elemental atomic absorption standard, ICP-MS Calibration Standard No. 1–2–3–4 (Perkin-Elmer), by dilution with demineralized water or synthetic sea water.

In the literature there are many examples of contamination derived from the pH probe, glass bottles and the reagents [12]. For this reason, all the sample and reagent preparations and handlings were conducted under a laminar-flow cleanhood (class 100) in order to reduce blank contaminations.

2.3. Procedure

A volume of 90 ml of the sample was buffered to 5.5 pH by adding 10 ml of 2.0 *M* ammonium acetate buffer solution (pH 5.5). An aliquot of 10 ml of this solution was loaded on to the Dionex MetPac-CC1 chelation column at 3 ml/min. The alkali and alkaline earth metals were eliminated by elution for 3 min at 3.0 ml/min with the ammonium acetate solution, and finally the elements under investigation were eluted with 2 *M* HNO_3 for 2 min at 3.0 ml/min. The operating programme and a scheme of the apparatus are reported in Table 1 and Fig. 1, respectively. The use of a multi-elemental technique such as ICP-MS allowed us to elute all the analytes in a single step with 2 *M* HNO_3 without considering the chromatographic separation,

Table 1
Ion chromatographic preconcentration programme

Step No.	Time (min)	Flow-rate (ml/min)	Eluent composition (%)			Valve position		Comments
			H_2O	CH_3COONH_4	HNO_3	V_5	V_6	
1	0.0	1.0	100	–	–	0	0	Start
2	0.1	3.0	–	100	–	1	1	Alkali metal elution
2f	2.9	3.0	–	100	–	1	1	
3	3.0	3.0	–	–	100	0	1	ICP-MS start reading
3f	5.5	3.0	–	–	100	0	1	ICP-MS end reading
4	5.6	3.0	–	–	100	1	1	Column washing
4f	7.5	3.0	–	–	100	1	1	
5	7.6	3.0	–	100	–	1	1	Column reconditioning
5f	11.0	3.0	–	100	–	1	1	
6	11.1	3.0	100	–	–	1	1	
7	14.0	3.0	100	–	–	0	0	Stand-by

therefore reducing the analysis time (see Table 2).

3. Results and discussion

In order to check the retention efficiency of the column with highly saline matrices, a series of preliminary off-line tests were performed. In these experiments we used the IC preconcentration unit separately from the ICP-mass spectrometer, and therefore the analysis consisted of two different steps: (1) loading of the sample and elution of the analytes from the column; and (2) the instrumental determination.

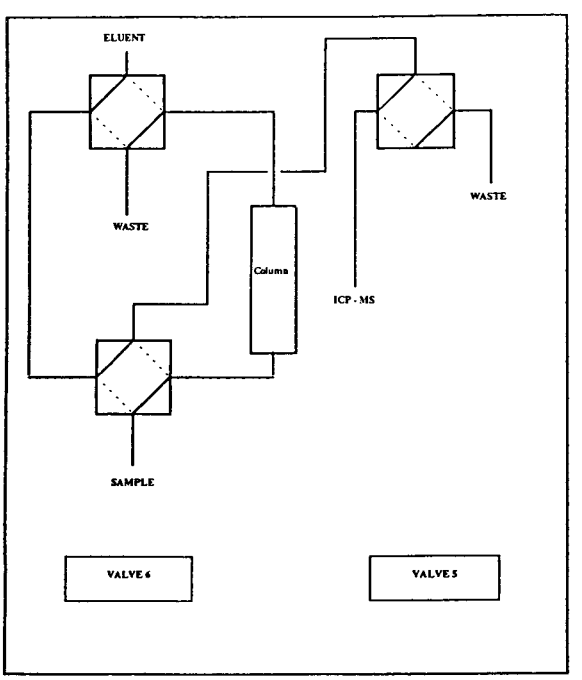

Fig. 1. Schematic diagram of the IC concentration system.

A multi-elemental standard solution (1 μg/l) was prepared in synthetic sea water by diluting the 10 mg/l multi-elemental atomic absorption standards (Perkin-Elmer). Different volumes (10, 100 and 500 ml) of the 1 μg/l multi-elemental synthetic sea water standard solution were loaded on the column, the alkali and alkaline earth metals were washed out according to the procedure described above and the elements under investigation were eluted with 10 ml of 2 *M* HNO_3. In this way, concentration factors of 1, 10 and 50 were obtained. The quantitative recoveries, calculated on the basis of three replicates and reported in Table 3, confirm that under the conditions tested the column permits the treatment of large volumes of highly saline samples.

In a second phase, in order to lower the volume of acid used for the elution of the metals, the handling of the samples and the consequent contamination of the system, we directly connected the IC and ICP-MS systems by means of PTFE tubing about 500 mm long. The IC concentration system is shown in Fig. 1. An increase

Table 2
Instrumental conditions for ICP-MS

Argon plasma flow (l/min)	14.5
Argon auxiliary flow (l/min)	0.95
Argon nebulizer flow (l/min)	1.00
Power (W)	1050
Sample uptake (ml/min)	1.0
Resolution (u)	0.8
Sweeps/readings	1
Readings/replicates	150
Point across peak	1
Dwell time (ms)	20
Scanning mode	Peak hop transient
Signal profile processing	Area integration

Element	Mass	Elemental equations
Mn	55	
Co	59	
Ni	60	
Cu	63	
Zn	66	
Y	89	
Cd	114	$Cd^{114} = Cd^{114} - 0.02747 \cdot Sn^{118}$
La	139	
Ce	140	
Pr	141	
Nd	144	$Nd^{144} = Nd^{144} - 0.2064 \cdot Sm^{147}$
Sm	152	$Sm^{152} = Sm^{152} - 0.01276 \cdot Gd^{157}$
Eu	153	
Gd	158	$Gd^{158} = Gd^{158} - 0.003604 \cdot Dy^{163}$
Tb	159	
Dy	164	$Dy^{164} = Dy^{164} - 0.04669 \cdot Er^{166}$
Ho	165	
Er	166	
Tm	169	
Yb	174	$Yb^{174} = Yb^{174} - 0.006632 \cdot Hf^{178}$
Pb	208	$Pb^{208} = Pb^{208} + Pb^{207} + Pb^{206}$
U	238	

Table 3
Recoveries (%) for preconcentration off-line tests on the MetPac-CC1 column

Element	Sample loaded (ml)[a]		
	10 ($f = 1$)[b]	100 ($f = 10$)	500 ($f = 50$)
Mn	105	102	102
Co	105	101	99
Ni	103	98	98
Cu	112	103	101
Zn	132	93	91
Y	106	111	100
Cd	85	95	96
La	101	102	100
Ce	104	104	99
Pr	103	99	99
Nd	106	99	98
Sm	102	96	96
Eu	99	96	96
Gd	102	100	99
Tb	97	96	96
Dy	88	96	97
Ho	87	95	95
Er	88	97	95
Tm	81	95	94
Yb	83	92	93
Pb	106	101	93
U	100	85	82

[a] Concentration of the multi-elemental solution = 1 μg/l (buffered at pH 5.5).
[b] f = Concentration factor: ml of solution loaded/ml of HNO_3 eluted.

in the sensitivity of detection and lower blank values were observed with this instrumental configuration.

A series of preliminary tests was carried out by loading various sample volumes in the range 5–200 ml. A sample volume of 10 ml was chosen as a compromise between the necessity for having detection limits adequate for the analytical needs and not too long analysis times. As an example, calibration with a blank and three standard solutions needs about 3.5 h: 3.3 min for the loading and 14 min for the analysis of each replicate, with three replicates for four solutions.

With very low concentrations of the analytes, as good retention on the column was observed, it will be possible to increase the enrichment factor by loading larger volumes of the samples.

Calibration of the ICP-MS system was performed by loading three times 10 ml of blank solution and three different multi-elemental standard solutions (1, 5, and 10 μg/l) in synthetic sea water. The linearity of the system was checked by calculating, on different days, the correlation coefficients of the curves; for all the elements these were better than 0.990.

The decrease in matrix interferences was con-

firmed by loading on the column 10-ml volumes of 1 μg/l multi-elemental standard solutions prepared in demineralized water and in synthetic sea water and comparing the respective intensities. The ratios of the instrumental signals (count/s), reported in Table 4, are close to 1 for all the elements.

These results confirm the possibility of using the Chelex 100 resin to eliminate the saline matrix of samples and to determine the analytes by ICP-MS after elution of trace metals with 2 *M* HNO_3.

In order to check the contamination that occurs in the system, we compared the contents of each analyte in the blank solutions: 10 ml of ammonium acetate buffer and 90 ml of demineralized water or synthetic sea water. As can be seen in Table 5, whereas for the REE there is no significant difference between the two matrices, the concentrations of the most common transition metals vary dramatically, confirming the presence of these elements in the salts used for the preparation of the synthetic sea water. This fact negatively influences the detection limits.

The detection limits for all the elements, calculated as three times the standard deviation of three replicates of the blank solution, are reported in Table 6, where the results obtained by loading a sample volume of 10 ml (demineralized and sea water solutions) and 100 ml of sea water solution are compared. The values obtained for the REE in demineralized and sea water are similar to those determined using the continuous pneumatic aspiration system. This means that the matrix elimination achieved by the IC system permits the determination of REE in sea water with the same detection limits as in demineralized water. An increase in the sample volume loaded resulted in a sensitive improvement of the performance.

The same behaviour was not observed for the transition and heavy metals, for which we noted higher contamination problems when using synthetic sea water. In this case only the values obtained in the demineralized water are similar to those determined by continuous aspiration; a

Table 4
Signal ratio between 1 μg/l multi-elemental standard in demineralized water and sea water solution

Element	Ratio: sea water/ demineralized water	Element	Ratio: sea water/ demineralized water
Mn	1.05	Sm	0.93
Co	0.91	Eu	0.94
Ni	0.88	Gd	0.93
Cu	0.85	Tb	0.92
Zn	0.85	Dy	0.91
Y	0.89	Ho	0.92
Cd	0.90	Er	0.89
La	0.98	Tm	0.90
Ce	0.99	Yb	0.92
Pr	0.90	Pb	0.86
Nd	0.92	U	0.85

Table 5
Typical values for a blank solution

Element	Concentration (ng/l)	
	Demineralized water	Sea water
Mn	80	141
Co	80	154
Ni	70	250
Cu	90	250
Zn	90	250
Y	3	7
Cd	20	186
La	4	14
Ce	20	82
Pr	1	4
Nd	3	8
Sm	10	19
Eu	4	13
Gd	10	10
Tb	1	5
Dy	10	7
Ho	1	3
Er	4	7
Tm	2	5
Yb	5	6
Pb	20	85
U	3	8

Sample volume loaded: 10 ml.

Table 6
Detection limits (ng/l) for on-line concentration method

Element	Continuous aspiration: demineralized water	On-line concentration		
		Demineralized water, 10 ml	Sea water	
			10 ml	100 ml
Mn	7	9	56	189
Co	19	8	14	25
Ni	36	49	102	104
Cu	11	50	63	37
Zn	44	100	123	102
Y	5	3	8	3
Cd	15	9	40	58
La	2	7	7	38
Ce	5	10	13	17
Pr	3	5	1	1
Nd	6	8	2	2
Sm	2	2	1	1
Eu	2	3	5	1
Gd	6	4	3	1
Tb	3	3	4	1
Dy	5	1	6	1
Ho	1	4	8	1
Er	4	3	9	1
Tm	2	4	3	1
Yb	3	1	5	18
Pb	5	16	50	145
U	2	15	12	21

worsening of the results was observed on increasing the sample volume from 10 to 100 ml.

We determined the precision of the determination by analysing three replicates of a 1 μg/l multi-elemental standard solution and calculating the relative standard deviation (R.S.D.). The precision was about 1% for Y, La, Ce, Pr, Nd, Sm and Eu, 2% for Gd, Tb, Tm and U, 3% for Dy, Ho, Er and Yb, 5% for Co, Cd, Mn and Pb and 10% for Ni, Cu and Zn.

Further purification of synthetic sea water and the insertion of a Chelex column in the buffer solution line significantly reduced the amount of metal ions introduced with the buffer or avoided large blank values for certain metals owing to accidental contamination of the buffer. This is particularly true for Zn, which usually gives high blank levels and is often subject to contamination from the laboratory environment.

4. Conclusions

Ion chromatography can be successfully used with ICP-MS for the simultaneous determination of transition metals and REE in sea water. The system makes it possible to remove the saline matrix and concentrate the analytes of interest. The instrumental conditions adopted allow 22 elements to be detected with detection limits, for 10 ml of sample, in the range 1–50 ng/l.

The precision of the results found for 1 μg/l of different analytes in sea water varied between 0.5 and 3% for REE and between 5 and 10% for transition elements. The use of a multi-elemental technique such as ICP-MS, moreover, permitted the throughput of the samples to be increased, as no separation of the different analytes was required.

This work confirmed that on-line preconcen-

tration is one of the best methods of sample pretreatment in ICP-MS. The procedure requires very few sample manipulations and reagent additions and for this reason very low blank levels are obtained.

References

[1] A.R. Date and A.L. Gray, Application of Inductively Coupled Plasma Mass Spectrometry, Blackie, London, 1989.
[2] U. Vollkopf and M. Paul, The Analysis of Environmental Samples by ICP-MS, Perkin-Elmer Technical Information N.4E, Perkin-Elmer, Norwalk, CT.
[3] A Stroh, At. Spectrosc., 13 (1992) 89.
[4] J.W. McLaren, D. Beauchemin and S.S. Berman, J. Anal. At. Spectrom., 2 (1987) 277.
[5] E.H. Evans and J.J. Giglio, J. Anal. At. Spectrom., 8 (1993) 1.
[6] A.R. Date, Y.Y. Cheung and M.E. Stuart, Spectroschim. Acta, Part B, 42 (1987) 3.
[7] C.J. Cheng, T. Akagi and H. Haraguchi, Anal. Chim. Acta, 198 (1987) 173.
[8] W.W. Van Berkel, A.W. Overbosch, G. Feenstra and F.J.M. Maessen, J. Anal. At. Spectrom., 3 (1988) 249.
[9] J.W. McLaren, J.W.H. Lam, S.S. Berman, K. Akatsuka and M.A. Azeredo, J. Anal. At. Spectrom., 8 (1993) 279.
[10] ASTM D1141, Specification for Substitute Ocean Water 1989, Annual Book of ASTM Standards, Vol. 11.02, Water (II), ASTM, Philadelphia, 1989.
[11] R. Boniforti, R. Ferraroli, P. Frigeri, D. Heltai and G. Queirazza, Anal. Chim. Acta, 162 (1984) 33.
[12] D. Beauchemin, J.W. McLaren, A.P. Mykytiuk and S.S. Berman, J. Anal. Atom. Spectrom., 3 (1988) 305.

ELSEVIER

Journal of Chromatography A, 709 (1995) 283–290

JOURNAL OF CHROMATOGRAPHY A

Computer program for simulating the performance of thick-bed diffusive samplers: predicted and experimental sample loss due to reversible adsorption

E. Nordstrand

Department of Analytical Chemistry, Stockholm University, 106 91 Stockholm, Sweden

First received 13 January 1995; revised manuscript received 7 April 1995; accepted 7 April 1995

Abstract

Using experimentally determined adsorption isotherm constants, a computer model of the performance characteristics of thick-bed diffusive samplers was developed. The model has previously been used to calculate effective uptake rates, and it is now shown that it will predict the loss of sample due to reversible adsorption. The predicted losses of pentane, hexane, heptane and toluene from Tenax® TA and Chromosorb® 106 compare well with experimental data. The samplers were exposed for 2–16 h, followed by desorption for 2–21 h. The largest deviation between predicted and experimental values was found for pentane on Tenax TA, where the average experimental loss was 30% and the average predicted loss was 41%. Pentane on Chromosorb 106 showed an average experimental loss of 20% while the predicted loss was 19%. Possible applications are the measurements of strongly bound compounds in air, determined with high accuracy, while doing screening measurements of weaker bound compounds, with a less but estimated accuracy, on the same adsorbent.

1. Introduction

Diffusive sampling, where air pollutants are collected on a sorbent by diffusion rather than by active pumping, is a continuously growing technique. The applications include sampling of both organic and inorganic compounds in air [1–5]. The growing interest in the technique is due to its relatively low price and simplicity; no pumps are needed and the sampler can be made small and low-weight. Diffusive samplers are, therefore, well suited for long-time personal exposure measurements and for other long-time measurements requiring a large number of sampling points.

The practical use of diffusive samplers, containing an adsorbent, is usually limited to compounds that are strongly retained by the sorbent. The uptake rate for strongly retained compounds will essentially be constant, irrespective of concentration levels and exposure time. Weakly retained compounds will not show constant uptake rates, as the sorption is balanced by desorption. The problems are generally greater for samplers designed for thermal desorption than for samplers intended for liquid desorption, as the adsorbents used for thermal desorption usually are weaker than those used for liquid desorption.

In the present work a thick-bed tubular diffu-

0021-9673/95/$09.50
SSDI 0021-9673(95)00445-9

sive sampler containing adsorbents designed for thermal desorption has been studied in view of this problem.

It is now possible to predict the effective (reduced) uptake rates for thick-bed diffusive samplers by a computer model based on experimentally determined adsorption isotherms [6–8]. Prediction can also be based on retention volumes [9,10]. However, the applicability of retention volumes is limited to the linear region of the adsorption isotherm, whereas an accurate determination of the adsorption isotherm constants gives the possibility to describe the adsorption/desorption behavior of the sampler over the entire range of the measured adsorption isotherms.

Severe problems arise when adsorbents having a weak interaction with a specific analyte are used for monitoring of that compound if the air concentration decreases. In such cases, a net loss of the analyte will occur due to desorption. Such desorptive losses can be large, and the suitability of an adsorbent for specific analytes and sampling conditions should be evaluated bearing this in mind [11,12]. If the concentration of an analyte varies greatly during the sampling period, the average concentration could be greatly underestimated if the analyte is lost by reversible adsorption; high concentrations in the beginning or in the end of a sampling period would thus give different time weighted average (TWA) concentrations. In terms of the error bounds in diffusive sampling, the effects of such sample losses on sampling precision have been discussed by Underhill [11] and Bartley et al. [12,13].

The loss of weakly sorbed analytes from different types of diffusive samplers has been described by assuming a linear sorption isotherm [14,15]. This approximation is valid for liquid sorbents, but for solid sorbents it is applicable only over a limited concentration range. Some adsorbent/adsorbate interactions, e.g. the adsorption of benzene and chloroform on Tenax® TA, are adequately described by linear adsorption isotherms at low concentrations [11]. At higher concentrations the adsorption isotherms for solid adsorbents are, in most cases, non-linear [11,14], and thus the desorptive losses are not accurately described by models based on linear adsorption isotherms.

Van den Hoed and Van Asselen [7] presented a computer program for predicting effective uptake rates by thick-bed diffusive samplers, based on experimentally determined adsorption isotherms. Nordstrand and Kristensson [6] expanded this program to include, among other things, a model for net desorption effects due to reversible adsorption. A test of the capability of this computer model to estimate desorptive losses is presented here. The method was to load the sampling tube with the investigated compound by diffusion and then study the loss of the compound from the adsorbent in clean air. This loss is not very dependent upon a stable exposure concentration, as long as it is continuous and at about the same level of concentration over the whole exposure period. Chromosorb® 106 and Tenax TA were used as adsorbents, and *n*-pentane, *n*-hexane, *n*-heptane and toluene as adsorbates.

2. Experimental

2.1. Generation of test atmospheres

An exposure chamber consisting of a brass tube (50 × 3 cm I.D.) with fittings to attach 12 diffusive samplers was fed with compressed air via PTFE tubing. A short section of PTFE tubing was replaced by silicon tubing which led the vapour, via a fused-silica capillary, from the vapour generator (vide infra) into the air stream. The linear airflow, calculated from the airflow and the cross-sectional area, was 12 cm/s.

The standard gas atmosphere was generated either by diffusion cells or static pressure pumps. The diffusion cell was a stainless steel container, coupled to a piece of stainless steel tubing, simplified after Schoene and Steinhanses [16] (no electronic flow control valve or differential manometer). A static pressure pump was obtained by putting one end of a fused-silica capillary under the surface of the liquid under investigation and applying pressure with compressed air (Fig. 1).

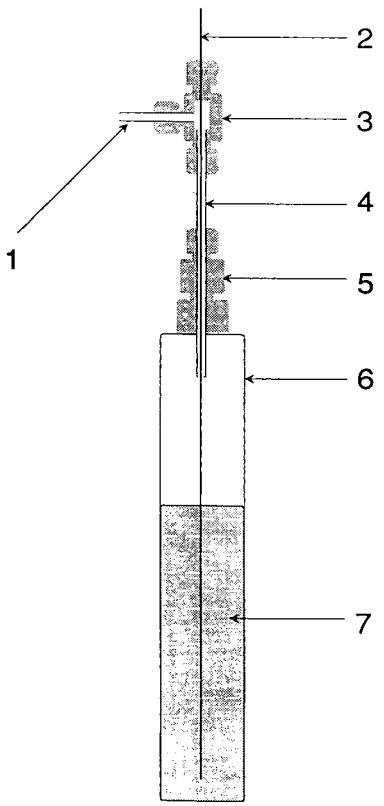

Fig. 1. Constant pressure pump for the exposure system. (1) Inlet for compressed nitrogen, pressure controlled; (2) fused-silica capillary; (3) Swagelock T-piece (1/16″); (4) steel tubing (1/16″); (5) Swagelock reducer (1/16″ to 1/4″); (6) stainless steel canister; (7) liquid to be introduced into the exposure system.

The free end of the capillary was placed in the airstream by piercing the silicon tubing. The liquid was pressed at a constant speed into the air stream, vaporized, and further transported to the exposure chamber. The dimensions of the stainless steel tubing and fused-silica capillary (length and internal diameter) as well as the air pressure were adjusted to give the desired air concentrations in the exposure chamber.

Due to the high heat of vaporization of some analytes, such as pentane, water will condensate from the air and freeze on the tip of the capillary. To avoid this, a section of stainless steel tubing was inserted into the air stream, after the silicon tubing. The free end of the capillary was put into contact with the wall of the stainless steel tube, which would then conduct a sufficient amount of heat to the tip of the capillary to keep the capillary tip free from frost.

The concentrations generated were determined at the beginning and the end of each exposure period by pumping air from the exposure chamber (50–250 ml) through two or three adsorbent tubes containing Tenax TA. The concentrations determined in this way differed in most cases by less than 2%, but at the most by 20%. The largest differences occurred when long exposure periods and low concentrations were used. The diffusion cell was preferable when low concentrations were desired, whereas the constant pressure pump was used to generate the higher concentrations.

The sample loss due to reversible adsorption was studied in a separate chamber under a flow of clean air. No special measures were taken to filter the air, since no detectable amounts of the investigated or other similar compounds were found when sampling actively one litre of the air onto an adsorbent tube.

2.2. Exposure of the diffusive samplers

Diffusive samplers, ATD (automatic thermal desorption) diffusive tube (mean cross-sectional area of 0.193 cm^2, a mean air gap length of 1.51 cm [9]; Perkin-Elmer, Beaconsfield, Buckinghamshire, UK [17]), containing either Tenax TA (60/80, Alltech Associates, Deerfield, IL, USA) or Chromosorb 106 (60/80, Alltech), were exposed at 22°C unless otherwise specified. Twelve samplers could be exposed in each experiment. There was no detectable difference in analyte uptake among the twelve sampling positions. After exposure, four samplers were used to determine how much of the analyte had been taken up, the other tubes were sealed and removed to the clean air chamber for study of the loss due to reversible adsorption. In each experiment, four tubes were subject to the short desorption time (time 1) and four to the long desorption time (time 2), except where otherwise stated. The tubes were removed from the clean air chamber and sealed at the end of the

desorption periods. Exposure times were between 2 and 16 h, followed by desorption in the clean air chamber for 2 to 21 h.

2.3. Instrumentation

The samplers were analyzed on a Perkin-Elmer automatic thermal desorption unit, ATD 50, coupled to a Perkin-Elmer GC-8500 equipped with a flame ionization detector (FID). The desorption temperature varied between 220°C and 250°C depending on the adsorbent/analyte combination. Helium was used as desorption gas. The cold-trap was packed with Tenax TA, and the split flow was varied depending on the exposure concentration and sampling time, so as to give good peaks on the GC. The column was a CPWAX 52 CB (25 m × 0.32 mm I.D., 1.2 μm film thickness, Chrompak International, Middelburg, Netherlands) with helium at 1.6 ml/min as carrier gas. The temperature programme was adjusted to suit the individual analytes.

2.4. Determination of the adsorption isotherm constants

The adsorption isotherms used in this study have been measured for equilibrium concentrations on Tenax TA up to 30 ppm for pentane and up to 80 ppm for toluene [7]. The highest concentrations used for Chromosorb 106 were between 40 ppm (hexane) and 70 ppm (pentane and toluene) [7]. Adsorption isotherm constants for many compounds can be found in the literature. Adsorption isotherm constants for many compounds on Tenax TA, Chromosorb 106, Carbopack B can be found in Refs. [7,8,18,19].

3. Results and discussion

3.1. Experimental and predicted retention of compounds by the adsorbent

Experimentally determined and calculated exposure concentrations are presented in Tables 1 and 2. The calculated exposure concentrations are based on the amount of the analyte adsorbed by the adsorbent tube after exposure, the exposure time, and the adsorption isotherm constants [6,7]. These are used by the programme to estimate sample loss due to reversible adsorption. The ratio between effective and ideal uptake rates, (U_{eff}/U_{id}), shows the error that results from using the ideal instead of the effective uptake rate for calculating the exposure concentration. The analyte loss ratio $(W_x/W_{exp}$, where $x = 1$ or 2) after each desorption period is calculated from the amount initially adsorbed in each exposure experiment.

The deviations between calculated and experimental results are summarized in Table 3. The average sum of the difference between the calculated and experimental desorption losses is a measure of the systematic deviation between model and experimental results. There is no apparent general trend of the model to under- or overestimate the loss. The size of the prediction error is given by the average absolute differences of the calculated and experimental desorption losses. With the exception of pentane, the deviations could result from imprecision in the determination of the different ratios.

In the early studies of this computer model, the relative standard error of the prediction of effective uptake rates was determined to be 8% [7]. The average experimental desorption loss in the present study was 15%. The losses calculated by the computer program differed, on average, from the experimental value by 6% of the whole (Table 3). In a study of sample loss due to reversible adsorption, using trichloroethylene at 25 ppm and activated charcoal [14], the random error for the deviation between model and experimental results during the desorption period was 6%.

The largest deviation between model and experimental results in Table 3 is found for pentane on Tenax TA, where the loss is overestimated by more than 10%. This is the weakest combination of adsorbent/adsorbate in this study. It indicates a deficiency in the model when used to describe either the transport from the adsorbent to the air, or the transport within the adsorbent bed, when high concentrations of

Table 1
Experimental and calculated results from exposure of Tenax TA

Compound	C [ppm (v/v)]		Exposure time (min)	W_{exp} (μg) (R.S.D.)	U_{eff}/U_{id}	Desorption time 1 (min)	W_1/W_{exp} (R.S.D.)	Calc W_1/W_{exp}	Desorption time 2 (min)	W_2/W_{exp} (R.S.D.)	Calc W_2/W_{exp}
	Exp	Calc									
Pentane	34	33	180	5.7 (5%)	0.51	147	0.81[d] (8%)	0.69	417	0.65 (6%)	0.54
Pentane[a]	51	54	131	7.2 (2%)	0.54	179	0.71[d] (2%)	0.62	361	0.65 (3%)	0.52
Hexane	0.46	0.3	635	0.39 (4%)	0.78	300	0.91 (7%)	0.88	530	0.80 (5%)	0.84
Hexane	7.8	7.6	240	2.8[d] (4%)	0.74	180	0.88[d] (5%)	0.83	360	0.74[d] (8%)	0.76
Hexane	15	13	246	4.5[d] (4%)	0.70	182	0.87 (5%)	0.82	371	0.68 (5%)	0.74
Hexane	16	10	120	1.9 (3%)	0.81	182	0.81 (4%)	0.80	360	0.74 (4%)	0.73
Hexane	134	165	180	35.8 (7%)	0.58	–	–	–	480	0.74 (8%)	0.61
Heptane	4.5	3.0	240	2.0[d] (6%)	0.97	183	0.97 (7%)	0.95	363	0.92[d] (7%)	0.93
Heptane	29	26	115	5.9[d] (4%)	0.90	175	1.02 (8%)	0.90	360	0.94 (5%)	0.87
Heptane	180	154	176	41 (7%)	0.67	183	0.76 (15%)	0.83	364	0.77[d] (8%)	0.78
Toluene	0.35	0.2	312	0.15[d] (1%)	1.0	251	1.02[d] (6%)	1.0	1252	0.90[d] (7%)	0.98
Toluene	0.4	0.25	971	0.54 (4%)	0.97	240	0.94 (4%)	0.98	739	0.85[d] (6%)	0.96
Toluene[b]	12	12	178	4.6[d] (8%)	0.95	363	0.89[d] (10%)	0.90	1130	0.80[d] (11%)	0.83
Toluene[c]	241	299	182	94[d] (1%)	0.74	181	0.76 (2%)	0.83	354	0.73[d] (4%)	0.76

[a] $T = 23.5$°C.
[b] $T = 27.0$°C.
[c] $T = 27.5$°C.
[d] $n = 3$, all others $n = 4$.
C = Concentration of the analyte in air. Exp/Calc = measured experimental concentration/calculated concentration according to computer program, collected mass and exposure time. W_{exp} = mass of analyte taken up by the adsorbent and relative standard deviation (R.S.D.). U_{eff}/U_{id} = the effective uptake rate calculated according to the computer program/the ideal uptake rate according to the computer program. W_x/W_{exp} = the mass of the analyte on the adsorbent after the desorption period, x (1 or 2), divided by W_{exp}. W_x/W_{exp}, R.S.D. = relative standard deviation of the ratio, approximated as the square root of the sum of the relative variances of the respective measurements. Calc W_x/W_{exp} = the mass of the analyte on the adsorbent after clean air exposure, as calculated in the computer program, divided by W_{exp}.

analyte are present. The highest equilibrium concentration used for calculating the adsorption isotherm for pentane on Tenax TA was approximately 30 ppm [7]. The experiments in this study have thus been performed near the upper limit of the described adsorption isotherm, and an

Table 2
Experimental and calculated results from exposure of Chromosorb 106

Compound	C [ppm(v/v)]		Exposure time (min)	W_{exp} (mg) (R.S.D.)	U_{eff}/U_{id}	Desorption time 1 (min)	W_1/W_{exp} (R.S.D.)	Calc W_1/W_{exp}	Desorption time 2 (min)	W_2/W_{exp} (R.S.D.)	Calc W_2/W_{exp}
	Exp	Calc									
Pentane	12	12	290	5.5 (5%)	0.88	215	0.81 (8%)	0.90	395	0.77 (5%)	0.84
Pentane[a]	51	45	122	9.7 (8%)	0.92	354	0.85 (9%)	0.81	539	0.79[d] (9%)	0.76
Hexane	0.40	0.38	760	0.58 (3%)	0.99	390	1.01 (5%)	0.98	715	1.01 (8%)	0.97
Hexane	132	160	200	63 (11%)	0.95	235	0.79 (14%)	0.92	740	0.79 (14%)	0.84
Toluene	1.3	1.8	312	1.3[d] (3%)	1.0	692	0.94[d] (4%)	1.0	1172	0.88[d] (3%)	0.99
Toluene	241	227	180	94 (2%)	0.98	182	1.01[d] (10%)	0.96	353	0.94[d] (2%)	0.94

See Table 1 for explanation of headings and footnotes.

Table 3
Summary of the deviation between calculated and experimental results

Adsorbent and compound	Average experimental desorption loss (%)		Average (Calc − Exp) desorption loss (%)		Average |Calc − Exp| desorption loss (%)	
	Time 1	Time 2	Time 1	Time 2	Time 1	Time 2
Tenax TA						
Pentane	24	35	+11	+12	11	12
Hexane	13	26	+4	−3	4	5
Heptane	9	12	+2	+3	6	3
Toluene	10	18	−3	−6	3	6
Chromosorb 106						
Pentane	17	22	−3	+2	7	5
Hexane	10	10	−6	−1	8	4
Toluene	3	9	+2	−6	2	6
Average	12	19	+1	+0.4	6	6

Time 1/Time 2 = Shorter/longer desorption period in each experiment, see Table 1,2. Calc = calculated loss of analyte according to computer program. Exp = experimental loss of analyte.

expansion of the isotherm could solve some of the above problems.

When comparing C_{exp} and C_{calc} in Table 1 and according to Refs. [7,9], it seems possible to estimate the exposure concentration for the poor combination of pentane on Tenax TA in spite of the strongly reduced uptake rate. This could give a false impression of the possibility to analyze pentane using diffusive samplers packed with Tenax TA, since the possible errors due to reversible adsorption and concentration fluctuations, in this case, can be very high.

Table 1 shows that when pentane (33 ppm, Tenax TA) is present in the first 180 min of the 597 min (10 h) total sampling period (exposure + long desorption time) the sample loss equals 35%. For the whole sampling period of 597 min, the correct TWA concentration should be 10 ppm (v/v). Applying the computer program on the residual experimental mass after the end of the 597 min gives an estimated concentration of 9 ppm, a deviation of 10% from the correct TWA. If the exposure to pentane had been performed in the last, instead of in the first, part of the sampling period, the calculated concentration would, instead, be 14 ppm, a deviation of 40%.

It is evident that the decrease in sampling rate resulting from the high concentration pulse in the beginning of the sampling period, has been reduced in the computer model by the prolonged total sampling period (exposure + desorption), thereby counterbalancing the effects of sample loss incurred by reversible adsorption. These factors have the opposite effect for a concentration pulse at the end of the sampling period. It is therefore possible to use Tenax TA for measuring pentane in a stable environment without fluctuating concentrations, provided that the adsorbent is not saturated during the exposure period. In an environment with unstable concentrations, it would be possible to estimate maximum sampling errors based on prior knowledge, or assumption, of the fluctuation pattern in the studied air.

It is interesting to note that a strong combination of adsorbent/adsorbate, such as toluene on Tenax TA, also suffers from sample loss due to high concentrations or long sampling times (Table 1). The resulting loss is not negligible and

should be considered when sampling toluene for several hours, or at high concentrations, utilising Tenax TA. However, the reduction in uptake rate is a minor problem compared with the potential net sample loss in an environment with strongly fluctuating concentrations.

The calculations of effective uptake rates and losses due to reversible adsorption are based on the measured adsorption isotherm of the adsorbent and the adsorbate in single combination [7]. This works well in single-component atmospheres where no interfering compounds are present. However, the adsorption isotherm for a particular compound may change if another compound is present at high concentrations. Vejrosta et al. [20] showed that the adsorption of 0.5 ppmv benzene, by Tenax GC, decreased even in the presence of about 10 ppbv of *o*-xylene. Increasing the concentration of *o*-xylene by three orders of magnitude decreased the partition coefficient of benzene by a factor of approximately 5. Coadsorption could thus limit the applicability of these methods when interfering compounds are present in the sampled atmosphere. This study [20] was performed under equilibrium conditions. However, a prerequisite for a well functioning diffusive sampler is that equilibrium is never attained. More work has to be done to investigate the severeness of competitive adsorption during diffusive sampling.

4. Conclusion

For thick-bed diffusive samplers, the computer program [6] offers the possibility to calculate effective (reduced) uptake rates and estimate possible net sample loss due to reversible adsorption, provided that the adsorption isotherm for the adsorbent/adsorbate pair is known. It is then possible to calculate the effective uptake rates and also to estimate sample loss due to reversible adsorption during fluctuating concentrations of adsorbate. The errors can be estimated and compared with the need for accuracy of the measurement.

When screening for the presence of compounds in air, the demand of accuracy of a TWA is less than 50% expressed as relative overall uncertainty [21]. If the adsorption isotherms are determined, thick-bed diffusive samplers could thus be used for the screening of many, weak bound, compounds. For instance, it could be possible to measure styrene with high accuracy with Tenax TA and at the same time performing screening measurement of hexane with a less, but estimated, accuracy.

The presence of coadsorbing compounds in the air could however change the adsorption isotherm of the analyte on the sorbent [20]. This could severely limit the applicability of the suggested approach to describe the performance of the diffusive sampler.

Acknowledgement

The author is grateful to Dr. Henrik Kylin for his help in the preparation of the manuscript.

References

[1] R. Williams, A. Collier and J. Lewtas, Indoor Environ., 2 (1993) 98.
[2] M. Lee, Y. Yanagisawa, M. Hishinuma, J.D. Spengler and I.H. Billick, Environ. Sci. Technol., 26 (1992) 697.
[3] J.-M. Lin and T.-S. Lin, Toxicol. Environ. Chem., 39 (1993) 229.
[4] W. Mailahn, B. Seifert, D. Ullrich and H.-J. Moriske, Environ. Int., 15 (1989) 537.
[5] T. Yasugi, T. Kawai, K. Mizunuma, S. Horiguchi, H. Iguchi and M. Ikeda, Int. Arch. Occup. Environ. Health, 63 (1992) 449.
[6] E. Nordstrand and J. Kristensson, Am. Ind. Hyg. Assoc. J., 55 (1994) 935.
[7] N. van den Hoed and O.L.J. van Asselen, Ann. Occup. Hyg., 35 (1991) 273.
[8] J. Unwin, Report, 93/7, Health and Safety Executive, Research and Laboratory Services Division, Occupational Medicine and Hygiene Laboratory, Broad Lane, Sheffield S3 7HQ, UK.
[9] M.D. Wright, Report, 93/3, Health and Safety Executive, Research and Laboratory Services Division, Occupational Medicine and Hygiene Laboratory, Broad Lane, Sheffield S3 7HQ, UK.
[10] R.W. Coutant, R.G. Lewis and J. Mulik, Anal. Chem., 57 (1985) 219.
[11] D.W. Underhill, Talanta, 40 (1993) 143.

[12] D.L. Bartley, G.J. Deye and M.L. Woebkenberg, Appl. Ind. Hyg., 2 (1987) 119.
[13] D.L. Bartley, Am. Ind. Hyg. Assoc. J., 44 (1983) 879.
[14] D.L. Bartley, M.L. Woebkenberg and J.C. Posner, Ann. Occup. Hyg., 32 (1988) 333.
[15] J.C. Posner and G. Moore, Am. Ind. Hyg. Assoc. J., 46 (1985) 277.
[16] K. Schoene and J. Steinhanses, Fresenius J. Anal. Chem., 335 (1989) 557.
[17] R.H. Brown, J. Charlton and K.J. Saunders, Am. Ind. Hyg. Assoc. J., 42 (1981) 865.
[18] N. van den Hoed and M.T.H. Halmans, Am. Ind. Hyg. Assoc. J., 48 (1987) 364.
[19] K. Schoene, J. Steinhanses and A. König, Fresenius J. Anal. Chem., 336 (1990) 114.
[20] J. Vejrosta, M. Roth and J. Novak, J. Chromatogr., 265 (1983) 215.
[21] Workplace atmospheres–General requirements for the performance of procedures for the measurement of chemical agents. European Committee for Standardization, EN 482 (1994).

ELSEVIER

Journal of Chromatography A, 709 (1995) 291–301

JOURNAL OF CHROMATOGRAPHY A

Characterization of micropacked alkyl-bonded silica columns for gas chromatographic analyses of light hydrocarbons in planetary atmospheres

S.O. Akapo

NASA–Ames Research Center, Mail Stop 239-12, Moffett Field, CA 94035-1000, USA

First received 3 March 1995; revised manuscript received 18 April 1995; accepted 18 April 1995

Abstract

Micropacked columns of different types of chemically bonded *n*-octyl- and *n*-octadecyl stationary phases were prepared and evaluated for the separation of light hydrocarbons under isothermal conditions. Column selectivities and efficiencies varied with surface coverage and the functionality of the silanizing agents. As might be expected, solute retentions are higher on the C_{18} phases than on the C_8 phases due to the increased effective interactive surface between the solute and the stationary phase. Among the phases examined, the polymeric *n*-octadecyl packings gave the highest plate number and better retention characteristics for the test solutes. The H versus $\bar{u}$ plots obtained revealed the applicability of the columns for fast analysis at low linear carrier-gas velocities and correspondingly low volumetric flow-rates without any substantial loss in efficiency. Within the temperature range investigated, thermal-stability experiments indicate that the polymeric *n*-octadecyl phase can be used at temperatures up to 250°C with little or no column bleed.

1. Introduction

The understanding of chemical evolution and the origin of life in the solar system form part of NASA's exobiology program. Clearly such investigations require the development of analytical techniques that are both highly sensitive and precise for the identification of compounds that might be present in planetary atmospheres. Even though conventional chromatography was successfully used for in situ analyses of the atmospheric constituents of Mars [1,2] and Venus [3], the relatively long time required to complete each analysis prevented the collection and analyses of more samples while the probe descends [4]. Similar problems are anticipated in future planetary missions such as the Galileo, Cassini, Mars Pathfinder, Mars Surveyor, and Rosetta missions. For instance, the proposed NASA–ESA Cassini mission, planned to be launched in 1997 [5] to explore the atmosphere of Titan, will involve the collection and analyses of complex mixtures of low-molecular-mass hydrocarbons, nitriles, dinitriles, CO, H_2, and CO_2 in the presence of large amounts of methane, N_2, and Ar during the probe descent.

To solve some of these problems, Do and Raulin [6,7] studied the chromatographic behavior of PoraPLOT and Al_2O_3–KCl porous-layer open tubular (PLOT) capillary columns for the analysis of light gases. While the columns produced good resolution of the test solutes in a

0021-9673/95/$09.50
SSDI 0021-9673(95)00479-3

relatively short time, they were, however, found unsuitable for gas chromatographic experiments aboard spacecraft due to their poor mechanical strength. Also, bleeding of the stationary phase encountered during temperature programming make CP-Sil-5 CB WCOT capillary columns unviable for space applications [8]. Although a Molsieve PLOT capillary column allows the separation of permanent gases in the presence of hydrocarbons and nitriles, its mechanical strength appears too weak to withstand the rigors of launch and space flight [9,10].

In the light of the aforementioned, micropacked columns might be a suitable alternative for capillary columns because of their high sample-loading capacity, low flow-rate, low bleeding of the liquid phase, and small value of the mass-transfer coefficient, C, of the van Deemter equation [11–14]. Such columns with narrow inner column diameter ($d_c \leq 1$ mm) have been shown to give high efficiency and outlet flow-rates that satisfy the optimum flow conditions into the mass spectrometer, making them suitable for gas chromatography–mass spectrometry (GC–MS) coupling [15–17]. In view of the anticipated limitations in terms of size, weight, power, and consumables in future planetary missions, the above properties of micropacked columns could be of special benefit for GC–MS experiments aboard a spacecraft [4,18].

More recently, de Vanssay et al. [10] showed that molecular sieve 5A micropacked could be used for fast analysis of permanent gases under isothermal conditions with high efficiency and low column-head pressure. However, the C_2 hydrocarbons were poorly resolved on this column due to their long retention times and poor peak shape. Therefore, micropacked GC columns containing chemically bonded stationary phases with the ≡Si–O–Si bond type may be a better choice for the determination of low-molecular-mass hydrocarbons. Since this type of packing material can provide high separation efficiency, sample capacity, and high stability capable of withstanding the rigors of launch and space flight, its potential importance in future space missions is currently under investigation. The present paper describes the synthesis of a series of alkyl-bonded silica packings using mono-, di-, and trifunctional chlorosilanes. Data on gas flow and chromatographic characteristics of the columns, including van Deemter curves for selected light hydrocarbons, are reported.

2. Experimental

2.1. Materials and chemicals

Porasil C (particle size 149–177 μm, surface area 100 m^2/g, pore diameter 300 Å) silica was purchased from Waters Associates (Millipore, Milford, MA, USA). Octyldimethylchlorosilane, octylmethyldichlorosilane, and octyltrichlorosilane were prepared by hydrosilation reaction [19] of distilled octene (Aldrich, Milwaukee, WI, USA) with the appropriate hydrosilane (United Chemical Technologies, Bristol, PA, USA). Each reaction was catalyzed by chloroplatinic acid (Aldrich). Octadecyldimethylchlorosilane and octadecyltrichlorosilane were obtained from United Chemical Technologies and used as received. Toluene, tetrahydrofuran, methylene chloride, and methanol were obtained from general sources and used as received.

2.2. Synthesis of stationary phases

Prior to the preparation of the stationary phases, about 20 g of silica were refluxed with 3 *M* HCl at 100°C for 2 h, rinsed thoroughly with deionized water, and dried overnight at ca. 150°C in an oven. The monomeric phases were prepared under anhydrous conditions, as follows. About 3 g of silica was added to a warm solution of 30 ml dry toluene and 10 ml of the appropriate monofunctional silane in a 100-ml two-neck round-bottom flask. The slurry was refluxed for 4 h at 110°C under gentle helium (99.999% UHP He) flow. After cooling, the silylated silica was transferred into a sintered glass crucible and washed with dry toluene, methylene chloride, methanol, methanol–water (50:50, v/v), and finally with methanol under

suction. The cleaned particles were then end-capped by refluxing for 2 h in a mixture of 30 ml toluene and 8 ml HMDS–TMCS (hexamethyldisilaxane–trimethylchlorosilane, 1:1 molar ratio) at 100°C. The final product was again washed as described above, dried under vacuum in a desiccator, and stored in a dry bottle for characterization. In a similar manner, monomeric phases using di- or trifunctional silanes were prepared. However, prior to endcapping, the bonded phases were refluxed with 50% THF–H_2O for 1 h at 80°C to remove any unreacted chlorine atoms.

The following procedure was employed for the preparation of the polymeric phases using di- or trifunctional silanes. About 3 g of silica were dispersed in a warm solution of 30 ml dry toluene and 10 ml of the appropriate silane in a two-neck round-bottom flask. One milliliter of water was immediately added to the mixture to initiate self-polymerization of the silane and the slurry was refluxed for 5 h under a slow helium flow. The derivatized silica was filtered using a sintered glass crucible and washed as described above. Samples were dried under vacuum in a desiccator and kept in dry bottles for evaluation.

The amounts of stationary phase on the bonded supports were determined by elemental carbon analysis of the dried samples.

2.3. Column packing

The bonded phases were packed into stainless-steel tubes (2.0 m × 1.07 mm I.D.; No. 304) which had been pretreated by washing successively with HCl (20%), distilled water, methanol, and acetone and then purged with helium gas. The tubes were fitted with Swagelok low dead volume connectors. The columns were dry packed in vertical position with one end, loosely plugged with silanized glass wool, connected to a vacuum pump and a small stainless-steel reservoir was attached to the open end. The packing material was slowly added to the reservoir on starting the vacuum pump and the particles were continuously transported into the column while moving a hand vibrator along the column. The column was considered filled when there was no reduction in the volume of the packing material after a few minutes of vibration. The column inlet was then sealed with silanized glass wool and installed in the gas chromatograph. All columns were conditioned overnight at 110°C under helium-gas purge at 5 ml/min before use.

2.4. Gas chromatograph

The columns were evaluated on a gas chromatograph equipped with a micro thermal conductivity detector (TCD) and control (Carle Instruments, Fullerton, CA, USA) and a Hewlett-Packard HP 3396 Series II integrator (Hewlett-Packard, Avondale, PA, USA). UHP helium (99.999% He) was used as carrier gas for all measurements. To remove traces of water and oxygen from the helium, the carrier gas line was connected to a Matheson Hydrox purifier, Model 8301 (Matheson Gas Products, Secaucus, NJ, USA). A gas mixture of 1000 ppm each of methane (C_1), ethane (C_2), propane (C_3), and butane (C_4) in helium (Matheson Gas Products) was used to evaluate the chromatographic performance of the columns. The sample mixture was injected into the column with an eight-port Valco (Alltech, Deerfield, IL, USA) valve fitted with two 100-μl sample loops. All experiments were performed under isothermal conditions.

2.5. Chromatographic parameters

The capacity factor, k', was determined from the expression $k' = (t_R - t_o)/t_o$, where t_R is the retention time of the solute and t_o is the hold-up time determined by injecting nitrogen as a marker. The average linear gas velocity values ($\bar{u}$), calculated from the expression $\bar{u} = L/t_o$ (where L is the column length in cm), were obtained by varying the inlet pressures of the carrier gas from 1.38 to $4.14 \cdot 10^5$ Pa at the operating temperature. The carrier gas flow-rate was measured at the column outlet using a soap-bubble flow meter. Assuming the peaks to be symmetrical and Gaussian, the theoretical plate height, H, for the test solutes were calculated from

$$H = \frac{L}{5.54}\left[\frac{w_{0.5}}{t_R}\right]^2, \quad (1)$$

where $w_{0.5}$ is the peak width at half height in time units. The separation factor, α, and column plate number, N, were calculated in the usual manner.

3. Results and discussion

The objective of this study was to investigate the viability of micropacked columns containing alkyl-bonded silicas for GC analysis of light hydrocarbons in planetary atmospheres. These columns are considered suitable for this application due to their high efficiency, speed, selectivity, and thermal stability when compared with conventionally coated columns. The physical characteristics of the packing materials are shown in Table 1. The surface coverage of each bonded phase was calculated from its percentage carbon load (%C) according to the equation [20]

$$\text{surface coverage } (\mu\text{mol/m}^2) = \frac{\%C \times 10^6}{1200 N_c \times S_{BET}}, \quad (2)$$

where N_c is the number of carbon atoms in the bonded ligand and S_{BET} is the surface area of the silica as given by the manufacturers. As can be seen, the carbon contents of the polymeric phases are relatively higher than the corresponding monomeric phases and this, in a few cases, results in exceptionally high surface coverage of the packing. Thus, beside the di- and trifunctional silanes undergoing a 1:1 or 1:2 stoichiometric reaction with the silanols [21] as expressed by Eqs. 3 and 4, respectively, addition of water to the reaction mixture probably increased the carbon content of the phases by increasing the amount of bonded chains through self-polymerization of the hydrolyzed product of the silanes according to Eqs. 5a and 5b [22]:

$$\equiv \text{Si–OH} + \text{Cl–Si(Me)}_x\text{(Cl)}_y\text{R} \rightarrow \equiv \text{Si–O–Si(Me)}_x\text{(Cl)}_y\text{R}, \quad (3)$$

$$\equiv \text{Si–OH} + \text{Cl–Si(Me)}_x\text{(Cl)}_y\text{R} \rightarrow \equiv \text{Si–O–Si(Me)}_x\text{(O–Si)(Cl)}_{y-1}\text{R}, \quad (4)$$

$$\text{ClSi(Me)}_x\text{(Cl)}_y\text{R} + y\text{H}_2\text{O} \rightarrow \text{HO–Si(Me)}_x\text{(OH)}_y\text{R} + y\text{HCl}, \quad (5a)$$

$$\equiv \text{Si–OH} + \text{HO–Si(Me)}_x\text{(OH)}_y\text{R} \rightarrow \equiv \text{Si–O–[R–Si(Me)}_x\text{–O–]}_n\text{–H}, \quad (5b)$$

where $x = 1$ or 0 and $y = 1$ or 2 for di- or trifunctional silane, respectively; R is $CH_3(CH_2)_{17}-$ or $CH_3(CH_2)_7-$ and n is an integer equal to or greater than 1.

The gas flow properties of the columns are presented in Table 2. Using a value of $2.018 \cdot 10^{-4}$ g cm^{-1} s^{-1} for the viscosity, η, of helium at 25°C [23], the specific permeabilities, κ_o, were

Table 1
Characteristics of the bonded phases[a]

Column no.	Phase type	%C	Surface coverage (μmol/m^2)
1	monomeric monofunctional C_8	2.46	2.05
2	monomeric difunctional C_8	3.58	3.31
3	polymeric difunctional C_8	4.22	3.91
4	monomeric trifunctional C_8	4.67	4.86
5	polymeric trifunctional C_8	4.78	4.98
6	monomeric monofunctional C_{18}	8.60	3.98
7	monomeric trifunctional C_{18}	8.81	4.08
8	polymeric trifunctional C_{18}	10.72	4.96

[a] Silica: Porasil C, 80/100 mesh.

Table 2
Columns gas flow characteristics[a]

Column no.	Packing density (g/cm^3)	Porosity, ϵ	Permeability, κ_o ($\times 10^{-7}$ cm^2)
1	0.508	0.404	2.74
2	0.497	0.402	2.69
3	0.502	0.398	2.57
4	0.499	0.405	2.78
5	0.510	0.398	2.57
6	0.498	0.401	2.66
7	0.500	0.400	2.64
8	0.503	0.407	2.83
Mean ± S.D.	0.502 ± 0.005	0.402 ± 0.003	2.69 ± 0.09
C.V. (%)	1.0	0.7	0.3

[a] Columns: 2.0 m × 1.07 mm I.D.; helium, 25°C.
S.D. = standard deviation; C.V. = coefficient of variation.

determined from the slopes of the plots of F_o versus $p_i^2 - p_o^2$ derived from [24]

$$F_o = \frac{3.0 \cdot 10^7 A \kappa_o [p_i^2 - p_o^2]}{\eta L p_o}, \quad (6)$$

where F_o is the carrier gas flow-rate at the column outlet, A is the cross-sectional area of the column, and p_i and p_o are the column inlet and outlet pressure, respectively. The column porosity, ϵ, was calculated from the expression $\epsilon = 1 - m\rho_b/V_c$, where ρ_b and m are the bulk density and mass of packing, respectively, and V_c is the column volume. As can be seen, column porosities were almost identical and very close to the theoretical value of 0.42 reported for random close packing of spheres with small diameter range [25]. The insignificant differences in column permeability (coefficient of variation, C.V. = 0.3%) and packing densities (C.V. = 1.0%) showed that the packing procedure is reasonably uniform and reproducible.

Fig. 1 shows the chromatograms illustrating the separation performance of the selected columns. Better separation of the analytes was possible using the polymeric surface modification process, as indicated by the resolution of the test solutes which improved from monomeric to polymeric phases. While baseline separation was achieved only on the polymeric C_{18} column (column 8), the overall time required for the elution of butane (last peak) ranged from about 1.0 min in column 1 to 2.2 min in column 8 at the operating conditions.

The chromatographic properties of the columns in terms of their capacity factor, selectivity, and efficiency of the solutes are listed in Table 3. In general, higher k' and plate numbers were obtained on the polymeric phases than on the monomeric phases and these were greater on octadecyl columns, as expected. Also, the solutes were retained longer on the octadecyl phases than on the corresponding octyl phases. This is probably the result of their high carbon content rather than the nature of the stationary phase. Therefore, the analytes interact with the bonded ligands almost exclusively by dispersive forces which increase with the molecular contact area between the solutes and the hydrocarbonaceous layer of the stationary phases. As might be expected, the k' for methane remains substantially constant ($k' = 0.06 \pm 0.01$) on all the columns, since it's dispersive interaction with the stationary phase is very small compared to, for example, that of butane, where the overlap between the chains leads to a significant dispersive interaction.

According to Ettre and March [26], plots of resolution versus retention time for a given pair of peaks provides a good comparison of the

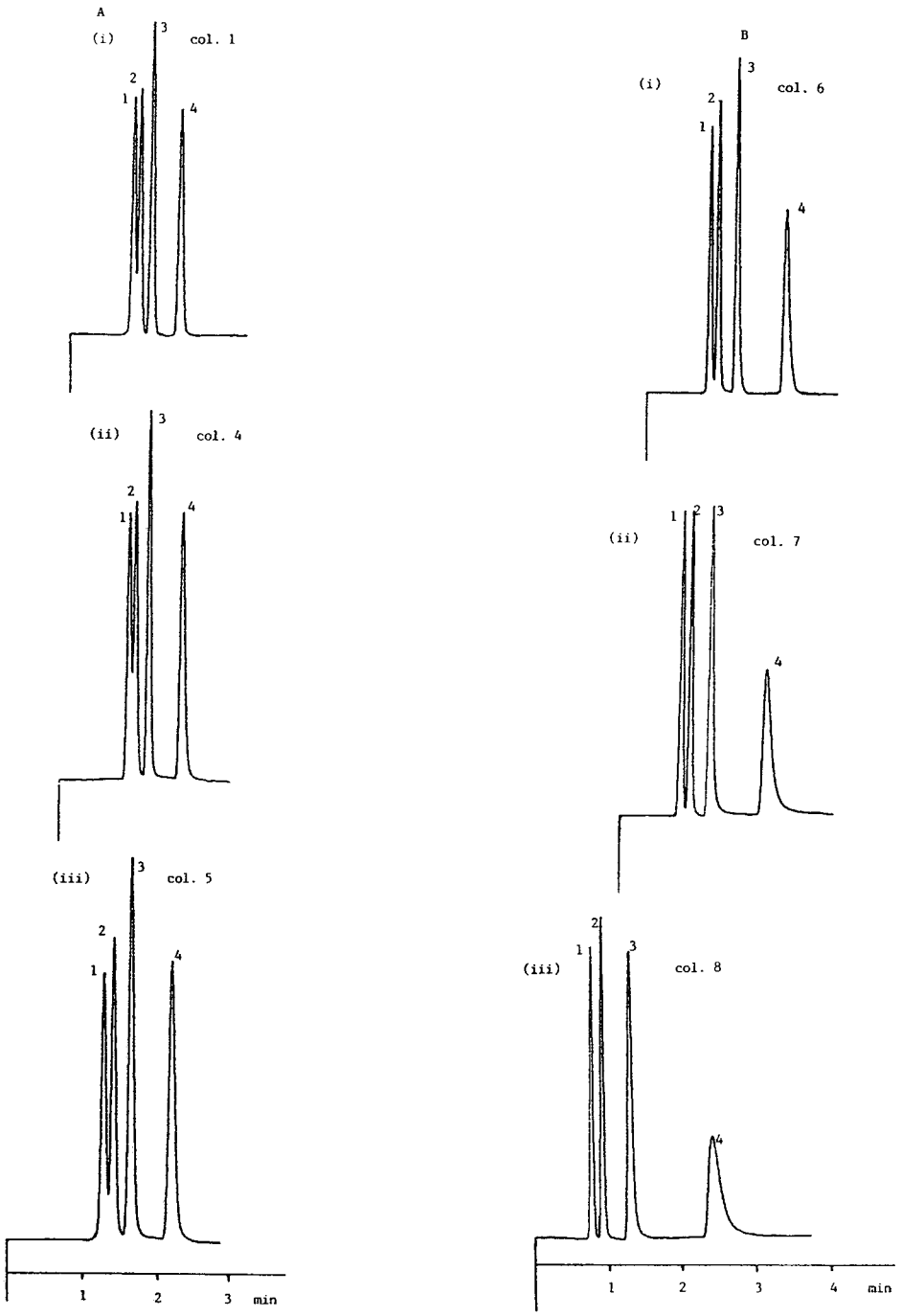

Fig. 1. Gas chromatogram of light hydrocarbons on 2.0 m × 1.07 mm I.D. columns of various: (A) octyl- and (B) octadecyl phases. (i) Monomeric monofunctional, (ii) monomeric trifunctional, (iii) polymeric trifunctional syntheses. Conditions: temperature, 25°C; TC detector; carrier gas: He, 5.5 ml/min; 100-μl injection loop. Peaks: (1) methane, (2) ethane, (3) propane, (4) butane.

Table 3
Chromatographic properties of columns[a]

Column no.	Capacity factor				Separation factor			Efficiency[b] (plates/m)
	k'_{C_1}	k'_{C_2}	k'_{C_3}	k'_{C_4}	α_1^2	α_2^3	α_3^4	
1	0.05	0.12	0.30	0.65	2.40	2.50	2.17	1112
2	0.06	0.18	0.38	0.85	3.00	2.11	2.24	1217
3	0.07	0.19	0.39	0.87	2.05	2.47	2.23	1264
4	0.06	0.15	0.34	0.76	2.50	2.27	2.24	1246
5	0.06	0.16	0.35	0.78	2.67	2.19	2.23	1263
6	0.06	0.19	0.50	1.30	3.17	2.63	2.60	1332
7	0.06	0.22	0.58	2.22	3.67	2.64	3.83	1477
8	0.07	0.28	0.85	2.67	4.00	3.04	3.14	1513

[a] Temperature: 25°C; column length: 2.0 m; carrier gas: He, 5.5 ml/min.
[b] Column efficiency based on butane peak.

"true" performance of different columns in gas chromatography. Fig. 2 shows these plots for the propane/butane peak pair for all the columns. The resolution, R_s, for the two peaks was calculated from the expression

$$R_s = \frac{1}{4}\frac{\alpha - 1}{\alpha}\frac{k'}{1+k'}\sqrt{N}. \quad (7)$$

The differences in selectivity of the columns is reflected in the shape of the curves. Thus, the high retention capacity of the solutes on columns 7 and 8 results in high resolution. As shown in Fig. 2, column 8 gave a much better resolution

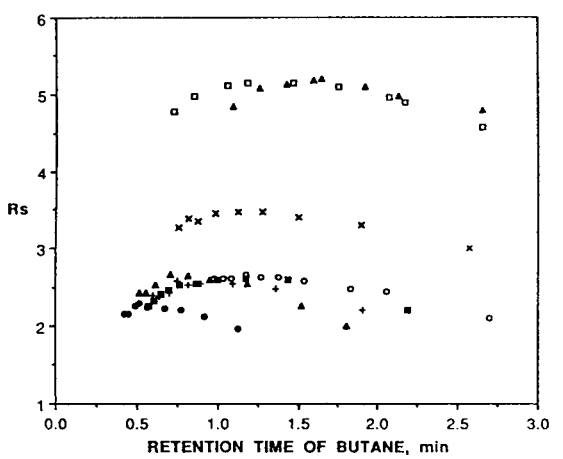

Fig. 2. Plots of resolution of the propane/butane peak pair against the retention time of butane. Column identifications: (●) 1, (■) 2, (+) 3, (△) 4, (○) 5, (×) 6, (▲) 7, (□) 8.

than column 7 in a short analysis time. The best resolution that could be achieved on column 1 is about 2.3, after which the resolution decreases markedly with increasing analysis time. At high velocities, the maximum R-values for columns 2, 3, 4, and 5 are almost identical. In general, the resolutions of the octadecyl phases are significantly higher than those of the octyl phases, presumably due to their high hydrocarbon character and hence high retention capacity of the solutes.

Fig. 3 shows the column efficiencies expressed in terms of HETP (height equivalent of a theoretical plate) as a function of average linear gas velocity, $\bar{u}$. The fit of the experimental data to the van Deemter equation ($H = A + B/\bar{u} + C\bar{u}$) [27] by the least-squares method gave negative values for the constant A. Therefore, in agreement with previous data for packed columns [28,29], a constant value of zero was assumed and the contributions of B (axial diffusion in the column) and C (mass transfer in the column packing material) terms of the equation to the total plate height for butane are listed in Table 4 together with the minimum column plate heights (H_{min}) at optimum carrier gas velocities ($\bar{u}_{opt}$). The plots show the expected improvement in column efficiency as the B term contribution diminishes, with each plot exhibiting a shallow and broad minimum at the optimum region. While the linear part of the curves for methane

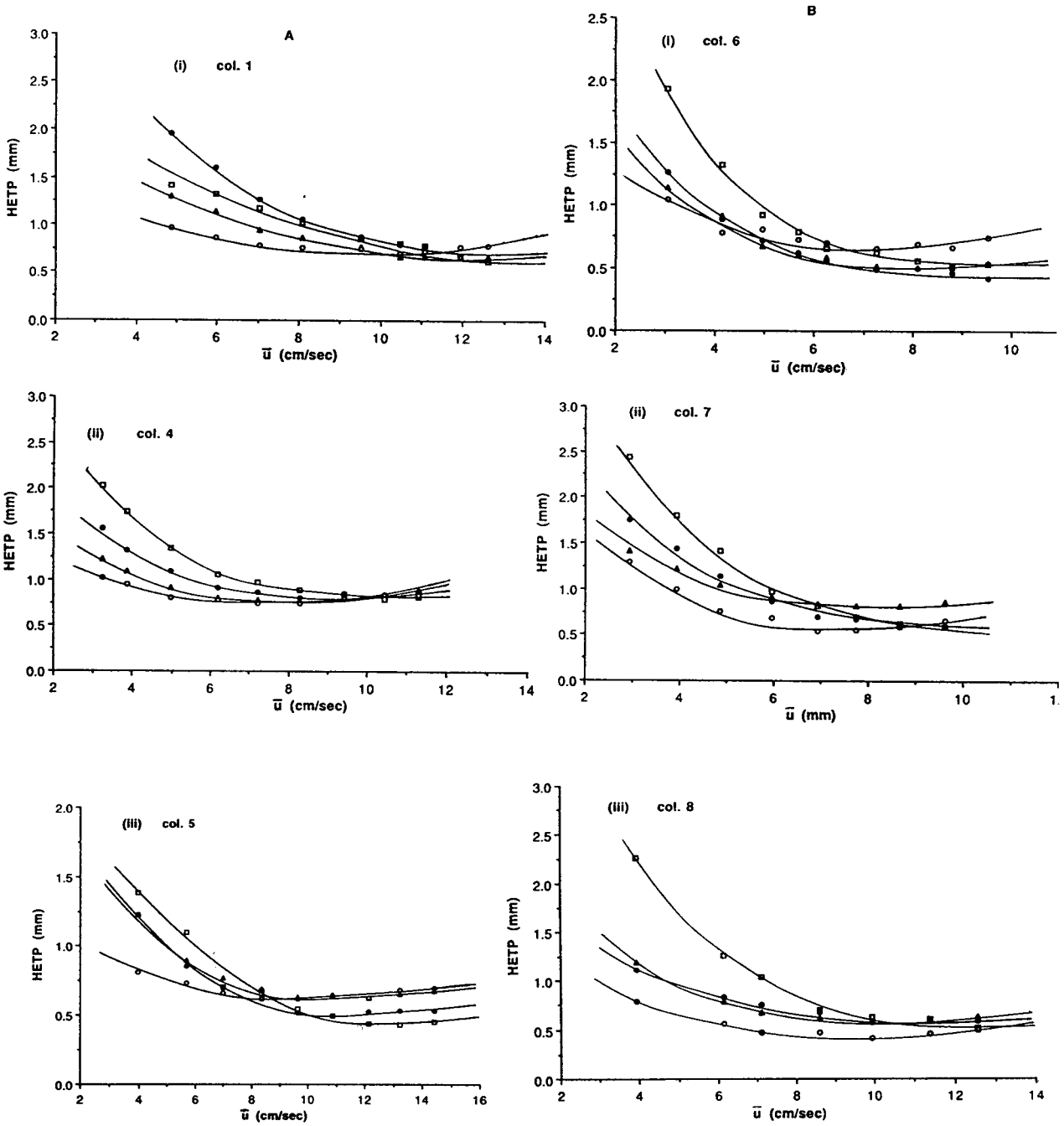

Fig. 3. Dependence of H on average linear gas velocity ($\bar{u}$) of test solutes on 2.0 m × 1.07 mm I.D. columns of various (A) octyl- and (B) octadecyl phases. (i) Monomeric monofunctional, (ii) monomeric trifunctional, (iii) polymeric trifunctional syntheses. Carrier gas: helium, $T = 25$°C. Symbols represent: (□) methane, (●) ethane, (△) propane, (○) butane.

Table 4
Kinetic properties of the columns for butane at 25°C

Column no.	ΔP ($\times 10^5$ Pa)	ϕ_{min} (ml/min)	$\bar{u}_{opt}$ (cm/s)	$HETP_{min}$ (mm)	B (cm^2/s)	C ($\times 10^{-3}$ s)
1	2.39	11.1	6.69	0.66	0.28	5.2
2	2.38	10.9	7.35	0.59	0.20	5.0
3	2.21	11.2	7.08	0.62	0.22	5.5
4	2.12	12.0	7.09	0.68	0.28	5.2
5	2.20	11.0	8.43	0.64	0.23	6.3
6	2.40	11.8	7.69	0.69	0.21	6.4
7	2.17	12.0	7.94	0.58	0.25	6.6
8	2.28	12.3	7.72	0.46	0.23	7.0

(least retained solute) remains almost constant at high velocities, those of other solutes, especially butane, increased slowly with increasing gas velocity. This may be due to the low diffusion coefficient of butane in the gas phase, which probably leads to low plate heights at low velocities where the B term is large ($B/\bar{u}$&z.Gt;$C\bar{u}$) and large plate heights at higher gas velocities where the C term predominates ($C\bar{u}$&z.Gt;$B/\bar{u}$).

As shown in Table 4, the C terms for the polymeric packings are slightly higher than those of the corresponding monomeric phases. This is probably caused by the low diffusion coefficient of the solute within the cross-linked polymer structure of the bonded ligands. The above phenomenon might account for the relatively high C-value of column 5 compared to that of column 3. Thus, column 3 may be thought of possessing a less cross-linked polymer structure than column 5 and therefore offering a small resistance to mass transfer. Since B is directly proportional to the diffusion coefficient of the solute in the carrier gas, which is the same for molecules of the same size and shape, the value of B is almost constant for all the columns. Similar trends were observed for other solutes. The minimum flow-rate, ϕ_{min} (mean = 11.54 ml/min; C.V. = 4.72%), and $\bar{u}_{opt}$ (mean = 7.50 cm/s; C.V. = 7.42%) are not significantly different in all the columns and are within the range of values obtained in gas–liquid chromatography [30]. From the data presented in Table 4, column 8, which yields a minimum plate height of 0.46 mm (2174 theoretical plates/m) with butane, appeared to be the best column. This minimum value of H was achieved at an average linear gas velocity of 7.72 cm/s, corresponding to a flow-rate of 12.3 ml/min and a pressure drop of $2.28 \cdot 10^5$ Pa.

The thermal stability of the phases was examined by determining the capacity factors of the test solutes at 25°C after purging the columns at high temperatures ranging from 100 to 250°C for 2 h under dry helium flow. A change of about 10% or higher in k'-values indicates that the packing material was affected at the purging temperature. Fig. 4 shows the effect of the purging temperature on the capacity factor of butane. It can be seen that the k' of butane did not vary greatly within the temperature range investigated. In fact, increasing the purging tem-

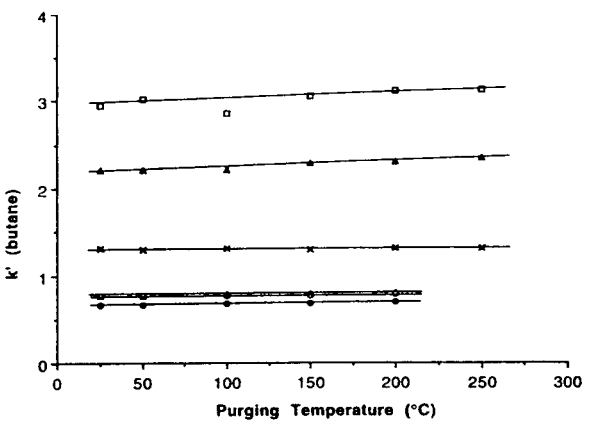

Fig. 4. Effect of purging temperature on capacity factor, k' of butane. Column identifications: (●) 1, (△) 4, (○) 5, (×) 6, (▲) 7, (□) 8.

perature of columns 6, 7, and 8 to 250°C results in 5.4, 6.0, and 6.5% loss, respectively, in k'-values of butane, which could well be due to removal of residual solvents from the pores of the packings at elevated temperatures. Therefore columns 6, 7, and 8 can be operated at temperatures up to 250°C without any appreciable column bleed. This temperature is notably higher than that obtained on isocyanate packings [31]. Consequently, the packing materials investigated in this study, particularly the polymeric C_{18} phase (column 8), can be employed with ionization detectors where high stability and minimum column bleed are required.

To further illustrate the performance of column 8, being the most efficient column, Fig. 5 shows the chromatogram of a ten-hydrocarbon mixture of C_1 to C_4 compounds. Although not capable of producing baseline separation of all the compounds (Fig. 5A), the analysis was much faster (<6 min) than that obtained on isocyanate columns (ca. 15 min) under similar conditions but at a lower carrier gas flow-rate [31]. At a column temperature of 50°C, the time required for such analysis was reduced almost by half (Fig. 5B). Even though propadiene and propene and isobutane and butane co-eluted, respectively, ethane was separated from ethene under these conditions. Thus, column selectivity could presumably be improved by temperature programming and/or optimization of the column parameters such as column length and particle diameter. It is worth mentioning that the high power consumption of temperature programming may be detrimental to spacecraft applications since one of the major constraints in space missions is power budget.

4. Conclusion

This study has demonstrated the potential importance of micropacked alkyl-bonded silica columns, particularly polymeric octadecyl packings, for GC analysis of light hydrocarbons due to their good chromatographic performance compared to conventional packed columns. Even though a WCOT capillary column with chemical-

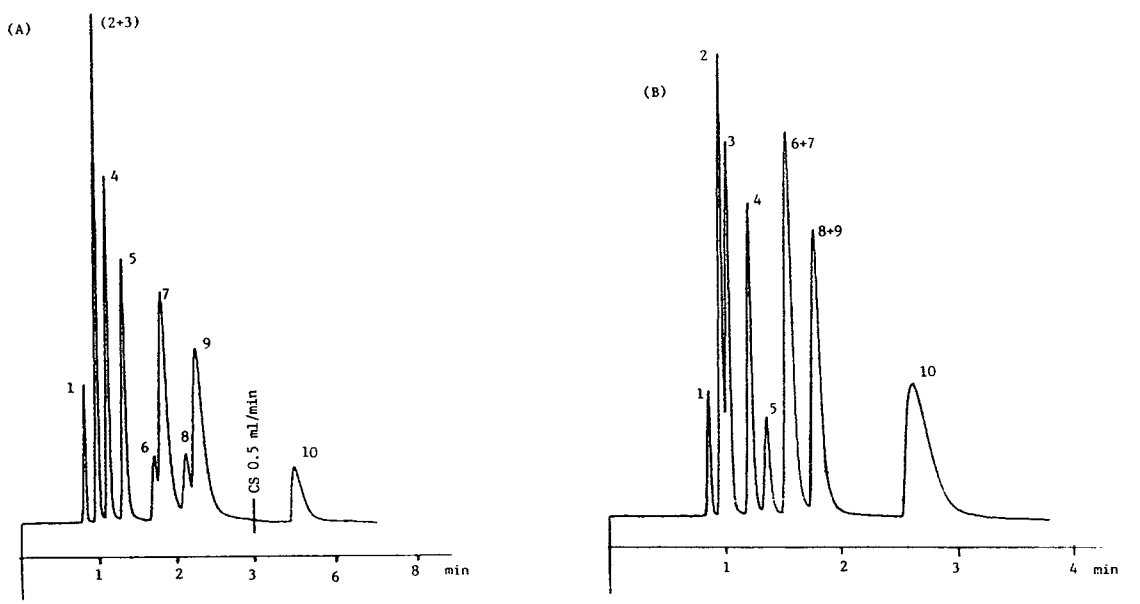

Fig. 5. Separation of hydrocarbon mixtures on polymeric octadecyl bonded phase (column 8). Conditions: temperature (A) 25°C, (B) 50°C; TC detector; carrier gas: He, 8.34 ml/min; 100-μl injection loop; chart speed (CS); 2.0 ml/min at start, changed to 0.5 ml/min at 3.0 min. Peaks: (1) methane, (2) ethane, (3) ethene, (4) propane, (5) acetylene, (6) propene, (7) propadiene, (8) isobutane, (9) butane, (10) propyne.

ly bonded stationary phase (dimethyl polysiloxane) provides fast and efficient analysis of low-molecular-mass hydrocarbons and nitrile [8], the high thermal stability of the present columns coupled to the capability of micropacked columns to handle much larger samples without overloading appear to make them suitable for GC instrumentation in future space missions. In view of the complex nature of gas mixtures in planetary atmospheres, the chromatographic behavior of the column with N-organics including nitriles is worth investigating.

Acknowledgements

This work was performed while the author held a National Research Council–NASA Research Associateship. The support of NASA–Ames Research Center through the Exobiology Program is acknowledged. The helpful comments of Dr. Jose R. Valentin and Glenn Carle of that center during the preparation of this work has been found invaluable. Finally, I thank Dr. C.F. Simpson of Birkbeck College, University of London, London, UK, for his assistance with the elemental carbon analysis.

References

[1] V.I. Oyama and B.J. Berdahl, J. Geophys. Res., 82 (1977) 4669.
[2] F.S. Brown, H.E. Adelson, M.C. Chapman, O.W. Clausen, A.J. Cole, J.T. Cragin, R.J. Day, C.H. Debenhnam, R.E. Fortney, R.I. Gilje, D.W. Harrey, J.L. Logan, Jr., W.D. Potter and G.T. Rosiak, Rev. Sci. Instrum., 49 (1978) 139.
[3] V.I. Oyama, G.C. Carle, F.H. Woeller, J.B. Pollack, R.T. Reynolds and R.A. Craig, J. Geophys. Res., 85 (1980) 7891.
[4] J.R. Valentin, LC·GC Int., 2 (1989) 32.
[5] CASSINI Report on the Phase A Study, European Space Agency, Report Reference SCI, (88)5, 1988.
[6] L. Do and F. Raulin, J. Chromatogr., 481 (1989) 45.
[7] L. Do and F. Raulin, J. Chromatogr., 514 (1990) 65.
[8] L. Do and F. Raulin, J. Chromatogr., 591 (1992) 297.
[9] E. de Vanssay, P. Capilla, D. Coscia, L. Do, R. Sternberg and F. Raulin, J. Chromatogr., 639 (1993) 255.
[10] E. de Vanssay, S. Zubrzycki, R. Sternberg, F. Raulin, M. Sergent and R. Phan-Tan-Luu, J. Chromatogr. A, 688 (1994) 161.
[11] C.A. Cramers and J.E. Rijks, Adv. Chromatogr., 17 (1979) 101.
[12] T. Herraiz, G. Reglero, M. Herraiz, R. Alonso and M.D. Cabezudo, J. Chromatogr., 388 (1987) 325.
[13] J.F.K. Huber, H.H. Lauer and H. Poppe, J. Chromatogr., 112 (1975) 377.
[14] R.J. Jonker and H. Poppe, Anal. Chem., 54 (1982) 2447.
[15] F. Bruner, P. Ciccioli, E. Brancalleoni and A. Longo, Chromatographia, 8 (1975) 503.
[16] V.S. Gavrichev, V.G. Berezkin, A.R. Jumaev, A. Malik, Yu M. Borisov, I.A. Lvov, Yu M. Lyubitov, V.I. Mikhailov and V.D. Sokovikh, J. Chromatogr., 365 (1986) 237.
[17] D.A. Lewis, P. Vouros and B.L. Karger, Chromatographia, 15 (1982) 117.
[18] F. Raulin, E. de Vanssay, L. Do and P. Paillous, LC·GC Int., 5 (1992) 32.
[19] J.L. Speier, Adv. Organomet. Chem., 17 (1979) 407.
[20] S.O. Akapo and C.F. Simpson, J. Chromatogr. Sci., 32 (1994) 86.
[21] S.O. Akapo and C.F. Simpson, J. Chromatogr. Sci., 28 (1990) 186.
[22] J.K. Haken, J. Chromatogr., 300 (1984) 1.
[23] E.A. Moelwyn-Hughes, Physical Chemistry, Pergamon Press, London, 2nd ed., 1964, p. 609.
[24] J. Bohemen and J.H. Purnell, J. Chem. Soc., 360 (1961).
[25] J. Bohemen and J.H. Purnell, in D.H. Desty (Editor), Gas Chromatography, Academic Press, New York, 1958, p. 6.
[26] L.S. Ettre and E.W. March, J. Chromatogr., 91 (1974) 5.
[27] J.J. van Deemter, F.J. Zuiderweg and A. Klinkenberg, Chem. Eng. Sci., 5 (1956) 271.
[28] J.C. Giddings and R.A. Robison, Anal. Chem., 34 (1962) 885.
[29] W.L. Jones, Anal. Chem., 33 (1961) 829.
[30] A.B. Littlewood, Gas Chromatography, Acdemic Press, New York, 1970.
[31] G.E. Pollock, D.R. Kojiro and F.H. Woeller, J. Chromatogr. Sci., 20 (1982) 176.

ELSEVIER

Journal of Chromatography A, 709 (1995) 303–311

JOURNAL OF CHROMATOGRAPHY A

Determination of aliphatic aldehydes as their thiazolidine derivatives in foods by gas chromatography with flame photometric detection

Hiroyuki Kataoka*, Akihiko Sumida, Naoko Nishihata, Masami Makita

Faculty of Pharmaceutical Sciences, Okayama University, Tsushima, Okayama 700, Japan

First received 2 January 1995; revised manuscript received 18 April 1995; accepted 18 April 1995

Abstract

A selective and sensitive gas chromatographic method for the determination of saturated and unsaturated aliphatic aldehydes in foods has been developed. After extraction of the sample with acetonitrile, aldehydes were converted into their thiazolidine derivatives by the reaction with cysteamine, and then measured by gas chromatography with flame photometric detection. The calibration curves for aliphatic aldehydes in the range 20–2500 ng were linear and the detection limits at a signal-to-noise ratio of 3 were ca. 4–100 pg injected. Aliphatic aldehydes in foods could be selectively determined by this method without any interference from coexisting substances. Overall recoveries of aldehydes added to food samples were 82–111%. Analytical results for the determination of aliphatic aldehydes in various food samples are presented.

1. Introduction

Low-molecular-mass aldehydes, which have unpleasant pungent odors, are usually present at trace amounts in various complex materials such as foods, tobacco smoke, air and water pollution samples and physiological fluids. In fat-containing foods, these compounds are formed during maturation by enzymatic and nonenzymatic reactions, especially by oxidation of unsaturated fatty acids [1–4]. Rancidity, caused by lipid peroxidation, has long been recognized as a problem in the storage of fat and oils. Lipid peroxidation is also associated with numerous pathological conditions such as atherosclerosis, cardiovascular diseases, carcinogenesis, inflammatory disease, mammographic dysplasia, chronic gastritis, precancerous dysplasia and postischemic reperfusion injury [5–10]. Aldehydes formed during lipid peroxidation are shown to be highly cytotoxic and genotoxic [11–15] and to react with functional groups such as amino and sulphydryl groups of biomolecules, such as proteins, nucleic acids, glutathione, cysteine, lysine and coenzyme A [16–22]. Therefore, measurement of aldehydes in foodstuff is very important.

The determination of aliphatic aldehydes has been carried out by high-performance liquid chromatography (HPLC) or gas chromatography (GC). However, these methods have some inherent problems related to the difficulty in handling low-molecular-mass aldehydes because of their high water solubility, volatility and reactivity. HPLC analyses of aldehydes with

* Corresponding author.

0021-9673/95/$09.50
SSDI 0021-9673(95)00478-5

ultraviolet (UV) [23–26] and fluorescence [27–29] detection require derivatization in order to increase the detection sensitivity. Although some of the derivatization methods are very sensitive, they require time-consuming preliminary clean-up of the sample to remove excess reagent and coexisting substances. Headspace GC analysis [30,31] of underivatized aldehydes presents a simple technique that measures volatile compounds in equilibrium with liquid or solid samples, but it requires a closed system to prevent loss of volatile aldehydes. On the other hand, GC methods based on the derivatization with 2,4-dinitrophenylhydrazine [32–34], methylhydrazine [35], benzyloxyamine [36], pentafluorobenzyloxyamine [37,38], N-benzylethanolamine [39], hydroxylamine/*tert.*-butyldimethylsilyltrifluoroacetamide [40,41] and morpholine [42] by flame ionization detection, nitrogen–phosphorus detection (NPD), electron-capture detection and GC–mass spectrometry with selected-ion monitoring have been reported. However, with some of these methods the aldehyde peaks are difficult to identify because of the inevitable formation of both *syn* and *anti* forms. Therefore, simultaneous determination of different aldehydes is almost impossible with these derivatization methods. Moreover, some of these methods require strong acidic conditions for derivatization that may cause undesirable reactions, such as decomposition of carbohydrates or proteins in the case of food samples. Recently, Shibamoto and co-workers [4,43–46] developed a new derivatization method of saturated aldehydes with cysteamine (2-aminoethanethiol) to form stable thiazolidine derivatives. This method gives only one derivative for each aldehyde with almost quantitative yield under mild conditions, and excess of the reagent (cysteamine) does not interfere with GC analysis. Furthermore, the resulting thiazolidine derivatives can be separated perfectly with fused-silica capillary columns and detected selectively with nitrogen–phosphorous detection (NPD). However, this method has not been applied to the determination of unsaturated aldehydes.

In this work, we report a method for the determination of saturated and unsaturated aliphatic aldehydes as their thiazolidine derivatives by GC with flame photometric detection (FPD–GC). By using this method, the contents of these aldehydes in food samples, and the effects of heat treatment and UV irradiation on the formation of aliphatic aldehydes by lipid peroxidation of food oils were also studied.

2. Experimental

2.1. Reagents

Butanal (C_4) and acetaldehyde (C_2) were purchased from Nacalai Tesque (Kyoto, Japan) and E. Merck (Darmstadt, Germany), respectively. Propanal (C_3), isobutanal (i-C_4), pentanal (C_5), isopentanal (i-C_5), hexanal (C_6), heptanal (C_7), octanal (C_8), nonanal (C_9), decanal (C_{10}), *trans*-2-hexenal (C_{6-1}) and 2,4-hexadienal (C_{6-2}) were purchased from Tokyo Kasei Kogyo (Tokyo, Japan). Each aldehyde was dissolved in 20% methanol to make a stock solution with a concentration of 2 mg/ml and used after dilution with 20% methanol to the required concentration (1–5 μg/ml). Phenyl sulphide (Tokyo Kasei Kogyo) as an internal standard (I.S.) was dissolved in ethyl acetate at a concentration of 0.5 μg/ml. Cysteamine (Nacalai Tesque) was dissolved in distilled water at a concentration of 2 mg/ml. All other chemicals were of analytical-reagent grade.

2.2. Preparation of samples

Food samples were purchased at local retail markets and were treated for analyses on the same day. Food oil samples (ca. 0.1 ml) and solid fat samples (ca. 0.1 g) were extracted twice with 0.5 ml of acetonitrile, and 0.1 ml of the combined extracts was used as the sample for derivatization. For solid samples containing lipid, e.g. cheese, chocolate and potatochips, an aliquot (ca. 1 g) was homogenized in 4 ml of acetonitrile with a Model LK-21 ultra-disperser (Yamato Kagaku, Tokyo, Japan). After centrifugation at 3000 *g* for 10 min, the precipitate was re-extracted with 4 ml of acetonitrile. The super-

natants were combined and 0.1 ml of the combined solution was used as the sample for derivatization.

2.3. Derivatization procedure

To the standard solution containing 20–2000 ng of each aldehyde or the sample prepared by the above method were added 0.2 ml of 0.2 mg/ml cysteamine and 0.1 ml of 0.1 *M* sodium hydroxide, and the total volume was made up to 1 ml with distilled water. The mixture was shaken with a Model SR-II shaker set (Taitec, Saitama, Japan) up and down at 3000 rpm for 10 min at room temperature and to the reaction mixture 0.5 ml of distilled water was added. After saturation with sodium chloride, the mixture was extracted with 0.2 ml of ethyl acetate containing 1 μg/ml phenyl sulphide (I.S.) and 1 μl of this extract was injected onto the FPD–GC system. The derivatization process is shown in Fig. 1.

2.4. Gas chromatography

GC analysis was carried out with a Shimadzu Model 12 A gas chromatograph equipped with FPD (S-filter). A fused-silica capillary column (J&W, Folsom, CA, USA) connected DB-17 (15 m × 0.53 mm I.D., 1.0 μm film thickness) and DB-210 (15 m × 0.53 mm I.D., 1.0 μm film thickness) was used. The operating conditions were as follows: column temperature, programmed at 6°C/min from 100 to 240°C; injection and detector temperature, 250°C; nitrogen flow-rate, 10 ml/min (flow-velocity, 76 cm/s). The peak height ratios against the I.S. were measured and the peak-height ratios against the I.S. were calculated.

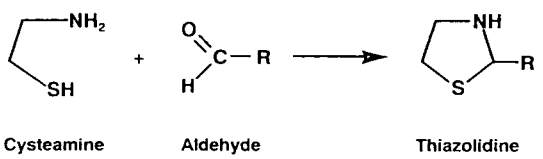

Fig. 1. Derivatization reaction of aldehydes. R = alkyl group.

2.5. Gas chromatography–mass spectrometry (GC–MS)

A Hewlett-Packard Model 5890A gas chromatograph was operated in conjunction with a VG Analytical Model 70-SE mass spectrometer and a VG-11-250J mass data system. A fused-silica capillary column containing cross-linked OV-1 (Quadrex, New Haven, CT, USA, 25 m × 0.25 mm I.D., 0.25 μm film thickness) was used. Column temperature: programmed at 8°C/min from 100 to 270°C; injection temperature, 280°C; ion-source temperature, 270°C; ionizing voltage, 40 eV; helium flow-rate, 8 ml/min.

2.6. Heat treatment and UV irradiation of food oil samples

Food oil (ca. 0.1 ml) was heated at 100°C in a Model TB-320 hot block bath (Advantec Toyo, Tokyo, Japan) or irradiated in a Model H-400 UV lamp (λ = 250–400 nm) house (Irie, Tokyo, Japan) from a distance of 40 cm for various times and then the aldehyde content in the sample was measured by the above method.

3. Results and discussion

Shibamoto and co-workers [44–46] developed a new derivatization method based on the reaction of aldehyde with cysteamine and applied to the determination of various volatile aldehydes in heated pork fat, cooking oils and automobile exhaust after headspace sampling. Although this method is sensitive and specific by using NPD, it is time-consuming because of the two-phase reaction with gaseous aldehyde and cysteamine solution, and has not yet been applied to unsaturated aldehydes. Therefore, we re-examined the reaction conditions of saturated and unsaturated aldehydes with cysteamine. The reaction of alde-

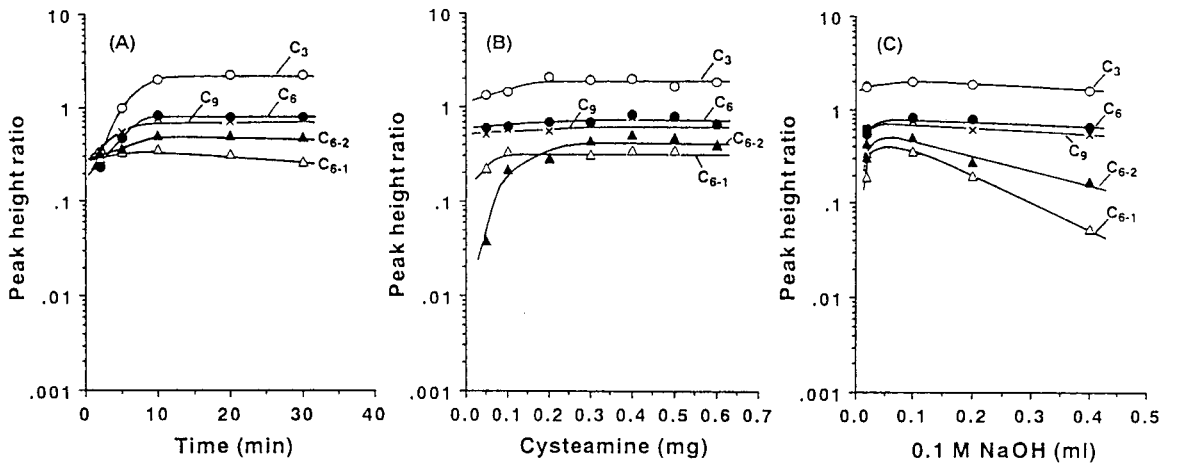

Fig. 2. Effects of (A) reaction time, (B) cysteamine and (C) sodium hydroxide on the formation of thiazolidine derivatives of aldehydes.

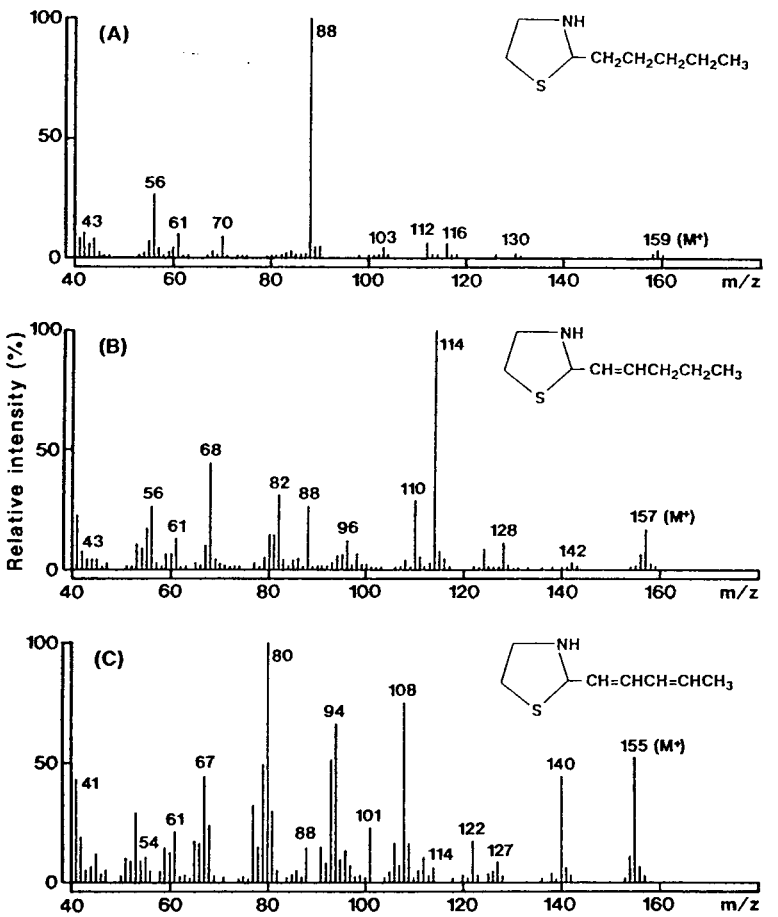

Fig. 3. Mass spectra of the thiazolidine derivatives of aldehydes. (A) Hexanal (C_6), (B) *trans*-2-hexenal (C_{6-1}), (C) 2,4-hexadienal (C_{6-2}).

hydes with cysteamine proceeds rapidly in aqueous alkaline media. As shown in Fig. 2A,B, with 0.4 mg of cysteamine the reaction is accomplished within 10 min at room temperature by shaking. Although saturated aldehydes readily reacted with 0.05 *M* sodium hydroxide, the derivatization yield of unsaturated aldehydes decreased by the excess of sodium hydroxide (Fig. 2C). It seems that unsaturated aldehydes are preferentially oxidized in stronger alkaline media. Subsequently, the thiazolidine derivatives produced by this reaction were extracted into the solvent and injected onto the GC system. Of the several solvents tested, ethyl acetate proved to be the most satisfactory for the rapid and quantitative extraction of thiazolidines. Although Shibamoto et al. used dichloromethane as extraction solvent, sampling of the organic layer was difficult because this solvent was found in the bottom layer. By using this improved method, preparation of the derivative could be performed within 15 min, and several samples could be treated simultaneously.

The structures of the thiazolidine derivatives of aldehydes were confirmed by GC–MS analysis. As shown in Fig. 3, a molecular ion peak $[M]^+$ was observed for each of the derivatives and other common ion peaks which were useful for structure elucidation, were $[M-15]^+$ (CH_3), $[M-88]^+$ (SCH_2CH_2NHCH) and *m/z* 88. As shown in Table 1, the derivatives of saturated aldehydes were stable under normal laboratory conditions, and no decomposition was observed during GC analysis. On the other hand, the

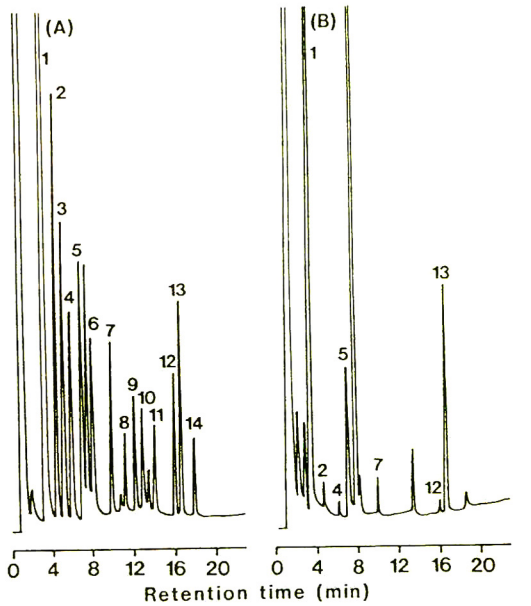

Fig. 4. Typical gas chromatograms obtained from standard and food sample. (A) Standard (containing 100 ng of C_2–C_8 and 500 ng of C_9, C_{10}, C_{6-1} and C_{6-2}). (B) sesame oil (10 *m*l). GC conditions are given in Experimental. Peaks: 1 = acetaldehyde (C_2), 2 = propanal (C_3), 3 = isobutanal (i-C_4), 4 = butanal(C_4), 5 = isopentanal (i-C_5), 6 = pentanal (C_5), 7 = hexanal (C_6), 8 = *trans*-2-hexenal (C_{6-1}), 9 = heptanal (C_7), 10 = 2,4-hexadienal (C_{6-2}), 11 = octanal (C_8), 12 = nonanal (C_9), 13 = phenyl sulphide (I.S.), 14 = decanal (C_{10}).

derivatives of unsaturated aldehydes were stable for 24 h but decomposed to below 60% of their original value over a 3-day period when these derivatives were stored as ethyl acetate solution at 4°C. This seems to be due to the oxidation of

Table 1
Stability of thiazolidines derived from aldehyde

Aldehyde	Storage time[a] (days)			
	0	1	2	3
Propanal (C_3)	2.02 ± 0.09	2.03 ± 0.12	2.04 ± 0.10	1.93 ± 0.07
Hexanal (C_6)	0.82 ± 0.02	0.82 ± 0.05	0.84 ± 0.04	0.84 ± 0.03
Nonanal (C_9)	0.76 ± 0.01	0.72 ± 0.02	0.79 ± 0.04	0.73 ± 0.02
trans-2-Hexenal (C_{6-1})	0.35 ± 0.02	0.32 ± 0.01	0.24 ± 0.01	0.20 ± 0.01
2,4-Hexadienal (C_{6-2})	0.52 ± 0.03	0.48 ± 0.03	0.42 ± 0.03	0.31 ± 0.02

[a] Samples were analysed immediately after derivatization and after 1, 2 and 3 days' storage as thiazolidine derivatives in ethyl acetate at 4°C. Each value, mean ± S.D. ($n = 4$), represents peak-height ratio against the I.S.

the unsaturated bonds. Thus, the samples must be analysed at least on the day after derivatization. The within-run C.V.s for the aldehydes were 1.3–7.1% ($n = 4$) and between-run C.V.s over a period of 4 days were 2.6–15.2% ($n = 4$). The derivatives were volatile and eluted as separate symmetrical peaks within 18 min by using connected DB-17 and DB-210 capillary columns (Fig. 4A). The derivatives gave an excellent FPD response and minimum detectable amounts of C_3,C_6, C_9, C_{6-1} and C_{6-2} (at a signal-to-noise ratio of 3 under the instrumental conditions used) were ca. 4, 10, 60, 100 and 100 pg injected, respectively. In order to test the linearity of the calibration curve, various amounts of aldehydes ranging from 20–500 ng (for C_3, C_4, *i*-C_4, C_5, *i*-C_5, C_6, C_7 and C_8) and 100–2500 ng (for C_9, C_{10}, C_{6-1} and C_{6-2}) were derivatized in a mixture and aliquots representing 0.1–2.5 ng (for C_3, C_4, *i*–C_4, C_5, *i*-C_5, C_6, C_7 and C_8) and 0.5–12.5 ng (for C_9, C_{10}, C_{6-1} and C_{6-2}) were injected onto the FPD–GC system. In each case, a linear relationship was obtained and the reproducibility was found to be satisfactory, when the peak-height ratios were measured with reference to the I.S. (Table 2). On the other hand, C_2 was detected with satisfactory sensitivity, but reproducibility was poor because of interference from background C_2 originating from the laboratory atmosphere and the reagents used.

Table 2
Linear regression data for aliphatic aldehydes

Aldehyde[a]	Regression line[b]		
	s	*b*	*r*
Propanal (C_3)	1.886	−3.466	0.9926
Isobutanal (*i*-C_4)	1.799	−3.450	0.9981
Butanal (C_4)	1.750	−3.523	0.9942
Isopentanal (*i*-C_5)	1.869	−3.660	0.9982
Pentanal (C_5)	1.778	−3.639	0.9975
Hexanal (C_6)	1.854	−3.795	0.9970
Heptanal (C_7)	1.842	−3.968	0.9972
Octanal (C_8)	1.782	−3.991	0.9960
Nonanal (C_9)	1.884	−5.202	0.9906
Decanal (C_{10})	1.818	−5.329	0.9905
trans-2-Hexenal (C_{6-1})	1.963	−5.748	0.9941
2,4-Hexadienal (C_{6-2})	2.129	−6.035	0.9977

[a] Range: 20–500 ng for C_3, *i*-C_4, C_4, *i*-C_5, C_5, C_6, C_7 and C_8; 100–2500 ng for C_9, C_{10}, C_{6-1} and C_{6-2}.
[b] $\log y = s \log x + b$; y = peak-height ratio, x = amount of aldehyde (ng), s = slope, b = intercept, r = correlation coefficient ($n = 15$).

For aldehyde analysis of foodstuffs, acetonitrile was used as extraction solvent. Aliphatic aldehydes were quantitatively extracted from food samples by extraction twice with 0.5 ml of

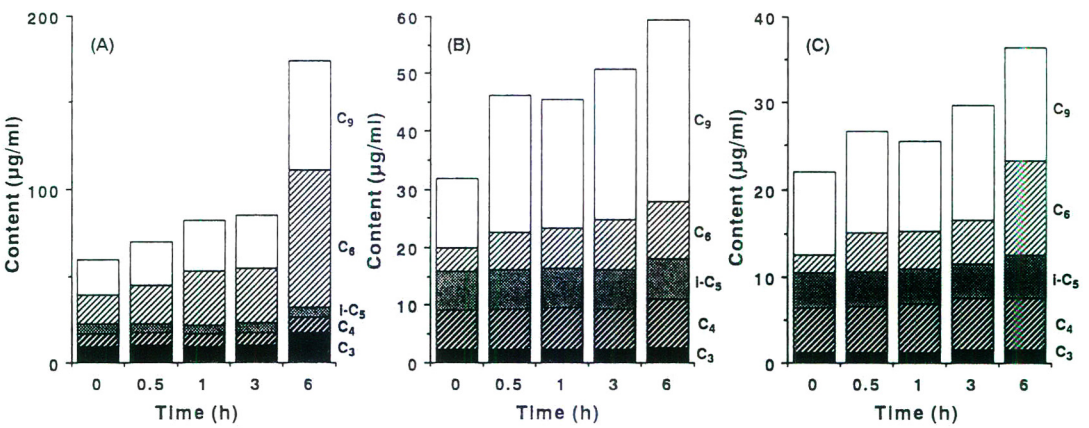

Fig. 5. Effect of heat treatment at 100°C on the formation of aldehydes in (A) salad oil, (B) sesame oil and (C) corn oil.

Table 3
Recoveries of aliphatic aldehydes added to food samples

Aldehyde[a]	Added	Amount found[b]		Recovery (%)
		Non-addition	Addition	
Sesame oil	(μg/ml)	(μg/ml)	(μg/ml)	
C_3	10	2.4 ± 0.1	10.6 ± 0.6	82
i-C_4	10	ND[c]	8.9 ± 0.4	89
C_4	10	6.9 ± 0.3	15.9 ± 0.9	90
i-C_5	10	6.7 ± 0.1	17.5 ± 1.3	108
C_5	10	ND	10.5 ± 0.6	105
C_6	10	4.0 ± 0.1	13.1 ± 0.5	91
C_7	10	ND	8.4 ± 0.2	84
C_8	10	ND	9.2 ± 0.4	92
C_9	50	11.9 ± 0.7	58.8 ± 1.7	94
C_{10}	50	ND	48.7 ± 1.3	97
C_{6-1}	50	ND	41.6 ± 1.1	83
C_{6-2}	50	ND	46.3 ± 1.8	93
Margarine	(μg/g)	(μg/g)	(μg/g)	
C_3	10	1.9 ± 0.2	11.6 ± 0.4	97
i-C_4	10	ND	10.2 ± 0.4	102
C_4	10	5.1 ± 0.4	15.8 ± 0.8	107
i-C_5	10	4.8 ± 0.3	15.2 ± 0.8	104
C_5	10	ND	10.3 ± 0.4	103
C_6	10	1.2 ± 0.1	12.0 ± 1.0	108
C_7	10	ND	10.4 ± 0.2	104
C_8	10	ND	10.3 ± 0.2	103
C_9	50	8.6 ± 0.8	53.1 ± 1.1	89
C_{10}	50	ND	50.6 ± 0.9	101
C_{6-1}	50	ND	49.2 ± 3.3	98
C_{6-2}	50	ND	55.5 ± 1.0	111

[a] C_3 = propanal; *i*-C_4 = isobutanal; C_4 = butanal; *i*-C_5 = isopentanal; C_5 = pentanal; C_6 = hexanal; C_7 = heptanal; C_8 = octanal; C_9 = nonanal; C_{10} = decanal; C_{6-1} = *trans*-2-hexenal; C_{6-2} = 2,4-hexadienal.
[b] Mean ± S.D. ($n = 4$).
[c] Not detectable.

acetonitrile. Fig. 4B shows the chromatogram obtained from a food sample. Although background peaks originating from the laboratory atmosphere and the reagents used were observed between *i*-C_5 and C_5, and between C_{6-2} and C_8, aldehydes in the sample could be detected without any interference from coexisting substances. As shown in Table 3, the overall recoveries of aliphatic aldehydes added to several food samples were 82–111% and the relative standard deviations were 1.2–9.3% ($n = 4$). The aliphatic aldehyde contents in various food samples determined by this method are summarized in Table 4. It can be seen from our data that sardine oil and chocolate contained high concentrations of C_4, C_6, C_7 and C_9. Unsaturated aldehyde C_{6-1} was found in milk and chocolate. On the other hand, *i*-C_4, C_5, C_8, C_{10} and C_{6-2} were not detected at all in any of the sample investigated in this study. By using this improved method, production of aldehydes in salad oil (mixture of soybean oil and rapeseed oil), sesame oil and corn oil was measured during heat treatment and UV irradiation. As shown in Figs. 5 and 6, the total contents of aldehydes in these food oils increased by 1.3–1.9 and 2.3–5.0

Table 4
Aliphatic aldehyde contents in various foods from commercial sources

Sample	Aldehyde[a] content (μg/ml or g) (mean ± S.D., $n = 4$)						
	C_3	C_4	i-C_5	C_6	C_7	C_9	C_{6-1}
Sesame oil	2.4 ± 0.1	6.9 ± 0.3	6.7 ± 0.1	4.0 ± 0.1	ND[b]	11.9 ± 0.7	ND
Soybean oil	1.6 ± 0.1	5.4 ± 0.3	5.1 ± 0.3	1.8 ± 0.1	ND	8.1 ± 0.5	ND
Rapeseed oil	2.5 ± 0.1	5.3 ± 0.3	4.9 ± 0.3	3.6 ± 0.2	ND	10.6 ± 0.6	ND
Cottonseed oil	1.6 ± 0.1	5.3 ± 0.3	5.1 ± 0.3	2.3 ± 0.02	ND	10.0 ± 0.6	ND
Corn oil	1.3 ± 0.1	5.0 ± 0.2	4.0 ± 0.4	2.2 ± 0.1	ND	9.5 ± 0.2	ND
Olive oil	1.8 ± 0.1	5.5 ± 0.2	4.8 ± 0.3	3.5 ± 0.2	ND	12.6 ± 1.0	ND
Sardine oil	5.9 ± 0.1	6.2 ± 0.2	3.3 ± 0.2	6.5 ± 0.2	5.3 ± 0.2	23.7 ± 1.2	ND
Beef fat	2.7 ± 0.3	5.1 ± 0.3	5.4 ± 0.2	2.4 ± 0.2	ND	12.6 ± 1.7	ND
Lard	3.8 ± 0.2	5.5 ± 0.3	4.7 ± 0.3	2.6 ± 0.1	ND	9.0 ± 0.9	ND
Butter	2.1 ± 0.1	4.9 ± 0.2	5.1 ± 0.3	2.0 ± 0.2	ND	13.0 ± 0.8	ND
Margarine	1.9 ± 0.2	5.1 ± 0.4	4.8 ± 0.3	1.2 ± 0.1	ND	8.6 ± 0.8	ND
Mayonnaise	2.1 ± 0.3	3.8 ± 0.2	3.8 ± 0.4	2.2 ± 0.2	ND	10.6 ± 0.5	ND
Cheese	2.4 ± 0.1	4.6 ± 0.2	3.4 ± 0.1	3.5 ± 0.1	ND	22.8 ± 1.3	ND
Egg yolk	2.7 ± 0.3	4.0 ± 0.2	3.5 ± 0.2	1.5 ± 0.1	ND	9.0 ± 0.2	ND
Fresh milk	3.0 ± 0.5	3.7 ± 0.4	5.1 ± 0.1	1.5 ± 0.1	ND	9.4 ± 0.5	17.8 ± 2.1
Chocolate	1.9 ± 0.2	4.4 ± 0.3	3.5 ± 0.4	5.1 ± 0.2	3.4 ± 0.1	19.1 ± 0.5	18.7 ± 0.8
Potatochips	2.0 ± 0.1	3.2 ± 0.2	4.1 ± 0.2	1.8 ± 0.1	ND	9.9 ± 0.9	ND

[a] C_3 = propanal; C_4 = butanal; i-C_5 = isopentanal; C_6 = hexanal; C_7 = heptanal; C_9 = nonanal; C_{6-1} = *trans*-2-hexenal.
[b] Not detectable.

fold during heat treatment and UV irradiation, respectively. Particularly C_6 and C_9 increased with time during both treatments. Increases of these aldehydes were approximately 1.4–5.0 fold for heat treatment (6 h) and 2.1–30.9 fold for UV irradiation (5 h). The levels of the other aldehydes were not affected by both treatments.

4. Conclusion

A convenient and reliable method for the determination of saturated and unsaturated aliphatic aldehydes in food samples has been established by modification of Shibamoto's method. Although this method is less sensitive than

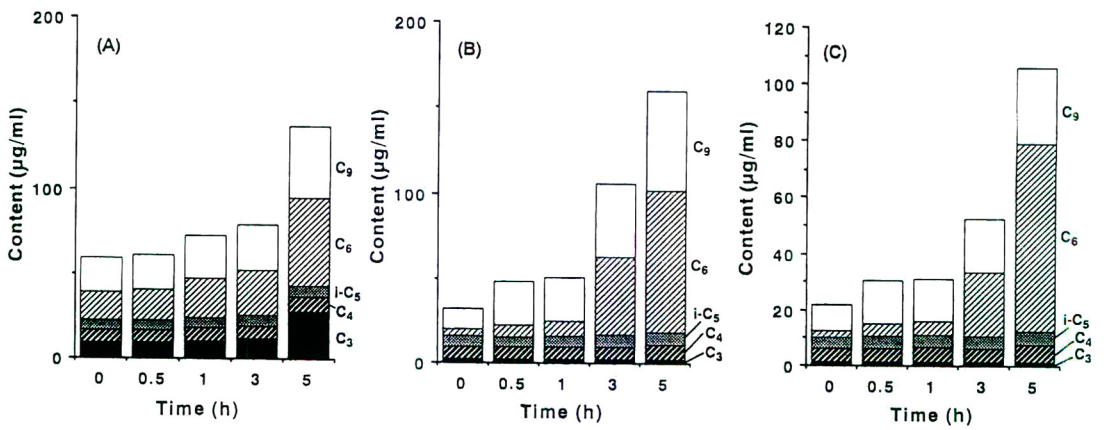

Fig. 6. Effect of UV irradiation on the formation of aldehydes in (A) salad oil, (B) sesame oil and (C) corn oil.

Shibamoto's method, this method is more simple and rapid, and sufficiently applicable for various foodstuffs. Moreover, with the present method food samples can be directly analysed without pre-treatment clean-up and without any interference from other coexisting substances. Therefore, we believe that this method provides a useful tool for routine analysis of foodstuffs.

5. References

[1] G. Ohloff, in J. Solms (Editor), Functional Properties of Fats in Foods, Forster, Zurich, 1973.
[2] B. Reindl and H.J. Stan, J. Agric. Food Chem., 30 (1982) 849.
[3] D.S. Mottram, S.E. Croft and R.L.S. Patterson, J. Sci. Food Agric., 35 (1984) 233.
[4] K. Umano and T. Shibamoto, J. Agric. Food Chem., 35 (1987) 14.
[5] T.F. Slater, Biochem. J., 222 (1984) 1.
[6] J.M.C. Gutteridge and B. Halliwell, Trends Biochem. Sci., 15 (1990) 129.
[7] J. Emerit, J.M. Klein, A. Coutellier and F. Congy, Pathol. Biol., 39 (1991) 316.
[8] M. Aviram, Atherosclerosis, 98 (1993) 1.
[9] B. Halliwell, Haemostasis, 1 (1993) 118.
[10] B.N. Ames, M.K. Shigenaga and T.M. Hagen, Proc. Natl. Acad. Sci. USA, 90 (1993) 7915.
[11] L.J. Marnett, H.K. Hurd, M.C. Hollstein, D.E. Levin, H. Esterbauer and B.N. Ames, Mutat. Res., 148 (1985) 25.
[12] A. Benedetti and M. Comporti, Bioelectrochem. Bioenerg., 18 (1987) 187.
[13] H. Esterbauer, P. Eckl and A. Ortner, Mutat. Res., 238 (1990) 223.
[14] V.J. Feron, H.P. Til, de Vrijer, R.A. Woutersen, F.R. Cassee and P.J. Van Bladeren, Mutat. Res., 259 (1991) 363.
[15] H. Esterbauer, Am. J. Clin. Nutr., 57 (suppl.) (1993) 779s.
[16] H. Esterbauer, in D.C.H. McBrien and T.F. Slater (Editors), Free Radicals, Lipid Peroxidation and Cancer, Academic Press, New York, 1981, p. 101.
[17] K. Kikugawa, T. Kato and A. Iwata, Lipids, 24 (1989) 962.
[18] H. Seto and T. Okubo, J. Chromatogr., 570 (1991) 301.
[19] C.E. Vaca, P. Vodicka and K. Hemminki, Carcinogenesis, 13 (1992) 593.
[20] A. Kautiainen, C.E. Vaca and F. Granath, Carcinogenesis, 14 (1993) 705.
[21] M. Tornqvist and A. Kautiainen, Environ. Health Perspect., 99 (1993) 39.
[22] P. Douki and B.N. Ames, Chem. Res. Toxicol., 7 (1994) 511.
[23] S. Selim, J. Chromatogr., 136 (1977) 271.
[24] B. Reindl and H.J. Stan, J. Agric. Food Chem., 30 (1982) 849.
[25] M.X. Coutrim, L.A. Nakamura and C.H. Collins, Chromatographia, 37 (1993) 185.
[26] J. Iehotay and F. Halmo, J. Liq. Chromatogr., 17 (1994) 847.
[27] W.L. Stahovee and K. Mopper, J. Chromatogr., 298 (1984) 399.
[28] K. Yoshino, T. Matsuura, M. Sana, S. Saito and I. Tomita, Chem. Pharm. Bull., 34 (1986) 1694.
[29] B.E. Miller and N.D. Danielson, Anal. Chem., 60 (1988) 622.
[30] E.N. Frankel, M.L. Hu and A.L. Tappel, Lipids, 24 (1989) 976.
[31] Y. Hoshika and G. Muto, J. High Resol. Chromatogr., 14 (1991) 330.
[32] Y. Hoshika and Y. Takata, J. Chromatogr., 120 (1976) 379.
[33] K. Kuwata, M. Uebori, H. Yamasaki and Y. Kuge, Anal. Chem., 55 (1983) 2013.
[34] S.B. Tejada, Int. J. Environ. Anal. Chem., 26 (1986) 167.
[35] H. Tamura and T. Shibamoto, Lipids, 26 (1991) 170.
[36] S.P. Levine, T.M. Harvey, T.J. Waeghe and R.H. Shapiro, Anal. Chem., 53 (1981) 805.
[37] H. Nishikawa, T. Hayakawa and T. Sakai, Bunseki Kagaku, 36 (1987) 381.
[38] M. Tomita, I. Ijiri, K. Shimosata and S. Kawai, J. Chromatogr., 414 (1987) 454.
[39] E.R. Kennedy and R.H. Hill, Anal. Chem., 54 (1982) 1739.
[40] C. Norsten-Hoog and T. Cronholm, Anal. Biochem., 189 (1990) 131.
[41] M. Kinter, S. Sullivan, R.J. Roberts and D. Spitz, J. Chromatogr., 578 (1992) 9.
[42] K. Umano and T. Shibamoto, J. Agric. Food Chem., 35 (1987) 909.
[43] T. Hayashi and T. Shibamoto, J. Agric Food Chem., 33 (1985) 1090.
[44] A. Yasuhara and T. Shibamoto, J. Food Sci., 54 (1989) 1471.
[45] A. Yasuhara and T. Shibamoto, J. Chromatogr., 547 (1991) 291.
[46] A. Yasuhara and T. Shibamoto, J. Chromatogr. A, 672 (1994) 261.

ELSEVIER

Journal of Chromatography A, 709 (1995) 313–317

JOURNAL OF CHROMATOGRAPHY A

Analysis of trichloroacetic acid in the urine of workers occupationally exposed to trichloroethylene by capillary gas chromatography

G.E. O'Donnell*, A. Juska, R. Geyer, M. Faiz, S. Stalder

Laboratory Services, WorkCover Authority of N.S.W., 5A Pioneer Avenue, Thornleigh, N.S.W. 2120, Australia

First received 27 December 1994; revised manuscript received 28 March 1995; accepted 4 April 1995

Abstract

A gas chromatographic procedure is described for the determination of trichloroacetic acid in urine, the major metabolite of trichloroethylene exposure. Trichloroacetic acid was derivatised to its methyl ester with BF_3/methanol reagent and then extracted into toluene and analysed by capillary gas chromatography using electron-capture detection. The response was linear in the range 0.4–100 mg/l of trichloroacetic acid in urine and showed a relative recovery of 99.6%. The procedure is suitable for monitoring occupational exposure to trichloroethylene.

1. Introduction

Trichloroethylene is widely used in industry as a degreaser for metal parts, dry cleaning agent, thinner for paints and lacquers, and for extracting oils, fats and waxes from vegetable and animal products. In occupational exposure, inhalation is the main route of absorption, however, significant skin absorption can occur upon contact with liquid trichloroethylene [1]. The absorbed trichloroethylene is mainly metabolised into trichloroacetic acid (TCA) (18%) and trichloroethanol (TCOH) (33%) which are eliminated in urine. The fate of 20–30% of the absorbed amount of trichloroethylene remains unknown [2]. Minor metabolites, such as chloroform, chloral hydrate and monochloroacetic acid have been suggested [3]. The relationship between the degree of exposure and excretion of TCA remains linear if the exposure concentration does not exceed 50 ppm (268 mg/m^3) in air [2,4–6]. When measuring both major metabolites, TCA and TCOH, the sampling time is quite critical because of differences in elimination half-lives of the metabolites (TCA 50–100 h; TCOH 12–26 h [7]). Hence, TCA concentration in urine reflects exposure over the working week while TCOH reflects exposure over the previous day.

Our laboratory previously used a spectrophotometric method based on the Fujiwara reaction [8]. However, this method involved the use of toxic solvents, such as pyridine, and it has shown to lack selectivity, due to interferences from similar halogenated organic compounds [9], and to lack stability of the Fujiwara reaction product. Other gas chromatographic methods which require derivatisation with reagents such as diazomethane [10–12] have the disadvantages of needing the use of concentrated acid and the

* Corresponding author.

0021-9673/95/$09.50
SSDI 0021-9673(95)00423-8

performance of multiple solvent extractions to achieve a reasonable extraction recovery. Furthermore, the use of a dangerous, toxic, carcinogenic derivatisation reagent is most undesirable. Other methods which have been reported include high-performance liquid chromatography [13], ion chromatography [14] and headspace gas chromatography [15–17]. Headspace analysis is attractive if one has an appropriate autosampler, but little time is saved due to the long incubation period. Analysis using dual columns and electron-capture detection (ECD) offers good specificity comparable to that of gas chromatographic–mass spectrometric determinations, e.g. the difluoroanilide derivatisation method [18]. The difluoroanilide derivatisation method looses specificity by monitoring an ion fragment which originates from the difluoroanilide reagent. Furthermore, difluoroanilide derivatives have shown to be unstable due to sensitivity to light [18]. Hence, the current method was developed to be simple, accurate and not requiring the use of toxic reagents or solvents such as pyridine. It involves the derivatisation of TCA to its methyl ester using methanol/BF_3 reagent. The ester is then partitioned into an organic solvent and analysed by capillary gas chromatography with electron-capture detection. The results obtained using this procedure were compared with those obtained using the Fujiwara spectrophotometric method.

The present method was developed to monitor occupational exposure to trichloroethylene. The occupational exposure limit is equivalent to 100 mg/l [19]. Therefore, the method was developed to monitor concentrations between 0.4 and 100 mg/l. The limit of quantitation of the method was hence designed to be 0.4 mg/l as concentrations below this level are not considered relevant to occupational exposure.

2. Experimental

2.1. Reagents and chemicals

The borontrifluoride–methanol complex, 14% BF_3 content was obtained from BDH Laboratory Supplies (Poole, UK); the toluene was nanograde obtained from Mallinckrodt (Germany); sodium trichloroacetic acid (97%) was obtained from Aldrich (Milwaukee, OR, USA); trichloroacetic acid methyl ester (>96%) from Tokyo Kasei Kogyo (Tokyo, Japan); Biorad Lyphochek Urine Metals Quality Control Level 1 from Bio-Rad Laboratories (Anaheim, CA, USA); anhydrous sodium sulphate (99.0%) from Ajax Chemicals (Sydney, Australia).

2.2. Apparatus

A Hewlett-Packard Model 5890 series II gas chromatograph with an electron-capture detection system, Model 7673A automatic liquid sampler and HP 3396 ChemStation data analysis system was used. The gas chromatographic capillary columns used were DB-17 (0.25 μm film thickness; 30 m × 0.32 mm I.D.) and DB-5.625 (0.25 μm film thickness; 30 m × 0.32 mm I.D.) from J&W Scientific (Folsom, CA, USA).

2.3. Instrumental conditions

The gas chromatograph was used with dual capillary columns of different polarities, as above, to give added certainty to positive identification. A split injection mode was used as electron-capture detection was highly sensitive to the TCA-methyl ester. The inlet injection temperature was 240°C and a detector temperature of 300°C was used. The temperature program of the chromatograph was initial temperature 55°C for 0.5 min, then at a rate of 3°C/min to 80°C, then at a second rate of 50°C/min to 280°C and held for 4.17 min. This gives a total run time of 17.00 min. Hydrogen was used as carrier gas at a flow-rate of 2 ml/min. The split vent was equal to 40 ml/min and detector make up gas (5% methane in argon) was equal to 80 ml/min. The injection volume used was 1 μl. A 100 mg/l spiked urine sample chromatogram can be seen in Fig. 1.

2.4. Preparation of standards

A stock standard was prepared by weighing 0.5 g of sodium trichloroacetate and making up to volume in a 1-l volumetric flask with distilled

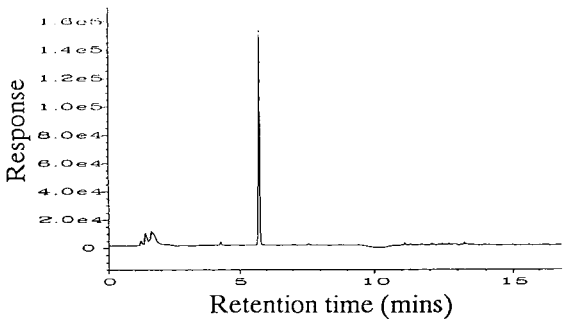

Fig. 1. Gas chromatogram of 100 mg TCA/l urine using a DB-17 (0.25 μm film thickness; 30 m × 0.32 mm I.D.) capillary column from J&W Scientific.

water. A range of working standards were prepared from this stock by appropriate dilutions to give a range of 0.5–100 mg/l. The sodium salt of TCA was preferred to the acid form because it was less hygroscopic. A Bio-Rad commercial quality control sample was used to determine the accuracy and precision of the method. The absolute recovery of the procedure was determined using standards prepared from the TCA-methyl ester made up directly in toluene.

2.5. Procedure

A 200-μl aliquot of urine sample was added to a 12-ml stoppered test tube. A 0.5-ml volume of BF_3–methanol complex was added to the sample in the test tube. The mixture was heated at 60°C for 30 min. After cooling, the sample was extracted with 8.0 ml of toluene for one hour on a rotator. A 2-ml volume of the toluene extract was then taken and shaken with anhydrous sodium sulphate in a glass vial. A portion of this dried toluene extract was then transferred to a vial for gas chromatographic analysis.

The standards and the quality control sample were prepared according to the same procedure as used for the samples.

3. Results and discussion

Gas chromatographic analysis of chlorinated hydrocarbons using electron-capture detection is a very sensitive detection technique. Hence, efforts were made in this procedure to optimise the linear range of the detector to the concentration range encountered in occupational exposures. A large volume of extracting solvent was used to give the effect of (1) dilution and (2) a satisfactory extraction efficiency of greater than 90%. It was found that at least a 1:2 ratio of sample to derivatising reagent was necessary for the maximum level of derivatisation to occur.

3.1. Recoveries

Absolute recoveries were quantified against a TCA-methyl ester standard, which was diluted to the appropriate concentration in nanograde toluene. The absolute recovery of TCA-methyl ester in water was 48.8% with a standard deviation of 1.9 ($n = 30$) over the range 0.1–100 mg/l. In urine the absolute recovery was 48.5% with a standard deviation of 2.5 ($n = 30$) over the range 0.1–100 mg/l. The fact that both water and urine have the same recoveries allows the use of water as the standard matrix.

The relative recoveries were obtained by comparing the spiked urine results to the water standards, which had both been subjected to the same procedure. This gave a relative recovery in urine of 99.6% ($n = 30$).

3.2. Accuracy and precision

The precision of the procedure was determined by using a commercially available quality control standard known as Lyphochek Urine Metals Control Level 1 obtained from Bio-Rad Laboratories (Anaheim, CA, USA). The mean value of this control was specified by the manufacturers as 24.4 mg/l with an acceptable range of 19.5–29.3 mg/l. This control standard was analysed, and gave a mean value of 28.45 mg/l with a standard deviation of 1.14 mg/l ($n = 11$). This gave a 95% confidence interval of the mean as 27.7–29.2 mg/l based on the two-sided t-test of $\times \pm ts/n^{1/2}$. A slightly higher bias can be seen in the mean of the procedure when compared to mean value given by the manufacturer. However, the confidence limits of the mean lie within the acceptable range given by the manufacturer.

The precision of the procedure can be seen by observing the relative standard deviations (R.S.D.) over the range of concentrations shown in Table 1. This concentration range of 0.1–100 mg/l TCA gave a range of R.S.D. of 2.2–4.9% with an overall mean of the R.S.D. of 3.3%.

3.3. Linearity

The procedure shows good linearity (Fig. 2) over the range 0.4–100 mg/l with a correlation coefficient of 1.000. However, to extend the range of analysis to 0.05–100 mg/l it was found that a power function was necessary to achieve the same correlation coefficient.

Figure 2. Linearity of TCA Analysis in Urine

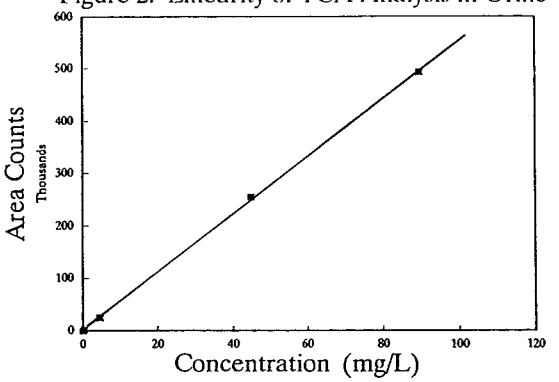

Fig. 2. Linearity of TCA analysis in urine over the range 0.4–100 mg/l with a correlation coefficient of 1.000.

3.4. Detection limits

The detection limit of this procedure was found to be 0.05 mg/l based on a signal-to-noise ratio of 5 and a power regression curve. This detection limit can easily be lowered by using a splitless chromatographic injection mode and less toluene to extract the TCA-methyl ester.

3.5. Comparison to the Fujiwara method

Urine samples were taken in the field from 10 workers employed in a degreasing operation who had been exposed to trichloroethylene. These urine samples were analysed by both the above procedure and the Fujiwara method [8]. The two procedures are compared in Fig. 3 which shows the values obtained from the gas chromatographic procedure plotted against the values obtained for the same samples analysed by the Fujiwara method. For the procedures to give identical values the points should lie on the 45° angle line. There appears to be a positive bias towards the Fujiwara reaction method. This is not unreasonable as the Fujiwara reaction is not absolutely specific for TCA [9]. This bias may be attributable to chloroform and chloral hydrate which have been suggested as a minor metabolites of trichloroethylene [3].

Table 1
The absolute and relative recoveries of TCA in water and urine

Range studied (mg/l)	Absolute recovery in water[a]		Absolute recovery in urine[a]		Relative recovery of urine to water[a]	
	Mean	R.S.D.	Mean	R.S.D.	Mean	R.S.D.
0.1 ($n = 6$)	50.9	2.1	46.4	3.1	91.2	3.7
0.4 ($n = 6$)	45.7	1.2	46.6	4.8	102.0	4.9
5.0 ($n = 6$)	49.2	1.7	49.5	1.7	100.6	2.4
50.0 ($n = 6$)	50.8	1.8	50.9	1.3	100.2	2.2
100.0 ($n = 6$)	47.2	2.4	49.1	1.4	104.0	3.2
Overall mean ($n = 30$)	48.8	1.9	48.5	2.5	99.6	3.3

[a] Values are in %.

Figure 3. Comparision of GC to Fujiwara Method

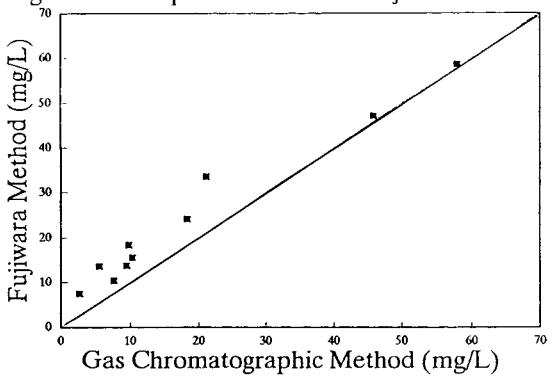

Fig. 3. Comparison of the gas chromatographic procedure to the Fujiwara reaction method with 10 urine specimens taken from trichloroethylene exposed workers.

4. Conclusion

The present method was developed for the purpose of monitoring exposure of workers to trichloroethylene in the workplace. Hence, it was optimised to determine TCA in the range 0.4–100 mg TCA/l urine. However, this method could easily be made more sensitive by using a splitless injection mode and a lower volume of toluene for the extraction step and still achieve satisfactory recoveries. It is a simple method which gives an accurate and sensitive analysis and does not suffer from the interferences of the Fujiwara method and avoids the use of toxic solvents such as pyridine.

References

[1] A. Sato and T. Nakajima, Br. J. Ind. Med., 35 (1978) 43.
[2] T. Ertle, D. Henschler, G. Mueller and M. Sparsowski, Arch. Toxikol., 29 (1972) 171.
[3] B. Soucek and D. Vlachova, Br. J. Ind. Med., 17 (1960) 60.
[4] A. Sato, T. Nakajima, Y. Fujiwara and N. Marayama, Br. J. Ind. Med., 34 (1977) 56.
[5] M. Ikeda, H. Ohtsuji, T. Imamura and Y. Komoika, Br. J. Ind. Med., 29 (1972) 28.
[6] S. Tanaka and M. Ikeda, Br. J. Ind. Med., 25 (1968) 214.
[7] V. Bartonicek, Br. J. Ind. Med., 19 (1972) 134.
[8] R. Frant and J. Westendorp, Ind. Hyg. Occup. Med., 1 (1950) 308.
[9] J.F. Reith, W.C. van Ditsmarsch and T. de Ruiter, Analyst., 99 (1974) 652.
[10] J.W. Miller, P.C. Uden and R.M. Barnes, Anal. Chem., 54 (1982) 485.
[11] H. Nomiyama, K. Nomiyama and H. Uchiki, Am. Ind. Hyg. Assoc. J., 39 (1978) 506.
[12] R.F. Christman, D.L Norwood, D.S. Millington, J.D. Johnson and A.A. Stevens, Environ. Sci. Technol., 17 (1983) 625.
[13] M. Ogata and Y. Yamazaki, Acta. Med. Okayama, 33 (1979) 479.
[14] H. Itoh, Analyst, 114 (1989) 1637.
[15] V. Senft, J. Chromatogr., 337 (1985) 126.
[16] J.M. Christensen, K. Rasmussen and B. Koppen, J. Chromatogr., 442 (1988) 317.
[17] D.D. Breimer, H.C.J. Ketelaars and J.M. Van Rossum, J. Chromatogr., 88 (1974) 55.
[18] H. Ozawa, J. Chromatogr., 644 (1993) 375.
[19] Threshold Limit Values and Biological Exposure Indices, 1993–1994 American Conference of Governmental Industrial Hygienists.

ELSEVIER

Journal of Chromatography A, 709 (1995) 319–331

JOURNAL OF CHROMATOGRAPHY A

Determination of organophosphorus pesticides in environmental samples by capillary gas chromatography–mass spectrometry

Tameo Okumura, Yoshinori Nishikawa*

Environmental Pollution Control Center, 62-3, 1 Chome, Nakamichi, Higashinari-ku, Osaka City 537, Japan

First received 29 November 1994; revised manuscript received 13 April 1995; accepted 18 April 1995

Abstract

Traces of fourteen organophosphorus pesticides in environmental samples such as river water, sediment and fish were determined by capillary GC–MS with selected-ion monitoring. The pesticides could be determined within the range 0.02–0.75 ng/ml in water with relative standard deviations (R.S.D.s) of 1.0–31.4% (except for MPP, 1.0–10.9%). The detection limits of the pesticides were 0.013–0.120 ng/ml in water. Their recoveries from river water, sea water, sediment and fish samples were 101–132%, 103–145%, 93–166% (except for isoxathion) and 67–101% (except for isoxathion and phosmet), with R.S.D.s of 1.1–8.0%, 0.9–8.2%, 6.2–28.5% and 4.2–10.8%, respectively.

1. Introduction

Organophosphates are well known as powerful insecticides and organophosphorus pesticides (OPs) have been widely used since the use of organochlorine pesticides was prohibited, as they do not have such adverse decomposition and bioaccumlative properties in the environment. However, care must be taken with the use of OPs because they are cholinesterase inhibitors in living bodies [1].

Chromatographic methods such as GC [2–7] and LC [8–10] have been used for the simultaneous determination of pesticides. However, it is very difficult to determine trace amounts in the presence of various kinds of interfering substances that occur in the environment, especially in fish samples. Moreover, few reports have appeared concerning detection limits, which are related to the standard deviations of the measured values at near zero concentrations of the analyte.

The aim of this study was to develop a practical method for the determination of the OPs in water, sediment and fish samples for use in an actual survey. In this work, fourteen OPs were selected for the survey on the basis of the amounts manufactured, their forms of use and other factors of concern to the Japan Environmental Agency. A convenient method is presented for determining these OPs in environmental samples by capillary GC–MS with selected-ion monitoring (SIM) and with detection limits at sub-ng/ml levels. The analytical methodologies were improved by using a clean-up pro-

* Corresponding author.

0021-9673/95/$09.50
SSDI 0021-9673(95)00477-7

cedure with both normal- and reversed-phase column chromatography for fish samples.

2. Experimental

2.1. Reagents and apparatus

OP standards were obtained as pure solids or liquids from Wako (Osaka, Japan). The structures of the fourteen OPs studied are shown in Fig. 1. Phenanthrene-d_{10}, fluoranthene-d_{10} and chrysene-d_{12}, used as internal standards, were obtained from MSD Isotopes (Montreal, Canada). Dichloromethane, acetone, hexane and methanol of pesticides grade and the other reagents used of special grade were purchased from Wako and Tokyo Kasei (Tokyo, Japan).

Wako gel C-200 and polyamide C-200 of column chromatographic grade were purchased from Wako. Hydrated silica gel columns were prepared as follows. Wako gel C-200 was activated overnight at 130°C and kept in a desiccator. A 100-g amount of the activated silica gel was placed in a stoppered conical flask, then 5 or 40 ml of pure water were added and the flask was shaken to ensure homogeneity and then allowed to stand for 4–5 h. A 2-g amount of the hydrated (100 + 5) silica or 5 g of the hydrated (100 + 40) silica was packed in a 1 cm I.D. column chromatographic tube using the hexane slurry method and anhydrous Na_2SO_4 was added to make a ca. 2 cm upper layer of the column packing. The polyamide column was prepared by packing 1 g of polyamide C-200 in 1 cm I.D. column chromatographic tube using the methanol–water (50:50) slurry method. The hydrated (100 + 5) silica columns were used to clean up sediment samples and the hydrated (100 + 40) silica and the polyamide columns were used for fish samples.

A Waters (Milford, MA, USA) Model 600E liquid chromatograph equipped with a Model 717 autosampler and a Nihonbunko (Tokyo, Japan) Model 870-UV absorbance detector adjusted to 210 nm was employed for the determination of *n*-octanol–water partition coefficients and for pesticide degradation tests. The analytical column used was a 25 cm × 4.6 mm I.D. stainless-steel tube packed with Develosil ODS-5 (Nomura Kagaku, Aichi, Japan).

A Branson B-220 ultrasonic extractor and a Poly Toron PT10-30 homogenizer were used for extraction from sediment and fish samples, respectively. A Tomy Seiko (Tokyo, Japan) LC06-SP centrifuge was employed for phase separation of sediment or fish samples.

2.2. Gas chromatography–mass spectrometry

A Hewlett-Packard (Avondale, PA, USA) HP 5790 gas chromatograph and a Nihondenshi (Tokyo, Japan) JEOL-DX303 mass spectrometer with a DA-5000 data processing system were employed. The analytical column used was Ultra-2 cross-linked with 5% phenylmethylsilicone (25 m × 0.32 mm I.D., 0.52 μm film thickness). The GC temperature programme was an initial temperature of 70°C, increased at 3°C/min to 250°C. The temperatures of the injector, transfer line and ion source were 250°C. The carrier gas was helium at 7.5 p.s.i. (61 cm/s). Samples were injected in the splitless mode with 1.5 min purge off. The mass spectrometer was operated at 70 eV and 300 μA in the electron-impact mode using scanning or SIM. The ions of the pesticides and the internal standards monitored are shown in Table 1. As the retention times of the OPs vary widely, it is preferable to use several internal standards, and in this work three deuterated hydrocarbons whose retention times covered the appropriate interval were used. The m/z values monitored were selected in consideration of selectivity and sensitivity. Fig. 2 shows typical GC–MS total ion and SIM traces for the pesticides and the internal standards.

2.3. Analytical procedure

The procedure for the determination of the OPs in environmental samples is outlined in Fig. 3. A 1000-ml volume of water sample was added to 50 g of NaCl and extracted twice with 100 and 50 ml of dichloromethane, then the organic

①IBP($C_{13}H_{21}O_3PS$:288.4)
S-benzyl O,O-diisopropyl phosphorothioate

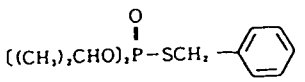

②MEP($C_9H_{12}NO_5PS$:277.2)
O,O-dimethyl O-4-nitro-m-tolyl phosphorothioate

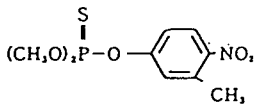

③Diazinon($C_{12}H_{21}N_2O_3PS$:304.4)
O,O-diethyl O-2-isopropyl-6-methyl-pyrimidine-4-yl phosphorothioate

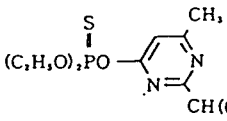

④MPP($C_{10}H_{15}O_3PS_2$:279.3)
O,O-dimethyl O-4-methylthio-m-tolyl phosphorothioate

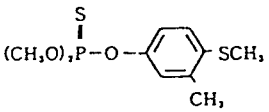

⑤EDDP($C_{14}H_{15}O_2PS_2$:310.4)
O-ethyl S,S-diphenyl phosphorodithioate

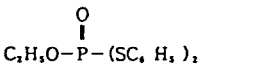

⑥Malathion($C_{10}H_{19}O_6PS_2$:330.4)
S-1,2-bis(ethoxycarbonyl)ethyl O,O-dimethyl phosphorodithioate

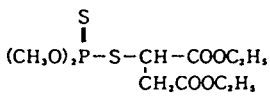

⑦Isoxathion($C_{13}H_{16}NO_4PS$:313.3)
O,O-diethyl O-5-phenylisoxazol-3-yl phosphorothioate

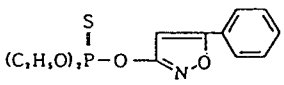

⑧EPN($C_{14}H_{14}NO_4PS$:323.3)
O-ethyl O-p-nitrophenyl phenyl phosphorothioate

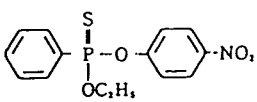

⑨Methidathion($C_6H_{11}N_2O_4PS_3$:302.3)
S-2,3-dihydro-5-methoxy-2-oxo-1,3,4-thiadiazol-3-ylmethyl O,O-dimethyl phosphorodithioate

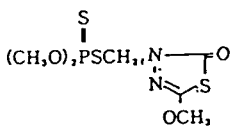

⑩Salithion($C_8H_9O_3PS$:216.2)
2-methoxy-4H-1,3,2-benzodioxaphosphinine

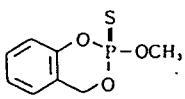

⑪Phosalone($C_{12}H_{15}ClNO_4PS_2$:367.8)
S-6-chloro-2,3-dihydro-2-oxobenzoxazol-3-ylmethyl O,O-diethyl phosphorodithioate

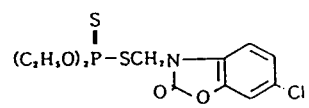

⑫Phosmet($C_{11}H_{12}NO_4PS_2$:317.3)
O,O-dimethyl S-phthalimidomethyl phosphorodithioate

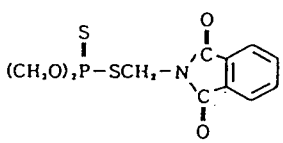

⑬α-CVP($C_{12}H_{14}Cl_3O_4P$:359.6)
2-chloro-1-(2,4-dichlorophenyl)vinyl diethylphosphate

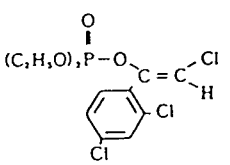

⑭β-CVP($C_{12}H_{14}Cl_3O_4P$:359.6)
2-chloro-1-(2,4-dichlorophenyl)vinyl diethylphosphate

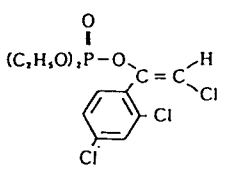

Fig. 1. Structures of the OPs studied.

Table 1
Monitor ions for the pesticides and the internal standards

No.	Compound	Monitor ion (m/z)		
a	Phenanthrene-d_{10}		188	
10	Salithion	(183)		216
3	Diazinon	(179)		304
1	IBP	204		(288)
b	Fluoranthene-d_{10}		212	
2	MEP	(260)		277
6	Malathion	(127)		173
4	MPP	(169)		278
13	α-CVP	323		(325)
14	β-CVP	323		(325)
9	Methidathion	(125)		145
7	Isoxathion	(177)		313
c	Chrysene-d_{12}		240	
5	EDDP	(173)		310
12	Phosmet	160		(317)
8	EPN	(169)		185
11	Phosalone	182		(367)

The monitor ions in parenthesis are used for identification, not for quantitation.

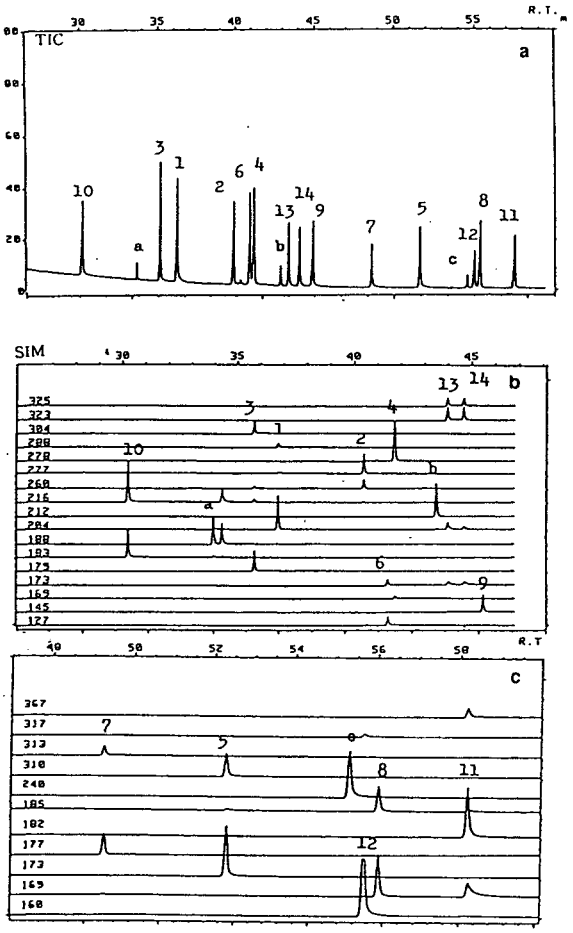

Fig. 2. Typical GC–MS TIC and SIM traces for the OPs and the internal standards. (a) Phenanthrene-d_{10}; (b) fluoranthene-d_{10}; (c) chrysene-d_{12}. Peaks: 1 = IBP; 2 = MEP; 3 = diazinon; 4 = MPP; 5 = EDDP; 6 = malathion; 7 = isoxathion; 8 = EPN; 9 = methidathion; 10 = salithion; 11 = phosalone; 12 = phosmet; 13 = α-CVP; 14 = β-CVP.

phases were combined and dehydrated by passing through anhydrous Na_2SO_4. The organic phase was concentrated to 3–5 ml in a Kuderna–Danish (KD) evaporative concentrator and further evaporated to 0.5 ml under a stream of nitrogen. A 0.5-ml volume of internal standard solution (each 1 mg/l) was added and then an aliquot was analysed by GC–MS–SIM.

For sediments, 10 g of sample were added to 30 ml of acetone with stirring and then sample was extracted twice in an ultrasonic extractor for 10 min and then centrifuged at 3000 rpm (1600 g) for 10 min. The supernatant solutions were combined in a separating funnel and 200 ml of 5% NaCl solution and 50 ml of dichloromethane were added, then the mixture was extracted, dehydrated and concentrated to dryness. One should be careful not to over-dry with heating, otherwise the recovery will be low. Hexane (2 ml) was added to the dry sample, which was subjected to hydrated (100 + 5) silica column chromatography. The column was first washed with 20 ml of hexane and then the fourteen OPs were eluted with 30 ml of acetone–hexane (10:90). The eluate was treated using the same procedure as for water samples.

For fish samples, 10 g of sample were homogenized, centrifuged, extracted and concentrated to dryness in a similar manner to sediment. Next, 2 ml of azobenzene in hexane solution (500 mg/l) were added to the dry sample and subjected to hydrated (100 + 40)

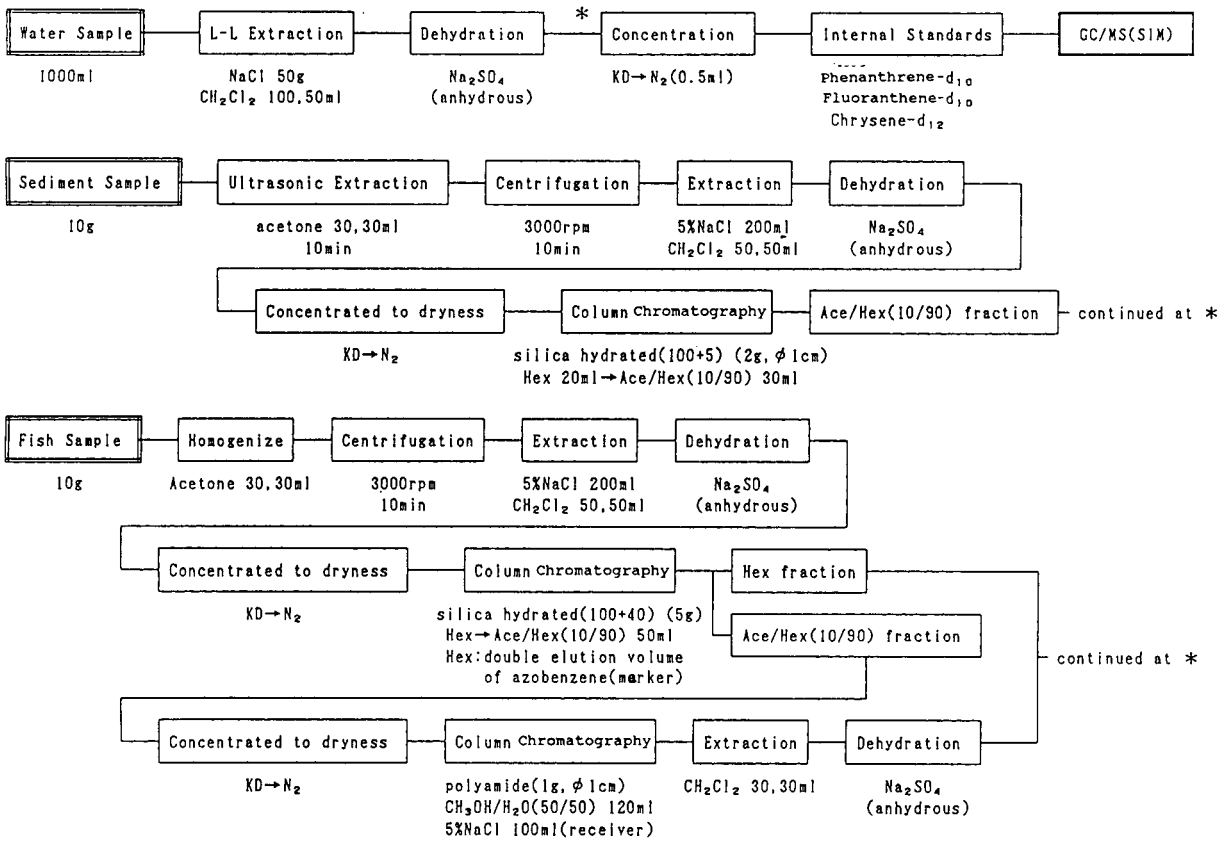

Fig. 3. Flow scheme for the determination the OPs in environmental samples.

silica column chromatography. Azobenzene was used as an elution marker, being observed visually as a yellow band in the column. The hexane fraction was obtained using double the volume (14 ml) used in azobenzene elution. As it was difficult to charge the sample on the column due to its low solubility in CH_3OH–H_2O (50:50), the acetone–hexane (10:90) fraction (50 ml) was concentrated to dryness 0.3 g of polyamide was added to the residue and then the adsorbed particles were charged on the polyamide column. The charged sample was washed on the column with 120 ml of CH_3OH–H_2O (50:50) to remove interfering biota components. The eluate was extracted twice with 30 ml of dichloromethane and then the organic phase was dehydrated with anhydrous Na_2SO_4. The organic phase and the preceding hexane fraction were combined and the procedure was continued from the asterisk marked in Fig. 3.

3. Results and discussion

3.1. Octanol–water partition coefficients

The *n*-octanol–water partition coefficients (P_{ow}) of organic chemicals are an important parameter for predicting bioconcentration factors for fish and their water solubility. It is easy to calculate log P_{ow} as a function of the logarithm of the capacity factor with the use of a

reversed-phase HPLC system [11,12]. Benzene, bromobenzene and biphenyl were used for calibration. The analytical column was used Develosil ODS-5 (25 cm × 4.6 mm I.D.). The mobile phase was CH_3OH–H_2O (70:30) at a flow-rate 1.0 ml/min. The log P_{ow} data for the OPs are summarized in Table 2. The calculated values of log P_{ow} were 1.90–3.97 and the experimental values were 1.8–4.30.

3.2. Degradation test

In any method, it is necessary to elucidate the stability of the analytes. A degradation screening test for the pesticides was investigated under different pH conditions. Table 3 shows residual percentage of the OPs after 1 h and 5 days at pH 5, 7 and 9, adjusted using the buffer solutions 65 m*M* KH_2PO_4, 65 m*M* KH_2PO_4–65 m*M* Na_2HPO_4 (40:60) and 65 m*M* Na_2HPO_4, respectively. The pesticides did not decompose under acidic conditions (pH 5), but EDDP, salithion and phosmet decomposed at pH 7 and 9 and malathion at pH 9. MPP decomposed on exposure to light.

3.3. Clean-up procedure for column chromatography

Clean-up of sediment extracts was carried out with the use of the hydrated (100 + 5) silica column. Fig. 4 shows typical elution pattern of the OPs with hexane and acetone–hexane (10:90) as eluents. The OPs were not eluted with 20 ml of hexane, but they completely eluted with 30 ml of acetone–hexane (10:90). For fish or biota samples, it is difficult to apply a clean-up procedure similar to that for sediment owing to unavoidable interfering components in the samples. Most OPs are relatively polar compounds, so the hydrated (100 + 40) silica column was used. The polar acetone–hexane (10:90) fraction was further cleaned up by means of polyamide column chromatography in order to separate biota interferents.

3.4. Calibration

The calibration graph for the OPs was obtained by plotting the concentration ratio against peak-area ratio of the analyte to internal stan-

Table 2
HPLC capacity factors and calculated log P_{ow} values for the pesticides

Compound	Capacity factor (k')[a]	Log k'	Calculated log P_{ow}	Reported log P_{ow}
IBP	9.16	0.96	3.19	3.34[b], 2.6 [7]
MEP	6.06	0.78	2.70	2.94[b], 2.2 [7]
Diazinon	11.31	1.05	3.43	1.92[b], 2.9 [7]
MPP	11.03	1.04	3.40	3.57[b], 3.0 [7]
EDDP	10.18	1.01	3.31	2.31[b], 2.6 [7]
Malathion	5.08	0.71	2.49	2.45[b], 1.9 [7]
Isoxathion	13.14	1.12	3.61	3.93[b], 2.9 [7]
EPN	17.88	1.25	3.97	2.00[b]
Methidathion	3.63	0.56	2.10	2.42[b], 2.5 [7]
Salithion	3.05	0.48	1.90	2.67[b], 2.3 [7]
Phosalone	13.70	1.14	3.66	4.30 [12], 3.0 [7]
Phosmet	3.75	0.57	2.14	2.83 [12], 1.8 [7]
α-CAVP	13.95	1.14	3.68	3.54[b]
β-CVP	11.45	1.06	3.45	2.7 [7]
Benzene	3.97	0.60		2.13 [11]
Bromobenzene	6.97	0.84		2.99 [11]
Biphenyl	15.61	1.19		3.76 [11]

[a] $k' = (t_R - t_0)/t_0$; $t_0 = 1.55$ min.
[b] From materials supplied by Japan Environmental Agency.

Table 3
Degradation tests for the pesticides at pH 5, 7 and 9

Compound	pH	Concentration (mg/l)	Residual (%)		
			After 1 h	After 5 days	
				Dark	Light
IBP	5	2.0	100	105	–
	7	2.0	100	101	103
	9	2.0	100	107	–
MEP	5	1.0	87	87	–
	7	1.0	84	84	80
	9	1.0	89	78	–
Diazinon	5	3.0	103	32	–
	7	3.0	95	86	84
	9	3.0	105	83	–
MPP	5	2.0	94	81	–
	7	2.0	95	70	30
	9	2.0	98	90	–
EDDP	5	2.0	99	67	–
	7	2.0	90	15	9
	9	2.0	10	0	–
Malathion	5	5.0	109	102	–
	7	5.0	107	71	52
	9	5.0	59	0	–
Isoxathion	5	2.0	89	81	–
	7	2.0	84	73	64
	9	2.0	87	72	–
EPN	5	2.0	87	31	–
	7	2.0	94	26	16
	9	2.0	105	16	–
Methidathion	5	3.0	102	86	–
	7	3.0	100	78	67
	9	3.0	99	46	–
Salithion	5	1.0	108	74	–
	7	1.0	84	0	0
	9	1.0	103	0	–
Phosalone	5	2.0	90	63	–
	7	2.0	97	57	51
	9	2.0	94	19	–
Phosmet	5	1.0	112	84	–
	7	1.0	63	0	0
	9	1.0	0	0	–
α-CVP	5	1.0	87	95	–
	7	1.0	98	98	95
	9	1.0	109	103	–
β-CVP	5	2.0	96	107	–
	7	2.0	97	95	94
	9	2.0	98	101	–

dard. An example is shown in Fig. 5. The concentration ratio of the OPs to the internal standards was determined from the peak-area ratio with the use of a calibration graph and then the detected amounts were calculated from the amounts of internal standards added. The con-

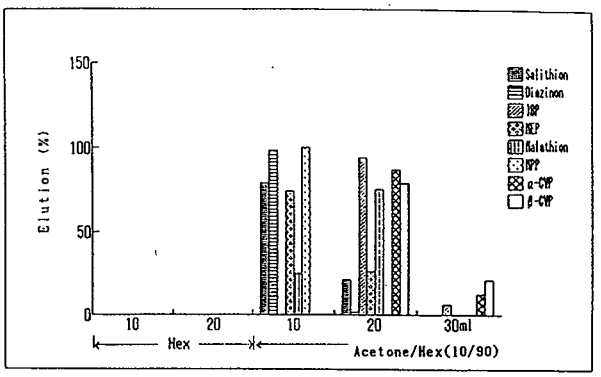

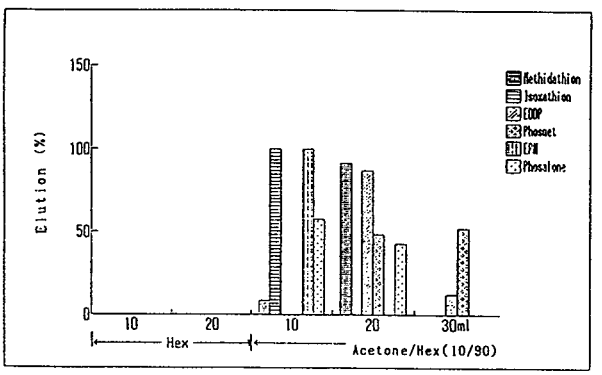

Fig. 4. Typical elution patterns of the OPs on the hydrated (100 + 5) silica column.

centration of OPs in environmental samples was calculated with the following equation:

concentration (ng/ml or ng/g)

= amount detected (ng)/sample size (ml or g)

3.5. Preservation in river water

A 1000-ml river water sample spiked with 60–750 ng of the OPs was stored in a refrigerator and their concentrations were determined after 7 and 14 days. Fig. 6 shows stability of the OPs in river water. Phosmet was somewhat decomposed, but the other OPs virtually did not decompose in the river water when stored cool and in the dark place for 7–14 days. However, it is preferable that the analysis is carried out as soon as possible after sampling.

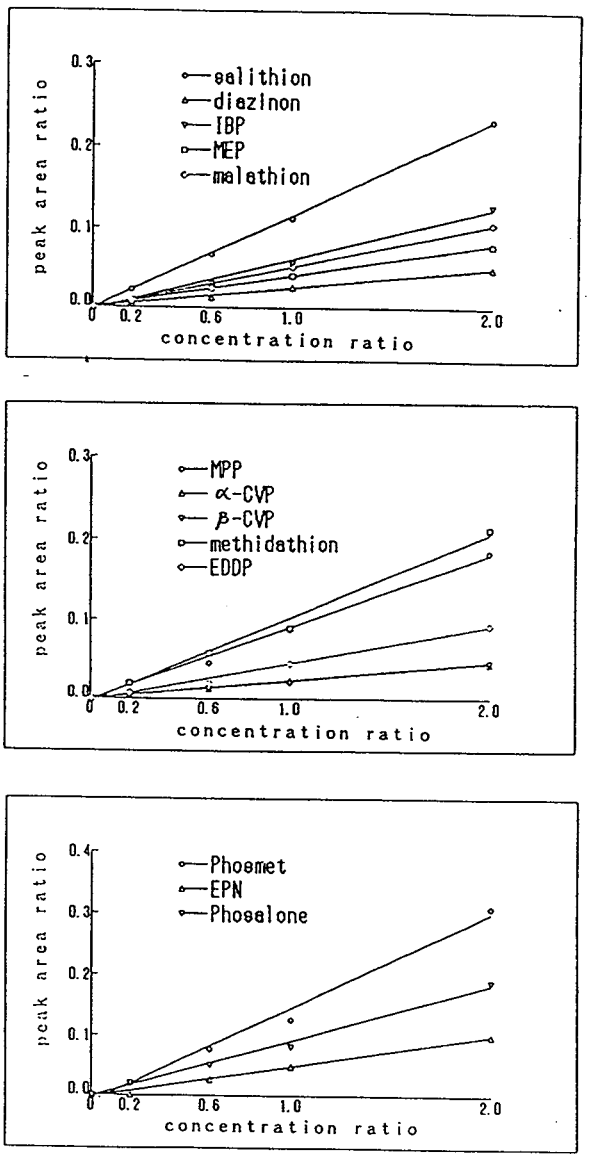

Fig. 5. Typical calibration graphs for the OPs.

3.6. Detection limits and analytical precision

Table 4 reports the detection limits and precision for the OPs. A blank test was performed with using 1000 ml of pure water and with other chemicals used in the analysis. No blank peaks corresponding to the OPs were observed in the chromatogram. Detection limits (DL) were

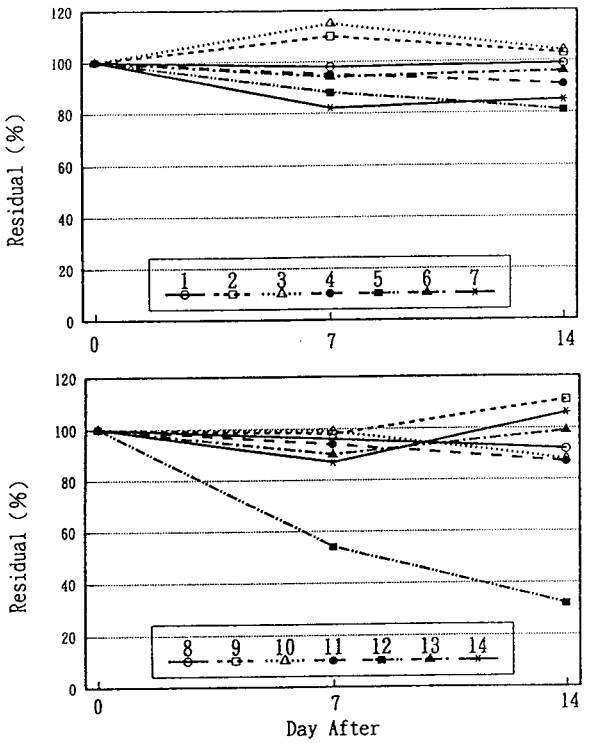

Fig. 6. Stability of the OPs in river water. Initial concentrations of the pesticides were as follows: (1) IBP 105; (2) MEP 150; (3) diazinon 90; (4) MPP 150; (5) EDDP 450; (6) malathion 300; (7) isoxathion 600; (8) EPN 750; (9) methidathion 450; (10) salithion 60; (11) phosalone 600; (12) phosmet 450; (13) α-CVP 150; (14) β-CVP 150 ng/l.

calculated from the sensitivity of the response estimating the standard deviation as follows:

$$D = t_{(n-1,0.05)}\ \sigma\ /\ \sqrt{n} \times \mathrm{d}C/\mathrm{d}R \qquad \mathrm{DL} = 3\bar{D}$$

where D is detection potential and $\bar{D}$ is the average value of D calculated using different concentrations (DL were defined as three times the detection potential), $t_{(n-1,0.05)}$ the t-distribution at 95% reliability, σ the standard deviation of the response, n the number of replicates, C the concentration of the pesticides and R the peak-area ratio of the analyte to the internal standard.

The pesticides (except for MPP) were determined with relative standard deviations (R.S.D.s) of 0.9–10.9% at levels in the range 0.035–0.750 ng/ml in water samples. The detection limits of the pesticides in water were calculated to be 0.013–0.120 ng/ml for 1000 ml of water. The detection limits of several OPs obtained using LC–MS–SIM [9,10] were reported to be 1–100 ng (signal-to-noise ratio 3–6) and those obtained using GC with nitrogen–phosphorus detection (NPD) [5] were 1 ng/l for 1000–4000 ml of water. Although they have been defined differently, comparison of the detection limits given by these methods showed that the values with GC–MS–SIM might be superior to those with LC–MS–SIM and inferior to those with GC–NPD. However, the detection limits in this work have been presented in order to assess the overall analytical procedure on the basis of statistical considerations with a view to using the method in an actual survey.

3.7. Recovery test

Analyte recoveries were investigated by using 1000 ml of river and sea water and 10 g of sediment and fish sample spiked with 120–1500 ng of the OPs. Table 5 gives the recoveries of the pesticides from these environmental samples. The OP recoveries were 101–145% from river and sea water with R.S.D.s of 0.9–8.2%. For sediment and fish samples, the recoveries were 93–166% (except for isoxathion) and 66–101% (except for phosmet), with R.S.D.s of 6.2–28.5% and 4.2–35.3%, respectively. Diazinon, MEP, malathion, β-CVP and phosalone could be detected at sub-ng/ml or -ng/g levels in the environment. Fig. 7 shows examples of their chromatograms for non-spiked and spiked samples of river water, sediment and fish.

4. Conclusions

The proposed method involving a column clean-up procedure and GC–MS–SIM determination may be useful for the routine analysis of environmental samples at low-ng/ml levels. Especially trace levels of the OPs in fish samples were successfully separated from interfering biota materials with the use of both normal- and

Table 4
Detection limits and analytical precision for the pesticides

Compound	Detection limit (ng/ml)	Analytical precision		
		Concentration (ng/ml)	Response[a]	R.S.D. (%)
IBP	0.027	0.035	117	7.7
		0.070	272	8.7
		0.105	387	5.3
MEP	0.032	0.05	108	10.9
		0.10	204	4.1
		0.15	306	3.7
Diazinon	0.013	0.03	116	2.9
		0.06	224	8.3
		0.09	306	2.1
MPP	0.120	0.05	58	31.4
		0.10	152	9.2
		0.15	222	25.7
EDDP	0.034	0.15	118	2.4
		0.30	252	3.6
		0.45	366	1.0
Malathion	0.044	0.10	108	7.1
		0.20	238	4.3
		0.30	348	4.3
Isoxathion	0.110	0.20	125	2.5
		0.40	274	7.6
		0.60	420	4.9
EPN	0.120	0.25	100	3.2
		0.50	206	6.1
		0.75	312	4.0
Methidathion	0.072	0.15	118	3.2
		0.30	246	7.4
		0.45	357	3.8
Salithion	0.013	0.02	111	0.9
		0.04	206	7.6
		0.06	258	6.5
Phosalone	0.073	0.20	109	5.8
		0.40	242	6.3
		0.60	363	1.4
Phosmet	0.048	0.15	123	3.0
		0.30	250	5.6
		0.45	384	1.3
α-CVP	0.023	0.05	121	7.8
		0.10	276	8.1
		0.15	402	1.2
β-CVP	0.024	0.05	123	4.1
		0.10	258	7.5
		0.15	372	3.0

[a] Average of four experiments.

Table 5
Recovery of the pesticides from environmental samples

Compound	Sample	Sample amount	Added (ng)	Recovery (%)	Number of samples (*n*)	R.S.D. (%)
IBP	River water	1000 ml	210	123	4	5.4
	Sea water	1000 ml	210	127	4	6.9
	Sediment	10 g	1000	119	7	13.1
	Fish	10 g	1000	96	7	4.6
MEP	River water	1000 ml	300	116	4	1.2
	Sea water	1000 ml	300	115	4	5.4
	Sediment	10 g	1000	113	7	25.8
	Fish	10 g	1000	99	7	6.6
Diazinon	River water	1000 ml	180	122	4	2.3
	Sea water	1000 ml	180	115	4	5.4
	Sediment	10 g	1000	97	7	6.2
	Fish	10 g	1000	91	7	4.7
MPP	River water	1000 ml	300	112	4	1.1
	Sea water	1000 ml	300	108	4	5.3
	Sediment	10 g	1000	109	7	21.9
	Fish	10 g	1000	97	7	4.7
EDDP	River water	1000 ml	900	125	4	2.1
	Sea water	1000 ml	900	122	4	4.7
	Sediment	10 g	1000	112	7	28.5
	Fish	10 g	1000	67	7	9.8
Malathion	River water	1000 ml	600	126	4	3.5
	Sea water	1000 ml	600	125	4	5.7
	Sediment	10 g	1000	93	7	14.8
	Fish	10 g	1000	101	7	7.1
Isoxathion	River water	1000 ml	1200	128	4	3.4
	Sea water	1000 ml	1200	145	4	3.2
	Sediment	10 g	1000	–	7	–
	Fish	10 g	1000	66	7	35.3
EPN	River water	1000 ml	1500	101	4	2.6
	Sea water	1000 ml	1500	104	4	1.8
	Sediment	10 g	1000	125	7	11.7
	Fish	10 g	1000	91	7	10.8
Methidathion	River water	1000 ml	900	121	4	7.5
	Sea water	1000 ml	900	125	4	5.0
	Sediment	10 g	1000	133	7	20.4
	Fish	10 g	1000	94	7	5.0
Salithion	River water	1000 ml	120	101	4	3.3
	Sea water	1000 ml	120	121	4	5.7
	Sediment	10 g	1000	102	7	17.7
	Fish	10 g	1000	89	7	5.1
Phosalone	River water	1000 ml	1200	101	4	4.7
	Sea water	1000 ml	1200	103	4	0.9
	Sediment	10 g	1000	166	7	15.5
	Fish	10 g	1000	85	7	8.7
Phosmet	River water	1000 ml	900	132	4	3.7
	Sea water	1000 ml	900	119	4	3.2
	Sediment	10 g	10000	113	7	6.4
	Fish	10 g	1000	11	7	23.9
α-CVP	River water	1000 ml	300	128	4	8.0
	Sea water	1000 ml	300	135	4	8.2
	Sediment	10 g	1000	114	7	16.9
	Fish	10 g	1000	93	7	4.4
β-CVP	River water	1000 ml	300	125	4	7.2
	Sea water	1000 ml	300	128	4	5.8
	Sediment	10 g	1000	116	7	15.7
	Fish	10 g	1000	90	7	4.2

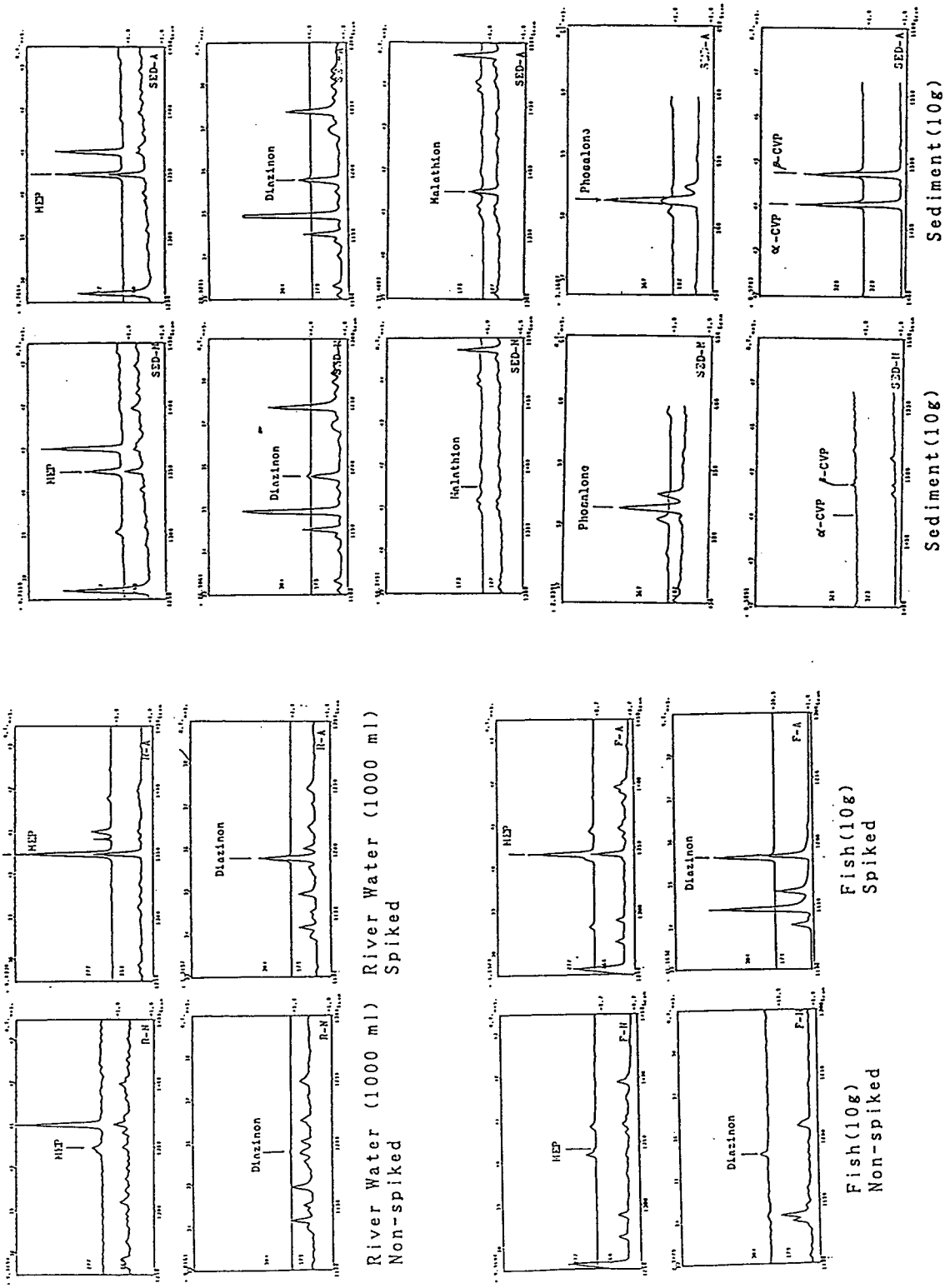

Fig. 7. Determination of the OPs in normal and spiked river water, sediment and fish samples.

reversed-phase column chromatography. Determination of the OPs with this method could probably be applicable to many other kinds of chemicals in environmental samples.

Acknowledgement

This work was supported by the Office of Health Studies, Environmental Health Department, Japan Environmental Agency (Project for Development of Analytical Method).

References

[1] S. Onodera, S. Wakabayashi, N. Furukawa, T. Ogawa, Y. Matsuura, K. Manabe, S. Suzuki, S. Ishikura and S. Suzuki, J. Environ. Chem., 2 (1992) 547.
[2] P.R. Loconto and A.K. Gaind, J. Chromatogr. Sci., 27 (1989) 569.
[3] M. Matsumoto, Shokuhin Eiseigaku Zasshi., 25 (1984) 410.
[4] A. Neicheva, D. Karageorgiev and T. Konstantinova, Sci. Total Environ., 123/124 (1992) 29.
[5] M. Mansour, D. Barcelo and J. Albaiges, Sci. Total Environ., 123/124 (1992) 45.
[6] K. Nishio and Y. Hayakawa, J. Jpn. Soc. Water Environ., 16 (1993) 55.
[7] T. Okumura and K. Imamura, Jpn. J. Water Pollut. Res., 14 (1991) 109.
[8] D. Barcelo and J. Albaiges, J. Chromatogr., 474 (1989) 163.
[9] D. Barcelo, G. Durand, R.J. Vreeken, G.J. Jong and U.A.Th. Brinkman, Anal. Chem., 62 (1990) 1696.
[10] S. Kawasaki, H. Ueda, H. Itoh and J. Tadano, J. Chromatogr., 595 (1992) 193.
[11] G.D. Veith, N.M. Austin and R.T. Morris, Water Res., 13 (1979) 43.
[12] C.T. Chiou, V.H. Freed, D.W. Schmedding and R.L. Kohnert, Environ. Sci. Technol., 11 (1977) 475.

ELSEVIER

Journal of Chromatography A, 709 (1995) 333–344

JOURNAL OF CHROMATOGRAPHY A

Atomic emission detection for the quantitation of trimethylsilyl derivatives of chemical-warfare-agent related compounds in environmental samples

William R. Creasy*, Alex A. Rodríguez, John R. Stuff, Robert W. Warren

AMC Treaty Laboratory Division, EAI Corporation, 1308 Continental Drive, Suite J, Abingdon, MD 21009, USA

First received 17 January 1995; revised manuscript received 7 April 1995; accepted 10 April 1995

Abstract

Quantitation of nerve agent degradation products is needed to develop methods for analysis of environmental samples for verification of the Chemical Weapons Convention. A procedure has been characterized which involves formation of the trimethylsilyl esters of alkylmethylphosphonic acids using 1% trimethylchlorosilane in bis-(trimethylsilyl)trifluoroacetamide as a derivatizing agent. Eight phosphorus-containing acids were extracted from spiked water, wipes, and two soil samples at low ppm levels, prepared using solid-phase extraction with a strong anion-exchange column, and derivatized. A gas chromatograph (GC) interfaced to an atomic emission detector (AED) was used to quantitate the derivatives in order to determine the extraction and derivatization efficiencies for environmental sample preparation. Because elemental response factors for the AED are independent of the type of compound, quantitation can be accomplished using an external standard, for which dimethylmethylphosphonate (DMMP) is used. The derivatization efficiencies ranged from 80% to 110% (six trials, with R.S.D. in the range 2–7%). The extraction efficiencies ranged from 13% to 99% in water, and they were lower from the soil and wipes. Gas chromatography–mass spectrometry of the derivatives was used to provide positive identifications.

1. Introduction

International treaties regarding the use, production, storage and destruction of chemical warfare (CW) agents, as well as current bilateral agreements between the United States and Russia, have created a need for analytical capabilities for inspection and verification [1]. These requirements include capabilities for sampling, sample preparation, and analysis of CW agents, precursors, byproducts, and degradation products. Because of the range of chemical warfare agents that are included in the treaties, chemicals with a wide range of polarities and solubilities must be detected.

One type of specified CW inspection, called a "challenge inspection", is required by the treaty to be carried out in a way to protect the industrial and national security of the installations that are inspected [1]. The best way to achieve this requirement is by the use of instrumentation that can be set up and operated "on-site", or at the location of the site to be inspected. This approach eliminates the need to transport sam-

* Corresponding author.

0021-9673/95/$09.50
SSDI 0021-9673(95)00451-3

ples to a remote laboratory, reducing chain-of-custody requirements and improving the protection of confidentiality. GC–MS equipment is now commercially available for use in on-site analysis that gives analytical data of equivalent quality to laboratory instrumentation [2,3]. In addition to the availability of on-site equipment, however, it is also necessary to develop sample preparation methodologies that can be efficiently carried out in non-laboratory settings. Optimally, the analytical procedures should be as simple and general as possible to facilitate their use on-site as well as to minimize the quantities of solvents, consumables, and extra equipment that must be transported. These methods must be characterized to the greatest extent possible for many different matrices in order to provide results of the highest confidence in legally binding inspections.

Among the CW-related compounds are alkyl methylphosphonic acids, which are degradation products of nerve agents. These chemicals are non-volatile and strongly acidic in water solution. The currently used methods for determination of these compounds on-site involve solid-phase extraction, concentration, derivatization, and analysis of the derivatized products by gas chromatography–mass spectrometry (GC–MS) [4]. The derivatizing agent is 1% trimethylchlorosilane in bis(trimethylsilyl)trifluoroacetamide (BSTFA), which forms the trimethylsilyl (TMS) derivatives of the acids.

The goal of this study is the optimization and validation of these methods in a variety of matrices. The sensitivity of these methods has been targetted for concentrations of 10 ppm or more (by mass) for soil, water, and wipe samples to give identifications with high confidence. The analysis is by GC–MS with a full-scan mass spectrum with library matching to give a positive identification even in the presence of compounds extracted from the matrices that may interfere. This goal has been achieved for distilled water, wipe, sandy loam soil, and sandy clay soil. Distilled water was chosen as a benchmark matrix, since the method involves water extractions from the other matrices which will add impurities to the water. Additional work is in progress to validate the methods in other matrices, including a humic soil, decontamination solutions, and environmental water samples, and for other chemicals, including mustard-gas degradation products. A parallel effort is under way for the analysis of CW agents and other non-polar, volatile compounds in these matrices.

Previously published studies have validated or characterized similar methods for a smaller subset of compounds [5–8]. However, no previously published study has reported a systematic characterization of a particular method for on-site analysis of as wide a range of CW-related compounds.

In order to optimize the methods for on-site analysis, it is advantageous to know the efficiency of each step of the process, particularly the derivatization efficiency and the extraction efficiencies from water, soil and wipe matrices. Quantitation can be accomplished using gas chromatography coupled with phosphorus-specific atomic emission detection (GC–AED). AED has previously been evaluated as a screening method for CW-related samples [9]. The compound-independent nature of the AED response makes it ideal for quantitation [10–12]. An external standard which contains phosphorus can be used to determine a calibration curve for all phosphorus-containing compounds. In addition, AED is better suited for quantitative analysis of TMS derivatives than some other methods. For example, the flame-photometric and nitrogen–phosphorus detectors are fouled from silica deposits which form on the detector when silyl derivatizing agents are used. The deposits result from injection of excess derivatizing reagent into the detector. GC–MS requires standards of each individual derivatized compound for quantitation, even though it is used qualitatively to confirm the identities of the derivatives in the gas chromatograph.

A procedure for the quantitation of the alkyl methylphosphonic acids using phosphorus-specific atomic emission detection is described. The quantitation of the derivatives enables calculation of the derivatization efficiencies of these acids and the extraction efficiencies from the various matrices. The relative standard devia-

tions (R.S.D.s) of these quantities are used to assess the reliability of the methods.

2. Experimental

2.1. Chemicals and matrices

The following standard chemicals were obtained from the Edgewood Research, Development, and Engineering Center (Aberdeen Proving Ground, MD, USA): ethylmethylphosphonic acid (EMPA), isopropylmethylphosphonic acid (IPMPA), pinacolylmethylphosphonic acid (PMPA), cyclohexylmethylphosphonic acid (CMPA), isobutylmethylphosphonic acid (IBMPA), ethylmethylphosphonothioic acid (EMPTA), and isobutylmethylphosphonothioic acid (IBMPTA). Purity of the chemicals was determined by NMR. Methylphosphonic acid (MPA, 98%) was obtained from Johnson Matthey (Ward Hill, MA, USA). Hexane (HPLC grade, 97% *n*-hexane) and acetonitrile (99.9%) were from J.T. Baker (Phillipsburg, NJ, USA). Dichloromethane (99.9%), methanol (99.9+%), ammonium hydroxide (ACS reagent), 2-propanol (99.9%), and DMMP (97%) were obtained from Sigma–Aldrich Chemical Co. (Milwaukee, WI, USA). The derivatizing agent, Sylon-BFT [1% trimethylchlorosilane in bis-(trimethylsilyl)trifluoroacetamide, BSTFA], was obtained from Supelco (Bellefonte, PA, USA). Distilled/deionized water (18 MΩ) was generated internally using a Barnstead (Dubuque, IA, USA) Nanopure system.

Cotton wipe material was purchased from VWR Scientific (Bridgeport, NJ, USA). Wipes are used for collecting samples by wiping off solid surfaces, possibly after wetting the surface with solvent. This particular material was characterized in order to be consistent with previous international field trials.

The first soil type was a sandy soil from California. It has been characterized in detail by Kingery et al. [13]. In brief, it is neutral (6.6) in pH and 88% sand. It has a fairly high phosphate content (47 mg/kg), possibly because of modification with fertilizer. It was obtained from farmlands near Lawrence Livermore National Laboratory, California. Sorption of alkyl methylphosphonic acids was measured to be low (53 μg/g for MPA, 3.3 μg/g for IPMPA, and 1.1 μg/g for EMPA). Degradation of EMPA on the soil was observed in about 350 h, which was attributed to biological activity, but this time scale was much longer than the present measurements. Degradation of IPMPA was first order and much slower, indicating that no biological degradation was involved.

The second soil type was a sandy clay, also from California. It was characterized [13] to be 46% sand, 28% silt, and 26% clay. The pH was 7.9, more basic than the sandy soil. Phosphate content was also high (76 mg/kg), and there was higher potassium (156 mg/kg) and calcium (2280 mg/kg) than the sandy soil. Sorption of MPA, IPMPA, and EMPA was low and very similar to the sandy soil. EMPA decomposed after 150 h, probably also due to biological activity, but IPMPA degradation was again first order and slow.

2.2. Equipment and chromatographic conditions

A Hewlett-Packard Model 5890 Series II gas chromatograph interfaced to a Hewlett-Packard Model 5921A atomic emission detector was used for all analyses. The gas chromatograph was fitted with a 30 m × 0.25 mm I.D. HP-5 (cross-linked 5% phenyl methyl silicone) fused-silica capillary column, film thickness 0.25 μm. Helium was used as a carrier gas at linear velocity of 32 cm/s. The oven temperature was set initially at 60°C, programmed from 60 to 200°C at 10°C/min. Splitless injections of 2 μl were used with a solvent delay of 4.00 min for the analytes and 1.80 min for the external standard. The injector port temperature was set at 275°C, the transfer line temperature at 300°C, and the cavity block temperature in the AED at 300°C. Hydrogen, at high flow, was used as the reagent gas. Peaks were detected by measuring phosphorus emission at 186 nm. Sulfur emission was monitored at 181 nm to help establish retention times for the two thioic acids.

For mass spectral work, a Hewlett-Packard

Model 5890 Series II gas chromatograph and Model 5971 MSD were used. Similar GC conditions were used, although the starting temperature was 60°C, held for 2 min, and ramped at 15°C/min to 250°C. The MSD was operated in scan mode from 50 to 300 amu. The retention times are different for the two instruments, but the elution orders are identical.

2.3. Preparation of standards

DMMP standards were prepared gravimetrically in acetonitrile and run on the AED. A typical calibration curve is shown in Fig. 1. The correlation coefficient of 0.9992 shows good linearity. The curve also includes points for a series of dialkyl methylphosphonates of varying concentrations and molecular masses. The correspondence between the calibration curve for DMMP and the signals of the other compounds is good.

Individual standards of the alkyl methylphosphonic and thioic acids were prepared in acetonitrile and hexane due to limited solubility in hexane. An amount of 300 μl of the standards was added to 200 μl of Sylon-BFT. The samples were sealed and heated at 60°C for 15 min. The derivatized acids were analyzed by GC–AED to determine the efficiency of the derivatization for each of the acids under these conditions, and five trials were averaged (except for CMPA, for which three trials were done). Measurements indicated that there was no significant difference in derivatization efficiency between hexane and acetonitrile as solvents.

Standard solutions of a mixture of MPA and the other acids were prepared in isopropanol and were used to spike the soils, water, and wipes.

2.4. Sample preparation method

Samples were made by spiking the matrix with stock solution, allowing the solvent to dry, and extracting, all within a few hours. The samples were then prepared in accordance with the current standard method [4]. For water samples or extracts, a volume of 10 ml aqueous solution was concentrated using a strong anion-exchange (SAX) solid-phase extraction cartridge (Baker-bond Quaternary Amine, J.T. Baker, Phillipsburg, NJ, USA). Analytes retained on the cartridge were eluted with 1.0% (v/v) ammonium hydroxide in methanol. The eluent was evaporated to dryness at 60°C under nitrogen. The sample residue was derivatized using a mixture of 200 μl of Sylon-BFT and 300 μl of

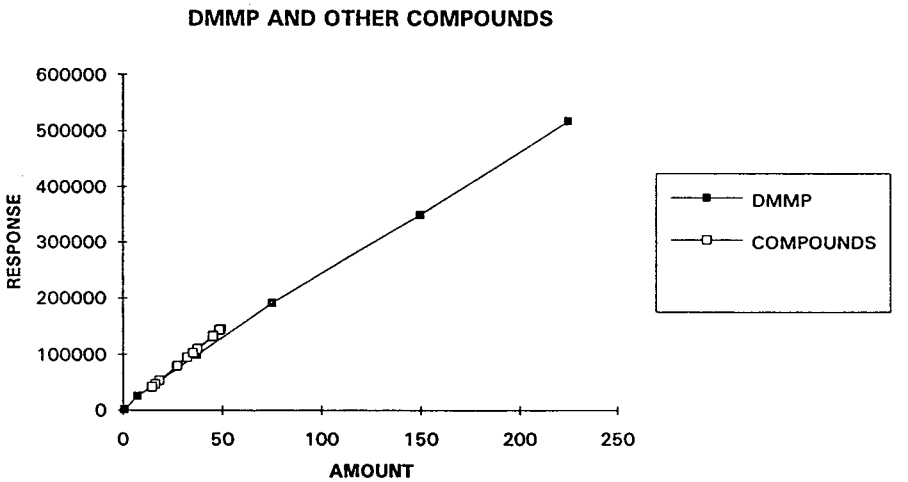

Fig. 1. Calibration curve of the GC–AED using standard DMMP solutions (solid squares). Points for other phosphonates are also shown to indicate that the signal is compound independent. Twelve compounds that were used of the type $CH_3PO_3R_1R_2$, for R_1 and R_2 selected from methyl, ethyl, isopropyl, *n*-propyl, pinacolyl (1,2,2-trimethylpropyl), hexyl, 2-methoxyethyl, 2-butoxyethyl, and cyclohexyl. Amount is in nanograms of P.

hexane, immediately sealed in an autosampler vial, and heated at 60°C for 15 min. The derivatized samples were analyzed by GC–AED or GC–MSD usually on the same day and always within a few days.

Soil (5 g sample weight) and wipe (1 g weight) samples were extracted twice with approximately 10 ml each of water. The water was filtered and analyzed following the same procedure as the aqueous samples. Soil, water, and wipe samples were spiked with the standard solutions of the acids in isopropanol to 10 ppm by mass: wipes at 10 μg/1 g of sample, water at 100 μg/10 ml of sample, and soil at 50 μg/5 g of sample. Three repetitions were done for each.

3. Results and discussion

Past studies have used several different types of derivatives to analyze alkylmethylphosphonic acids, including trimethylsilyl (TMS) [6], *tert.*-butyldimethylsilyl (TBDMS) [5,7], methyl [8,15–17], and perfluorobenzyl [14]. Each type of derivative has some advantages.

Methylation of alkylmethylphosphonic acids using diazomethane has been reported [15], but the use of diazomethane is inappropriate for field work due to its hazardous and difficult preparation and its lack of stability [16,17]. Methylation using trimethylphenylammonium hydroxide by co-injecting the underivatized acid and the hydroxide into a heated GC injector port has been done [8]. However, results indicate that the derivatization efficiency using this method is not good, especially for low concentrations of acid, and detection of MPA is difficult for solution concentrations below 150 ppm [18]. In addition, this method requires a GC injector port that is heated to 300°C, which can be difficult to achieve on some fieldable instruments due to limited power. This technique requires additional development work.

Perfluorobenzyl derivatives may provide greater sensitivity in negative chemical ionization MS detection [14], although currently negative-ion detection is not available on fieldable instrumentation. These derivatives may be valuable with additional field-instrument development.

Use of TBDMS derivatives of alkylmethylphosphonic acids [5,7] has been reported to give some advantages compared to TMS derivatives in terms of hydrolytic stability and ease of MS detection [7], although a direct comparison of sensitivity or stability has not been done. It has also been reported that, for some inorganic oxygen-containing anions, the TMS derivatives degrade rapidly at room temperature even in the derivatization solution, while TBDMS derivatives are stable [19], although this degradation was not observed for phosphate. To see whether this type of degradation was a problem for alkylmethylphosphonic acids, solutions of the acid derivatives still in BSTFA solution were analyzed after being stored in sealed vials for seven months at room temperature. It was still possible to detect and positively identify all the derivatives, although some degradation may have occurred. In fact, EMPA, IPMPA, PMPA, and MPA derivatives could be positively identified in BSTFA solutions prepared from wipe and soil extracts at spiking levels of 5 ppm after seven months of storage. Thus, degradation of these TMS derivatives does not appear to be a problem.

For the methods used in the current study, TMS derivatization was chosen on the basis of cost and availability of reagents and consistency with established recommended operating procedures [20]. The current results indicate that TMS derivatives are adequate for this purpose. Bauer and Vogt [21] have reported that BSTFA has a high hydrolytic sensitivity, requiring the use of special vials for derivatization. In our experience, Sylon-BFT can be routinely exposed to air with no significant degradation. The reagent is added to autosampler vials and sealed with crimp-type caps with no further precautions. Bauer and Vogt also reported that a variety of alkylphosphonic acids did not dissolve in BSTFA without the use of methanol as a solvent, which reacted vigorously to the BSTFA [21]. The alkylmethylphosphonic acids in this study are reproducibly derivatized without using polar solvent. However, the acids that were

spiked were all in the form of free acids rather than salts. Some studies have indicated that inorganic sodium or potassium salts are difficult to derivatize with BSTFA because they do not dissolve, although ammonium salts can be derivatized when dissolved in dimethylformamide [21,22]. This point will be addressed in more detail later.

Hexane and acetonitrile were compared as solvents for diluting the BSTFA. No significant difference was observed for the derivatization efficiency in hexane compared to acetonitrile. Hexane was found to give much better chromatography, since the GC peaks from solutions in acetonitrile can give broad, poorly defined peaks [7]. It is suspected that this problem is caused by poor solvent focusing on the non-polar GC column. The use of an uncoated precolumn or the initiation of the GC run at 90–100°C, above the acetonitrile boiling point, improved the chromatography.

Using the described methods, the spiked samples were prepared, derivatized, and analyzed. The peaks in the gas chromatogram were positively identified by using GC–MS. Fig. 2 shows a total ion chromatogram, top panel, along with extracted ion chromatograms for the ions of mass 153, 169, and 225. MPA, which is doubly substituted with TMS, has a base peak of 225 corresponding to the $[M-15]^+$ ion [23]. The other alkylmethylphosphonic acid derivatives have a base peak for the fragment ion at 153, corresponding to the $[CH_3PO_3HSi(CH_3)_2]^+$ ion, making this ion very characteristic of TMS derivatives of these compounds. This ion mass is also fairly uncommon as the base peak in mass spectra of other compounds, so it is a preferred extracted ion for locating the derivatives in a complex spectrum. The alkylmethylphosphonic derivatives also give an ion of mass 169, corresponding to $[CH_3PO_3H_2Si(CH_3)_3]^+$. The alkylmethylphosphonothioic acids have analogous ions at 169 and 185, due to the substitution of S for O. A custom library database was

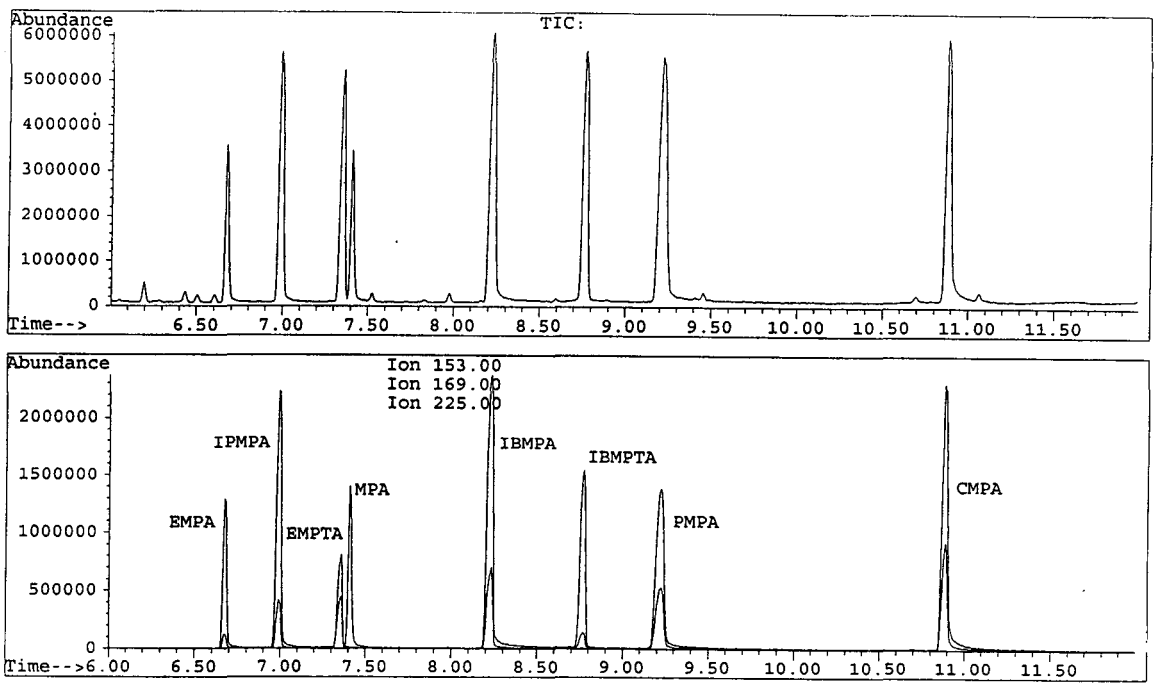

Fig. 2. GC–MS chromatograms for analysis of a mixture of alkylmethylphosphonic acids. Top panel: total-ion chromatogram. Bottom panel: extracted ion chromatograms for ions of mass 153, 169, and 225. The peaks corresponding to the TMS derivatives of the acids are labelled according to the abbreviations in the text.

assembled from mass spectra taken of separate standard solutions of each compound. The mass spectrum for each peak of the prepared samples was searched in the library and a positive identification was obtained. The elution order of the derivatives was determined.

In addition to EI mass spectra, chemical ionization mass spectra were collected of selected samples to confirm the identifications. Methane or ammonia were used as chemical ionization reagents. Both reagents gave parent ion signals for the TMS derivatives, although the methane spectra showed more fragmentation than the ammonia spectra for the acids with the larger alkyl groups. These results will be published separately.

A GC–AED chromatogram showing the separation of the derivatized alkylmethylphosphonic and thioic acids is shown in Fig. 3. The compounds are baseline resolved with the exception of EMPTA and MPA, which overlap slightly.

Table 1
Derivatization efficiencies of the alkyl methylphosphonic acids

Compound	Derivatization efficiency (%)	*N*	%R.S.D.
EMPA	99	6	6.5
IPMPA	84	6	4.0
EMPTA	93	6	6.0
MPA	80	6	7.4
IBMPA	110	6	3.1
IBMPTA	86	6	4.2
PMPA	107	6	3.4
CMPA	109	3	1.8

The peak shapes are good. The separation time is under 10 min.

The average derivatization efficiencies that were determined are listed in Table 1. They range from 80% for MPA to 110% for IBMPA. The R.S.D.s are in the range of 2–7%. The

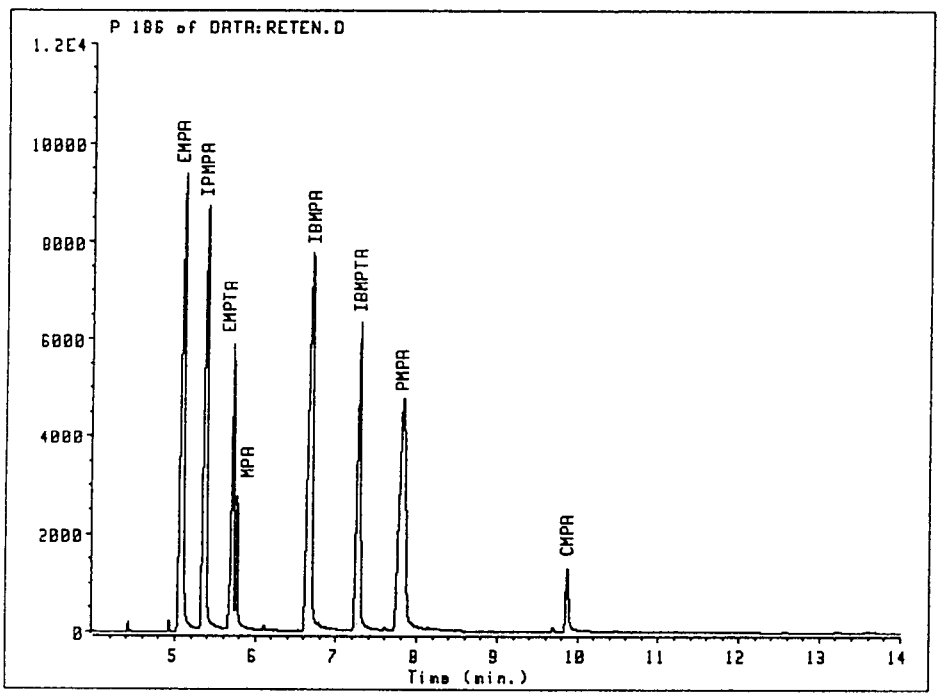

Fig. 3. GC–AED chromatogram with phosphorus detection of a sample spiked with seven alkylmethylphosphonic acids and derivatized in hexane. MPA was present as an impurity from the other seven acids. GC conditions were 60°C (no hold) to 200°C at 10°C/min. The peaks correspond with the abbreviations in the text.

efficiencies for IBMPA, PMPA, and CMPA, which are above 100%, are high by more than two standard deviations, suggesting that there may be a small systematic error in determining the concentrations. The volume change from mixing the BSTFA and acetonitrile solvents was measured and corrected for. In all cases, the derivatization efficiencies are high enough to give good recoveries of these compounds.

The efficiencies for recovery of the eight acids from three matrices are listed in Table 2. The recoveries are corrected for the derivatization efficiencies. The recoveries for water range from 13 to 99% for the acids at a concentration of 10 μg/ml.

The recovery for MPA is the lowest at 13%. The pH of the 18-MΩ water used in this study is approximately 6. At this pH, the MPA is singly ionized, which may affect its recovery. However, the optimal pH for recovery of MPA from the solution can only be determined experimentally. Preliminary results indicate that MPA is not observed from basic solutions, even though it would be doubly ionized. It is possible that the MPA forms a salt when the solution is dried and the salt does not dissolve and derivatize in the BSTFA, similar to salts of inorganic anions [21,22]. This is consistent with results of Black et al. [5], who reported that treating aqueous extract by passing it through a cation-exchange column (H^+ form) increased their sensitivity to MPA substantially. Use of a cation-exchange column would make the solution acidic, rather than basic, and it would remove metal ions that could form salts with the MPA. However, we have also found in preliminary work that basic water solutions and basic extractions of the soil improve the recoveries of the other alkylmethylphosphonic acids. Since the recovery at neutral pH is high enough to detect all the acids by GC–MS, no changes to the sample preparation method have been instituted. However, further research on the effects of pH and metal-ion concentration is under way. If it is found that improved recovery is required, it may be necessary to determine the optimal pH and change the method accordingly, although it may not be possible to optimize for both MPA and the mono-esters under the same conditions.

The R.S.D.s for the recoveries from water solution are in the range of 15–20%. The source of the error is not well characterized. In the sample preparation procedure, it is necessary to use a strong anion-exchange column in order to trap the strongly acidic species, which are in anionic form in pH 7 water. Non-polar cartridges such as C_{18} cartridges would be adequate for the alkylmethylphosphonic acids with large alkyl groups [14], but they will not trap smaller acids such as MPA. In order to elute the acids off the SAX cartridges, it is necessary to use a strong base. This solution can also strip some of the bonded phase and dissolve silicates from the cartridge. These species appear to react with the derivatizing agent, causing background in the chromatograms and decreasing the amount of

Table 2
Recovery efficiencies of each of the alkyl methylphosphonic acids from three matrices, along with the relative standard deviations from three trials

Compound	Water rec. (%)	%R.S.D.	Sandy soil rec. (%)	%R.S.D.	Swipes rec. (%)	%R.S.D.
EMPA	36	19	18	21	9	59
IPMPA	59	18	39	14	18	30
EMPTA	64	19	48	7	23	15
MPA	13	21	4	1	2	37
IBMPA	95	18	35	44	40	17
IBMPTA	64	14	41	11	42	15
PMPA	99	13	54	12	48	6
CMPA	79	15	2	10	29	14

Table 3
Recovery efficiencies of the alkyl methylphosphonic acids from sandy clay soil, using two different extraction conditions

Compound	Recovery (%) Case 1[a]	Recovery (%) Case 2[b]
EMPA	14.5	52
IPMPA	15	47
EMPTA	15	48
IBMPA	29	74
IBMPTA	15	46
PMPA	22.5	53
CMPA	3	7

[a] Case 1: two sequential extractions of 10 ml each of water. Average of two trials.
[b] Case 2: two sequential extractions, first 10 ml, second 20 ml. Fractions combined and then prepared the same as Case 1. One trial.

reagent that is available to react with the analytes. This may give rise to some of the variations in the recovery efficiencies.

Previously, a procedure was used which called for elution of the column with 10% ammonium hydroxide in methanol. This method gave even poorer R.S.D.s for the recoveries. Indeed, in some cases some of the acids were entirely missing from the chromatograms. This was attributed to loss of derivatizing agent due to reaction with chemicals that were stripped from the cartridges. Measurement showed that twice as much material by mass (silicates, etc.) was eluted from the columns using 10% NH_4OH compared to 1% NH_4OH. Reduction of the ammonium hydroxide concentration to 1% improved the R.S.D.s. Lower levels than 1% hydroxide were not effective in eluting the acids from the column.

The recoveries for the soils and wipe samples are in general lower than that for the water samples, as expected since the wipe and soil samples involve the extra step of water extraction from the two media. This extraction introduces an additional efficiency factor for each acid, since each may have a different affinity for the solid material. The wipes have the lowest recovery values, indicating some affinity of the

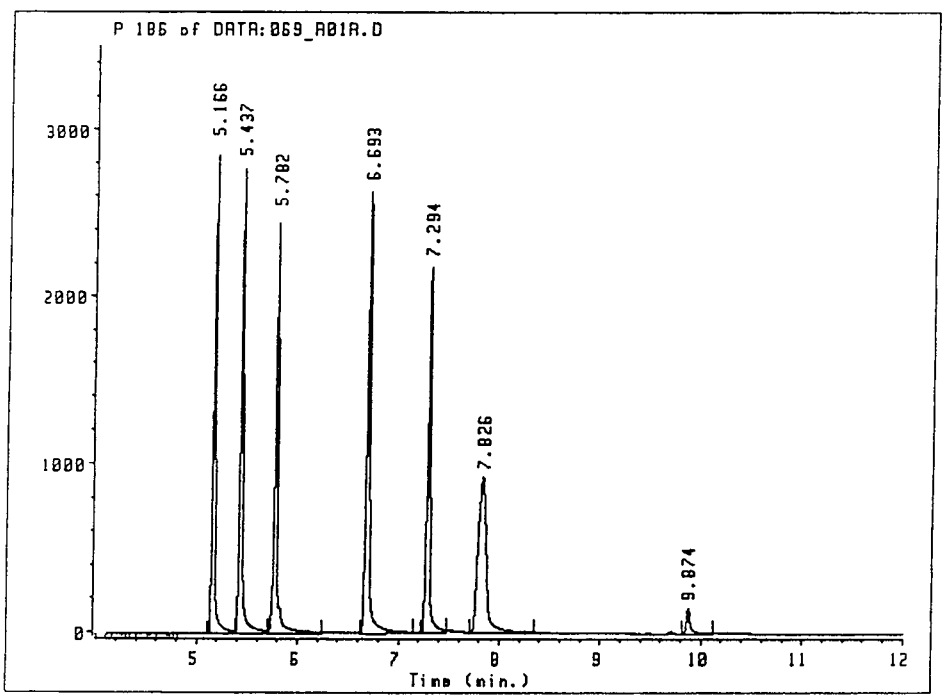

Fig. 4. GC–AED chromatogram with phosphorus detection of an extract from the sandy clay soil.

acids for the wipe material. However, the wipe samples also have the smallest quantity of spiked chemical, which decreases the signal level and is likely to be responsible for the high %R.S.D. On the other hand, the R.S.D.s for some of the sandy soil recoveries are smaller than the R.S.D.s for the water extractions, which is likely to be fortuitous.

Table 3 shows the recoveries of the mono-esters from the sandy clay soil with two slightly different extraction conditions. In the first case (two trials), the previously described method was done with two extractions of 10 ml of water. In the second case (one trial), the first extraction was 10 ml and the second was 20 ml. In both cases, extracts were combined before passing through the solid-phase extraction cartridge, and the rest of the preparation was identical. The second case shows a marked improvement in the recoveries for all the acids. However, the first case was adequate for positive identifications, and it is advantageous to keep the volume of water used for the extraction at a minimum.

MPA was not spiked on these samples and was not quantified, since it is being analyzed as a separate set of runs, although a small amount was present as a contaminant in some of the mono-esters.

For these matrices, there are no interfering compounds that prevent the identification of the analytes of interest. The wipes contain some extractable fatty acids which are derivatized and can cause congestion in the chromatogram, but which do not interfere in the identifications. The sandy soil was quite clean.

The sandy clay soil had some extracted contaminants, but they did not present a problem. Fig. 4 shows the GC–AED of one of the extracts of the sandy clay soil. There are no major phosphorus signals besides the acids of interest. The EMPTA and MPA peaks, at retention times of 5.782, were not resolved, since the EMPTA has a strong signal and MPA was a minor contaminant. Both were identified in the GC–MS run in the extracted ion chromatogram of the same sample, shown in Fig. 5. The TIC in the

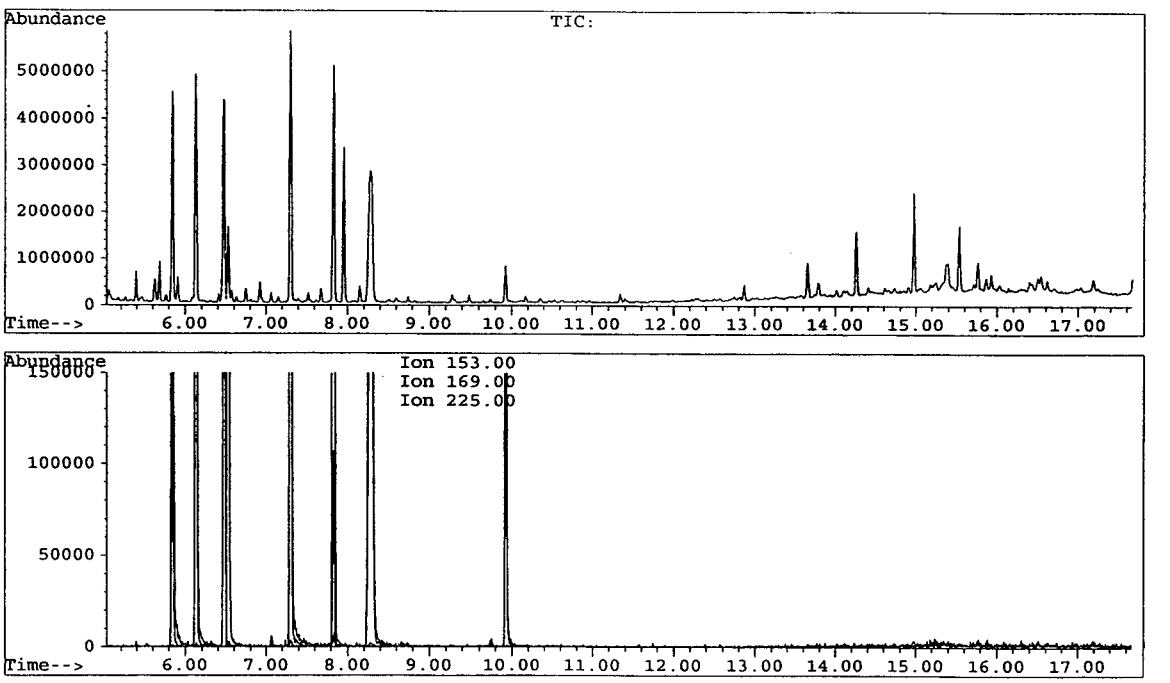

Fig. 5. GC–MS chromatogram of an extract from the sandy clay soil. Top panel: total-ion chromatogram. Bottom panel: extracted ion chromatogram of the ions of mass 153, 169, and 225, with the scale expanded to show the baseline.

top panel shows that many peaks are present from contaminants. However, the extracted ion chromatogram in the bottom panel shows that the ions at mass 153, 169, and 225 can be used to identify the peaks for the acid derivatives unambiguously for this matrix. As a result, it is appropriate to use these ions for a single-ion monitoring (SIM) method to screen for these types of compounds, although a SIM method may not be considered to be a positive identification for treaty verification purposes.

The soils contain phosphate, which is also derivatized. The phosphate derivative does not produce a significant peak in the GC–AED chromatogram, possibly because it is obscured by the tail from the acid peaks. It was found in the mass spectra at very low levels by extracting the 299 ion, which is the base peak of the mass spectrum [22–24]. The retention time of the triply derivatized phosphate is different from the alkylmethylphosphonic acids, so it does not interfere with the quantitation. In Fig. 5, it was actually only a small shoulder on the interference peak at 8.0 min.

Further trials are in progress to validate the method for other matrices and, if necessary, refine it further. If possible, the validation for lower detection limits will also be obtained.

4. Conclusions

Gas chromatography coupled to an atomic emission detector is a valuable tool for the quantitation of trimethylsilyl derivatives of alkylmethylphosphonic and thioic acids. The quantitative results helped pinpoint areas for method improvement. The results showed that the derivatization efficiencies for all the acids were sufficiently high for detection by GC–MS. However, the extraction efficiencies, even from water solution, using the solid-phase extraction procedure are substantially lower, and the R.S.D.s are rather high, suggesting that further improvements are still possible. In general, though, this procedure for detecting alkylmethylphosphonic acids in these matrices gives reliable detection at the 10 ppm level, the current goal, so it is adequate for reliable qualitative analysis of environmental samples for treaty verification. Work is in progress to characterize the methods for other matrices, including salt water solutions and decontamination solutions, and for other analytes of interest for CW verification.

Acknowledgements

The authors thank Dr. Dennis Reutter and Dr. Lynn Hoffland of the Army Materials Command (AMC) Treaty Laboratory for funding. The work was performed at Edgewood Research, Development and Engineering Center, Aberdeen Proving Ground, Edgewood Area, MD, USA, under contract No. DAA15-91-0019.

References

[1] Convention on the Prohibition of the Development, Production, Stockpiling, and Use of Chemical Weapons and their Destruction, United States Control and Disarmament Agency, Washington, DC, 1993.
[2] W.C. McDonald, M.D. Erickson, B.M. Abraham and A. Robbat, Jr., Environ. Sci. Technol., 28 (1994) 336A–343A.
[3] W. Creasy, T.G. Albro, R.L. Cheicante and J.R. Stuff, Spectroscopy, 9(9) (Dec. 1994) 42–47.
[4] J.R. Stuff (Editor), On-Site Sample Preparation Method for Soil, Water, and Wipe Samples for the Qualitative Determination of Chemical Warfare (CW) Related Compounds, U.S. Army Chemical and Biological Defense Command, Aberdeen Proving Ground, MD, in press.
[5] R.M. Black, R.J. Clarke, R.W. Read and M.T.J. Reid, J. Chromatogr. A, 662 (1994) 301–321.
[6] P.A. D'Agostino and L.R. Provost, J. Chromatogr., 589 (1992) 287–294.
[7] J.G. Purdon, J.G. Pagotto and R.K. Miller, J. Chromatogr., 475 (1989) 261–272.
[8] J.A. Tornes and B.A. Johnsen, J. Chromatogr., 467 (1989) 129–138.
[9] T.G. Albro, in Proceedings of the 1994 ERDEC Scientific Conference on Chemical and Biological Defense Research, 15–18 Nov. 1994, Aberdeen Proving Ground, MD, in press.
[10] B.D. Quimby and J.J. Sullivan, J. High Resolut. Chromatogr., 12 (1989) 282–286.
[11] T.G. Albro, P.A. Dreifuss and R.F. Wormsbecher, J. High Resolut. Chromatogr., 16 (1993) 13–17.

[12] S.R. Goode and C. Thomas, Spectroscopy, 9(9) (Dec. 1994) 14–18.
[13] A.F. Kingery, K.P. Lee, S.E. Bufflap and H.E. Allen, Characterization and Fate of Alkyl Methylphosphonates in Standard Soils Used in the Provisional Technical Secretariat Inter-Laboratory Comparison, Final Report to EAI Corporation, 1994. Available on request.
[14] M.L. Shih, J.R. Smith, J.D. McMonagle, T.W. Dolzine and V.C. Gresham, Biol. Mass Spectrom., 20 (1991) 717–723.
[15] A. Verweij, H.L. Boter and C.E.A.M. Degenhardt, Science, 204 (1979) 616–618.
[16] J. Askew, J.H. Ruzicka and B.B. Wheals, J. Chromatogr., 41 (1969) 180–187.
[17] H. Schlenk and J.L. Gellerman, Anal. Chem., 32 (1960) 1412–1414.
[18] T.G. Albro, Evaluation of Trimethylphenylammonium Hydroxide (TMPAH) as a Derivatization Agent for the Methylation of Methylphosphonic Acid (MPA), EAI Report 14/93/002D2, Abingdon, MD, 1993. Available on request.
[19] T.P. Mawhinney, J. Chromatogr., 257 (1983) 37–44.
[20] M. Rautio (Editor), Recommended Operating Procedures for Sampling and Analysis in the Verification of Chemical Disarmament, 1994 Edition, Ministry of Foreign Affairs of Finland, Helsinki, 1994, ROP SP7.
[21] G. Bauer and W. Vogt, Anal. Chem., 53 (1981) 917–919.
[22] W.C. Butts and W.T. Rainey, Jr., Anal. Chem., 43 (1971) 538–542.
[23] D.J. Harvey and M.G. Horning, J. Chromatogr., 79 (1973) 65–74.
[24] M. Zinbo and W.R. Sherman, Tetrahedron Lett., 33 (1969) 2811–2813.

ELSEVIER

Journal of Chromatography A, 709 (1995) 345–349

JOURNAL OF CHROMATOGRAPHY A

Supercritical fluid chromatography of free resin acids on an ODS-silica gel column

Aya Yamada[a,*], Yoichiro Ezaki[a], Kohtaro Matsuo[a], Takashi Yarita[b], Akira Nomura[b]

[a]*Tsukuba Research Laboratory, Arakawa Chemical Industries Ltd., 5 Okubo, Tsukuba, Ibaraki 300-33, Japan*

[b]*Department of Analytical Chemistry, National Institute of Materials and Chemical Research, 1-1 Higashi, Tsukuba, Ibaraki 305, Japan*

First received 23 November 1994; revised manuscript received 6 April 1995; accepted 6 April 1995

Abstract

The supercritical fluid chromatographic behaviour of resin acids on an inert ODS-silica gel column using supercritical carbon dioxide as the mobile phase was studied. The separation of resin acids could be achieved considerably better by using methanol as a modifier. According to these results, the isomers of abietane-type acids could be separated by SFC without derivatization, particularly esterification.

1. Introduction

Rosin is a natural resin obtained from coniferous trees [1]. The main constituent of this industrially very important material is a mixture of several (usually seven to eight) diterpene monocarboxylic acids known as resin acids, as shown in Fig. 1 [2]. They are closely related to one another in their chemical structures, among which abietic acid and pimaric acid are representative ones for their skeletal features.

In practice, the gas chromatographic analysis of rosin is routinely carried out for quality control in industry following the procedure based on ASTM D3008 [3] using a packed column. This method, however, requires methylation of rosin to improve the volatility of resin acids. Although a capillary column can easily accomplish a better resolution of resin acids [4], the service life of capillary columns needs considerable improvement, in our experience.

The application of HPLC to the analysis of rosin has had limited success [5,6]. Otsuka and Kubo [6] were able to separate pine oleoresin to its components (resin acids) by HPLC on an ODS-silica gel column only after extensive recycling.

In recent years, supercritical fluid chromatography (SFC) has been developed as separation technique that is a bridge between GC and LC. Carbon dioxide is usually used as the mobile phase in SFC because of its properties, safety and cost. However, the addition of a modifier to the mobile phase is often required in order to improve the retention behaviour and the peak shapes [7–13]. An early study of the application

* Corresponding author.

0021-9673/95/$09.50
SSDI 0021-9673(95)00442-4

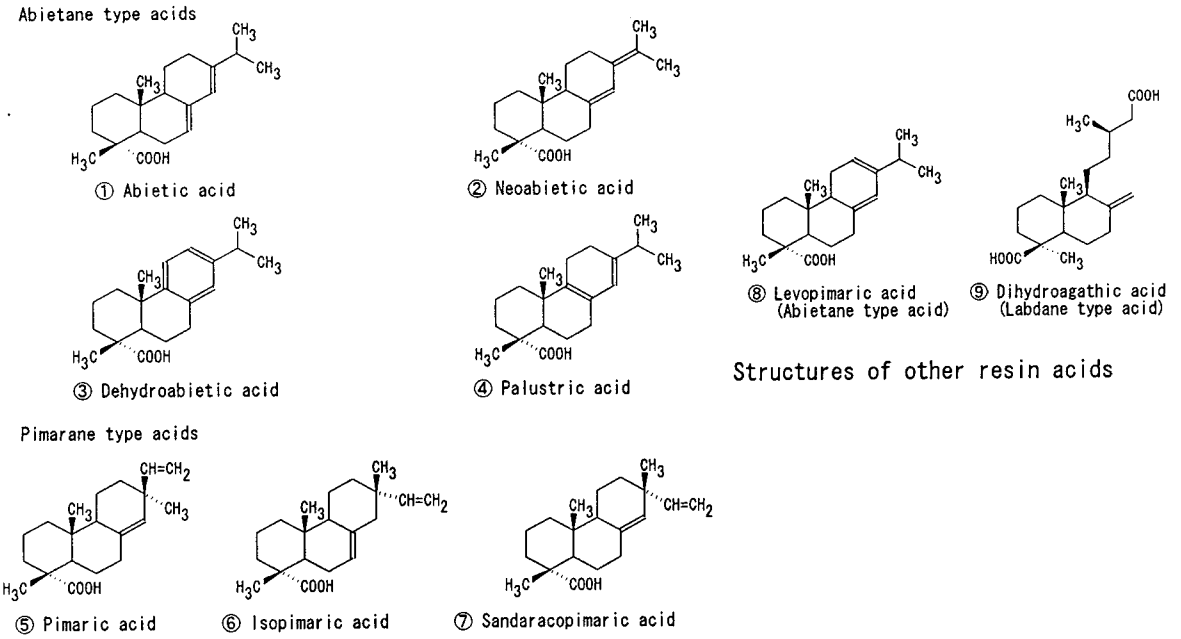

Fig. 1. Structures of resin acids in Chinese gum rosin.

of SFC to rosin analysis was reported by Gere [14], who was able to separate abietic and neoabietic acid on a polystyrene gel column. However, other resin acids were not investigated.

This paper describes the elution behaviour of free resin acids without any derivatization by SFC on an ODS-silica gel column.

2. Experimental

2.1. Apparatus

A Shimadzu (Kyoto, Japan) LC-6A pump was used to deliver carbon dioxide. The pump head was cooled so as to maintain a stable flow. An Isco (Lincoln, NE, USA) Model 100 DM pump was used to deliver modifier. A DKK (Tokyo, Japan) LSA-M mixer was used for mixing carbon dioxide and modifier. A Rheodyne (Cotati, CA, USA) Model 7125 sample injector with a 20-μl sample loop was used for sample injection. The separation column was kept at 40°C in a column oven from a Shimadzu LC-1 system. A Shimadzu SPD-6A UV detector was used for detection at 210 nm. The flow-rate of the mobile phase was controlled by a restrictor made of a capillary tube of 300 mm × 50 μm I.D. This SFC system is the same as described previously [15].

2.2. Materials

The separation column used in the SFC was an L-column ODS (250 mm × 4.6 mm I.D., particle size 5 μm, pore diameter 120 Å) from the Chemicals Inspection and Testing Institute (Tokyo, Japan). An ODS-silica gel column applied to the SFC separation of polar samples using carbon dioxide as the mobile phase without a modifier usually gives considerable tailing of peaks and retardation of sample elution, because polar compounds such as resin acids tend to adsorb to the residual silanol groups of the packing material. In the L-column ODS, the residual silanol groups are minimal.

The rosin sample was a commercial gum rosin, X grade, made in China, which is known to contain seven diterpene resin acids [2]. An aliquot of 0.5 μl of 5% rosin solution in chloro-

form was used for injection. The authentic pure resin acids, including levopimaric and dihydroagathic acids, used as the reference materials, were conventionally isolated by known methods [2].

3. Results and discussion

The chromatogram of Chinese gum rosin obtained by SFC without a modifier is shown in Fig. 2. The identification of each peak was based on the authentic reference materials.

As can be seen, pimarane-type acids eluted first in one peak followed by abietane-type acids. However, the separation of these acids into individual peaks was not accomplished and all the peaks had considerable tailing, presumably because of adsorption of resin acids on the residual silanol groups still remaining in the ODS-silica gel packing. The peak of neoabietic acid became very broad and could not be identified, for example. The chromatographic separation by SFC could not be improved by varying the carbon dioxide pressure from 12 to 21 MPa.

To improve the separation of resin acids, three types of modifier, water, 1,4-dioxane and methanol, were evaluated. With water, a water content of 0.31% (w/w) was the maximum amount that can be added as a modifier owing to its solubility in supercritical carbon dioxide. In such a case, the chromatogram was almost the same as that without a modifier (Fig. 2).

Using 2% (w/w) 1,4-dioxane as a modifier, a considerably better separation with less peak tailing compared with the result obtained with water as modifier could be achieved. The use of 1.2% (w/w) methanol instead of dioxane gave an even better result, as shown in Fig. 3. Although the elution pattern of the resin acids using methanol as a modifier was almost the same as that of dioxane modifier, higher chromatographic resolutions calculated for two adjacent peaks were obtained using methanol as a modifier, so further detailed studies were conducted with methanol as a modifier.

The elution behaviour of resin acids is affected by the addition of a methanol modifier, hence addition of less than 1% (w/w) of methanol made the resolution poorer because of peak tailing whereas too much methanol gave poorer resolution. As a result, the addition of 1.2% (w/w) methanol was adopted as the most suitable in further detailed studies. Fig. 4 shows the relationship between log k' of resin acids and the methanol concentration in the mobile phase. Chloroform was used to obtain t_0 for calculating k'. A linear relationship was obtained above a concentration of about 0.5% (w/w) of methanol,

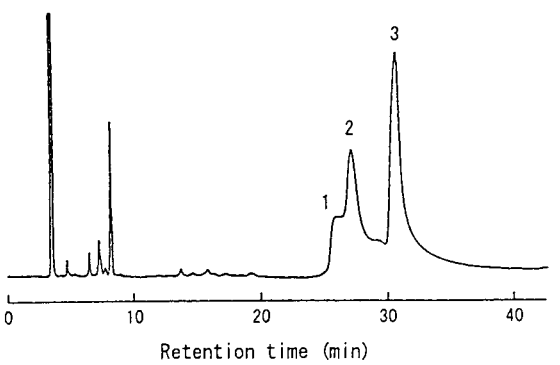

Fig. 2. Chromatogram of Chinese gum rosin. Peaks: 1 = pimaric acid, isopimaric acid; 2 = dehydroabietic acid, palustric acid; 3 = abietic acid. Conditions: CO_2 pressure, 12 MPa; CO_2 flow-rate, 430 ml/min at room temperature under 760 mmHg; other conditions as in text.

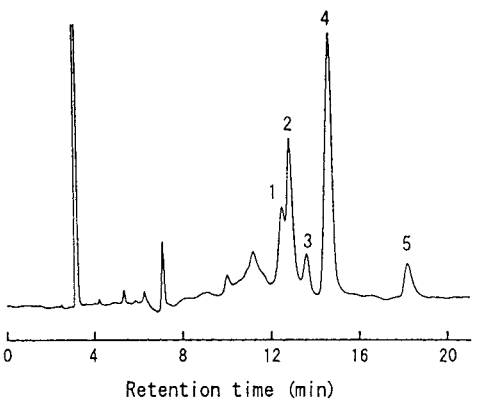

Fig. 3. Chromatogram of Chinese gum rosin [modifier: 1.2% (w/w) methanol]. Peaks: 1 = pimaric acid; 2 = sandaracopimaric acid, isopimaric acid, dehydroabietic acid; 3 = palustric acid; 4 = abietic acid; 5 = neoabietic acid. Other conditions as in Fig. 2.

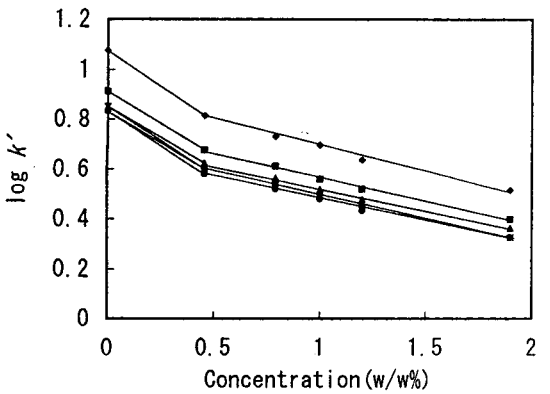

Fig. 4. Effect of methanol concentration in the mobile phase on k'. ◆ = Neoabietic acid; □ = abietic acid; ▲ = palustric acid; × = dehydroabietic acid; ◇ = sandaracopimaric acid, isopimaric acid; ○ = pimaric acid.

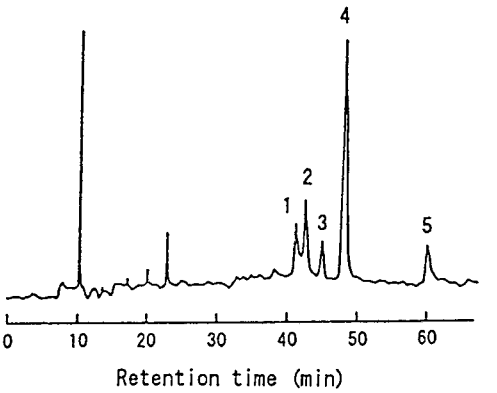

Fig. 5. Chromatogram of Chinese gum rosin on three columns [modifier: 1.2% (w/w) methanol]. Other conditions as in Fig. 2 and peak identifications as in Fig. 3.

although the elution order of the resin acids remained unaltered. The difference between the values obtained by extrapolating to the ordinate and those observed seems to be caused by adsorption of the resin acids on the residual silanol groups.

Although the chromatogram shown in Fig. 3 was better, some efforts were necessary to improve the separation of peaks 1–3 by connecting the same type of columns. The chromatogram obtained under the same conditions as in Fig. 3 except that three of the same ODS-silica gel columns were connected in series is shown in Fig. 5. The pressure of the mobile phase was adjusted so that the same mean pressure calculated from the inlet and outlet pressures of the columns could be established among three types of column connection, that is, single, double and triple connections. A three times longer analysis time was necessary, as in LC analysis, but considerably better resolution was obtained by tripling the column length, as expected.

Using a 50 cm (2 × 25 cm) column length, the elution behaviour of two important resin acids, levopimaric and dihydroagathic acids, both absent from Chinese gum rosin, was studied. As indicated before, levopimaric acid cannot be separated from palustric acid by GC under the current ASTM packed column standard conditions [3], but this resolution is readily accomplished with capillary columns [4]. Dihydroagathic acid, specifically contained in S. East Asian pine resin (*Pinus merkusii* Jungh. & de Vriese exudate) and easily separable by GC, has a characteristic structure with two carboxyl groups in the molecule. These two acids were mixed with Chinese gum rosin and subjected to SFC, giving the chromatogram shown in Fig. 6.

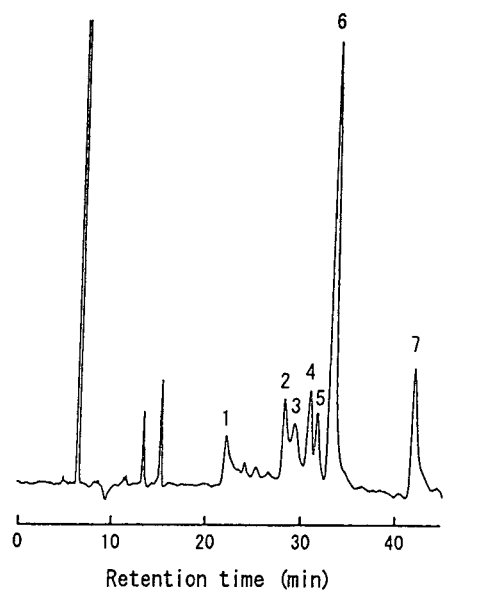

Fig. 6. Chromatogram of nine resin acids on two columns. Peaks: 1 = dihydroagathic acid; 2 = pimaric acid; 3 = sandaracopimaric acid, isopimaric acid, dehydroabietic acid; 4 = palustric acid; 5 = levopimaric acid; 6 = abietic acid; 7 = neoabietic acid. Other conditions as in Fig. 2.

Interestingly, dihydroagathic acid was eluted far ahead of others and levopimaric acid was eluted immediately after palustric acid.

4. Conclusion

The elution behaviour of resin acids by SFC on an inert ODS-silica gel column using supercritical carbon dioxide as the mobile phase was studied. The separation of resin acids could be considerably improved by using methanol as a modifier. According to the results, the isomers of abietane-type acids could be separated by SFC without derivatization, particularly esterification. Therefore, the development of a perfectly inert column is still required for the SFC separation of free resin acids (rosin per se without esterification, for example) without a modifier.

References

[1] H.I. Enos, Jr., G.C. Harris and G.W. Hedrich, Encyclopedia of Chemical Technology, Vol. 17, Interscience, New York, 2nd ed., 1968, p. 475.
[2] E.J. Soltes and D.F. Zinkel, in D.F. Zinkel and J. Russell (Editors), Naval Stores—Production, Chemistry, Utilization, Pulp Chemicals Association, New York, 1989, Ch. 9, p. 261.
[3] Standard Test Method for Resin Acids in Rosin by G.C., D3008-82, ASTM, Philadelphia, PA.
[4] D.F. Zinkel, Naval Stores Rev., 96, No. 2 (1986) 14.
[5] D.F Zinkel, in D.F. Zinkel and J. Russell (Editors), Naval Stores—Production, Chemistry, Utilization, Pulp Chemicals Association, New York, 1989, Ch. 24, p. 814.
[6] S. Otsuka and I. Kubo, in Proceedings of the 58th Meeting, Vol. 2, Chemical Society of Japan, Tokyo, 1989, p. 1156.
[7] A.L. Blilie and T. Greibrokk, Anal. Chem., 57 (1985) 2239.
[8] J,M Levy and W.M. Ritchey, J. High Resolut. Chromatogr. Chromatogr. Commun., 8 (1985) 503.
[9] J.M. Levy and W.M. Ritchey, J. Chromatogr. Sci., 24 (1986) 242.
[10] M.E. McNally, J.R. Wheeler and W.R. Melander, LC·GC, 6 (1988) 816.
[11] T.A. Berger and J.F. Deye, J. Chromatogr. Sci., 29 (1991) 141.
[12] T.A. Berger and J.F. Deye, J. Chromatogr. Sci., 29 (1991) 280.
[13] T.A. Berger and J.F. Deye, J. Chromatogr. Sci., 29 (1991) 390.
[14] D.R. Gere, Science, 222 (1983) 253.
[15] T. Yarita, A. Nomura, K. Abe and Y. Takeshita, J. Chromatogr. A, 679 (1994) 329.

ELSEVIER

Journal of Chromatography A, 709 (1995) 351–359

JOURNAL OF CHROMATOGRAPHY A

Combination of orthogonal array design and overlapping resolution mapping for optimizing the separation of heterocyclic amines by capillary zone electrophoresis

Jun Wu[a], Ming Keong Wong[a], Sam Fong Yau Li[a], Hian Kee Lee[a,*], Choon Nam Ong[b]

[a]*Department of Chemistry, National University of Singapore, Kent Ridge, Singapore 0511, Singapore*
[b]*Department of Community, Occupational, and Family Medicine, National University of Singapore, Kent Ridge, Singapore 0511, Singapore*

First received 10 January 1995; revised manuscript received 11 April 1995; accepted 11 April 1995

Abstract

This paper describes the application of combined orthogonal array design and overlapping resolution mapping to the optimization of capillary zone electrophoresis for the separation of heterocyclic amines. The factors affecting resolution, such as buffer pH, organic modifier, concentration of buffer solution, capillary tubing temperature, and electric field strength, were studied in two steps. In the first step, orthogonal array design was used to determine the most important factors and interactions. The experiments were carried out according to an OA_{16} (2^{15}) matrix through sixteen pre-designed trials. Based on the results of the first step, the second set of experiments was performed according to a three-dimensional overlapping resolution mapping scheme, in which eleven pre-planned trials were executed and global optimum conditions for the separation within a reasonable analysis time were obtained. The proposed conditions were successfully applied in the separation of thirteen heterocyclic amines.

1. Introduction

Since 1976, a series of mutagens and carcinogens, heterocyclic amines (HCAs), have been isolated and identified from heated amino acids or cooked meat products. Later, some of them have also been found in environmental samples [1–4]. These compounds have been found to be carcinogenic in rodents [5], non-human primates [6], and potentially carcinogenic to humans [7–13]. The knowledge of the distribution and contents of HCAs in environmental samples is essential for human health risk assessments and several methods have been developed for quantitating HCAs in various matrices. The commonly used ones are negative chemical ion GC–MS [14,15], LC–MS [16,17], HPLC [18–21], and immunoaffinity chromatography [22], but these techniques either require sophisticated and costly equipment which is beyond the reach of routine laboratories or are restricted to the determination of a selected group of HCAs.

Capillary electrophoresis (CE) has now been established as a powerful separation tool. Compared with HPLC, the technique is capable of

* Corresponding author.

0021-9673/95/$09.50
SSDI 0021-9673(95)00459-9

achieving higher separation efficiency, uses less organic solvents, and requires small amounts of samples. However, the migration behavior of ionized compounds is less well characterized than their retention behavior in HPLC. For the separation of compounds with very similar mobilities, such as isomers and analogues, more than one parameter (e.g. modifier concentration, pH, electrolyte concentration, nature of capillary tubing, capillary temperature, electric field strength, etc.) need to be incorporated in the optimization strategy to achieve an adequate separation of such complex mixtures.

Strategies for the systematic optimization of CE are few and most of the optimum separation conditions have been achieved using simple univariate optimization procedures. These techniques have been proven to be ineffective in locating the true optimum and are time-consuming.

The simultaneous multivariate optimization approach is usually the preferred method, but the application of it is often limited by the large trial size and the requirement of a sophisticated statistical background to implement. To alleviate these problems, systematic approaches are necessary.

The Plackett–Burman statistical design [23] has been used to optimize the resolution of testosterone esters. But there were no fixed rules for the selection of levels of factors and further optimization needed to be executed before the exact experimental conditions providing optimum separation could be determined. Other techniques also suffer from the limited number of parameters which can be varied, or from the difficulty in calculating the response function.

In our previous work, orthogonal array design (OAD) has been successfully applied in the optimization of analytical procedures such as chromatographic separation [24,25], solid-phase extraction [26], and others [27–31]. Orthogonal array design has some advantages over other optimization techniques in that as one kind of factorial design it can perform simultaneous multivariate optimization. Furthermore, since it is a fractional factorial design approach, the number of trials may be reduced greatly compared to the normal factorial designs by implementing a well-balanced assignment of all the factors and the interactions among them. In that way, when the effect of a factor is calculated, the influence of the other factors is canceled out. Therefore the term "orthogonal" means "balanced", "separable", or "not mixed" in this approach. A common mathematical procedure can be used to independently extract the main effects from factors and interactions amongst them quantitatively. The number of factors investigated can be up to thirty-one [32], which is decided by the size of the trials, the complexity of the system, and to what extent one wants the information. It can deal with both continuous and discrete factors. However, in the case of continuous factors the optimum conditions determined by OAD designs are limited to some discrete points, and in some cases the global optimum level lies between these points so that subsequent optimization steps may be necessary.

One of the mixture designs, the overlapping resolution mapping (ORM) scheme, has been adapted for the optimization of CE separations [33–35]. Although the considered number of factors by the two-dimensional ORM scheme is only two [33,34] and by the three-dimensional scheme three [35], ORM is capable of locating the global optimum within the selected range of experimental conditions instead of levels or points as in other approaches, and hence is faster in locating the optimum conditions.

The purpose of the present work is to demonstrate the advantages of combining the OAD design with the ORM scheme in optimizing the separation of eleven heterocyclic amines and two co-mutagenic β-carbolines (Table 1) by capillary zone electrophoresis (CZE).

2. Experimental

2.1. Chemicals

Chemicals and solvents were of HPLC or analytical grade. Water was obtained from a Milli-Q water purification system (Millipore, Bedford, MA, USA). IQ, MeIQx, 4,8-Di-

Table 1
Heterocyclic amines used in this investigation

Chemical name	Abbreviation
2-Amino-3-methylimidazo[4,5-*f*]quinoline	IQ
2-Amino-4-methylimidazo[4,5-*f*]quinoline	Iso-IQ
2-Amino-3,8-dimethylimidazo[4,5-*f*]quinoxaline	MeIQx
2-Amino-3,4,8-trimethylimidazo[4,5-*f*]quinoxaline	4,8-DiMeIQx
2-Amino-3,4,7,8-tetramethylimidazo[4,5-*f*]quinoxaline	4,7,8-TriMeIQx
2-Amino-1-methyl-6-phenylimidazo[4,5-*b*]pyridine	PhIP
3-Amino-1,4-dimethyl-5*H*-pyrido[4,3-*b*]indole	Trp-P-1
3-Amino-1-methyl-5*H*-pyrido[4,3-*b*]indole	Trp-P-2
2-Amino-6-methyldipyrido[1,2-*a*:3′,2′-*d*]imidazole	Glu-P-1
2-Amino-dipyrido[1,2-*a*:3′,2′-*d*]imidazole	Glu-P-2
2-Amino-9*H*-pyrido[2,3-*b*]indole	AαC
1-methyl-9*H*-pyrido[3,4-*b*]indole, β-carboline	H
9*H*-pyrido[3,4-*b*]indole, β-carboline	NH

MeIQx, and 4,7,8-TriMeIQx were kindly provided by Dr. K. Wakabayashi, National Cancer Center Research Institute, Japan. Iso-IQ, H, NH, PhIP, Trp-P-1, Trp-P-2, Glu-P-1, Glu-P-2, and AαC were purchased from Toronto Research Chemicals (Downsview, Ont., Canada). The compounds were dissolved in methanol at 250 ng/μl as stock solution, and a mixture solution containing 10 ng/μl of each compound in methanol was prepared from the stock and used as the working solution. Stock solutions of 1 *M* Na_2HPO_4, 1 *M* citric acid, and 1 *M* NaCl were obtained by dissolving the appropriate salts in water, and the buffer solutions were freshly prepared before use. The pH of the buffer was adjusted by adding H_3PO_4.

2.2. Instrumentation

The analysis was performed using a BioFocus 3000 automated capillary electrophoresis system (Bio-Rad, Hercules, CA, USA) with a multi-wavelength UV detector. The uncoated silica tubing was 51 cm in length and the effective length was 46.4 cm. Constant applied voltage was 18 kV (current 38 μA). UV absorbance was monitored at 190, 220, 240, and 263 nm. The injection was by the pressure mode, 1 p.s.i. s (1 psi = 6894.76 Pa) of a standard mixture solution (10 ng/μl). The capillary temperature was 25°C and the autosampler temperature was 15°C.

3. Results and discussion

3.1. OAD scheme

The assignment of factors and their levels for the first experiment is given in Table 2 according to an OA_{16} (2^{15}) matrix. The interaction between factors was also indicated as an independent factor in the table. Interaction is believed to occur between factors when the state or value of one factor influences the state or value of the other factor. After implementing sixteen predesigned experimental trials and obtaining the corresponding electropherograms, for each trial the resolution between each adjacent pair of peaks was calculated according to

$$R = 2(t_2 - t_1)/(w_2 + w_1) \quad (1)$$

The sums of all resolutions were calculated and are also listed in Table 2 as responses. The sums of responses at each level were computed as K_i in Table 2. Taking factor B as an example, K_1 is the sum of responses at level 1 (trials 1, 2, 3, 4, 9, 10, 11, and 12) and K_2 is the sum of responses at level 2 (trials 5, 6, 7, 8, 13, 14, 15, and 16). The sum of squares for each effect was obtained by using

$$Q_A = (K_1 + K_2)/a \quad (2)$$

where Q_A is the sums of squares of factor A, a is

Table 2
Assignment of the factors and their levels of the first experiment by using an OA_{16} (2^{15}) matrix along with the results of the effects of selected variables on the responses

	A pH	*B*	*A* × *B*	*C* NaCl	*A* × *C*	*E* × *F* *B* × *C*	*D*[a]	*C* × *F* *B* × *E*	*A* × *E*	*E* Temp.	*A* × *F*	*F* kV	*B* × *F* *C* × *E*	*R*[b]
1	2.5 (1)	0 (1)	(1)	50 (1)	(1)	(1)	(1)	(1)	(1)	20 (1)	(1)	20 (1)	(1)	6.06
2	2.5 (1)	0 (1)	(1)	50 (1)	(1)	(1)	(2)	(2)	(2)	30 (2)	(2)	15 (2)	(2)	10.91
3	2.5 (1)	0 (1)	(1)	0 (2)	(2)	(2)	(1)	(1)	(1)	20 (1)	(2)	15 (2)	(2)	8.05
4	2.5 (1)	0 (1)	(1)	0 (2)	(2)	(2)	(2)	(2)	(2)	30 (2)	(1)	20 (1)	(1)	8.20
5	2.5 (1)	30 (2)	(2)	50 (1)	(1)	(2)	(1)	(1)	(2)	30 (2)	(1)	20 (1)	(2)	14.12
6	2.5 (1)	30 (2)	(2)	50 (1)	(1)	(2)	(2)	(2)	(1)	20 (1)	(2)	15 (2)	(1)	8.28
7	2.5 (1)	30 (2)	(2)	0 (2)	(2)	(1)	(1)	(1)	(2)	30 (2)	(2)	15 (2)	(1)	12.19
8	2.5 (1)	30 (2)	(2)	0 (2)	(2)	(1)	(2)	(2)	(1)	20 (1)	(1)	20 (1)	(2)	13.36
9	3.5 (2)	0 (1)	(2)	50 (1)	(2)	(1)	(1)	(2)	(1)	30 (2)	(1)	15 (2)	(2)	3.84
10	3.5 (2)	0 (1)	(2)	50 (1)	(2)	(1)	(2)	(1)	(2)	20 (1)	(2)	20 (1)	(1)	5.13
11	3.5 (2)	0 (1)	(2)	0 (2)	(1)	(2)	(1)	(2)	(1)	30 (2)	(2)	20 (1)	(1)	0.66
12	3.5 (2)	0 (1)	(2)	0 (2)	(1)	(2)	(2)	(1)	(2)	20 (1)	(1)	15 (2)	(2)	2.67
13	3.5 (2)	30 (2)	(1)	50 (1)	(2)	(2)	(1)	(2)	(2)	20 (1)	(1)	15 (2)	(1)	3.65
14	3.5 (2)	30 (2)	(1)	50 (1)	(2)	(2)	(2)	(1)	(1)	30 (2)	(2)	20 (1)	(2)	0.32
15	3.5 (2)	30 (2)	(1)	0 (2)	(1)	(1)	(1)	(2)	(2)	20 (1)	(2)	20 (1)	(2)	7.35
16	3.5 (2)	30 (2)	(1)	0 (2)	(1)	(1)	(2)	(1)	(1)	30 (2)	(1)	15 (2)	(1)	2.09
K1	81.17	45.52	46.63	52.31	52.14	60.93	55.92	50.63	42.66	54.55	53.99	55.2	46.26	106.88
K2	25.71	61.36	60.25	54.57	54.74	45.95	50.96	56.25	64.22	52.33	52.89	51.68	60.62	
Δ[c]	55.46	15.84	13.62	2.26	2.60	14.98	4.96	5.62	21.56	2.22	1.10	3.52	14.36	

[a] Factor D was a dummy.
[b] Response = $R - 15.00$.
[c] $\Delta = |K_1 - K_2|$.

the number of levels, and K_1, K_2 are the sums of responses at level 1 and level 2, respectively.

Factor *D* is a dummy and was used for error estimation. During calculation, the sum of squares of the errors along with those of insignificant factors and interactions were combined and treated as the estimation of pooled error results so that the analysis of variance (ANOVA) could be conducted for data analysis.

The ANOVA results are shown in Table 3. It shows that within the selected range, buffer pH (*A*) was the most important factor (large sum of squares), and pH 2.5 was better than pH 3.5. The concentration of organic modifier (methanol) was the next important factor, and a buffer with the organic modifier (*B*) was better than one without it.

Although factors such as the concentration of supporting electrolyte (*C*), the capillary temperature (*E*), and applied voltage (*F*) were not as important as *A* or *B*, the effects of interactions between factor *A* and *E*, *E* and *F* plus *B* and *C*, *B* and *F* plus *C* and *E* are within the same order of magnitude as those of factor *B* or the interaction between *A* and *B*. In order to limit the trial number to a reasonable size, it was not necessary to distinguish the differences amongst these mixed effects. By some simple calculations, the optimum combination of these factors at certain levels could still be computed and the results of two single interactions between factors *A* and *B* along with *A* and *E* are shown in Tables 4 and 5.

The electrophoretic buffer is of key importance in CE because its composition basically determines the migration behavior of the analytes. The adjustment of pH changes electroosmotic flow (EOF), as well as the solute charge

Table 3
An ANOVA table for the first experiment

Source of variance	Sum of square	Freedom	Mean square	F-value	Significance[a]
A (pH)	192.38	1	192.38	125.4	$p < 0.001$
B (MeOH)	15.68	1	15.69	10.2	$p > 0.01$
$A \times B$	11.59	1	11.59	7.6	$p > 0.01$
$E \times F$ & $B \times C$	14.03	1	14.03	9.2	$p > 0.01$
$A \times E$	29.05	1	29.05	19.0	$p < 0.005$
$B \times F$ & $C \times E$	12.89	1	12.89	8.4	$p > 0.025$
C (NaCl)	0.32				
$A \times C$	0.42				
$C \times F$ & $B \times E$	1.97				
E (temp.)	0.31	9[b]	1.53[b]		
$A \times F$	0.08				
F (voltage)	0.77				
Errors	9.94				

[a] The critical F-value is 22.86 at 99.9% confidence, 13.61 at 99.5% confidence, 10.56 at 99.0% confidence, and 7.21 at 97.5% confidence.
[b] The insignificant factors (C, E and F) and interactions ($A \times C$, $A \times F$, $C \times F$ & $B \times E$) were pooled with the errors (D, dummy) for F-test calculation.

Table 4
The optimum combination of levels for buffer pH and capillary temperature of the first experiment (A_1E_2)

	E_1	E_2
A_1	35.75	**45.42**[a]
A_2	18.80	6.91

[a] This value was the best response.

and solute mobility. In CZE, both the electrophoretic mobility and electroosmotic mobility contribute to the migration velocity. To prevent elution of solutes before separation, a reduction of EOF may be necessary in certain cases. In the case of weak acids or bases, their degree of ionization depends on the pH of the solution,

Table 5
The optimum combination of levels for buffer pH and concentration of methanol of the first experiment (A_1B_2)

	B_1	B_2
A_1	33.22	**47.95**[a]
A_2	12.30	13.41

[a] This value was the best response.

which gives rise to differences in electrophoretic and electroosmotic mobilities. HCAs are a group of weak bases, hence they are converted to protonated species at low pH. That is why pH 2.5 provided a better separation.

The existence of the organic modifier, methanol, reduced the EOF significantly and improved the separation of HCAs to some extent. In addition, methanol improved the solubility of HCAs in the buffer, interacted strongly with the capillary wall, and therefore reduced the chance of interaction between solutes and the wall [36].

The results of both Table 2 and 3 show that factors such as concentration of buffer (C), applied voltage (F), and capillary temperature (E) are of less importance compared to pH (A) and concentration of organic modifier (B) in the selected experimental ranges, although all of them affected the resolution. At the same time, there were some strong interactions among these factors and therefore some of the effects were combined with each other.

Anions and cations present in the electrolyte system may affect the current and hence the electroosmotic flow, the heat generated, the interaction of analytes with the wall of the capillary, and the mobilities of the ions. The

ionic strength has significant effects on solute mobilities and separation efficiency. It has been found that addition of NaCl reduced EOF by decreasing the thickness of the double-layer [37]. In the present study, the existence of NaCl had no significant effect on the separation of HCAs within the selected variable ranges. The sum of resolutions of a buffer with 50 m*M* NaCl was even smaller than that of one without NaCl. It is likely that the effect was masked by relatively high concentrations of other electrolytes, such as Na_2HPO_4, in the system. But the addition of NaCl resulted in a competition between Na^+ and amines for cation-exchange sites on the silica surface and therefore reduced the adsorption of HCAs on the wall. The adverse effect of NaCl was that the increase of the ionic strength caused heat accumulation within the capillary tubing and therefore restricted further increment of the applied voltage.

The capillary temperature affects the resolution in two ways. First, the nature of the buffer medium will be affected by changes in temperature. As the temperature increases, the viscosity decreases and both the EOF and electrophoretic mobility increase. The mobility of most ions increases about 2%/°C [38]. Second, if the temperature gradients are steep enough, density gradients in the electrophoresis buffer can be induced, which in turn cause natural convection. A convection will remix separated sample zones and reduces separation performance severely. The results show that there is no significant difference between 20 and 30°C. However, the combinations of 20°C with other factors at certain levels were better than those of 30°C with the same factors.

The efficiency of separation is directly proportional to the capillary length, provided the field strength is kept constant. In other words, for a certain length of tubing, a high field strength, i.e. a high voltage, results in better resolution. In practice, the voltage is limited by the design of the instrument and the heat produced within the capillary.

In this work, voltage was not the most critical parameter in the resolution of the HCA mixture, according to the OAD. Rather, after pH and concentration of organic modifier, it was the third most important factor. However, it is acknowledged that this study considered only one specific category of compounds, and this observation may not be applicable to other compound classes.

3.2. ORM scheme

Based on the results of the first experiment, the optimum combination of minor conditions was selected. In the second set of experiments, emphasis was placed on the use of the three-dimensional ORM to optimize the important factors, namely pH and the concentration of methanol, along with another factor, the concentration of Na_2HPO_4, which had not been taken into consideration in the first experiment.

Since the principle and optimization strategy of ORM have been discussed in detail previously [33–35], only a brief description of the main steps of the method is given here. The ORM scheme consisted of a number of steps. First, the criteria for the optimum conditions were set. The criteria used were: (1) the resolution between all adjacent pair of peaks should be greater than unity and (2) the maximum analysis time should not exceed 20 min. Secondly, a set of trial experiments were chosen within the desired experimental ranges for the three variables, pH from 2.0 to 3.0, MeOH concentration from 15 to 35%, and concentration of Na_2HPO_4 from 20 to 60 m*M*, as shown in Table 6.

After implementing the eleven trials, the resolution between each adjacent pair of peaks for each trial was calculated (Eq. 1). The results are shown in Table 7. Subsequently, the *R*-values of each pair of peaks were fitted to the third-order polynomial equation

$$R = a_0 + a_1X_1 + a_2X_2 + a_3X_3 + a_4X_1X_2 + a_5X_2X_3 + a_6X_1X_3 + a_7X_1^2 + a_8X_2^2 + a_9X_3^2 + a_{10}X_1X_2X_3, \quad (3)$$

where a_i are coefficients and the X_i are the proportion of each variable between the maximum and minimum values expressed in percentages. With the aid of a modified version of

Table 6
Conditions of the eleven trials in the ORM scheme

Trial[a]	pH	MeOH (%)	Na_2HPO_4 (m*M*)
1	2.0	15	20
2	2.0	35	20
3	2.0	15	60
4	3.0	15	20
5	2.0	35	60
6	3.0	35	20
7	3.0	15	60
8	3.0	35	60
9	2.0	25	20
10	2.0	15	40
11	2.5	15	20

[a] Trials performed with 20 m*M* citric acid, 50 m*M* NaCl, 18 kV voltage, and capillary temperature at 25°C.

the BASIC program given in Ref. [39], the coefficients for each pair of peaks were determined. The *R*-values at other experimental conditions besides the eleven trial experiments were calculated using the above equation. These *R*-values were used to construct resolution plots. As there were twelve adjacent pair of peaks, twelve individual resolution plots were obtained. By overlapping all the resolution plots and retaining the minimum resolution values, the conditions which could provide resolution equal to or greater than unity for the twelve pair of peaks in the mixture could be determined.

Fig. 1 is the final overlapped resolution plot for all twelve pairs of peaks, where the region marked with "*" represents experimental conditions which provide resolution greater than unity for all peak pairs within the desired analysis time of 20 min. It indicates that the increase in concentration of the electrolyte, Na_2HPO_4, did not result in improvement in separation. The optimum region was found to lie in the pH range from 2.0 to 2.1, and concentration of methanol from 25% to 100%. The maximum response was 1.1936 at the point $A = 0$, $B = 80\%$, and $C = 0$ (marked as "1" in Fig. 1), which corresponds to pH 2.0, methanol concentration of 31%, and 20 m*M* of Na_2HPO_4.

To confirm the validity of the ORM scheme, experimental conditions corresponding to points 1 and 2 in Fig. 1 were chosen from the regions represented by the symbols "*" and "·", respectively. High resolution ($R > 1.0$) was expected for the condition represented by point 1 whereas poor resolution ($R \leq 0.5$) was expected for the condition represented by point 2. Typical electropherograms corresponding to these two conditions are shown in Figs. 2 and 3. Just as expected, not all peaks in Fig. 3 are well separated. In the case of Fig. 2, all the peaks are

Table 7
Resolution (*R*) between adjacent peaks calculated by using migration times obtained for the trials listed in Table 6

R	Trial										
	1	2	3	4	5	6	7	8	9	10	11
1	2.55	4.95	3.65	3.33	10.3	7.29	5.64	2.02	4.20	3.47	6.93
2	16.0	3.60	3.60	17.5	4.32	1.16	2.51	4.84	11.3	14.6	5.49
3	3.95	8.03	0	6.20	1.64	0	3.15	3.99	5.91	5.78	0
4	2.10	1.33	0	4.56	4.95	0	2.94	2.02	5.84	4.25	4.73
5	0	2.83	2.24	1.44	2.44	2.24	0	0.39	1.99	0.97	1.27
6	2.08	8.49	0	1.90	0	0	1.18	0.67	1.47	0.91	2.36
7	0	0.79	0	1.21	0	1.72	6.26	1.88	4.51	1.47	2.22
8	1.20	0.93	0.93	2.34	1.07	2.19	0	1.11	1.26	0	1.06
9	1.50	3.35	2.73	1.94	2.73	0	1.52	1.21	0	1.57	1.03
10	1.59	1.94	2.66	1.24	2.66	1.8	2.34	1.57	3.47	1.47	6.70
11	0	2.82	1.25	1.10	0	2.82	2.78	1.04	1.15	0.73	0
12	1.06	0.52	1.36	1.74	2.16	2.57	0.71	0.78	2.77	2.27	9.01

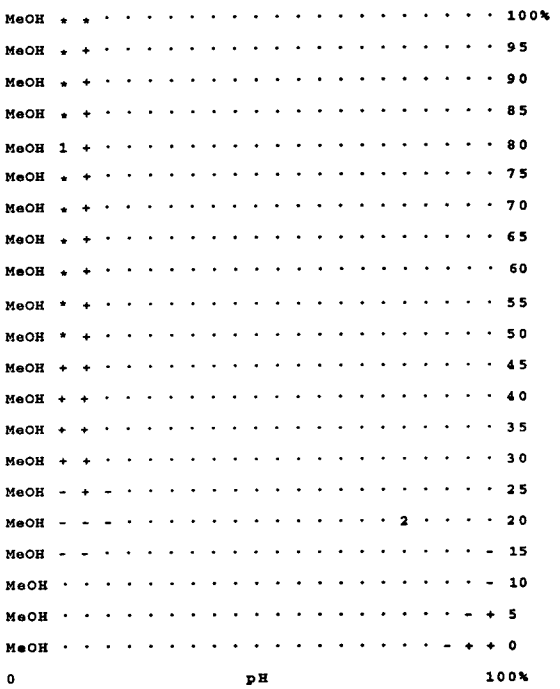

Fig. 1. Overlapped resolution diagram for the twelve pairs of HCA peaks. The minimum values of resolution among all the fifteen individual resolution diagrams are plotted in this overlapped diagram. The highest value of resolution (R = 1.1936) was obtained at point 1, which corresponds to x_1 = 0%, x_2 = 80%, and x_3 = 0%. Point 2 represents a typical set of conditions which give poor resolution. Notation: (·) $R \leq 0.5$, (−) $0.5 < R \leq 0.7$, (+) $0.7 < R \leq 1.0$, (*) $1.0 < R$.

baseline separated and the analysis time is within a reasonable range (< 20 min).

4. Conclusions

In this paper, the combination of the orthogonal array design and the overlapping resolution mapping scheme for the optimization of separation of a group of heterocyclic amines was demonstrated. The orthogonal array design method was used to perform preliminary screening to identify the important factors affecting resolution. Subsequently, the overlapping resolution mapping scheme was used to determine the global optimum conditions within the experimental ranges of the variables under consideration. The combination of the two methods overcomes the disadvantages of each individual method when used alone, and provides a powerful approach which can be utilized for the optimization of separation of complex mixtures.

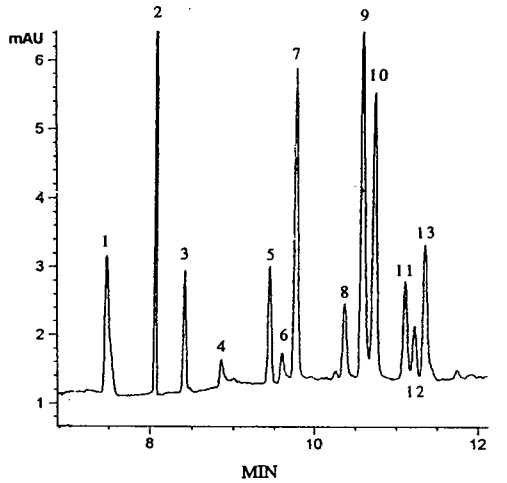

Fig. 2. Optimized electropherogram of the separation of the thirteen HCAs at point 1 (x_1 = 0%, x_2 = 80%, and x_3 = 0%) in ORM scheme. Electrophoretic conditions are given in the Experimental section. Peak identifications: 1 = Iso-IQ, 2 = IQ, 3 = NH, 4 = Glu-P-2, 5 = H, 6 = Glu-P-1, 7 = Trp-P-2, 8 = AαC, 9 = Trp-P-1, 10 = MeIQx, 11 = DiMeIQx, 12 = PhIP, 13 = TriMeIQx (see Table 1).

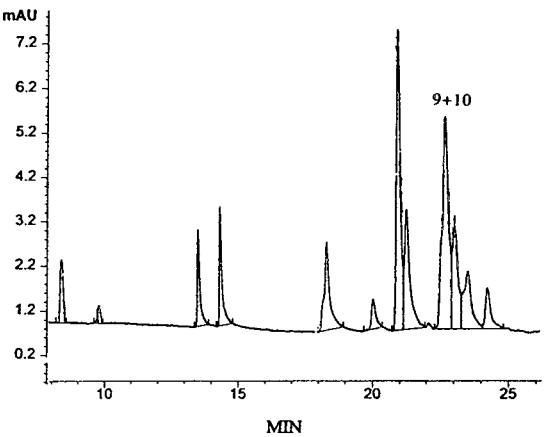

Fig. 3. Electropherogram of the separation of the thirteen HCAs at point 2 (x_1 = 80%, x_2 = 20%, and x_3 = 0%) in ORM scheme. Electrophoretic conditions are given in the Experimental section. Peak identifications are as given in Fig. 2.

Acknowledgements

The authors are grateful to Bio-Rad Laboratories (Singapore) Pte Ltd for the loan of a BioFocus 3000 automated capillary electrophoresis system, and to Ms. Veronica Tok of the same company for her assistance. J.W. wishes to thank the National University of Singapore for the award of a research studentship.

References

[1] J.S. Felton and M.G. Knize, in C.S. Cooper and P.L. Grover (Editors), Chemical Carcinogenesis and Mutagenesis, Vol. I, Springer Verlag, Berlin, 1990, p. 471.
[2] G. Eisenbrand and W. Tang, Toxicology, 84 (1993) 1.
[3] K. Wakabayashi, M. Nagao, H. Esumi and T. Sugimura, Cancer Res., 52 (Suppl.) (1992) 2092s.
[4] S. Manabe, O. Wada and Y. Kanai, J. Environ. Sci. Health A, 26 (1991) 1446.
[5] H. Ohgaki, S. Takayama and T. Sugimura, in H. Hayatsu (Editor), Mutagens in Food: Detection and Prevention, CTC Press, Boca Raton, FL, 1991, p. 219.
[6] R.H. Adamson, U.P. Thorgeirsson, E.G. Snyderwine, S.S. Thorgeirsson, J. Reeves, D.W. Dalgard, S. Takayama and T. Sugimura, Jpn. J. Cancer Res., 81 (1990) 10.
[7] Y. Yamazoe, M. Abu-Zeid, K. Yamaguchi and R. Kato, Jpn. J. Cancer Res., 79 (1988) 1159.
[8] T. Shimada, M. Iwasaki, M. Martin and F.P. Guengerich, Cancer Res., 49 (1989) 3218.
[9] M.A. Butler, M. Iwasaki, F.P. Guengerich and F.F. Kadlubar, Proc. Natl. Acad. Sci. USA, 86 (1989) 7696.
[10] R.J. Turesky, N.P. Lang, M.A. Butler, C.H. Teitel and F.F. Kadlubar, Carcinogenesis, 12 (1991) 1839.
[11] M. Abu-Zeid, Y. Yamazoe and R. Kato, Carcinogenesis, 13 (1992) 1307.
[12] R. Kato, CRC Crit. Rev. Toxicol., 16 (1986) 308.
[13] C.D. Davis, H.A.J. Schut, R.H. Adamson, U.P. Thorgeirsson, S.S. Thorgeirsson and E.G. Snyderwine, Carcinogenesis, 14 (1993) 61.
[14] S. Murray, N.J. Gooderham, A.R. Boobis and D.S. Davies, Carcinogenesis, 9 (1988) 321.
[15] A.M. Lynch, M.G. Knize, A.R. Boobis, N.J. Gooderham, D.S. Davies and S. Murray, Cancer Res., 52 (1992) 6216.
[16] Z. Yamaizumi, H. Kasai, S. Nishimura, C.G. Edmonds and J.A. McCloskey, Mutat. Res., 173 (1986) 1.
[17] R.J. Turesky, H. Bur, T. Huynh Ba, H.U. Aeschbacher and H. Milon, Food Chem. Toxicol., 26 (1992) 501.
[18] G.A. Gross, G. Philippossian and H.U. Aeschbacher, Carcinogenesis, 10 (1989) 1175.
[19] G.A. Gross, Carcinogenesis, 11 (1990) 1597.
[20] G.A. Gross and A. Grüter, J. Chromatogr., 592 (1992) 271.
[21] G.A. Gross, A. Grüter and S. Heyland, Food Chem. Toxicol., 30 (1992) 491.
[22] R.J. Turesky, C.M. Forster, H.U. Aeschbacher, H.P. Wuerzner, P.L. Skipper, L.J. Trudel and S.R. Tannenbaum, Carcinogenesis, 10 (1989) 151.
[23] J. Vindevogel and P. Sandra, Anal. Chem., 63 (1991) 1530.
[24] H.B. Wan, W.G. Lan, M.K. Wong and C.Y. Mok, Anal. Chim. Acta, 289 (1994) 371.
[25] W.G. Lan, K.K. Chee, M.K. Wong, H.K. Lee and Y.M. Sin, Analyst, 120 (1995) 281.
[26] H.B. Wan, W.G. Lan, M.K. Wong, C.Y. Mok and Y.H. Poh, J. Chromatogr. A, 677 (1994) 255.
[27] W.G. Lan, M.K. Wong, K.K. Chee and Y.M. Sin, Analyst, 120 (1995) 273.
[28] W.G. Lan, M.K. Wong, N. Chen and Y.M. Sin, Analyst, 119 (1994) 1659.
[29] W.G. Lan, M.K. Wong and Y.M. Sin, Analyst, 119 (1994) 1669.
[30] W.G. Lan, M.K. Wong, N. Chen and Y.M. Sin, Analyst, (1995), in press.
[31] W.G. Lan, M.K. Wong, N. Chen and Y.M. Sin, Talanta, 41 (1994) 1917.
[32] P.J. Oles, J. Assoc. Off. Anal. Chem. Int., 76 (1993) 615.
[33] S.K. Yeo, C.P. Ong and S.F.Y. Li, Anal. Chem., 63 (1991) 2222.
[34] C.L. Ng, H.K. Lee and S.F.Y. Li, J. Chromatogr., 598 (1992) 133.
[35] Y.F. Yik and S.F.Y. Li, Chromatographia, 35 (1993) 560.
[36] B.B. VanOrman, G.G. Liversidge and G.L. McIntire, J. Microcol. Sep., 2 (1991) 176.
[37] S. Fujiwara and S. Honda, Anal. Chem., 58 (1986) 1811.
[38] S. Hjerten, Chromatogr. Rev., 9 (1967) 122.
[39] J.C. Berridge, Techniques for the Automated Optimization of HPLC Separation, Wiley, New York, 1985, Appendix IV.

ELSEVIER

Journal of Chromatography A, 709 (1995) 361–366

JOURNAL OF CHROMATOGRAPHY A

Selective determination of aromatic amines in water samples by capillary zone electrophoresis and solid-phase extraction ☆

Aldo Cavallaro[a,*], Vittorio Piangerelli[a], Flavia Nerini[a], Silvano Cavalli[b], Claudio Reschiotto[b]

[a] *U.O. Chimica, Presidio Multizonale di Igiene a Prevenzione USSL 75/III, via Juvara 22, 20133 Milan, Italy*
[b] *Laboratorio Applicazioni, Dionex srl, via dei Tulipani 5, 20090 Pieve Emanuele MI, Italy*

First received 8 December 1994; revised manuscript received 1 April 1995

Abstract

The use of a 20:80 (w/w) mixture of keto-derivatized and underivatized poly(styrene–divinylbenzene) copolymer for the selective solid-phase extraction (SPE) of pollutants in environmental water samples is described. In previous paper work, this technique was used for phenol determination with amperometric detection. In this modification, the use of a selective separation technique such as capillary zone electrophoresis (CZE) limits the necessity for obtaining a selective class separation with the extraction procedure. In this case, the same extract as used for phenols was analysed by CZE in phosphate buffer with UV detection, and the cationic species of interest, aromatic amines, were well separated from all the other non-ionic and anionic compounds. Experimental conditions for the use of CZE and the extraction technique are described. Different recoveries of aromatic amines in environmental samples, linearity and detection limits are discussed.

1. Introduction

Substituted anilines and benzidines are widely used in the chemical industry as intermediates in the production of dyes, pesticides, pharmaceuticals, etc.. These compounds are very well known because of their high toxicity and suspected carcinogenicity [1]. Owing to their high solubility in water, aromatic amines can easily permeate through soil and contaminate groundwater.

This paper is based on previous research on the determination of phenolic compounds, also widely used in the chemical industry, in soil and groundwater of a heavily contaminated area.

The previously proposed method for the determination of phenolic compounds [2] was subject to interference due to contemporaneous extraction of compounds with an $ArNH_2$ group, so we sought an analytical method with high selectivity towards this category of substances, based mainly on differences in ionicity of the two classes. The most common technique used for the determination of aromatic amines in environmental samples is gas chromatography coupled with mass spectrometry (GC–MS). However, the use of this technique requires long and cumbersome purification steps before the analy-

* Corresponding author.

☆ Presented at the *International Ion Chromatography Symposium 1994, Turin, 19–22 September 1994.*

0021-9673/95/$09.50
SSDI 0021-9673(95)00435-1

sis. The high sensitivity of GC–MS is not always needed in investigations of known events and a simple, but highly selective, technique for a rapid throughput would be more convenient.

The use of capillary zone electrophoresis (CZE) allows the group separation of cationic aminocompounds from both neutral and anionic phenolic compounds present in SPE extracts, based on different migration times [3–5]. The same extract can be used to perform the two different analyses without changing the sample preparation steps dramatically.

2. Experimental

2.1. Instrumentation

A CES-1 capillary electrophoresis system equipped with a variable-wavelength spectrometric detector (Dionex, Sunnyvale, CA, USA) operating at 280 nm was used. Data manipulation and the operation of all components in the system were controlled by AI-450 chromatographic software (Dionex) interfaced via an Advanced Computer Interface ACI-2 (Dionex) to a 80486-based computer (Compaq, Milan, Italy). Water samples were extracted using the same glass apparatus as described in a previous paper [2].

2.2. Reagents and standard

Phosphoric acid, sodium dihydrogenphosphate, anhydrous sodium carbonate, anhydrous sodium sulfate and, 1,3-diaminopropane were of analytical-reagent grade (Novachimica, Milan, Italy) and acetonitrile, acetone and methylene chloride were of HPLC grade (Carlo Erba, Milan, Italy).

Standard of all amines were free base reagent grade with the exception of benzidine hydrochloride (Novachimica, Milan, Italy).

All reagent solutions were prepared daily with ultra-pure deionized water (DI water), with conductivity <0.1 μS at 25°C, obtained using a Milli-Q system (Millipore, Milford, MA, USA). A standard solution of each amine (1 g/l) was prepared by dissolution in acetonitrile. Working standard solution of amine mixtures in the concentration range 0.5–100 mg/l were obtained by serial dilution of stock standard solutions with 150 m*M* H_3PO_4.

2.3. Groundwater samples

Water samples were adjusted to pH 6.5–8 and then filtered through a 0.45-μm filter. Before use, the SPE cartridge was activated with sequential application of 5 ml of acetone, 5 ml of acetonitrile and 5 ml of DI water. This cartridge was made by filling an empty commercial SPE cartridge with a 20:80 (w/w) mixture of underivatized and keto-derivatized poly(styrene–divinylbenzene) copolymer prepared as described previously paper [2,6], Applying nitrogen pressure to the sample reservoir, 1 L of water sample was then passed through the cartridge at a flow-rate of 5 ml/min.

The cartridge was then dried under nitrogen for 5 min and retained compounds were eluted with 2 ml of 150 m*M* H_3PO_4 in water–acetone (80:20). The eluate was concentrated under a flow of nitrogen, diluted to a final volume of 1 ml and then analysed by CZE.

2.4. Soil samples

A 50-g amount of homogeneous soil sample from the dye industry was mixed with 50 g of sodium sulfate–sodium carbonate (2:1), washed with methylene chloride and over dried at 250°C. The mixture was then extracted twice with 50 ml of methylene chloride. The organic extract was collected over anhydrous sodium sulfate in a flask and evaporated to 5 ml with a rotary vacuum evaporator. The solution was mixed with 2 ml of 150 m*M* H_3PO_4, shaken and, after phase separation, the aqueous layer was analysed by CZE.

2.5. CE analysis

Capillary electrophoresis was performed in 65 cm (ca. 60 cm from injection to detection) × 50

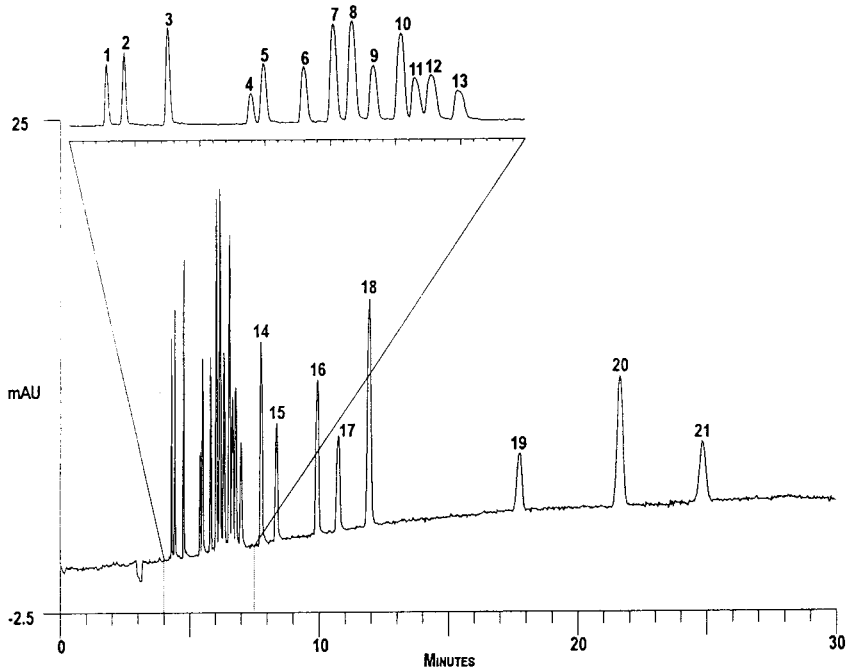

Fig. 1. Electropherogram for a standard solution of aromatic amines. Peaks: 1 = pyridine (35 mg/l); 2 = *p*-phenylenediamine (8 mg/l); 3 = benzidine (16 mg/l); 4 = *o*-toluidine (16 mg/l); 5 = aniline (8 mg/l); 6 = N,N-dimethylaniline (8 mg/l); 7 = *p*-anisidine (8 mg/l); 8 = *p*-chloroaniline (8 mg/l); 9 = *m*-chloroaniline (8 mg/l); 10 = ethylaniline (8 mg/l); 11 = α-naphthylamine (36 mg/l); 12 = diethylaniline (8 mg/l); 13 = N-(1-naphthyl)ethylenediamine (36 mg/l); 14 = 4-aminophenazone (16 mg/l); 15 = *o*-chloroaniline (16 mg/l); 16 = 3,4-dichloroaniline (16 mg/l); 17 = 3,3′-dichlorobenzidine (36 mg/l); 18 = 2-methyl-3-nitroaniline (16 mg/l); 19 = 2,4-dichloroaniline (36 mg/l); 20 = 2,3-dichloroaniline 16 mg/l); 21 = 2,5-dichloroaniline (36 mg/l). Buffer, 50 m*M* NaH_2PO_4–7 m*M* 1,3-diaminopropane (pH 2.35, adjusted with H_3PO_4); capillary, underivatized silica, 65 cm × 50 μm I.D.; applied potential, +30 kV; detection, UV at 280 nm.

μm I.D. fused-silica capillaries. The voltage was +30 kV (constant-voltage mode) and the capillary was cooled by an external forced air flow. Samples were injected by gravity raising the sample to 100 mm for 30 s. All experimental conditions were summarized in Table 1. 1,3-Diaminopropane as a surface modifier [7] was added to 50 m*M* phosphate buffer solution. pH 2.35 was chosen as the best compromise between analysis time and resolution, as shown in the

Table 1
Instrumental conditions used in the determination of aromatic amines by capillary zone electrophoresis

Capillary	Uncoated fused silica, 65 cm × 375 μm O.D. × 50 μm I.D.
Buffer	50 m*M* NaH_2PO_4–7 m*M* 1,3-diaminopropane, adjusted to pH 2.35 (H_2PO_4)
Rising cycle	Destination 6 s; capillary 120 s; source 6 s
Injection	Gravity at 100 mm for 30 s
Temperature control	Air cooling
Applied potential	+30 kV constant voltage
Current	ca. 55 μA
Wavelength	280 nm

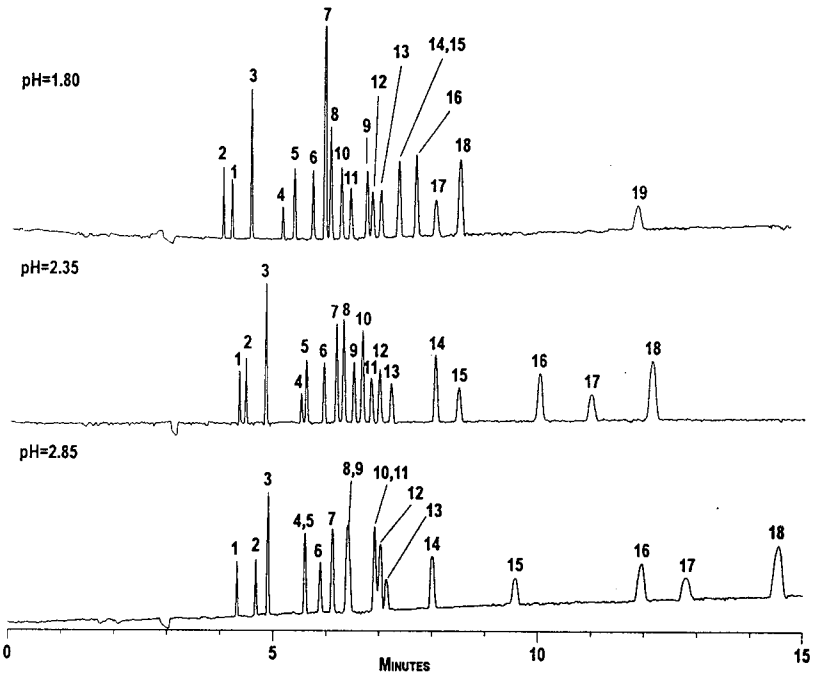

Fig. 2. Migration times of aromatic as a function of pH. Peaks as in Fig. 1. Buffer, 50 m*M* NaH_2PO_4–7 m*M* 1,3-diaminopropane with PH as shown; capillary, underivatized silica, 65 cm × 50 μm I.D.; applied potential, +30 kV; detection, UV at 280 nm.

electropherogram of an amine standard solution shown in Fig. 1. The influence of pH on the mobility of different amines is shown in the electropherograms in Fig. 2.

3. Results and discussion

3.1. Linearity, recovery and retention time stability

Linearity for all amines was verified by determining seven different concentrations of each amine in the range 0.5–100 mg/l. Regression coefficients and characteristics of the calibration plot were calculated. As shown in Table 2, good linearity for all amines was achieved over more than two orders of magnitude of concentration. The limits of detection ranged from 0.06 to 1.8 μg/ml; the limit of detection was calculated according IUPAC guidelines [8]. Recoveries were calculated from "CE clean" surface waters spiked with aromatic amine standards, and for the amines considered were better than 82% except for the most hydrophilic ones, the recovery of which ca. 60% under the same extraction conditions. In Table 3 are summarized the recoveries for representative amines.

In order to limit wall interactions and reduce retention time drift, a surface modifier such as 1,3-diaminopropane at a 7 m*M* concentration was added to the buffer.

3.2. Real samples

CZE was a valuable tool in the determination of cationic species in multi-component samples such as SPE extracts that we used in HPLC with amperometric detection for the determination of phenols. This analysis showed interfences due to aromatic amines, because of the sample origin, while GC–MS was complicated by a very large number of other compounds. Electropherograms b and c in Fig. 3 show a simplified "fingerprint" with few peaks certainly cationic and absorbance characteristics typical of aromatic substances.

Table 2
Parameters of calibration graphs and limits of detection for aromatic amines

Analyte	a	$b \cdot 10^6$	r^2	L.O.D.[a]
Pyridine	−1.679	0.505	0.989	0.65
p-Phenylenediamine	−0.373	0.134	0.997	0.12
Benzidine	−0.399	0.152	0.999	0.17
o-Toluidine	−0.359	0.199	0.998	0.44
Aniline	−0.308	9.801	0.997	0.12
N,N-Dimethylaniline	−0.244	9.507	0.998	0.12
p-Anisidine	−0.107	5.049	0.998	0.07
p-Chloroaniline	−0.145	4.638	0.999	0.06
m-Chloroaniline	−0.234	8.006	0.996	0.11
Ethylaniline	−0.146	4.912	0.999	0.07
α-Naphthylamine	−0.072	0.370	0.989	0.56
Diethylaniline	−0.084	8.003	0.998	0.11
N-(1-Naphthyl)ethylenediamine	−0.566	0.335	0.997	0.59
4-Aminophenazone	−0.477	8.542	0.999	0.18
o-Chloroaniline	−0.527	7.825	0.999	0.33
3,4-Dichloroaniline	−0.334	4.716	0.999	0.26
3,3′-Dichlorobenzidine	−1.331	0.136	0.992	1.5
2-Methyl-3-nitroaniline	−0.472	5.821	0.999	0.24
2,4-Dichloroaniline	0.145	6.275	0.992	1.8
2,3-Dichloroaniline	0.273	2.076	0.995	0.35
2,5-Dichloroaniline	1.627	6.612	0.975	1.6

Amount (mg/l) = $a + b \cdot$ response (area units).
[a] mg/l; L.O.D. calculated according IUPAC. Gravity injection at 100 mm for 30 s.

Identification of some of these peaks was achieved by spiking the sample with aromatic amines and cross-confirmation by GC–MS.

The sensitivity of the method is sufficient to give good accuracy in the determination of macro-contaminants, and further the intrinsic selectivity of the analytical approach helps to simplify the chromatograms. This kind of selectivity allows simpler sample preparation and purification and make this technique suitable for rapid control screening in situations that require evidence of contamination or accidents. On the other hand, the selectivity cannot compensate for the sensitivity, as can be seen in electropherogram a in Fig. 3, where there are no peaks, whereas the same sample analysed by GC–MS showed trace amounts of aromatic amines. As shown in Fig. 3c, for a soil sample, the suitability of the method for the analysis of samples extracted with a liquid–liquid extraction procedure was also verified.

The proposed method is simple and fast and its selectivity limits interferences from similar but differently charged compounds in complex matrices so that a complex procedure for sample preparation is not required. Conversely, it does not meet the sensitivity limits required by the

Table 3
Recovery of some representative aromatic amines from surface water samples by using SPE

Analyte	Recovery (%)[a]	R.S.A. (%)
Benzidine	47	6.0
Aniline	58	4.1
p-Anisidine	58	3.7
m-Chloroaniline	91	2.5
Diethylaniline	89	1.8
o-Chloroaniline	87	2.2
3,4-Dichloroaniline	87	1.4
3,3′-Dichlorobenzidine	82	2.4
2-Methyl-3-nitroaniline	97	1.1

[a] Surface water samples spiked with 20 μg/ml of amine; mean results ($n = 3$).

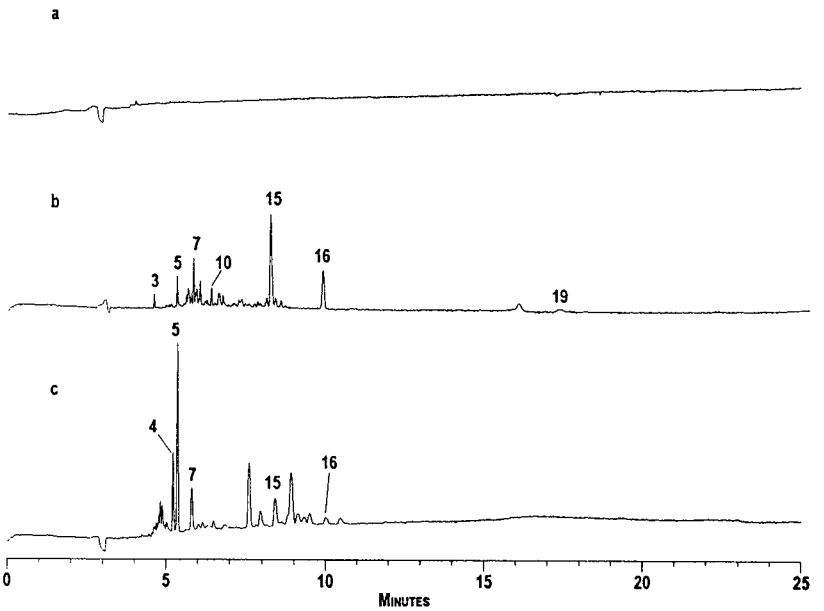

Fig. 3. Electropherograms of real samples after 1000-fold SPE preconcentration. (a) Tap water. (b) First layer groundwater. Peaks: 3 = benzidine (2.7 μg/l); 5 = aniline (1.8 μg/l); 7 = *p*-anisidine (1.5 μg/l); 10 = ethylaniline (0.5 μg/l); 15 = *o*-chloroaniline (9.9 μg/l); 16 = 3,4-dichloroaniline (2.9 μg/l); 19 = 2,4-dichloroaniline (1.1 μg/l). (c) Soil sample from industrial plant. Peaks: 4 = *o*-toluidine (600 μg/kg); 5 = aniline (801 μg/kg); 7 = *p*-anisidine (11.2 μg/kg); 15 = *o*-chloroaniline (15.2 μg/kg); 16 = 3,4-dichloroaniline (1.8 μg/kg). Sample preparation as described. Buffer, 50 m*M* NaH_2PO_4–7 m*M* 1,3-diaminopropane (pH 2.35, adjusted with H_3PO_4); capillary: underivatized silica, 65 cm × 50 μm I.D.; applied potential, +30 kV; detection, UV at 280 nm.

inherent toxicity and danger of the compounds concerned. This method could be useful in those situations of evident contamination or accidents, and when it is necessary to monitor rapidly a site of pollution in order to establish the borders of the contaminated areas.

Acknowledgement

The authors thank Mary Jo Wojtusik for valuable assistance with this project and for helpful discussions.

References

[1] B. Scholz and N. Palauschek, Fresenius' Z. Anal. Chim., 331 (1988) 282.
[2] V. Piangerelli, F. Nerini and S. Cavalli, Ann. Chim., 83 (1993) 331.
[3] J.W. Jorgenson and K.D. Lukacs, Anal. Chem., 53 (1981) 1298.
[4] J.W. Jorgenson and K.D. Lukacs, J. Chromatogr., 218 (1981) 209.
[5] J.W. Jorgenson and K.D. Lukacs, Science, 222 (1983) 266.
[6] J.J. Sun and J.S. Fritz, J. Chromatogr., 509 (1992) 197.
[7] D. Corradini, A. Rhomberg and C. Corradini, J. Chromatogr. A, 661 (1994) 305.
[8] G.L. Long and J.D. Winefordner, Anal. Chem., 55 (1983) 712A.

ELSEVIER

Journal of Chromatography A, 709 (1995) 367–374

JOURNAL OF CHROMATOGRAPHY A

Indirect fluorescence detection of free cyanide and related compounds by capillary electrophoresis

Vicente Martí[a], Manuel Aguilar[a], Edward S. Yeung[b,*]

[a] *Departament d'Enginyeria Química (E.T.S.E.I.B.), Universitat Politècnica de Catalunya, Av/Diagonal 647, Barcelona 08028, Spain*

[b] *Ames Laboratory-USDOE and Department of Chemistry, Iowa State University, Ames, IA 50011, USA*

First received 22 December 1994; revised manuscript received 22 March 1995; accepted 7 April 1995

Abstract

A capillary electrophoretic method to detect CN^- and some related compounds (CNO^-, SCN^-, and NO_3^-) using a prototype laser-based indirect fluorescence detector has been developed. This method avoids interferences from Cl^-, SO_4^{2-}, CO_3^{2-}, HCO_3^-, and ClO^- and allows the detection of CN^- in less than 4 min and the detection of related compounds in less than 8 min with precise migration times (R.S.D. about 1%). The measured detection limits of CN^- [5×10^{-6} *M* with DR = 90 (dynamic reserve)] are close to the expected theoretical value [$TR_{CN} = 0.44$ (transfer ratio)]. For the related compounds, the measured detection limits ranged from 10^{-5} to 2×10^{-6} *M*, depending on noise conditions (DR $\geq$ 300). The results showed that the chosen analytical conditions were appropriate and the detection limits could be improved using techniques to further decrease the noise (probably due to mechanical vibrations). Peak-height precision was about 10% R.S.D. and log–log regressions had slopes lower than one. These results seem to be due to instabilities in the indirect signal. The analysis of a quasi-real sample has been achieved, allowing identification of the related compounds present in a CN^-/SCN^- sample oxidized with ClO^- and determination of the CNO^- formed in this alkaline oxidation.

1. Introduction

Free cyanide (CN^- and HCN) is a very toxic contaminant with biocide effects that have to be controlled before reaching the environment. The presence of cyanide in natural waters is mainly due to the uncontrolled discharge of treated wastes from certain industrial processes (electroplating, ore cyanidation). The most extensive treatments of industrial water to eliminate CN^- are based on the alkaline oxidation with ClO^- to produce non-toxic CNO^- and, in a further oxidation step, HCO_3^- and N_2 [1,2], as well as UV oxidation [3,4], which yields the species CNO^-, NO_3^-, CO_3^{2-}, and HCO_3^-. The species SCN^- could be also present in some cyanide processes [5] or could be formed by the reaction with HS^- [6].

The classical procedures to determine total cyanide in liquid samples consist of acid distillation, collection of the released HCN(gas phase) on NaOH [7,8], and the determination of CN^- by colorimetric (LOD 0.5–20 ppb), electrochemical (LOD 3–50 ppb), or titrimetic methods (LOD 100–1000 ppb) [9–11]. When some metal–cyanide complexes and other species such as

* Corresponding author.

0021-9673/95/$09.50
SSDI 0021-9673(95)00446-7

NO_3^-, CO_3^{2-}, and HCO_3^- are present as interference, the distillation procedure will require sample pretreatment. The cited method can detect neither free cyanide (CN^- and HCN) nor CNO^- and SCN^- in the initial sample and is time-consuming. This prompts the development of new analytical methods for determining individually the amounts of free cyanide and cyanide-related species. These should be fast enough in total analysis time and should be able to detect total cyanide in concentrations lower than that required by law (normally from 10 to 50 ppb) to facilitate monitoring of cyanide in processes and in the environment.

There are several instrumental methods to analyze free cyanide and cyanide species. Atomic absorption spectroscopy (AAS)-based methods could only analyze metal–cyanide complexes with very good detection limits (0.2 to 2 ppb of cyanide) but with long analysis time [12]. GC methods could only analyze derivatized free cyanide also with very good LOD (0.3 to 100 ppb) [9–11]. HPLC-based methods show acceptable analysis time and selectivity. Several modalities and detection methods allow the detection of 20–500 ppb of metal–cyanide complexes [13] and 10–50 ppb of free [14] or derivatized cyanide [15]. As an alternative approach, capillary electrophoresis (CE) methods open the possibility of shorter analysis time, good resolution of sample components, and reasonable detection limits. Several metal–cyanide complexes have been separated in less than 5 min by using CE [16,17]

As CN^- and CNO^- do not absorb in the UV–Vis region [18,19], indirect detection methods have been used. Indirect detection techniques are based on the quantitation of the decrease of the signal due to the displacement of the chromophore ions by the sample ions. This method is used in LC and CE in combination with several detectors (refractive index, conductivity, polarimetry, absorption, and fluorescence) [20]. In the case of CE, indirect fluorescence is one of the most sensitive indirect detection methods and has been widely used for the detection of organic and inorganic anions [21,22]. For these reasons, a study on the determination of CN^- and some related compounds (CNO^-, SCN^-, and NO_3^-) by CZE using a laser-based indirect fluorescence detector will be discussed.

In this technique, the detection limits are directly proportional to the concentration of fluorophore and inversely proportional to the dynamic reserve (DR) and transfer ratio (TR) [21]. TR-values increase when the mobility of the analyte is close to the mobility of the fluorophore to a maximum value given by the ratio between analyte charge and fluorophore charge. Low concentrations of other co-ions (e.g. OH^-) improve the TR. The DR improves with absorption coefficient, quantum yield, and a stable excitation intensity. Increasing the fluorophore concentration and the optical power of the laser increases the signal, but noise is also increased, so it is necessary to operate at low concentrations and low optical power to obtain good DR-values [23].

2. Experimental

2.1. Instrumentation

In both detection modes that were used (indirect absorption and fluorescence) a bare fused-silica, 75 μm I.D., 360 μm O.D., capillary column (Polymicro Technologies, Phoenix, AZ, USA) was used. The total lengths used were 70 and 73 cm and the detection lengths were 44 and 38 cm for the case of indirect absorption detection and indirect fluorescence detection, respectively.

To operate in the absorption detection mode, the column was connected to a commercial electrophoresis instrument (ISCO, Model 3140; Lincoln, NE, USA). Data were collected using commercial software on an IBM-compatible 286 computer.

Fluorescence detection was achieved by replacing the absorption detector by a prototype fluorescence detector as shown in Fig. 1. The excitation source consisted of a 488-nm beam from an argon ion laser (1) (Model 2211-10SL; Cyonics, Uniphase, San Jose, CA, USA) that

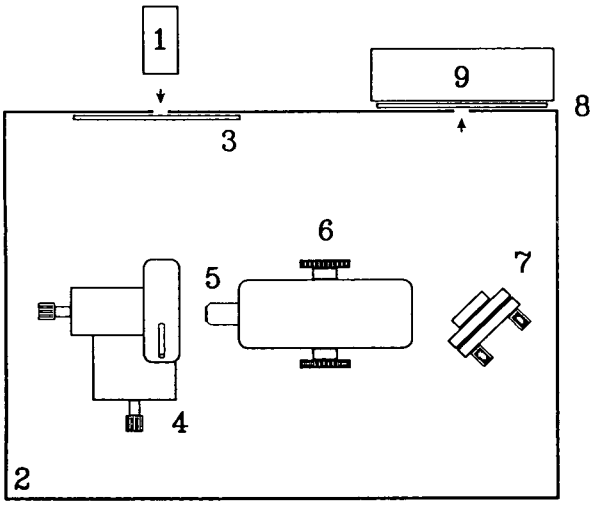

Fig. 1. Laser fluorescence detector setup. The different parts of the setup are explained in the text.

entered to a plexiglass box (2) through a 488-nm interference filter (3). The unfocused laser beam was directed perpendicularly to the capillary window. The capillary was connected to the commercial instrument by using a capillary holder (4). The fluorescence was collected by a 10 × microscope objective (5) placed in an objective holder (6) (Edmund Scientific, Barrington, NJ, USA) and was sent to a silicon photodetector (9) (HC 220-01; Hamamatsu, Bridgewater, NJ, USA) through a 500-nm long-pass cutoff filter (8) using a kinematic mirror mount (7) (Melles Griot, Irvine, CA, USA). Data were collected using an integrator (Datajet, Spectra-Physics, San Jose, CA, USA).

2.2. Operating conditions

The buffer solutions were filtered using a 0.2-μm membrane filter (Alltech, Deerfield, IL, USA) and were degassed for 15 min under vacuum with ultrasonication. After that, the buffer was stabilized at the running voltage for 4–5 h. Because the use of voltages above 25 kV requires increasing the stabilization time, equal or lower applied potentials were used. In all cases, a minimum optical power of 4 to 5 mW was used to avoid dark noise. The sample was introduced in the system by using vacuum injection.

2.3. Chemicals

Fluorescein disodium salt, 2-hydrate ($C_{20}H_{10}Na_2O_5 \cdot 2H_2O$, $M_r = 412.3$) was purchased from Eastman Kodak (Rochester, NY, USA). Sodium cyanate and sodium hypochlorite were obtained from Jansen Chimica (Gardena, CA, USA). The other cited chemicals were purchased from Fisher Scientific (Fair Lawn, NJ, USA).

2.4. Solutions and reagents

The main problem with free-cyanide samples is that hydrogen cyanide has a pK_a of about 9.2, so the pH has to be kept above this value to have more than 50% of free cyanide as CN^-. Another problem is that CNO^- is an expected species when starting from CN^- in aqueous medium, so the oxidizing properties of the sample matrix and buffer have to be taken into account [24]. Fluorescein solutions between 100 and 2000 μM adjusted to pH between 9.3 and more than 11 with NaOH or KOH were tested. Solutions below 100 μM were avoided because they would probably compromise the buffering capacity. The sodium cyanide standards were prepared every 2 or 3 days in concentrations from 1 to 10 g/l and were stored in the dark. Solutions above 10 ppm of NaCN were prepared each day and solutions lower than that concentration were prepared just before the analysis. Other solutions were prepared also every 2 or 3 days.

3. Results and discussion

3.1. Initial tests

Before using the prototype fluorescence detector, indirect absorption detection of CN^- at 238 nm using fluorescein was performed in order to check the chosen samples and the CE instrument. The best results are shown in Fig. 2(A), where a 1 mM fluorescein solution (pH 11) was

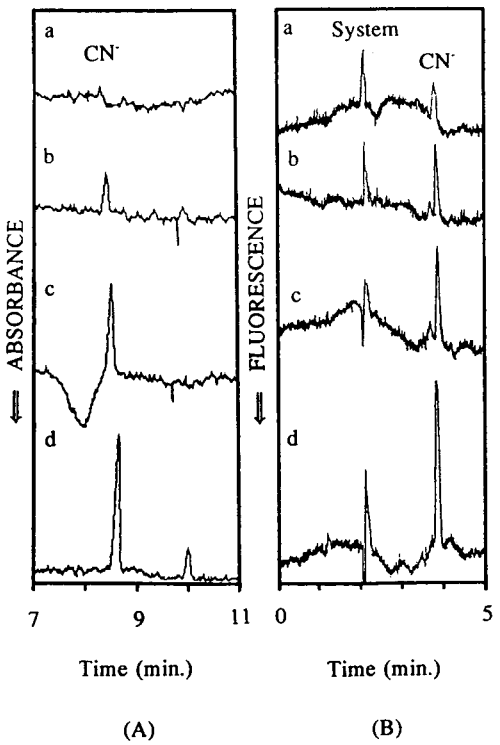

Fig. 2. Comparison of the indirect detection of CN^-: (a) 10^{-5} *M*; (b) 4×10^{-5} *M*; (c) 10^{-4} *M*; and (d) 2×10^{-4} *M*. (A) Absorption at 238 nm (1 m*M* fluorescein at pH 11, 5 kPa·s and 20 kV); (B) fluorescence at 4 mW (0.1 m*M* fluorescein at pH 10, 25 kPa·s and 25 kV).

used. It can be seen that detection limits were around 1 ppm of NaCN (2×10^{-5} *M*) and the analysis time was about 9 min.

One important factor to enhance indirect fluorescence detection is to apply high voltages and to operate with high net mobilities for the fluorophore to reduce bleaching. One can thus increase the background signal and reduce analysis time. The high pH-values and voltage used in these experiments produced these two effects [23]. Fluorescein samples were thus studied using direct fluorescence detection in order to evaluate system linearity and the extent of bleaching. The chosen optical power was 22 mW and the injection time and pressure was set to 5 kPa·s. Beyond this setting the peak height did not increase perceptibly, indicating the elimination of bleaching. LOD was around 2×10^{-10} *M* and the plot of the logarithm of peak height versus the logarithm of concentration (13 measurements) was linear ($r > 0.998$) in the range 2×10^{-10} to 10^{-6} *M* with a slope of 1.07 ± 0.01.

3.2. Indirect fluorescence detection of CN^-

After the above tests, solutions with lower concentrations of fluorescein and with different pH were tested in order to optimize the LOD of CN^-. The buffer solution had to be changed to 0.25 m*M* fluorescein and pH 9.6 to achieve an LOD similar to that for indirect absorption detection. By decreasing the concentration to 100 μM of fluorescein and pH 9.3 similar results were obtained, but the peaks were deformed. This is consistent with the fact that the chosen pH was close to the pK_a such that the sample was a mixture of CN^- and HCN with decreased TR.

After these observations, it was decided to increase the pH to see if there was some interference in the sample displacement by the fluorophore. The best results obtained for the detection of CN^- are shown in Fig. 2(B), where a 10^{-4} *M* fluorescein solution at pH 10 (KOH) was used. In this figure, it can be seen that the CN^- peak shape is satisfactory. To the degree that we can optimize each detection mode, the LOD was better for indirect fluorescence compared to indirect absorption, and the analysis time was shorter.

Table 1 shows some analytical results for CN^- and related compounds. The detection limits of all the anions studied were calculated from the peak height that is two times the peak-to-peak noise width of the same electropherogram [25]. In the case of CN^- the detection limit corresponds to 130 ppb. The dynamic reserve (DR) was calculated from the noise width and the measurement of the background signal obtained after blocking the laser beam and adjusting the output to zero. Depending on conditions, DR-values were between 75 and 300 for 100 μM fluorescein solutions. Operating under similar analytical conditions, the main factors affecting the noise were found to be mechanical vibration of the optics (movements in the order of 75 μm)

Table 1
Detection performance for various anions

	CN^-	CNO^-	SCN^-	NO_3^-
Migration time (min ± %R.S.D.)	3.7 ± 1.4[a]	5.7 ± 1.1	6.3 ± 0.9	7.9 ± 1.0
LOD (M)	5×10^{-6}	2×10^{-6}–9×10^{-6}	2×10^{-6}–10^{-5}	2×10^{-6}–10^{-5}
DR	90	⩾300	⩾300	⩾300
TR	0.44	0.07	0.05	0.05

[a] For CN^- $n = 6$, and for the other anions $n = 10$.

and the stabilization time of the solution in the column. This means that the experimental detection limits could be reduced if we were able to reduce the noise and further increase the DR.

Knowing C_{lim} (calculated as 0.5 times the LOD), DR-values, and fluorophore concentration, one can calculate the value of TR near the LOD. For monovalent anions, the maximum value of TR would be 0.5 because fluorescein at alkaline pH has two negative charges. The observed value of TR for CN^- is very close to the theoretical value. This means that the buffer was correctly optimized. Since sample displacement is charge based, one would reduce TR when the concentration of OH^- is similar to or larger than that of the chromophore. However, TR increases when the electrophoretic mobility of the analyte is similar to that of the chromophore. The mobility of OH^- is very high compared to that of the chromophore, so it is not possible to match the mobilities. Therefore low concentrations of the chromophore at a reasonably high pH were used as a compromise [26].

The LODs achieved are good, although marginal compared to the limit required by law and close to the theoretically expected values. The precision of the CN^- peak height was low, even when the samples were prepared just before the analysis. The linear regression of the logarithm of the concentration on the logarithm of the peak height from 10^{-5} to 2×10^{-3} M showed a slope that was different from one. Since for the direct detection of fluorescein with the same setup the slope was one, this deviation has to be due to the indirect technique that was used and not due to the instrument. Actually, TR-values are dependent on the concentrations of the sample and OH^-. Therefore this deviation in the slope could be expected.

3.3. Indirect fluorescence detection of related compounds

In this work, the detection of some anions related to CN^- (CNO^-, SCN^-, NO_3^-) and possible interfering anions (Cl^-, SO_4^{2-}, and CO_3^{2-}/HCO_3^-) were studied. Mixtures of these anions were analyzed using buffer solutions with fluorescein concentrations and pH in a similar range as used for CN^- detection. The separation of CNO^-, SCN^-, and NO_3^- from Cl^- and SO_4^{2-} was achieved, as shown in Fig. 3. In this electropherogram Cl^- and SO_4^{2-} were not resolved. This is, however, not important because it is only important to know if these two anions would interfere in the positions of the anions related to CN^-. In order to know the extent of the interference of these two anions, concentrations of Cl^- and SO_4^{2-} eleven times higher than that used in Fig. 3 (28 ppm Cl^- and 210 ppm SO_4^{2-}), which correspond to concentrations higher than those present in natural waters, were tested. The results showed that detection of CNO^- and SCN^- was possible even under these conditions.

Compared with other references [27,28], the relative elution order of the anions studied is the same, except for Cl^- and SO_4^{2-}. The CO_3^{2-}/HCO_3^- peak was not detected with the positive applied voltage because of their mobilities. All peaks showed tailing which would indicate that the anions have mobilities higher than those of

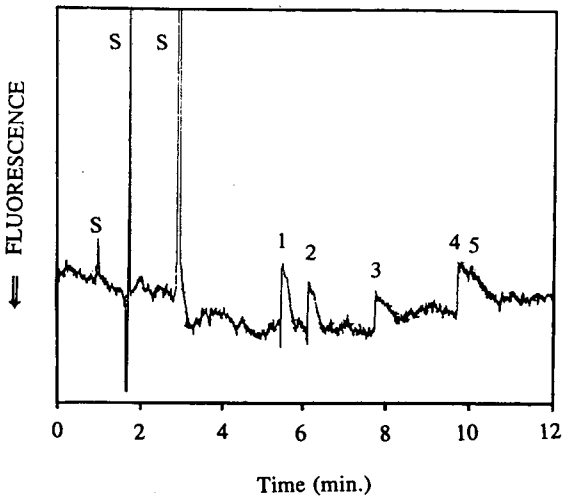

Fig. 3. Electropherogram of the indirect fluorescence analysis at 5 mW [0.1 m*M* fluorescein at pH 10 (KOH), 25 kPa · s and 25 kV]. Peaks: 1 = CNO^- 4.6×10^{-5} *M*; 2 = SCN^- 3.9×10^{-5} *M*; 3 = NO_3^- 3.4×10^{-5} *M*; 4 = Cl^- 7.2×10^{-5} *M*; 5 = SO_4^{2-} 2.0×10^{-4} *M*; and S = system peaks.

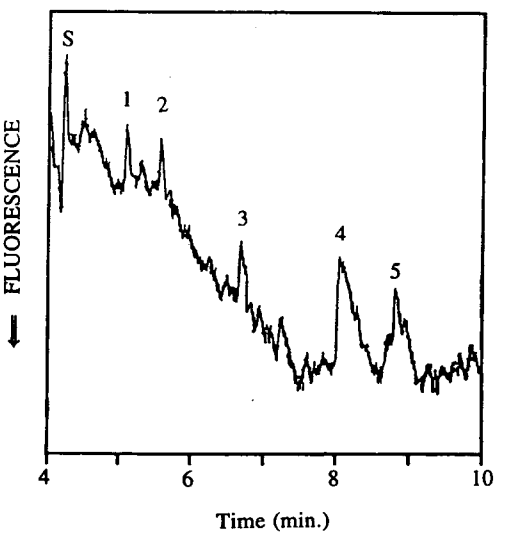

Fig. 4. Electropherogram of the analysis of anions near their LOD under favorable noise conditions [indirect fluorescence at 5 mW, 0.1 m*M* fluorescein at pH 10 (KOH), 25 kPa · s and 25 kV]. Peaks: 1 = CNO^- 2.7×10^{-6} *M*; 2 = SCN^- 2.3×10^{-6} *M*; 3 = NO_3^- 2.0×10^{-5} *M*; 4 = Cl^- 4.3×10^{-6} *M*; 5 = SO_4^{2-} 1.2×10^{-5} *M*; and S = system peaks.

the buffer anions [29]. This tailing is probably due to the relatively high concentration of OH^-.

Table 1 also shows the analytical parameters of CNO^-, SCN^-, and NO_3^-. It can be seen that one of the advantages of this method is that it is possible to analyze all anions of interest in less than 8 min, with good precision in the migration times. Once the fluorophore concentration and pH were chosen, the control of mechanical vibrations and stabilization of the buffer in the column became the limiting factors. By controlling the attachment of the detector to the instrument, the base leveling, vibration deadening, and by using a column stabilization time of 40 h, the results obtained were improved, as shown in Fig. 4, where it can be seen that Cl^- and SO_4^{2-} were clearly separated at low concentrations. The detection limits calculated from this figure are the lower values shown in Table 1. This low noise level lasted for several hours but it was not always possible to reproduce it. So, normal values for the detection limits with a good attachment of the detector and a stabilization time of 4 to 5 h were included in Table 1 as the higher values. Under these conditions DR values of 300 were obtained. Comparing the TR results between anions (including CN^-) in Table 1, it can be seen that they are consistent with the fact that TR increases when the mobility of the anion is closer to the mobility of the fluorophore. The calibration curves of the three anions of interest were plotted from concentrations close to the higher LOD to about 10^{-4} *M* of each anion. The precision of the peak heights and the linearity are similar to those for CN^-. Baseline fluctuations prevented us from evaluating the linearity of the response based on peak areas.

3.4. Study of the alkaline oxidation of CN^- and SCN^-

In order to assess if the analytical method is suitable for the study of the alkaline oxidation of cyanide with ClO^-, a sample of 100 ml consisting of 1.1×10^{-2} *M* of NaCN and 5.5×10^{-3} *M* of KSCN at pH 10 was oxidized using ClO^-. The oxidation method was based on standard assays [7,8] in which the same ClO^- molar concentration (24.8 g active chlorine/l) and the same oxidant-to-sample ratio were used. The sample

to be oxidized was placed in a dark kitasatos to avoid transformation due to sunlight. Through the top part of the kitasatos a pH electrode was inserted through a rubber stopper in order to monitor the alkalinity of the sample. The lateral part of the kitasatos was used to introduce solutions with the help of teflon tubes connected to plastic syringes. The oxidation consisted of the stepwise introduction of ClO^- solution (5 ml each 15 min) for one hour in the stirred sample, adding the necessary volume of 1 *M* NaOH to keep the pH between 10 and 11. Once this operation was completed, the solution was placed in a volumetric flask and made up to 200 ml by adding NaOH pH 10. In order to analyze the oxidized sample, 100 μl of this solution was diluted to 5 ml with the running buffer.

The electropherogram of this diluted sample is shown in Fig. 5. In this figure we can identify ClO^-, CNO^-, and system peaks by their migration times. The CNO^- anion was also identified by the addition of standard and was found not to be interfered with by ClO^- and other by-products. By using this method, the concentration of CNO^- was found to be between 1 and 2×10^{-4} *M* in the oxidized sample, but it was not possible to independently determine if all the CNO^- came from the CN^- plus SCN^- oxidation or only from CN^-.

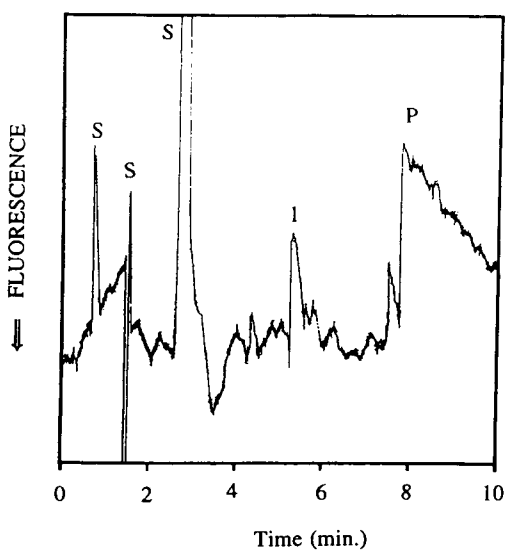

Fig. 5. Electropherogram of an oxidized sample of CN^- and SCN^- (see text) diluted 1/100. Indirect fluorescence detection at 5 mW, 0.1 m*M* fluorescein pH 10 (KOH), 25 kPa · s and 25 kV. Peaks: 1 = CNO^-; S = system peaks; and P = by-products (ClO^-, Cl^-).

Acknowledgements

The Ames Laboratory is operated for the U.S. Department of Energy by Iowa State University under Contract No. W-7405-Eng-82. This work was supported by the Director of Energy Research, Office of Basic Energy Sciences, Division of Chemical Sciences. Dr. A. Farran is also acknowledged for her valuable help. This work was also supported financially by Universitat Politècnica de Catalunya and Olivetti under the program "Ajuts de Curta Estada a l'Estranger" and by a scholarship from Comisionat per a Universitats i Recerca (Generalitat de Catalunya).

References

[1] D.J. Wedl and R.J. Fulk, Metal Finishing, 89 (1991) 33–37.
[2] C.M. Gerritsen and D.W. Margerum, Inorg. Chem., 29 (1990) 2757–2762.
[3] C.H. Pollema, J.L. Hendrix et al., J. Photochem. Photobiol., 66 (1992) 235–244.
[4] X. Domenech and J. Peral, Sol. Energy, 41 (1988) 55–59.
[5] J.C. Yannopoulos, The Extractive Metallurgy of Gold, Van Nostrand Reinhold, NY, 1991, p. 154.
[6] J. Marsden and I. House, The Chemistry of Gold Extraction, Ellis Horwood, NY, 1992, p. 491.
[7] APHA, AWWA and WEF, Standard Methods for the Examination of Water and Wastewater, APHA, AWWA and WEF, Washington, DC, 18th ed., 1992, pp. 4-18–4-35.
[8] ASTM, Annual book of ASTM standards, Vol. 11.02, ASTM, Washington, DC, 1991, pp. 90–129.
[9] P. McCarthy and R.W. Klusman, Anal. Chem., 65 (1993) 244R–292R.
[10] P. McCarthy, R.W. Klusman, S.W. Cowling and J.A. Rice, Anal. Chem., 63 (1991) 301R–342R.
[11] P. McCarthy, R.W. Klusman and J.A. Rice, Anal. Chem., 61 (1989) 269R–304R.
[12] J.J. Rosentreter and R.K. Skogerboe, Anal. Chem., 63 (1991) 682–688.

[13] C. Pohlandt and M.J. Hemmings, S. Afr. J. Chem., 41 (1988) 136–140.
[14] C. Pohlandt, S. Afr. J. Chem., 37 (1984) 133–137.
[15] P. Sillinger, Plating and Surface Finishing, 72 (1985) 82–85.
[16] M. Aguilar, A. Farran and M. Martínez, J. Chromatogr., 635 (1993) 127–131.
[17] M. Aguilar, X. Huang and R.N. Zare, J. Chromatogr., 480 (1989) 427–431.
[18] J. Brigando, Bull. Soc. Chim. Fr., 24 (1957) 503–516.
[19] R.P. Buck, S. Singhadeja and L.B. Rogers, Anal. Chem., 26 (1954) 1240–1242.
[20] E.S. Yeung, Acc. Chem. Res., 22 (1989) 125–130.
[21] Q. Xue and E.S. Yeung, J. Chromatogr. A, 661 (1994) 287–295.
[22] E.S. Yeung and W.G. Kuhr, Anal. Chem., 63 (1991) 275A–282A.
[23] W.G. Kuhr and E.S. Yeung, Anal. Chem., 60 (1988) 2642–2646.
[24] A.G. Sharpe, The Chemistry of Cyano Complexes of the Transition Metals, Academic Press, London, 1976, p. 3.
[25] C.F. Poole and S.A. Schuette, Contemporary Practice of Chromatography, Elsevier, Amsterdam, 1984, pp. 387–388.
[26] T.W. Garner and E.S. Yeung, J. Chromatogr., 515 (1990) 639–644.
[27] W.R. Jones and P. Jandik, J. Chromatogr., 608 (1992) 385–393.
[28] P. Jandik and G. Bonn, Capillary Electrophoresis of Small Molecules and Ions, VCH, New York, 1993, p. 261.
[29] F.P.E. Mikkers, F.M. Everaerts and Th.P.E.M. Verheggen, J. Chromatogr., 169 (1979) 1–10.

ELSEVIER

Journal of Chromatography A, 709 (1995) 375–380

JOURNAL OF CHROMATOGRAPHY A

Short communication

Highly sensitive high-performance liquid chromatographic method to discriminate enantiomeric monoacylglycerols based on fluorescent chiral derivatization with (*S*)-(+)-2-*tert*.-butyl-2-methyl-1,3-benzodioxole-4-carboxylic acid

Jeong-Hwan Kim, Yoshihiro Nishida, Hiroshi Ohrui, Hiroshi Meguro*

Department of Applied Biological Chemistry, Faculty of Agriculture, Tohoku University, 1-1 Tsutsumidori-Amamiyamachi, Aoba-ku, Sendai 981, Japan

First received 17 January 1995; revised manuscript received 11 April 1995; accepted 11 April 1995

Abstract

As an extension of previous methods for enantiomer analyses of diacylglycerols, a highly sensitive HPLC method was developed for the determination of the absolute configuration and optical purity of monoacylglycerols. Chiral derivatization by a fluorescent (*S*)-TBMB carboxylic acid followed by a normal-phase HPLC separation of the derived diastereomeric di-(*S*)-TBMB-carbonyl-*sn*-1- and -*sn*-3-monoacylglycerols provided useful tools to determine the chirality of a series of saturated and unsaturated monoacylglycerols ($C_{12:0}$–$C_{18:0}$, $C_{18:1}$, $C_{18:2}$ and $C_{18:3}$) [(*S*)-TBMB = (*S*)-(+)-2-*tert*.-butyl-2-methyl-1,3-benzodioxole]. In addition, the HPLC elution times of each diastereomeric isomer were correlated with the chain length (carbon number) and the double bond numbers of acyl groups.

1. Introduction

The development of a simple method to determine the enantiomeric distribution of monoacylglycerols (*sn*-1 and *sn*-3) will contribute to stereochemical studies of fatty acids, e.g., to study the stereoselectivity of lipase reactions or the biological functions of naturally occurring monoacylglycerols. Thomas et al. [1] developed a simple method to separate *sn*-1- and *sn*-3-monoacylglycerols from the *sn*-2-isomer by TLC on silica gel impregnated with boric acid. Other methods have been proposed for separating the homologous monoacylglycerols by reversed-phase HPLC without derivatization [2–4], but the enantiomeric separation of monoacylglycerols could not be achieved. Recently, Takagi and co-workers [5,6] reported the first successful separation of the enantiomeric monoacylglycerols using a chiral HPLC column coupled with di-3,5-dinitrophenylurethane derivatization.

Previously, we have reported highly sensitive methods for determining the optical purity and absolute configuration of diacylglycerols base on the fluorescent derivatization with (*S*)-(+)-2-*tert*.-butyl-2-methyl-1,3-benzodioxole [(*S*)-TBMB] carboxylic acid followed by HPLC separation of the derived diastereoisomers [7,8]. In this work, we extended this approach to mono-

* Corresponding author.

0021-9673/95/$09.50
SSDI 0021-9673(95)00460-2

acylglycerols and propose a simple and highly sensitive HPLC method for separating the enantiomers. Various normal-phase silica gel HPLC modes were tested for the diastereomeric separation of a series of monoacylglycerols ($C_{12:0}$–$C_{18:0}$, $C_{18:1}$, $C_{18:2}$ and $C_{18:3}$), and this paper describes the HPLC results, which allowed complete separation between the *sn*-1- and *sn*-3-isomers and also the *sn*-2-isomer within 80 min.

2. Experimental

2.1. Chemicals

Racemic monoacylglycerols with $C_{12:0}$–$C_{18:0}$, $C_{18:1}$, $C_{18:2}$ and $C_{18:3}$ acyl groups were purchased from Sigma (St. Louis, MO, USA). Optically active 3-monopalmitoyl-*sn*-glycerol and 2-monopalmitoylglycerol were also obtained from Sigma. (*S*)-(+)-2,2-Dimethyl-1,3-dioxolane-4-methanol was obtained from Tokyo Kasei (Tokyo, Japan) for the preparation of homologous diastereomeric 1,2-di-O-(*S*)-TBMB-carbonyl-3-O-acyl-*sn*-glycerol derivatives ($C_{12:0}$, $C_{14:0}$, $C_{18:0}$, $C_{18:1}$, $C_{18:2}$ and $C_{18:3}$). (*S*)-TBMB-COOH (100% e.e.) was synthesized according to the previously described method [9].

2.2. Di-(S)-TBMB derivatization of monoacylglycerols

Monoacylglycerols were derivatized with (*S*)-TBMB carbonyl chloride [8] as follows. A dry pyridine solution [0.2 ml containing 10% of 4-dimethylaminopyridine (DMAP)] of (*S*)-TBMB-COCl (20 mg, 0.08 m*M*) was added to a solution of 1-monopalmitoyl-*rac*-glycerol (7.0 mg, 0.02 m*M*) in dry CH_2Cl_2 (2 ml) with stirring at room temperature. After 2 h, the reaction mixture was diluted with CH_2Cl_2 (10 ml) and washed with saturated $NaHCO_3$ solution (3×10 ml) and water (20 ml). The methylene chloride solution was dried over $MgSO_4$, the latter was removed by filteration and the solvent was evaporated in vacuo at 40°C to afford 1,2-di-O-(*S*)-TBMB-carbonyl-3-O-palmitoyl-*rac*-glycerol, which was purified by preparative TLC [*n*-hexane–ethyl acetate (10:1, v/v)] (13 mg, yield 81%).

Di-(*S*)-TBMB-carbonyl derivatizations of 3- and 2-monopalmitoyl-*sn*-glycerols and other commercially available racemic monoacylglycerols ($C_{12:0}$, $C_{14:0}$, $C_{18:0}$, $C_{18:1}$, $C_{18:2}$ and $C_{18:3}$) were conducted in the same manners.

Optically active other homologous diastereomeric 1,2-di-O-(*S*)-TBMB-carbonyl-3-O-acyl-*sn*-glycerols ($C_{12:0}$, $C_{14:0}$, $C_{18:0}$, $C_{18:1}$, $C_{18:2}$ and $C_{18:3}$) were prepared via five steps (benzylation, deisopropylidenation, di-(*S*)-TBMB carbonylation, catalytic debenzylation and acylation using the corresponding acyl chloride) from an optically active (*S*)-(+)-2,2-dimethyl-1,3-dioxolane-4-methanol in a similar manner to that described in a previous paper [8] for the preparation of the 3-O-(*S*)-TBMB-carbonyl-1,2-di-O-acyl-*sn*-glycerol derivatives.

2.3. HPLC separations

Prior to the HPLC injection, the reaction mixture of di-(*S*)-TBMB-carbonyl-monoacylglycerol derivatives was preliminarily purified on silica gel TLC sheet [*n*-hexane–ethyl acetate (10:1, v/v)]. The TLC band of the derivatives was cut off from the TLC sheet and extracted with the HPLC solvents.

HPLC separations were conducted with a Jasco (Tokyo, Japan) Model 880-PU instrument connected to a Tosoh Model FS-8010 fluorescent detector with excitation at 310 nm and emission at 370 nm. Separations were performed on a Develosil 60-3 (Nomura Chemical) silica gel column (stainless steel, 50 cm × 4.6 mm I.D.). The analyses were carried out isocratically using HPLC-grade *n*-hexane–*tert.*-butyl alcohol (250:1, w/w; flow-rate 0.6 ml/min) as the mobile phase at ambient temperature. For quantitative determination, peak areas were calculated with a Model 807-IT integrator (Jasco).

3. Results and discussion

(*S*)-TBMB-COOH used in this study is optically pure to determine directly the optical

purities of monoacylglycerols as their diasteromeric di-(*S*)-TBMB-carbonyl derivatives. Di-(*S*)-TBMB-carbonyl derivatization of monoacylglycerols was performed in more than 80% yield using more than a four-fold excess of (*S*)-TBMB-COCl according to the optimized reaction conditions detailed under Experimental (Fig. 1). The same derivatization procedure as described under Experimental could be applied for analytical purposes to a sub-μg level of monoacylglycerols. In this case, the reaction mixture was directly spotted on the TLC sheet and developed with *n*-hexane–ethyl acetate (10:1, v/v). The fluorescent spots ($R_F = 0.30$–0.35) corresponding to di-(*S*)-TBMB-carbonylated monoacylglycerols were cut off from the TLC sheet and extracted with the HPLC solvents (*n*-hexane–*tert.*-butyl alcohol) for direct HPLC injection. This simple and convenient work-up procedure prior to the HPLC analysis was also employed in our previous study for the determination of diacylglycerols [8]. This procedure, taking a few minutes using a ready-made aluminium TLC sheet (5 cm × 5 cm), is recommended for eliminating pyridine and DMAP and their salts, which are unfavourable towards the silica column.

In contrast to the case of diacylglycerols in our previous study [8], the separation of enantiomeric monoacylglycerols as the (*S*)-TBMB-carbonyl derivatives could not be achieved straightforwardly. Various investigations of the HPLC conditions led us finally to use a longer silica gel column (Develosil 60-3, 50 cm) and *n*-hexane-*tert.*-butyl alcohol (250:1, w/w) as the mobile phase. Under these conditions, the separation of enantiomeric monoacylglycerols was accomplished in 80 min with a resolution factor (R_s) above 1.50.

Fig. 2 shows typical HPLC profiles of monoacylglycerols as the fluorescent diastereomeric di-(*S*)-TBMB-carbonyl derivatives. The *sn*-2-monoacylglycerol isomer could also be completely separated both from the monoacyl *sn*-1- and *sn*-3-isomers. The HPLC studies using chiral monoacylglycerols with known configurations indicated that the *sn*-1-isomers were eluted faster than the *sn*-3-isomers for any saturated and

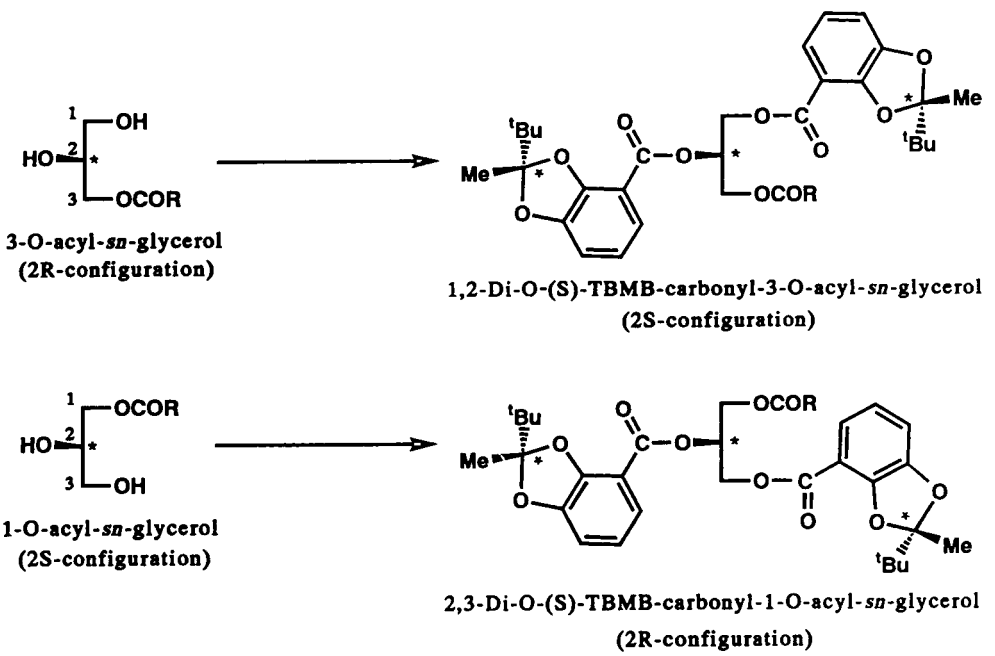

Fig. 1. Scheme for the direct derivatization of monoacylglycerols with (*S*)-TBMB-COCl forming diastereomeric derivatives: (*S*)-TBMB-COCl, pyridine, 4-dimethylaminopyridine (DMAP), room temperature.

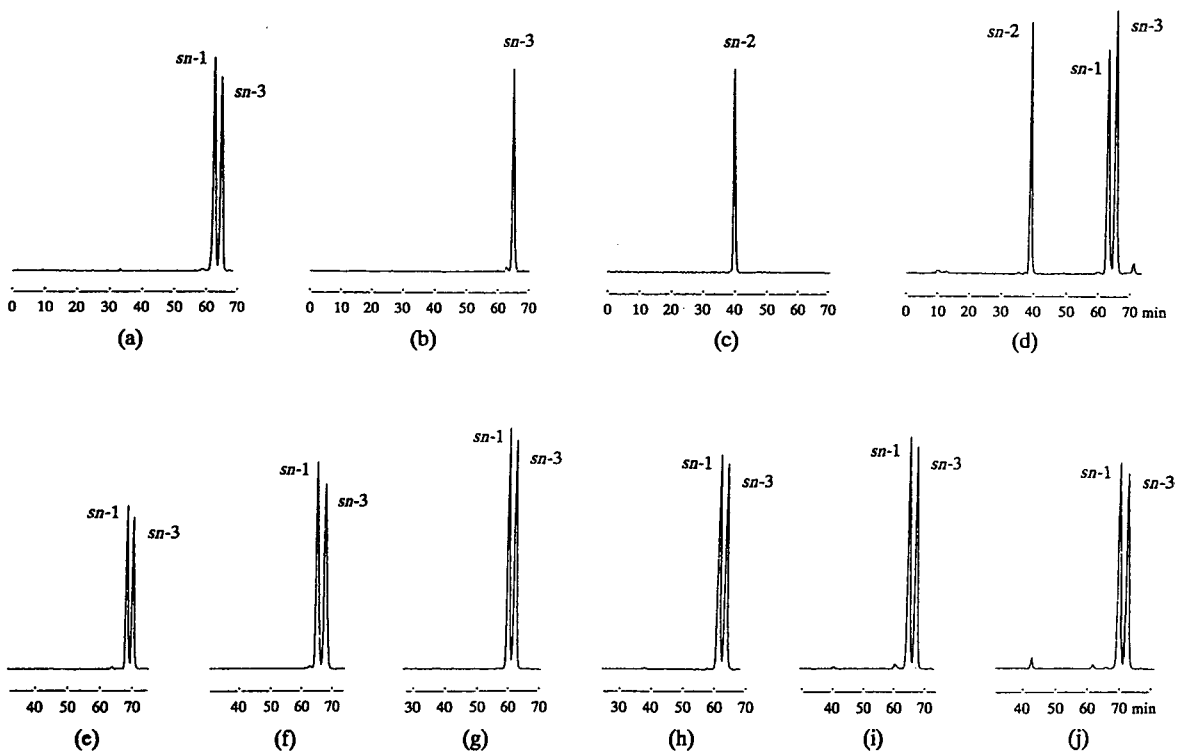

Fig. 2. Typical HPLC separations of each di-(*S*)-TBMB carbonylated homologous saturated and unsaturated monoacylglycerol. (a) *rac*-Monopalmitoyl-; (b) *sn*-3-monopalmitoyl-; (c) *sn*-2-monopalmitoyl-; (d) monopalmitoyl mixture [(a) + (b) + (c)]; (e) *rac*-monolauroyl-; (f) *rac*-monomyristoyl-; (g) *rac*-monostearoyl-; (h) *rac*-monooleoyl-; (i) *rac*-monolinoleoyl-; and (j) *rac*-monolinolenoyl-; *sn*-1, *sn*-2 and *sn*-3 in each chromatogram represent each position of the monoacyl group. HPLC conditions: silica gel column (Develosil 60-3, 50 cm × 4.6 mm I.D.); $\lambda_{ex} = 310$ nm, $\lambda_{em} = 370$ nm; eluent, *n*-hexane–*tert.*-butyl alcohol (250:1, w/w); flow-rate, 0.6 ml/min; temperature, 22–24°C.

unsaturated monoacylglycerols ($C_{12:0}$–$C_{18:0}$, $C_{18:1}$, $C_{18:2}$ and $C_{18:3}$) examined here. Although the separation of enantiomeric monoacylglycerols took longer with a longer silica column compared with the analysis of diacylglycerols (Develosil 60-3, 25 cm, $R_s > 2.0$), all enantiomers of saturated and unsaturated monoacylglycerols studied here could be separated with nearly identical separation coefficients ($\alpha = 1.05$) and peak resolutions ($R_s = 1.60$), as shown in Table 1.

In Fig. 3, we have plotted the logarithm of the retention volume (log V_r) versus the acyl carbon numbers (*CN*) and double (olefinic) bond numbers (*DN*) for each homologous series of isomeric *sn*-1- and *sn*-3-monoacylglycerols. Although some plots for the logarithmic retention volumes (log V_r) and various *DN* showed slightly positive deviations from the linear equation (Fig. 3B), their relationship could be approximated by the following equations: for the log V_r versus *CN* of saturated monoacylglycerols, log V_r (*sn*-1) = −0.011 *CN* + 1.67, log V_r (*sn*-3) = −0.012 *CN* + 1.70 and $E(CN) = \log V_r$ (*sn*-3) − log V_r (*sn*-1) ≈ 0.03; and for log V_r versus *DN* of unsaturated monoacylglycerols, log V_r (*sn*-1) = 0.027 *DN* + 1.47, log V_r (*sn*-3) = 0.028 *DN* + 1.49 and $E(DN) = \log V_r$ (*sn*-3) − log V_r (*sn*-1) ≈ 0.02, where *E* is the diastereomer separation factor.

In order to confirm the reproducibility and the quantitative aspects of the present method, monopalmitoylglycerols with known optical purities were derivatized with (*S*)-TBMB-COCl and subjected to the HPLC analysis (Table 2).

Table 1
Chromatographic data for homologous monoacylglycerols as their di-(*S*)-TBMB-carbonyl derivatives

Acyl group	Position	V_r (ml)	k'	α	R_s
Monolauroyl	*sn*-1	34.64	5.66	1.05	1.57
	sn-3	36.33	5.94		
Monomyristoyl	*sn*-1	32.88	5.37	1.05	1.60
	sn-3	34.54	5.64		
Monopalmitoyl	*sn*-2	18.38	3.00	1.69	19.95
	sn-1	31.11	5.08	1.05	1.58
	sn-3	32.56	5.32		
Monostearoyl	*sn*-1	29.75	4.86	1.04	1.55
	sn-3	31.01	5.07		
Monooleoyl	*sn*-1	31.03	5.07	1.04	1.54
	sn-3	32.40	5.29		
Monolinoleoyl	*sn*-1	33.16	5.42	1.05	1.60
	sn-3	34.90	5.70		
Monolinolenoyl	*sn*-1	35.77	5.85	1.05	1.67
	sn-3	37.57	6.14		

V_r = retention volume corrected by column void volume (6.12 ml); k' = capacity factor; α = separation coefficient; R_s = peak resolution.

Good agreement could be obtained for the optical purities assessed by the present HPLC method before and after the (*S*)-TBMB-carbonyl derivatization within the usual limit of variation (S.D. = 2.07, $n = 7$). The very small but significant deviation (ca. 2%) might be due mainly to the partial racemization of commercially available 3-monopalmitoyl-*sn*-glycerol during storage. In any event, this result showed that the peak areas of the two diastereomeric di-(*S*)-TBMB carbonylated monoacylglycerols can be used directly to determine the optical purities of original monoacylglycerols within a ca. 2% error without a calibration process. The detection limit of 3-monopalmitoyl-*sn*-glycerol (2*R*-configuration) as its di-(*S*)-TBMB carbonylate (2*S*-configuration) was 0.3 pmol on-column (signal-to-noise ratio = 3) owing to the fluorescence of the (*S*)-TBMB carbonyl chromophore.

We applied the method to check the racemization of chiral 3-monopalmitoyl-*sn*-glycerol under the acidic to basic conditions of pH 4.0 (phthalate buffer), 6.9 (phosphate buffer) and 9.2 (Na_2HCO_3 buffer). The results revealed that no racemization occurred in the pH range 4.0–9.2 at least for 1 week at room temperature; the optical purity of 3-monopalitoyl-*sn*-glycerol, initially ca. 96% e.e. as can be seen in Table 2, was kept constant at 95–96% e.e in all the pH solutions examined for 1 week. These results will be useful for studying the stereoselectivities of lipase-catalysed reactions at various pH values or the other enzymic and chemical reactions of glycerolipids.

In this work, we have extended our previous analytical strategy for diacylglycerols using (*S*)-TBMB-carbonyl labelling and HPLC analysis to monoacylglycerols to determine the optical purity and the absolute configuration. Under the present HPLC conditions using a normal-phase silica column (Develosil 60-3), the *sn*-1- and

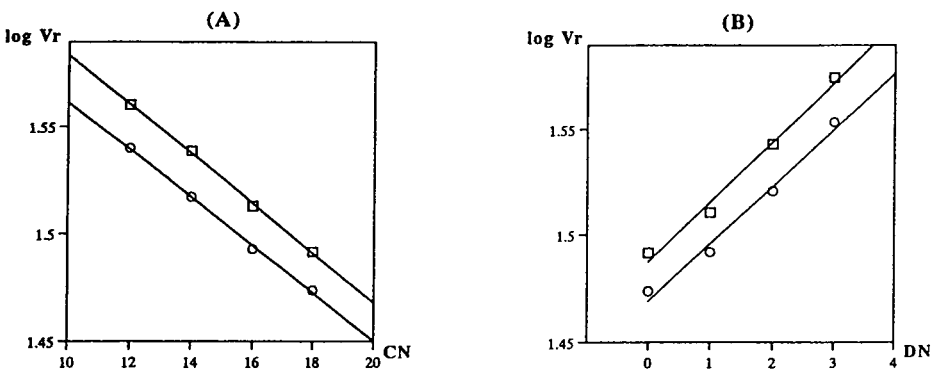

Fig. 3. Relationships between log V_r (retention volume) and (A) *CN* (number of acyl carbon atoms, $C_{12:0}$–$C_{18:0}$) and (B) *DN* (number of double bonds, $C_{18:0}$–$C_{18:3}$) for homologous and isomeric monoacylglycerols as their (*S*)-TBMB derivatives separated by HPLC on a silica gel column (Develosil 60-3). ○ = Log V_r (*sn*-1); □ = log V_r (*sn*-3).

Table 2
Comparison of optical purities before and after the derivatization of standard monoacylglycerols

Standard monoacylglycerol mixtures before derivatization[a]			After derivatization with (*S*)-TBMB-COCl[b]		
1-Monopalmitoyl-*rac*-glycerol (racemate) (mg)	3-Monopalmitoyl-*sn*-glycerol (*sn*-3) (mg)	Calculated optical purity (% e.e.)	Average observed optical purity (% e.e.)		S.D.
1.0	0	0	0.0	($n = 4$)	2.83
0.82	0.42	33.9	30.6	($n = 4$)	0.26
0.41	0.84	67.2	65.1	($n = 4$)	1.69
0	1.0	100	96.3	($n = 7$)	2.07

[a] Each standard solution was prepared by mixing the racemate and 3-monopalmitoyl-*sn*-glycerol in the appropriate ratio, and their optical purity was calculated from the ratio of the racemate and 3-monopalmitoyl-*sn*-glycerol contents [% e.e. before derivatization = *sn*-3/(racemate + *sn*-3) · 100].

[b] The HPLC peak areas of di-(*S*)-TBMB-carbonyl-monoacylglycerol derivatives (*sn*-1 and *sn*-3) derived from each standard monoacylglycerol mixture were used directly to determine the optical purity of the mixture of monoacylglycerols without correction [% e.e. after derivatization = (peak area of *sn*-3 − peak area of *sn*-1)/(peak area of *sn*-1 + peak area of *sn*-3) · 100].

sn-3-monoacyl enantiomers and the *sn*-2-isomer, in addition to the corresponding diacylglycerols, were simultaneously separated from each other within 80 min, and the analysis could be performed with less than 1 pmol of mono- and diacylglycerols, taking advantage of the strong fluorescence of the (*S*)-TBMB-carbonyl group.

We shall apply this approach to study the stereoselectivities of lipase reactions producing mono- and diacylglycerols and to clarify the separation mechanism of the enantiomeric mono- and diacylglycerols with this agent.

Acknowledgement

This work was partially supported by a Grant-in-Aid for Scientific Research from the Ministry of Education, Science and Culture of Japan.

References

[1] A.E. Thomas, III, J.E. Scharoun and H. Ralston, J. Am. Oil Chem. Soc., 42 (1965) 789.
[2] K. Maruyama and C. Yonese, J. Am. Oil Chem. Soc., 63 (1986) 902.
[3] S. Takano and Y. Kondoh, J. Am. Oil Chem. Soc., 64 (1987) 1001.
[4] B.G. Sempore and J.A. Bezard, J. Chromatogr. A, 596 (1992) 185.
[5] Y. Itabashi and T. Takagi, Lipids, 21 (1986) 413.
[6] T. Takagi and Y. Ando, Lipids, 25 (1990) 398.
[7] J.H. Kim, Y. Nishida, H. Ohrui and H. Meguro, J. Chromatogr. A, 677 (1994) 35.
[8] J.H. Kim, Y. Nishida, H. Ohrui and H. Meguro, J. Chromatogr. A, 693 (1995) 241.
[9] Y. Nishida, H. Ohrui and H. Meguro, Tetrahedron Lett., 30 (1989) 5277.

ELSEVIER

Journal of Chromatography A, 709 (1995) 381–386

JOURNAL OF CHROMATOGRAPHY A

Short communication

Separation of chromate and tungstate by reversed-phase high-performance chromatography using rutin as chelating reagent

Songbai Tian, Georg Schwedt*

Institut für Anorganische und Analytische Chemie, TU Clausthal, 38678 Clausthal-Zellerfeld, Germany

First received 10 February 1995; revised manuscript received 3 April 1995; accepted 3 April 1995

Abstract

Rutin was used as a chelating reagent to form ternary complexes with metal ions and hexadecyltrimethylammonium bromide (cetyltrimethylammonium bromide, CTAB). The retention behaviour of ternary complexes of Cr(VI) and W(VI) on a Nucleosil C_{18} column were examined. For chromatographic analysis the sample solution had to be changed because these ternary complexes did not give any peaks in aqueous medium. A solid-phase extraction step with polyethylene as sorbent and methanol as eluent was introduced. Cr(VI) and W(VI) complexes in methanolic medium gave sharp peaks in the chromatogram and were separated from each other and other metal ions by using a mobile phase of 42.5% (v/v) tetrahydrofuran containing 0.003 *M* CTAB. The method was applied to the analysis of chromate in geological samples.

1. Introduction

The application of surfactants in the photometric measurement of metal ions has been studied intensively for many years. The introduction of surfactants greatly increases the solubility of the metal complexes and the sensitivity of the photometric method; however, the selectivity of the method is not considerably improved.

High-performance liquid chromatography (HPLC) has the advantages of high sensitivity, selectivity and the possibility to simultaneously detect several analytes and has been widely used for the separation and determination of binary (metal ion and ligand) metal-ion complexes. Many metal ions that suffer from interference by other ions in spectrophotometry, can be separated and determined by HPLC. However, very little information is available in the literature on the direct HPLC analysis of ternary complexes with surfactants [1], although in some studies surfactants have been introduced into the mobile phase to increase the solubility of the metal complexes [2–5].

Rutin can form ternary complexes with Cr(VI) and W(VI) in the presence of cetyltrimethylammonium bromide (CTAB) [6,7]. Because their maximum absorption coefficients are very similar, Cr(VI) and W(VI) complexes can not be determined by spectrophotometry. The aim of this work was to examine the application of ion-pair reversed-phase chromatography to the analysis of these two ternary complexes. After solid-phase extraction the Cr(VI)- and W(VI)–rutin–CTAB ternary complexes in methanolic medium were separated with a mobile phase of

* Corresponding author.

0021-9673/95/$09.50
SSDI 0021-9673(95)00419-X

42.5% (v/v) tetrahydrofuran containing 0.003 *M* CTAB. CTAB, a surfactant with positive charge, was added to the mobile phase to improve the selectivity of the separation, whereas solid-phase extraction was used to change the sample medium in order to reduce the retardation of the ternary complexes.

2. Experimental

2.1. Apparatus

The liquid chromatograph consisted of a Bischoff 2200 pump, an injection valve with an injection volume of 20 μl, a Bischoff Lambda 1000 UV–Vis detector and a Shimadzu C-R6A integrator. A Nucleosil C_{18} column (250 × 4 mm I.D.) (Macherey-Nagel) was employed.

The spectral measurements were carried out in a Spectronic 20 D Model spectrophotometer (Milton Roy Company). The pH was adjusted with an E516 pH meter (Metrohm, Herisau).

A cartridge (plastic container, 60 × 9 mm I.D.) pre-packed with 250 mg of polyethylene was used for solid-phase extraction. The cartridge was connected to a SPE-21 vacuum pump (J.T. Baker), and the solutions were aspirated through. The cartridge was pre-conditioned by passing 2 ml methanol, then 2 ml acetic acid–sodium acetate buffer. At this stage the polyethylene in the cartridge had to be maintained moist.

2.2. Reagents

Rutin (Sigma) was dissolved in methanol to give 0.001 *M* solutions. Hexadecyltrimethylammonium bromide (CTAB) was obtained from Merck. A 0.01 *M* solution of CTAB was prepared by dissolving the solid in water. Acetic acid–sodium acetate (0.2 *M*, pH 5) buffer was used to control the pH of the pre-column derivatization. All chemicals used were of analytical-reagent grade.

2.3. Method

To a solution containing 5–100 μg CrO_4^{2-} and WO_4^{2-} were added 2 ml of 0.001 *M* rutin, 2.5 ml of 0.01 *M* CTAB and 2.5 ml of 0.2 *M* acetic acid–sodium acetate buffer. The mixed solution was diluted to 25 ml with deionized water and kept for 15 min in an ultrasonic bath for colour development.

A 5-ml volume of the above solution containing metal-ion complexes was aspirated through the pre-conditioned cartridge. The cartridge was then flushed with 2 ml of buffer. After drying of the column, the rutin–metal–CTAB ternary complexes were slowly eluted from the cartridge with 2 ml of methanol.

2.4. High-performance chromatography

A 20-μl methanolic sample solution was injected onto the liquid chromatographic system. The complexes were eluted with a mobile phase of 42.5% (v/v) [for the separation of Cr(VI) and W(VI)] or 40% (v/v) [for the determination of Cr(VI)] tetrahydrofuran containing 0.003 *M* CTAB at a flow-rate of 1 ml min^{-1}. The complexes were detected by a UV–Vis detector at 408 nm.

2.5. Determination of chromate in geological samples

A 0.1–0.5 g amount of sample was fused in an aluminium oxide crucible with 4 g of sodium peroxide at 700°C for 7 min. The melt was cooled and dissolved in 50 ml of water. The hydrogen peroxide was removed by boiling the solution for 10 min. After cooling, the solution was transferred to a volumetric flask and diluted to 100 ml with deionized water. A 5-ml volume of sample was transferred to a 25-ml flask and neutralised with diluted acetic acid. By using the above mentioned method chromate complexes were formed and then transferred to the methanolic medium by solid-phase extraction. Finally a 20-μl aliquot of the methanolic sample solution was injected onto the HPLC system.

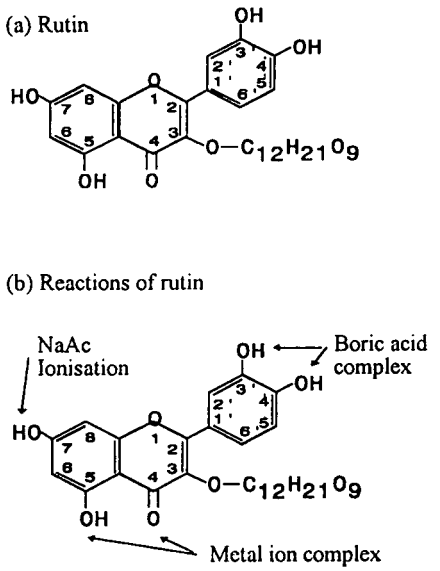

Fig. 1. Structure and reactions of rutin.

The amount of chromate in the sample solution was determined by measuring the peak height and comparison with calibration curves.

3. Results and discussion

3.1. Pre-column derivatization and solid-phase extraction of rutin complexes

The structure and reaction characteristics of rutin are shown in Fig. 1 [8]. With the hydroxyl group on C5 and the keto group on C4 rutin can form stable complexes with metal ions [9]. If the medium is not very acidic, the sugar moiety is stable [6] and the hydroxyl groups at the 3′, 4′ and 7 positions of rutin can be deprotonated differently. Therefore, rutin complexes are negatively charged and can form micellar ion-association compounds with CTAB. Table 1 shows some properties of the Cr(VI) and W(VI) ternary complexes. These two complexes are relatively stable and their extinction is stable for a period of at least two hours. The retention properties of the Cr(VI), W(VI) and other metal-ion complexes are discussed in Ref. [6].

Direct injection of non-pretreated aqueous solutions of Cr(VI) and W(VI) complexes did not yield any chromatographic peaks. This could be due to the strong hydrophobic character of the complexes. To reduce their adsorption on the stationary phase, the complexes were transferred to a methanolic medium by means of solid-phase extraction with polyethylene as the sorbent. The methanolic sample solution was injected onto the chromatographic system and separated peaks of the Cr(VI) and W(VI) complexes were obtained.

3.2. Chromatographic separation of ternary complexes of Cr(VI) and W(VI)

Table 1 shows that the ternary complexes of Cr(VI) and W(VI) have not only a similar λ_{max} but also a similar optimal pH. This non-selectivity of the complexation reactions leads to difficulties in the spectrophotometric detection but is a prerequisite for the simultaneous determination of metal-ion complexes by means of HPLC.

Separation of the Cr(VI) and W(VI) ternary complexes could be achieved by reversed-phase chromatography when the concentrations of tetrahydrofuran and CTAB were suitably selected. The rutin peak eluted early in the chromatogram and did not interfere with the solute peaks

Table 1
Properties of ternary complexes of rutin with metal and CTAB

Metal	λ_{max} (nm) (water)	λ_{max} (nm) (methanol)	pH_{opt}	Metal/ligand (molar-ratio)
Cr(VI)	429	416	5.0	1:2
W(VI)	417	408	4.4–5.1	1:2

because the rutin ternary complexes were more strongly retained by the column than non-complexed rutin.

The concentration of tetrahydrofuran in the mobile phase had a significant effect on the separation of the Cr(VI) and W(VI) complexes. The Cr(VI) and W(VI) complexes could be separated with a tetrahydrofuran content of 40% (v/v), but the retention time of the W(VI) complex was very long (15 min) and the peak was very wide. When the tetrahydrofuran content was higher than 45% (v/v), the Cr(VI) complex peak overlapped with the system peak and the Cr(VI) and W(VI) complexes could not be separated. A concentration of 42.5% (v/v) tetrahydrofuran was chosen for the separation of the Cr(VI) and W(VI) complexes. The mobile phase was carefully handled in a ultrasonic bath to prevent volatization of tetrahydrofuran.

The effect of CTAB in the mobile phase on the retention of Cr(VI) and W(VI) complexes was examined. With 42.5% tetrahydrofuran but no CTAB in the mobile phase the chromatographic peaks of the Cr(VI) and W(VI) complexes could not be resolved from each other and from the solvent peak. In contrast to the usual behaviour described in the literature [5], the addition of CTAB did not result in a decrease, but in an increase of the retention of the metal-ion complexes on the stationary phase. CTAB can act as counter ions in this system forming ion-pairs with complexes containing opposite charge. CTAB has a large hydrophobic group and can be adsorbed on the surface of the stationary phase. In this way a positively charged layer is formed on the surface of stationary phase. When the sample solution together with the mobile phase flows through the column, this positively charged layer competes with the CTAB in the mobile phase for the negatively charged binary rutin–metal-ion complexes. The higher the concentration of CTAB in the mobile phase, the more CTAB will adsorb on the stationary phase and the stronger the retention characteristics of the stationary phase. Because the W(VI) complexes were more sensitive to changes in the concentration of CTAB than the Cr(VI) complexes, the two ternary complexes could be separated. However, a too high concentration of CTAB gave an inferior baseline and resulted in a turbid mobile phase due to the limited solubility of CTAB. A concentration of 0.003 *M* CTAB was appropriate for the separation of the Cr(VI) and W(VI) complexes.

The pH of the eluent was 5.85. An increase or decrease of the pH neither improved the peak shape nor reduced the retention. Thus the eluent was used without pre-adjustment of the pH. In contrast to the results found with other ion-pair reversed-phase chromatographic separations of metal-ion complexes the addition of ligand and buffer to the mobile phase did not lead to any noticeable improvement in the separation of the complexes; it did however result in deformed peak shapes. Therefore, only 42.5% (v/v) tetrahydrofuran containing 0.003 *M* CTAB was chosen as the mobile phase.

It must be emphasised that the complexes of Cr(VI) and W(VI) could be not separated on a new column. Even when the tetrahydrofuran content in the mobile phase was increased to 60% (v/v), no W(VI)-complex peak did appear, whereas the Cr(VI) complex eluted together with other components with less retention. With the ageing of the column the retention of the Cr(VI) complex did not decrease substantially, whereas the retention of the W(VI) complex decreased dramatically. Thus, the Cr(VI) and W(VI) complexes could be separated on a used column with 42.5% (v/v) tetrahydrofuran containing 0.003 *M* CTAB.

An interesting phenomenon was observed in this experiment. When Cr(VI) and W(VI) were first mixed, coloured and then handled by solid-phase extraction, the peak height of tungstate was smaller than that of chromate, although the concentration of tungstate was 4-fold higher than that of chromate (Fig. 2a). When Cr(VI) and W(VI) were coloured separately, extracted and then mixed, a completely different chromatogram was obtained (Fig. 2b). The peak heights of the W(VI) and Cr(VI) complexes were almost identical, although the concentration of tungstate was only twice that of chromate. The reason could be that the chromate complex is more stable than the tungstate complex. Thus, the

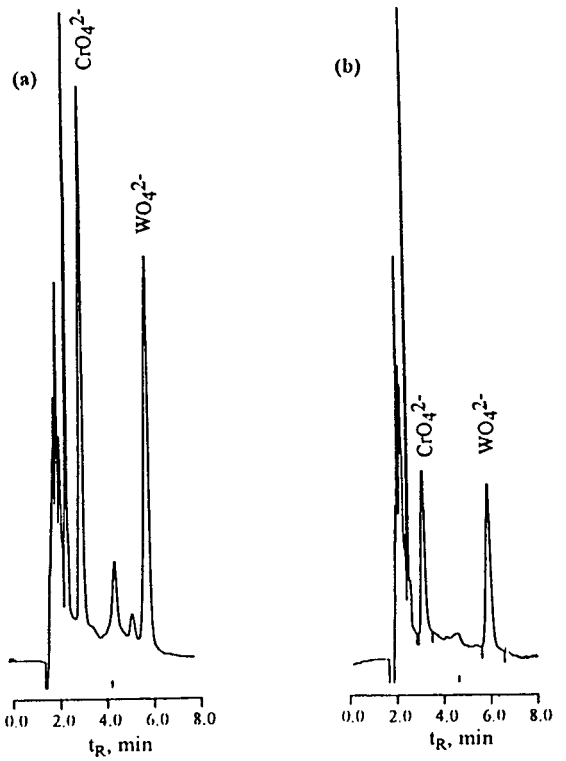

Fig. 2. Separation of the ternary complexes of Cr(VI) and W(VI). (a) Cr(VI), W(V) were first mixed, coloured and then handled by solid-phase extraction; concentration: 2 mg l^{-1} (chromate), 8 mg l^{-1}(tungstate); (b) Cr(VI), W(VI) were coloured first respectively, extracted and then mixed; concentration: 1 mg l^{-1} (chromate); 2 mg l^{-1}(tungstate). Mobile phase: 42.5% (v/v) tetrahydrofuran containing 0.003 *M* CTAB; column: Nucleosil C_{18}, 250 × 4 mm I.D.; flow-rate: 1 ml min^{-1}; detection: Vis (408 nm).

relatively stable complex between rutin and chromate is eluted first. Only excess of rutin is able to complex the tungstate completely; this will lead to a low absorbance of tungstate.

3.3. Determination of chromate in geological samples

Because no samples containing detectable W(VI) could be found, only the ion-pair reversed-phase chromatographic determination of the chromate–rutin–CTAB complex was performed as an example of the practical application of the method developed above (section 3.2). In order to obtain a more accurate measurement of the peak height, the concentration of tetrahydrofuran in the mobile phase was reduced to 40%.

This method was very sensitive. Even at a chromate concentration of 5 μg l^{-1}, the chromate peak could be still detected. The calibration curve is linear at least over the range 0.02–0.2 mg l^{-1} of chromate in the initial aqueous solutions.

Four geological samples were analysed and the results are summarised in Table 2. In order to evaluate the quantitative performance of the HPLC method, a photometric method [10] was used to compare the results. The results from the two methods show good agreement for the determination of chromate in geological samples.

The proposed HPLC method should be applicable to the determination of tungstate in the appropriate samples.

Table 2
Comparison of results for the determination of chromate in geological samples by HPLC and spectrophotometry [10]

Sample	Chromate content[a] (mg kg^{-1})	
	Proposed HPLC method	Spectrophotometry
Ore	174 ± 1.50	172 ± 0.52
Sediment	214 ± 2.07	230 ± 0.61
Grey soil	282 ± 3.49	260 ± 0.54
Red soil	910 ± 0.57	990 ± 0.09

[a] Mean ± R.S.D.% (n = 5).

4. Conclusions

A new ternary complex system has been developed for the separation of Cr(VI) and W(VI) by reversed-phase chromatography. Solid-phase extraction was used to transfer the ternary rutin–metal–CTAB complexes from an aqueous to a methanolic phase. Thus the interaction between the complexes and the stationary phase was reduced and separation of the complexes could be achieved. Due to the limited availability of samples the method was only applied for the determination of chromate in geological samples. When suitable samples are available the method should be applicable to the determination of tungstate or the simultaneous determination of chromate and tungstate.

References

[1] Y. Yuan, Fenxi Huaxue (Analytical Chemistry), 18 (1990) 87.
[2] Y. Zhao and Ch. Fu, Analyst, 116 (1991) 621.
[3] H. Sirén, Chromatographia, 29 (1990) 144.
[4] T. Okada, Anal. Chem., 64 (1992) 589.
[5] M.P. San Andrés, S. Vera and M.L. Marina, J. Chromatogr. A, 685 (1994) 271.
[6] M. Xu, Y. He and G.A. Parker, Fenxi Huaxue (Analytical Chemistry), 16 (1988) 207.
[7] S. Tian, Dissertation, Technical University of Clausthal, Germany, 1994.
[8] T.I. Khalifa, F.J. Muhtadi and M.M.A. Hassan, in K. Florey (Editor), Rutin, Analytical Profiles of Drug Substances, Vol. 12, Academic Press, New York, 1983.
[9] M. Katyal, Talanta, 15 (1968) 95.
[10] C. Harzdorf, in H. Hulpke, H. Hartkamp and G. Tölg (Editors), Spurenanalytik des Chroms, Analytische Chemie für die Praxis, Georg Thieme Verlag, Stuttgart, 1990, pp. 40–41.

ELSEVIER

Journal of Chromatography A, 709 (1995) 387–392

JOURNAL OF CHROMATOGRAPHY A

Short communication

Determination of aldehydes in basic medium by gas chromatography using O-benzylhydroxylamine derivatization

Vivek Jain*, Daniel Thielen

Occidental Chemical Corporation, 2801 Long Road, Grand Island, NY 14072, USA

First received 26 August 1994; revised manuscript received 4 April 1995; accepted 4 April 1995

Abstract

The O-benzylhydroxylamine hydrochloride derivatization of aldehydes, like most other aldehyde derivatization procedures, has historically been carried out under acidic conditions. An adaption of this procedure to basic samples, namely triethanolamine, is now reported whereby no acidification of the sample is required. This method has been shown to be capable of quantitatively determining up to at least the C_{10} aldehydes. Analysis by gas chromatography with flame ionization detection gave detection limits in the low μg/ml (ppm) range.

1. Introduction

Ethanolamines are commercially produced by reaction of ethylene oxide with ammonia. The various amines produced are separated by distillation to give monoethanolamine (MEA), diethanolamine (DEA) and triethanolamine (TEA). While MEA and DEA are usually water white in color, it is not uncommon for TEA to be highly colored. The color-producing impurities have been ascribed to the presence of aldehydes which are either impurities carried into the process with the ethylene oxide or are formed as a result of ethanolamine degradation. In order to study color formation during the production of these amines, it was necessary to have a method capable of determining trace levels of aldehydes in this matrix.

The determination of aldehydes either in total or as individual aldehydes has been described by many investigators. Gas chromatographic (GC) determination of free aldehydes present difficulties due to their reactive nature. Determination using liquid chromatography requires UV detection at 200 to 220 nm and presents a sensitivity issue since extinction coefficients of these aldehydes are not high. An alternative to direct determination is to react aldehydes with a derivatization agent which imparts either thermal stability for GC analysis or a more strongly absorbing chromophore in the UV or visible spectral range for liquid chromatographic analysis.

One of the most common derivatization agents for aldehydes is dinitrophenylhydrazine which when reacted with aldehydes produces a hydrazone product that is both thermally stable and has a strong chromophore. This method has been used for colorimetric [1–3], GC [4–6] and liquid chromatographic [7–9] determinations. This derivatization procedure, however, is an acid-catalyzed reaction which would require

* Corresponding author.

0021-9673/95/$09.50
SSDI 0021-9673(95)00422-X

acidification of a basic triethanolamine matrix. Acidification of this basic matrix could result in heat generation which would, in turn, increase the likelihood of losing the more volatile aldehydes. A second procedure involving the reaction of pentafluorobenzyloxyamine (PFBOA) with carbonyl compounds has been used for trace level detection of aldehydes [10–12]. Samples containing these fluorinated oxime derivatization products have been analyzed by GC with electron-capture detection (ECD). These reactions have been carried out in aqueous solutions and in media which are slightly acidic. A third method which involves formation of aldehyde oxazolidine derivatives is used extensively in air pollution work for screening and determination of various low-molecular-mass aldehydes. The most common reagent is 2-(hydroxymethyl)piperidine which is coated on XAD-2 resin for packing in solid adsorbent tubes [13]. This reagent was found by Kennedy and coworkers [14,15] to give the fastest reaction time for this class of reagents. This derivatization reaction has primarily been used in adsorbent tube reactions for gas-phase reactions rather than for solution-phase derivatizations.

This paper reports on an extension of the PFBOA procedure which demonstrates that the non-fluorinated O-benzylhydroxylamine (BOA) reagent is capable of derivatizing aldehydes in basic media to form aldehyde oxime products which can be quantitatively determined by GC using flame ionization detection (FID). While PFBOA gives good ECD sensitivity, this halogenated derivative decreases the FID response due to quenching of the flame signal by the fluorine. Therefore, the non-fluorinated BOA was chosen to maximize FID sensitivity.

2. Experimental

2.1. Reagents

O-Benzylhydroxylamine hydrochloride (Aldrich, Milwaukee, WI, USA) was prepared as a 5000 μg/ml solution in deionized (DI) water (Millipore, Bedford, MA, USA). Standard solutions (2500 μg/ml) of formaldehyde (Aldrich), acetaldehyde (Aldrich), propanal, butanal, pentanal, hexanal, heptanal (Alltech, Deerfield, IL, USA) were also prepared in DI water. Octanal and decanal standards can also be made in water but only at lower concentrations due to the limited aqueous solubility of these aldehydes. These solutions were diluted with DI water to prepare standards for standard addition and recovery studies. Similar standards were also prepared using TEA as a solvent. Hexane (Burdick & Jackson, Muskegon, MI, USA) was used for extractions.

2.2. Instrumentation

A Hewlett-Packard 5890A gas chromatograph equipped with a flame ionization detector was used for analysis. A 30 m × 0.25 mm I.D. DB-210 (J & W Scientific, Folsom, CA, USA) fused-silica capillary column (0.25 μm film thickness) was used for GC analysis. Helium was used as the carrier gas at 1.1 ml/min. The column temperature program was 50°C isothermal for 1 min, programmed to 200°C at 6°C min, held for 1 min, ramped again at 25°C/min to 225°C and held for 2 mins. Injection port and detector temperatures were held at 225 and 250°C, respectively.

2.3. Derivatization procedure

A 1-ml volume of sample was accurately weighed into a 4-ml screw-capped vial and 1 ml of the 5000 μg/ml BOA solution was added. The mixed solution was allowed to react at room temperature for 2 h. The derivative product was then extracted in the same vial with 1 ml of *n*-hexane by shaking vigorously for 1 min. The hexane extract was transferred to another vial using a transfer pipet and was shaken well with 4 ml of 0.15 *M* H_2SO_4 for 30 s. This removed excess TEA and BOA from the derivative product. The hexane layer was removed and analyzed for aldehyde content.

3. Results and discussion

BOA reacts with carbonyls (shown below) to form the corresponding oximes. Nonsymmetrical carbonyl compounds ($R_1 \neq R_2$) such as acetaldehyde react with BOA to give two geometrical isomers (based on the position of the R groups relative to the free electron pair of the nitrogen) and two peaks in the chromatogram when a polar column is used. Symmetrical carbonyls ($R_1 = R_2$) such as formaldehyde form a single isomer and give a single peak in the chromatogram. Doublet peaks in the chromatogram of an unknown will therefore give qualitative information regarding the presence of nonsymmetrical carbonyls.

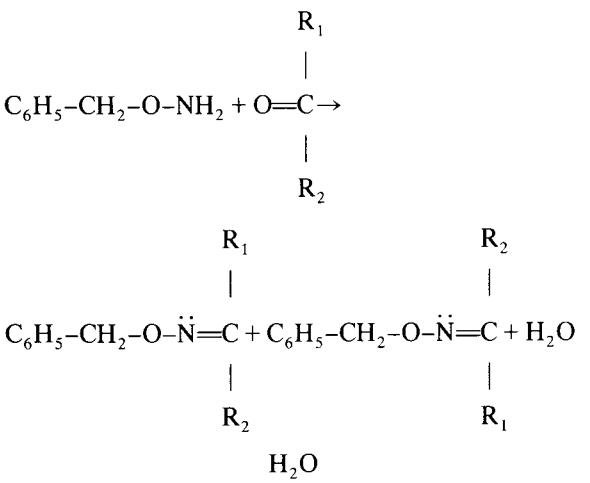

The work presented here shows that this method works effectively for linear straight-chain aldehydes up to at least C_{10} as well as for crotonaldehyde. Fig. 1 shows a standard chromatogram of the C_1–C_{10} aldehyde derivatives and illustrates that formaldehyde gives a single peak while the non-symmetrical aldehydes produce doublets.

The time required to carry out a BOA reaction was studied on TEA samples. A 1-ml volume of a 5000 μg/ml BOA solution was mixed with 1 ml of a TEA solution that had been spiked with known amounts of formaldehyde and acetaldehyde. The high concentration of BOA was used to ensure an excess of BOA. The vials were held at room temperature for periods

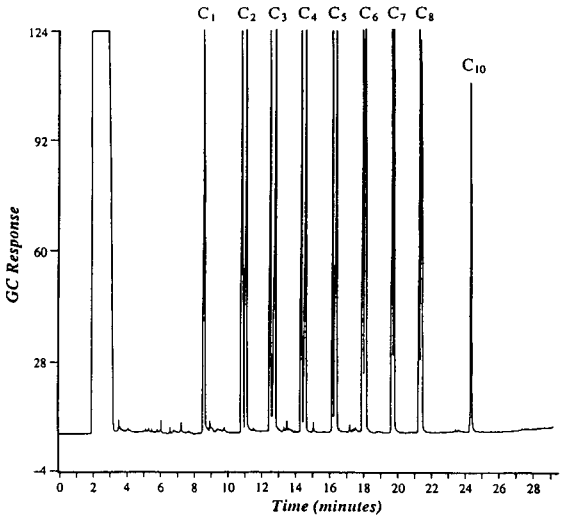

Fig. 1. Gas chromatogram of C_1–C_{10} straight-chain aldehydes using BOA derivatization.

of time ranging from 1 to 36 h. The TEA solutions were then extracted with hexane and analyzed. The results, shown in Fig. 2, indicate that the reaction reached completion in 1.5 to 2 h. The derivatives remained stable for at least 36 h in the TEA–BOA mixture and were also found to be stable in the hexane extract for an equivalent period of time. Since formaldehyde and acetaldehyde are often found in TEA, they were used for optimizing the reaction time. However, crotonaldehyde, hexanal and heptanal were also tested for optimum reaction conditions

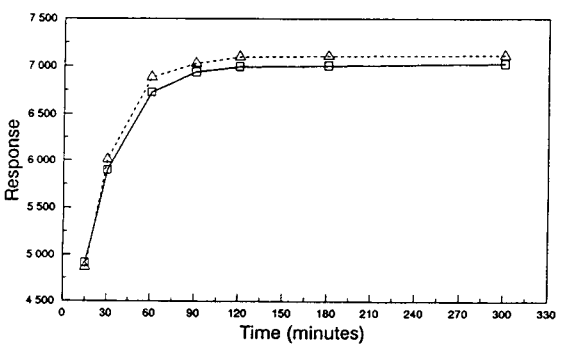

Fig. 2. Plot of flame ionization response versus BOA reaction time. △ = Formaldehyde; □ = acetaldehyde.

and they were found to react quantitatively and within the same time frame.

The derivatization method was confirmed in the TEA matrix by studying the spike recovery. TEA samples were spiked with known amounts (from 20 to 250 μg/ml) of formaldehyde, acetaldehyde, butyraldehyde and crotonaldehyde. The spiked samples were then analyzed using the above procedure and their typical recovery percentages are shown in Table 1. As predicted, two peaks were detected for each non-symmetrical aldehyde with recoveries calculated at greater than 90% for each.

A standard addition method was also used to confirm the concentration of aldehydes in a TEA sample. The concentrations for formaldehyde and acetaldehyde were found to be 18 and 50 μg/ml, respectively, as compared to 19 and 48 μg/ml using an external standard calibration. Since there did not appear to be any matrix effects, the external standard method was used for analyzing TEA samples.

Several TEA samples were then screened for individual aldehydes using the above procedure. Table 2 shows aldehydes found in the various TEA samples with the corresponding color description of the TEA. In all cases, only formaldehyde and acetaldehyde were found. It could not be determined whether formaldehyde and acetaldehyde are responsible for imparting color, however, they correlate with the color in these solutions. Since the method was tested for aldehydes only up to decanal, it could not be determined whether the TEA samples contained aldehydes higher than decanal or if higher-molecular-mass aldehydes were present which either did not elute from the column or which decomposed in the injection port of the chromatograph. At this time, another method [7–9] involving derivatization with dinitrophenylhydrazine was also explored for analyzing aldehydes in TEA samples using HPLC. It was found, however, that the method showed no reproducibility of response for various aldehydes especially formaldehyde and acetaldehyde present in TEA matrix. The non-reproducibility of response

Table 1
Spike recovery results for triethanolamine

Compound	Amount spiked (μg/ml)	Amount recovered (μg/ml)	Recovery (%)
Formaldehyde	20	18	90
	50	52	104
	100	96	96
	150	138	92
	250	235	94
Acetaldehyde	20	19	95
	50	47	94
	100	101	101
	150	140	93
	250	230	92
Butanal	20	18	90
	50	53	106
	100	90	90
	150	142	95
	250	238	95
Crotonaldehyde	20	21	105
	50	46	92
	100	93	93
	150	154	103
	250	228	91

Table 2
Aldehyde analysis in triethanolamine samples

Process sample	Formaldehyde (μg/ml)	Acetaldehyde (μg/ml)	APHA[a] color scale
1	3	24	25
2	6	100	45
3	5	100	55
4	7	110	70
5	7	150	300
6	17	180	500
7	12	260	1500

[a] Official method for color (APHA scale) issued by the American Oil Chemists' Society (AOCS), document no., TD1B, 1964.

could be attributed either to the formation of an unstable hydrazone derivative in TEA or degradation of the hydrazone derivative due to the extreme basic nature of TEA. No other methods were investigated further and the proposed method of BOA derivatization was used for routine aldehyde analysis in TEA.

3.1. Method sensitivity

To verify the linearity of the BOA derivatization method, a calibration for the analysis of formaldehyde, acetaldehyde, butyraldehyde and crotonaldehyde was done over a wide concentration range. The method was found to be linear from the detection limit of 1 μg/ml to approximately 2000 μg/ml with a correlation coefficient of 0.9998. A higher concentration of BOA solution can be used to obtain linearity for samples containing excessive amount of aldehydes. The upper detector linearities of octanal and decanal were 600 and 250 μg/ml, respectively, due to their limited solubilities.

Precision of this method was also investigated. Standards with known amount of formaldehyde and acetaldehyde were analyzed repeatedly up to 10 times. The relative standard deviation obtained for this method was 2.76%.

4. Conclusions

A method has been described for the determination of aldehydes in a basic medium, namely triethanolamine. While most aldehyde derivatization procedures are carried out under acidic conditions, this method provides the analyst with the additional capability of basic derivatization. This eliminates the need for any acidification of the sample prior to derivatization. The derivative products were found to be thermally stable and thus could be easily analyzed by GC. Excellent linearity of response with a correlation coefficient of 0.9998 was obtained, along with spike recoveries of greater than 90%, for all aldehydes studied.

References

[1] P.E. Toren and B.J. Heinrich, Anal. Chem., 27 (1955) 1986.
[2] L.J. Papa, Environ. Sci. Tech., 3 (1969) 397.
[3] Standard Test Method for Trace Quantities of Carbonyl Compounds with 2,4-Dinitrophenylhydrazine; Method E 411-92, American Society for Testing and Materials, Philadelphia, PA, Vol. 15.05.
[4] P. Ronkainen and S. Brummer, J. Chromatogr., 28 (1967) 253.
[5] L.J. Papa and L.P. Turner, J. Chromatogr. Sci., 10 (1972) 744.
[6] R.S. Smith and I. Drummond, Analyst, 104 (1979) 875.
[7] M.A. Carey and H.E. Persinger, J. Chromatogr. Sci., 10 (1972) 537.
[8] S. Selim, J. Chromatogr., 136 (1977) 271.
[9] F. Lipari and S.J. Swarin, J. Chromatogr., 247 (1982) 297.
[10] K. Kobayashi, E. Fukui, M. Tanaka and S. Kawai, J. Chromatogr., 202 (1980) 93.
[11] K. Kobayashi, M. Tanaka and S. Kawai, J. Chromatogr., 187 (1980) 413.

[12] M Tomita, I. Ijiri and K. Shimosato, J. Chromatogr., 414 (1987) 454.
[13] Manual of Analytical Methods, Vol. 1, National Institute of Occupational Safety and Health (NIOSH), Cincinnati, OH, 1989, Method 2539-1.
[14] E.R. Kennedy, P.F. O'Connor and Y.T. Gagnon, Anal. Chem., 56 (1984) 2120.
[15] E.R. Kennedy, Y.T. Gagnon, J.R. Okenfuss and A.W. Teass, Appl. Ind. Hyg., 3 (1988) 274.

ELSEVIER

Journal of Chromatography A, 709 (1995) 393–394

JOURNAL OF CHROMATOGRAPHY A

Book Review

Applied Pyrolysis Handbook, edited by Thomas P. Wampler; Marcel Dekker, New York, Basel, Hong Kong, 1995, ix + 361 pp., price US$ 135.00, ISBN 0-8247-9446-X.

About a decade ago a number of books on pyrolysis appeared at a time when the technique was rapidly emerging. In recent years such publications have been scant despite the wider application of the technique with improved chromatography due to the almost universal use of capillary columns and enhanced detection employing mass spectrometry, tandem mass spectrometry and Fourier transform infra-red spectrometry.

The work consists of 11 chapters, the first entitled "Analytical Pyrolysis: An Overview" by the editor illustrates briefly the principal degradation mechanisms and then introduces application to some of the major groups of materials most of which are further treated in subsequent chapters. Chapter 2 introduces pyrolysis instrumentation and analytical techniques and summarises the improvements that have evolved over 30 years. A disadvantage of Curie–Point systems is indicated to be possible catalytic effects due to the metals of the Curie–Point wire; however these metals are in part comparable to the constituents of resistively heated filaments. With filaments the resistance of the entire system must remain constant if the same energy is applied with the intention of providing the same temperature. Contact of parts of the filament and alloying must be avoided.

Chapter 3 describes Pyrolysis Mass Spectrometry and briefly shows instrument design, then chemometrics or methods of data analysis where multivariate statistics, techniques of Principal Component Analysis and artificial neutral networks are each described.

The Microstructure of Polyolefins forms Chapter 4 and here the various branching structures of polyethylene, the microstructure of polypropylene and the sequence distribution in ethylene–propylene copolymers are considered. It is apparent that the alternative to pyrolysis–gas chromatography in the measurement of these quantities is ^{13}C NMR and that the agreement of the two techniques is poor.

Chapter 6 entitled The Application of Analytical Pyrolysis to Cultural Materials is of considerable interest. Many common types of materials are considered but two additional features are described: (1) the effect of often centuries of exposure and (2) the representative nature of the sample. With the small samples available the analysis may be of a restorative material rather than of the original.

Environmental Applications of Pyrolysis forms Chapter 7 and a series of applications related to (1) air, i.e. smoke aerosols, vehicular traffic particulate matter and pollutants from thermal decomposition, (2) solids, i.e. waste plastic recycling, sewage sludge, soils and sediments, and (3) water, i.e. pulp mill effluents and groundwater, are decided.

The Examination of Forensic Evidence forms Chapter 8 and the examination of almost every material in common use, including paints, adhe-

SSDI 0021-9673(95)00547-1

sives, rubbers, fibres, oils and fats, cosmetics and inks, is considered. A particular feature of the chapter is the use of pyrolysis derivatization. In conventional chromatography derivative formation is a standard procedure and with pyrolysis high temperature derivative reactions have been developed where tetraalkylammoniumhydroxide reacts with hydrolyzable groups on pyrolysis products to produce alkyl derivatives which are readily detected.

The Characterization of Microorganisms by Pyrolysis–Gas Chromatography, Pyrolysis–Mass Spectrometry and Pyrolysis–Gas Chromatography–Mass Spectrometry forms Chapter 9 and although the individual techniques are described the advantages/disadvantages of each technique could be clearer. Selected applications include examples of gram-positive and gram-negative bacteria and of fungi.

Chapter 10 entitled Pyrolysis of Polar Macromolecules considers the pyrolysis of some synthetic polymers including polyalkyl methacrylates, polyethers, aromatic polyesters, cationic surfactants and sulphonamides.

The final chapter of the work is a compilation of 65 sample pyrograms of materials in common use. While the pyrolysis temperatures are shown the chromatographic conditions are omitted and this makes the collection of limited value.

The work assembles together many of the recent advances made in pyrolysis. Over half the citations have appeared in the last ten years and the work is recommended as an addition to the bookshelf of all interested in analytical pyrolysis. It is a pity that mass spectrometry as a detection method has not been treated in more detail and that the use of Fourier transform infrared detection has not been included.

Kensington, Australia J.K. Haken

ELSEVIER

Journal of Chromatography A, 709 (1995) 395–396

JOURNAL OF CHROMATOGRAPHY A

Book Review

Chromatography in the Petroleum Industry, Journal of Chromatography Library Series No. 56, edited by E.R. Adlard, Elsevier, Amsterdam, Lausanne, New York, Oxford, Shannon, Tokyo, 1994, XVIII + 434 pp., price Dfl. 435.00, ISBN 0-444-89776-3.

I can not claim to have read all, or even most, of the text in this book. In fact it is the kind of book that almost no-one would – or could – read all of. This is not a criticism. The book covers, so far as I can judge, the entire spectrum of common and uncommon chromatographic analyses carried out on petroleum or fractions thereof, and as such it encompasses a broader range than single individuals (certainly this individual) will have experience of. I personally was most interested in two of the chapters (Ch. 1 "The analysis of hydrocarbon gases" and Ch. 5 "Chromatography in petroleum geochemistry"), but then I am a geochemist. These were well written, although I found the chapter on petroleum geochemistry somewhat too concise (i.e. short) to be of practical use. This is not a criticism of the authors, who were presumably writing to a prescribed format.

Funnily enough, I found no chapter devoted to plain, straightforward gas chromatography, despite the fact that the editor states in the Foreword that "gas chromatography in particular is the most important analytical technique in petroleum analysis" (no-one would argue with that). After all, there are entire chapters on HPLC and column liquid chromatography (Ch. 12), supercritical fluid chromatography (Ch. 11), hydrodynamic chromatography (Ch. 4) and capillary electrophoresis (Ch. 14). It is true that gas chromatography is covered a lot along the way, for example in chapters 2 ("Advances in simulated distillation" – remarkable for a complete absence of figures), 3 ("The chromatographic analysis of refined and synthetic waxes") and 9 ("Multi-column systems in gas chromatography"), but why not a chapter devoted to the fundamental applications of this most important of techniques? This could have been in the form of an introductory chapter to the more specialised sections above. And why were the chapters dealing mostly with gas chromatography not grouped together, which would have been more logical and made it easier to grasp the scale and scope of the applications? As it is, the ordering of the chapters appears almost random.

Compared to the coverage of the basic gas chromatographic analysis, I thought there was an excessive amount of detail on rather less-common detectors. Microwave plasma detectors (Ch. 7) did not really merit 42 pages in my opinion, nor did the sulphur chemiluminescence detector (Ch. 8) demand so much as 29 pages.

As with all books, one has to put the question "who is going to read this?" The editor intends this one to be "primarily for those concerned with the analysis of crude oil and its products . . .". That encompasses a lot of people, but I am not sure that all of them will get much out of this book. Those already experienced people working in companies with well-developed methods probably will not read it – even

SSDI 0021-9673(95)00548-X

if they should – as it contains too much experimental detail for them. It could however be a good starting point for those trying to set up shop and who want to get a feel for how things are done. Despite the editor's undoubtedly correct belief that "many of the chapters have much broader applications", the apparent narrowness of the content suggested by the title may stifle the hope that "many outside the immediate sphere of petroleum analysis will find . . . it a worthwhile purchase."

Stavanger, Norway Richard Patience

ELSEVIER

Journal of Chromatography A, 709 (1995) 397

JOURNAL OF CHROMATOGRAPHY A

Book Review

Advances in Chromatography, Vol. 35, edited by P. Brown and E. Grushka; Marcel Dekker, New York, 1995; XVIII + 425 pp., price US$ 165, ISBN 0-8247-9361-7.

This volume, dedicated to Dr. J. Calvin Giddings, compiles a series of review articles dealing with the most rapidly developing areas in the field of chromatography and electrophoresis. In the Preface the editors quote Roy Keller who in the first volume of this series wrote that "even the explosive growth of chromatography (he meant mainly GC) has made it difficult for any single individual to maintain a coherent view of the field's progress". What was true some thirty years ago is valid even more today. In my opinion the editors of this volume succeeded very well in selecting the right topics. On the other hand, in contents the volume is a bit diversified spanning from Optical Detectors for Capillary Electrophoresis (E.S. Yeung), Capillary Electrophoresis Coupled with Mass Spectrometry (K. Pomer, L.J. Deterding and C.E. Parker), Approaches for Optimization of Experimental Parameters in CZE (H.J. Isaaq, G.M. Janini, K.C. Chan and Z. El-Rassi) and Pharmaceutical Analysis by CE (S.F.Y. Li, Choon Lan Ng and Chyl Peng Ong) to a review on chiral separations by C.J. Welch (Crawling out of the Chiral Pool: The Evolution of Pirkle-type Chiral Stationary Phases) and one review which is considerably more on the application side: R.E. Pauls, Chromatographic Characterization of Gasolines. The last two chapters deal with reversed-phase ion pair and ion interaction chromatography and error sources in the determination of chromatographic peak size ratios. When reading the book I was, for personal reasons, tempted to begin with the articles on capillary electrophoresis. Then I decided to start from the end with Veronika R. Meyer's contribution on Error Sources in Chromatography. This is a didactically sound piece of work. Moreover it is very valuable because particularly the newcomers to the field being impressed by the computerized systems are frequently overwhelmed by the beautiful peaks not realizing that without careful sample treatment the peaks need not necessarily reflect the reality. And they have to realize the limits of the procedures used, too.

It is always difficult with a good multiauthored book to stress one chapter and omitting the others. All of the reviews presented in this volume are not only pleasant to read but they offer a good survey of the latest achievements in the field, so they indeed help to invalidate the quotation of Roy Keller with which I started this report. Also in formal appearance the book is done on a highly professional level and the editors should be congratulated for a well done job. For its price the volume is a good buy. Except for the gasoline analysis review which is a bit too narrow-oriented, all the others, I believe, will find a very broad audience among chromatographers.

Prague, Czech Republic Zdeněk Deyl

SSDI 0021-9673(95)00561-7

Author Index Vol. 709

PUBLICATION SCHEDULE FOR THE 1995 SUBSCRIPTION

Journal of Chromatography A and *Journal of Chromatography B: Biomedical Applications*

MONTH	1994	J–A	M[a]	J	J	A	S	
Journal of Chromatography A	Vols. 683–688	689–698	699/1 + 2 700/1 + 2 702/1 + 2 703/1 + 2	704/1 704/2 705/1 705/2	706/1 + 2 707/1 707/2 708/1	708/2 709/1 709/2 710/1	710/2 711/1 711/2 712/1	The publication schedule for further issues will be published later.
Bibliography Section		713/1		713/2			714/1	
Journal of Chromatography B: Biomedical Applications		663–666	667/1 667/2	668/1 668/2	669/1 669/2	670/1 670/2	671/1 + 2	

[a] Vol. 701 (Cumulative Indexes Vols. 652–700) expected in October.

INFORMATION FOR AUTHORS

(Detailed *Instructions to Authors* were published in *J. Chromatogr. A*, Vol. 657, pp. 463–469. A free reprint can be obtained by application to the publisher, Elsevier Science B.V., P.O. Box 330, 1000 AH Amsterdam, Netherlands.)

Types of Contributions. The following types of papers are published: Regular research papers (full-length papers), Review articles, Short Communications and Discussions. Short Communications are usually descriptions of short investigations, or they can report minor technical improvements of previously published procedures; they reflect the same quality of research as full-length papers, but should preferably not exceed five printed pages. Discussions (one or two pages) should explain, amplify, correct or otherwise comment substantively upon an article recently published in the journal. For Review articles, see inside front cover under Submission of Papers.

Submission. Every paper must be accompanied by a letter from the senior author, stating that he/she is submitting the paper for publication in the *Journal of Chromatography A* or *B*.

Manuscripts. Manuscripts should be typed in **double spacing** on consecutively numbered pages of uniform size. The manuscript should be preceded by a sheet of manuscript paper carrying the title of the paper and the name and full postal address of the person to whom the proofs are to be sent. As a rule, papers should be divided into sections, headed by a caption (*e.g.*, Abstract, Introduction, Experimental, Results, Discussion, etc.). All illustrations, photographs, tables, etc., should be on separate sheets.

Abstract. All articles should have an abstract of 50–100 words which clearly and briefly indicates what is new, different and significant. No references should be given.

Introduction. Every paper must have a concise introduction mentioning what has been done before on the topic described, and stating clearly what is new in the paper now submitted.

Experimental conditions should preferably be given on a *separate* sheet, headed "Conditions". These conditions will, if appropriate, be printed in a block, directly following the heading "Experimental".

Illustrations. The figures should be submitted in a form suitable for reproduction, drawn in Indian ink on drawing or tracing paper. Each illustration should have a caption, all the *captions* being typed (with double spacing) together on a *separate sheet.* If structures are given in the text, the original drawings should be provided. Coloured illustrations are reproduced at the author's expense, the cost being determined by the number of pages and by the number of colours needed. The written permission of the author and publisher must be obtained for the use of any figure already published. Its source must be indicated in the legend.

References. References should be numbered in the order in which they are cited in the text, and listed in numerical sequence on a separate sheet at the end of the article. Please check a recent issue for the layout of the reference list. Abbreviations for the titles of journals should follow the system used by *Chemical Abstracts*. Articles not yet published should be given as "in press" (journal should be specified), "submitted for publication" (journal should be specified), "in preparation" or "personal communication".

Vols. 1–651 of the *Journal of Chromatography*; *Journal of Chromatography, Biomedical Applications* and *Journal of Chromatography, Symposium Volumes* should be cited as *J. Chromatogr.* From Vol. 652 on, *Journal of Chromatography A* (incl. Symposium Volumes) should be cited as *J. Chromatogr. A* and *Journal of Chromatography B: Biomedical Applications* as *J. Chromatogr. B.*

Dispatch. Before sending the manuscript to the Editor please check that the envelope contains four copies of the paper complete with references, captions and figures. One of the sets of figures must be the originals suitable for direct reproduction. Please also ensure that permission to publish has been obtained from your institute.

Proofs. One set of proofs will be sent to the author to be carefully checked for printer's errors. Corrections must be restricted to instances in which the proof is at variance with the manuscript.

Reprints. Fifty reprints will be supplied free of charge. Additional reprints can be ordered by the authors. An order form containing price quotations will be sent to the authors together with the proofs of their article.

Flow-Through (Bio)Chemical Sensors

By **M. Valcárcel** and **M.D. Luque de Castro**

Techniques and Instrumentation in Analytical Chemistry Volume 16

Flow-through sensors are more suitable than classical probe-type sensors for addressing real (non-academic) problems. The external shape and operation of flow-through (bio)chemical sensors are of great practical significance as they facilitate sample transport and conditioning, as well as calibration and sensor preparation, maintenance and regeneration, all of which result in enhanced analytical features and a wider scope of application. This is a systematic presentation of flow-through chemical and biochemical sensors based on the permanent or transient immobilization of any of the ingredients of a (bio)chemical reaction (i.e. the analyte, reagent, catalyst or product) where detection is integrated with the analytical reaction, a separation process (dialysis, gas diffusion, sorption, etc.) or both.

The book deals critically with most types of flow-through sensors, discussing their possibilities and shortcomings to provide a realistic view of the state-of-the-art in the field. The large numbers of figures, the wealth of literature references and the extensive subject index complement the text.

Contents: 1. Sensors in Analytical Chemistry. Analytical chemistry at the turn of the XXI century. Analytical information. What is a sensor? Sensors and the analytical process. Types of sensors. General features of (bio)chemical sensors. (Bio)chemical sensors and analytical properties. Commercial availability. Trends in sensor development. **2. Fundamentals of Continuous-Flow (Bio)Chemical Sensors.** Definition. Classification. The active microzone. Flow-through cells. Continuous configurations. Regeneration modes. Transient signals. Measurement modes. The role of kinetics. Requirements for proper sensor performance. **3. Flow-Through Sensors Based on Integrated Reaction and Detection.** Introduction. Flow-through sensors based on an immobilized catalyst. Flow-through immunosensors. Flow-through sensors based on an immobilized reagent. Flow-through sensors based on an *in situ* produced reagent. **4. Flow-Through Sensors Based on Integrated Separation and Detection.** Introduction. Integrated gas diffusion and detection. Integrated liquid-liquid separation and detection. Integrated retention and detection. Flow-through sensors for multideterminations based on integrated retention and detection. Ion-selective electrodes (ISEs) and ion-sensitive field-effect transistors (ISFETs). **5. Flow-Through Sensors Based on Integrated Reaction, Separation and Detection.** Introduction. Integration of gas-diffusion, reaction and detection. Integration of dialysis, reaction and detection. Integration of sorption, reaction and detection. **Index.**

©1994 332 pages Hardbound
Price: Dfl. 355.00 (US$ 208.75)
ISBN 0-444-89866-2

ELSEVIER
An imprint of Elsevier Science

ORDER INFORMATION

ELSEVIER SCIENCE
Customer Service Department
P.O. Box 211
1000 AE Amsterdam
The Netherlands
Fax: +31 (20) 485 3432

For USA and Canada:
ELSEVIER SCIENCE
Customer Service Department
P.O. Box 945, New York
NY 10159-0945
Fax: +1 (212) 633 3764

US$ prices are valid only for the USA & Canada and are subject to exchange rate fluctuations; in all other countries the Dutch guilder price (Dfl.) is definitive. Customers in the European Union should add the appropriate VAT rate applicable in their country to the price(s). Books are sent postfree if prepaid.